Landfill Response to In-situ Stabilisation

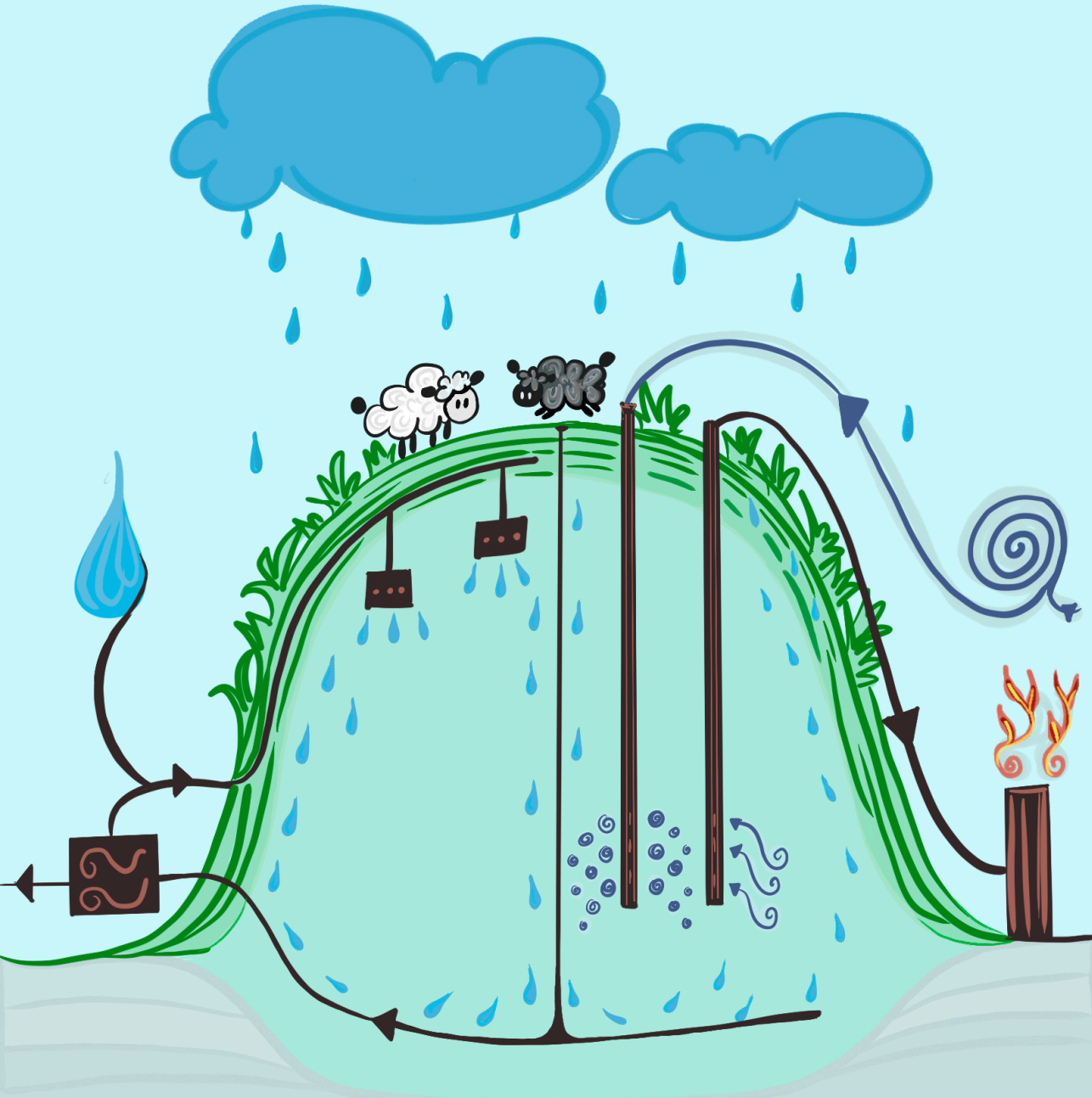

Paola Nathali Meza Ramos

Landfill Response to In-situ Stabilisation

Dissertation

for the purpose of obtaining the degree of doctor
at Delft University of Technology
by the authority of the Rector Magnificus,
Prof.dr.ir. H. Bijl,
chair of the Board for Doctorates
to be defended publicly on
Monday, 13 April 2026, 15:00

by

Paola Nathali MEZA RAMOS

This dissertation has been approved by the promotors.

Composition of the doctoral committee:

Rector Magnificus,	chairperson
Prof. dr. ir. T. J. Heimovaara,	Delft University of Technology, promotor
Prof. dr. J. Gebert,	Delft University of Technology / Technische Universität Braunschweig, Germany, promotor

Independent members:

Prof. dr. H.M. Jonkers,	Delft University of Technology
Prof. dr. J.F. Cuevas Rodriguez,	Autonomous University of Madrid, Spain
Prof. dr. M. Huber-Humer,	University of Natural Resources and Life Sciences, Austria
Dr. B.M. van Breukelen,	Delft University of Technology
Prof. dr. D. van Halem,	Delft University of Technology, reserve member

Keywords: Landfill in-situ stabilization; landfill aeration; water recirculation; spatial variability; landfill gas generation; carbon and nitrogen mass balance; nitrogen transformation; landfill biogeochemistry; full-scale monitoring.

Printed by: Gildeprint B.V.
Cover design by: Paola Nathali Meza Ramos
Cover ilustration by: Ana María Restrepo Sierra

ISBN/EAN: 978-94-6384-940-1

An electronic copy of this dissertation is available at: http:repository.tudelft.nl/

To my dad, who always believed I would be a doctor...
even if not the kind he had in mind

Table of contents

Summary

Many landfills still pose significant emission and pollution risks because decomposition is incomplete, and contaminants persist. To mitigate these risks and reduce the duration of aftercare, in-situ stabilization techniques have been developed to accelerate waste degradation. Two methods have been tested in this context: recirculation of water to stimulate microbial activity and aeration to promote aerobic degradation. Both alter the composition of organic matter as readily degradable fractions are consumed, while more resistant components remain.

Although numerous projects worldwide have shown encouraging results, landfill stabilization remains challenged by the inherent heterogeneity of the waste body. This complexity limits uniform treatment and leaves uncertainties about the physical, chemical, and biological interactions at play. Addressing these knowledge gaps, this thesis investigates the effectiveness of aeration and water recirculation in three Dutch pilot landfills: Braambergen and Wieringermeer (aerated), and Kragge (water recirculation).

The pilots revealed that the effects of aeration are highly variable in space and time. At Braambergen, variability in aeration performance revealed the strong influence of site heterogeneity. Differences in water levels in aeration wells affected gas composition and flow, yet high water columns alone could not explain the observed contrast between compartments. Other factors, such as spatial variability in gas permeability within the waste body, also played a role. Where aeration was more effective, higher gas extraction, elevated temperatures, and greater settlement indicated enhanced microbial activity and carbon mineralization.

Beyond gas monitoring, stabilization was assessed by comparing the carbon generation of waste samples under aerobic and anaerobic conditions with model predictions and with carbon actually recovered on-site. The heterogeneity of the waste samples was reflected in the carbon potential and decay rate constants (k-values). Aerated pilots showed reduced aerobic carbon potential, reflecting advanced stabilization, while the recirculated pilot retained substantial degradable organic matter. These results highlight both the large potential of aeration to accelerate stabilization and the persistence of heterogeneity that complicates prediction and management.

A further focus was placed on building a comprehensive carbon and nitrogen balance across the solid, aqueous, and gas phases at field scale. Over seven years, aerated pilots exhibited higher organic matter degradation than the anaerobic pilot with a significant share of carbon and nitrogen released through the gas phase. In contrast, the recirculated pilot retained larger amounts of degradable carbon and poorly mobilizable nitrogen.

Importantly, the analysis revealed that a substantial fraction of nitrogen remains fixed in solid or microbial pools, potentially delaying compliance with leachate emission targets.

Taken together, these findings advance understanding of how aeration and water recirculation influence landfill stabilization. They demonstrate the benefits of aeration for accelerating degradation while also underlining the challenges posed by spatial variability and persistent nitrogen pools. Such insights are crucial for improving the design and implementation of in-situ stabilization strategies and for reducing the long-term aftercare needs of landfills.

Samenvatting

Veel stortplaatsen vormen nog steeds een aanzienlijk risico voor emissies en verontreiniging, omdat de afbraak van het afval onvolledig is en verontreinigende stoffen achterblijven. Om deze risico's te beperken en de duur van de nazorg te verkorten, zijn in-situ stabilisatietechnieken ontwikkeld die de afbraak van afval versnellen. Twee methoden zijn in dit verband onderzocht: recirculatie van water om de microbiële activiteit te stimuleren en beluchting om de aerobe afbraak te bevorderen. Beide processen veranderen de samenstelling van organische stof doordat de gemakkelijk afbreekbare fracties worden geconsumeerd, terwijl de meer resistente componenten achterblijven.

Hoewel wereldwijd talrijke projecten veelbelovende resultaten hebben laten zien, blijft de stabilisatie van stortplaatsen een uitdaging vanwege de inherente heterogeniteit van het stortlichaam. Deze complexiteit belemmert een uniforme behandeling en zorgt voor onzekerheden over de onderliggende fysische, chemische en biologische processen. Om deze kennishiaten aan te pakken, onderzoekt dit proefschrift de effectiviteit van beluchting en waterrecirculatie in drie Nederlandse pilotstortplaatsen: Braambergen en Wieringermeer (belucht) en De Kragge (met waterrecirculatie).

De pilots toonden aan dat de effecten van beluchting sterk variëren in ruimte en tijd. In Braambergen liet de variabiliteit in beluchtingsprestaties de sterke invloed van locatie-specifieke heterogeniteit zien. Verschillen in waterstanden in de beluchtingsputten beïnvloedden de gassamenstelling en -stroom, maar hoge waterkolommen alleen konden het waargenomen contrast tussen compartimenten niet verklaren. Andere factoren, zoals de ruimtelijke variatie in gasdoorlatendheid binnen het stortlichaam, speelden eveneens een rol. Waar de beluchting effectiever was, wezen hogere gasextractie, verhoogde temperaturen en grotere zetting op een verbeterde microbiële activiteit en koolstofmineralisatie.

Naast gasmonitoring werd de mate van stabilisatie beoordeeld door de koolstofproductie van afvalmonsters onder aerobe en anaerobe omstandigheden te vergelijken met modelvoorspellingen en met de daadwerkelijk op locatie teruggewonnen koolstof. De heterogeniteit van de afvalmonsters kwam tot uiting in het koolstofpotentieel en de afbraaksnelheidsconstanten (k-waarden). De beluchte pilots vertoonden een lager aerobe koolstofpotentieel, wat wijst op een verder gevorderde stabilisatie, terwijl de pilot met waterrecirculatie nog aanzienlijke hoeveelheden afbreekbare organische stof bevatte. Deze resultaten onderstrepen zowel het grote potentieel van beluchting om de stabilisatie te versnellen als de blijvende invloed van heterogeniteit die voorspelling en beheer bemoeilijkt.

Een bijkomende focus lag op het opstellen van een uitgebreide koolstof- en stikstofbalans

over de vaste, vloeibare en gasfase op veldschaal. Over een periode van zeven jaar vertoonden de beluchte pilots een hogere afbraak van organische stof dan de anaerobe pilot, waarbij een aanzienlijk deel van koolstof en stikstof via de gasfase werd vrijgegeven. Daarentegen behield de pilot met waterrecirculatie grotere hoeveelheden afbreekbare koolstof en moeilijk mobiliseerbare stikstof. De analyse liet bovendien zien dat een aanzienlijk deel van de stikstof vast blijft zitten in vaste of microbiële fracties, wat naleving van emissiedoelwaarden voor percolaat kan vertragen.

Gezamenlijk dragen deze bevindingen bij aan een beter begrip van hoe beluchting en waterrecirculatie de stabilisatie van stortplaatsen beïnvloeden. Ze tonen de voordelen van beluchting aan voor het versnellen van afbraak, maar benadrukken ook de uitdagingen die gepaard gaan met ruimtelijke variabiliteit en hardnekkige koolstof- en stikstofvoorraden. Dergelijke inzichten zijn essentieel voor het verbeteren van het ontwerp en de uitvoering van in-situ stabilisatiestrategieën en voor het verkorten van de lange-termijn nazorg van stortplaatsen.

1

General Introduction

1.1. Waste generation and landfilling

1.1.1. Global and European waste generation

Since the beginning of human civilization, waste generation has been a byproduct of human activity. With ongoing economic development and rapid population growth, the volume of waste has increased dramatically. Globally, more than two billion tons of municipal solid waste (MSW) are generated each year, a figure projected to increase by 56% by 2050 unless urgent action is taken (United Nations Environment Programme, 2024). While nearly all MSW is collected in high-income countries, less than 40% is collected in low-income regions. Globally, approximately 30% of collected MSW is disposed of in landfills, making it the most widely used waste management method. By 2050, it is estimated that more than one billion tons of MSW will be landfilled (United Nations Environment Programme, 2024).

In the European Union, 52 million tons of MSW were landfilled in 2022 which represented 23% of total waste generation (Eurostat, 2025).

Among EU member states, the Netherlands present a distinctive case: despite its high recycling and recovery rates (Lieten & Dijcker, 2018), landfills still play an essential role for specific waste streams such as contaminated soils and hazardous residues.

1.1.2. Waste management and landfilling in the Netherlands

In 2022, Dutch municipalities disposed of approximately two million tons of waste in landfills, more than half of which consisted of soil, remediation residues, and hazardous waste (Table 1.1). All household waste was treated through waste processing facilities (0.3 Mton in 2022) and biological treatment such as fermentation and composting (1.5 Mton in 2022, Werkgroep Afvalregistratie, 2024).

Table 1.1. Amounts of landfilled waste in the Netherlands in 2022 (Werkgroep Afvalregistratie, 2024).

Waste category	tons	%
Household waste	0.00	0
Commercial waste	306,976.00	15
Waste separation (residuals)	227,848.00	11
Soil and soil remediation residues	705,329.00	34
Construction and demolition	140,838.00	7
Other waste (mainly reprocessing residues bottom ash, and hazardous waste like asbestos containing, and residual waste from incineration plants)	712,967.00	34
Total	2,093,958.00	100

The Netherlands has an estimated 4,000 to 6,000 former landfill sites that ceased operations before September 1996, most of which are non-sanitary landfills (Lieten & Dijcker, 2018). These sites typically lack environmental protection measures such as impermeable liners, leachate collection systems, and gas management infrastructure, as defined under the Landfill Directive 1999/31/EC (Council of the European Union, 1999) and relevant Dutch

regulations, including the Environmental Management Act (Wet milieubeheer-Wm) and the Decree on Landfills and Waste Dumping Bans (Besluit stortplaatsen en stortverboden afvalstoffen) (Government of the Netherlands, 2024, 2025).

Since 1980, all active landfills have been required to comply with stringent environmental regulations, having been constructed or upgraded as sanitary landfills. From September 1996 onward, landfills have been subject to the Environmental Management Act (Wm) and are referred to as Wm-landfills. These sites are required to comply with mandatory provisions, including long-term environmental monitoring and aftercare. Upon closure, the responsibility for aftercare is transferred to the respective provincial authority. Currently, there are 19 operational sanitary Wm-landfills in the Netherlands. A dedicated aftercare fund, established by the provinces and financed by landfill operators, ensures the long-term environmental management of these sites (Lieten & Dijcker, 2018).

1.1.3. Principles of sanitary landfilling

The goal of sanitary landfilling is to minimize environmental contamination by isolating the waste using impermeable liners and by capturing and treating gas and leachate which was generated through microbial degradation and infiltration of water (Lee et al., 2022). However, while these protective measures are essential for environmental control, they also inhibit conditions necessary for comprehensive waste degradation.

Impermeable liners prevent the infiltration of water, thereby limiting the transport of leachable substances, but also reducing moisture availability within the waste body. As a result, the waste may dry out over time, hindering microbial activity. Furthermore, the sealed landfill environment remains anaerobic, which slows degradation and prevents the complete breakdown of organic matter compared to aerobic conditions (Ritzkowski & Stegmann, 2012). Together, these factors reduce the potential for natural stabilization and prolong the aftercare period.

1.1.4. Landfill stability and emission potential

Upon closure, Dutch landfills are sealed with impermeable cover layers, and residual emissions of gas and leachate are continuously monitored and treated until the site no longer poses an environmental risk. Stabilized landfills may then be repurposed for use such as cycling parks, golf courses, recreational facilities, and office spaces. In a land-scarce country such as the Netherlands, recovering and repurposing former landfill sites is a strategic priority. However, the time required for a landfill to reach a stable state remains uncertain (Ritzkowski, 2021; van Turnhout et al., 2018).

The anaerobic environment typically prevailing in waste limits the rate of organic waste degradation (Brand et al., 2016; X. Zhang et al., 2019), resulting in extended aftercare periods, potentially spanning hundreds of years, before waste reactivity declines to negligible levels (van Turnhout et al., 2018). Theoretically, aftercare obligations could persist indefinitely unless emission potential is sufficiently reduced (Ritzkowski, 2021). Therefore, minimizing

the emission potential is essential to concluding aftercare responsibilities and unlocking land for future use (Scharff, 2014). Emission potential refers to the landfill's long-term capacity to release harmful substances, via leachate or gas, that may affect soil, groundwater, or surface water quality (Brand et al., 2014).

1.1.5. In-situ stabilization techniques

"Landfill Stability" is not universally defined. In the USA, a landfill is considered biologically stabilized when it produces negligible gas, the leachate is non-polluting, and subsidence is complete, typically marking the end of anaerobic microbial activity (Anex, 1996). In England and Wales, a risk assessment approach is used, meaning the criteria for completion are not absolute (Rich et al., 2008). Generally, stability is reached when biodegradable waste has mineralized or become inert, gas and leachate production has declined to safe levels, and structural settlement has ceased (G. Zhang et al., 2023). Nevertheless, many older landfills still present significant emission and pollution risks due to incomplete decomposition and residual contaminants (Tintner et al., 2012).

To address these challenges, in-situ stabilization techniques have been developed to accelerate waste degradation and reduce the aftercare period to within a single generation. Several methods are used to enhance stabilization (Hrad & Huber-Humer, 2017; Raga et al., 2015; Ritzkowski et al., 2006; Ritzkowski & Stegmann, 2012; Stegmann & Heyer, 2003). One such method involves water recirculation to increase moisture content and stimulate microbial activity (Lee et al., 2022; van Turnhout et al., 2018), although heterogeneity and anisotropy in the waste body often impede uniform distribution (Fei et al., 2016). Another promising method is landfill aeration, which introduces oxygen to enhance aerobic microbial activity. Aerobic degradation yields more energy and enables the activation of oxygen-dependent enzymes, thereby facilitating faster breakdown of organic matter (Ritzkowski et al., 2016). Both anaerobic and aerobic degradation processes alter the molecular structure and composition of the remaining organic matter, as easily digestible components are broken down more rapidly (Brandstätter et al., 2020).

Several in-situ stabilization projects worldwide have demonstrated promising results. In Austria and Germany, in-situ aeration significantly reduced gas and leachate emissions and promoted biological stabilization. However, total organic carbon (TOC) reductions in solid waste were modest, often due to the presence of inert materials such as plastics, wood, and textiles, and the challenges of representative sampling in heterogeneous waste bodies (Brandstätter et al., 2020; Ritzkowski et al., 2006). While aeration is commonly applied to older, more stabilized landfills, it can also be effective in younger sites. For example, a large-scale remediation project at the Jinkou Landfill in China applied in-situ aeration to zones containing biologically active waste. After 12 months, the site met national reuse standards and was repurposed as a public park. However, managing elevated temperatures and installing control systems significantly increased project costs (Cao et al., 2016).

Similarly, water recirculation projects have shown potential in accelerating stabilization. In China, recirculation reduced nitrogen concentrations and waste reactivity, although changes in solid waste composition remained limited due to the aged, heterogeneous nature of the material (Chung et al., 2015). In the United States, early experiences with in-situ leachate recirculation improved gas production and stabilization, though technical challenges, particularly related to system design and moisture management, persisted (Reinhart, 1996).

In the Netherlands, the Dutch Sustainable Landfill Management programme (iDS) applies these principles to three pilot landfills to reduce long-term aftercare by actively lowering emission potential through aeration and water recirculation. These pilot compartments are part of the larger landfills Braambergen, Wieringermeer, and Kragge. For clarity, the landfill areas under in-situ stabilization are referred to here as BRA, WIE, and KRA, respectively.

1.2. Background

The Dutch Sustainable Landfill Management program (iDS) was initiated in 2010 by the Dutch Sustainable Landfill Foundation, in collaboration with the Dutch Ministry of Infrastructure and the Environment, provincial governments, scientific institutes, and the Dutch Waste Management Association (Sustainable Landfill Foundation, 2010).

The project was structured in two phases. The first phase (2010) involved a conceptual and computational model which was developed to derive Emission Testing Values (ETVs) for leachate based on environmental protection criteria and existing Dutch and EU regulations. The approach focused on using the receptor (soil/groundwater) as the starting point rather than the landfill itself. Key recommendations included using background concentrations plus maximum permissible additions to define acceptable pollutant levels (Versluijs et al., 2011). In the second phase (2011–2014), the concept of Emission Testing Values (ETVs), later referred to as Environmental Protection Criteria (EPCs), was refined, and landfill-specific ETV proposals were developed for pilot sites (Dijkstra et al., 2018).

Ammonium was identified as a key contaminant, with an ETV of 50 mg/L defined as leachate concentration. However, it was recommended that the degradation behavior of ammonium during treatment be studied further to enable future refinement of this value (Brand et al., 2014; Dijkstra et al., 2018).

The overarching aim of iDS is to reduce the costs and duration of landfill aftercare by accelerating stabilization and thereby reducing environmental emission potential (Sustainable Landfill Foundation, 2010). From late 2017 and early 2018, in-situ stabilization measures, including aeration and water recirculation, were implemented at BRA (aeration), WIE (aeration), and KRA (recirculation). These pilots are expected to undergo active treatment for approximately 10 years. Following this period, ETVs will be used to assess whether environmental risks have been sufficiently mitigated, potentially allowing landfills to be closed without a top cover (Brand et al., 2014, 2016; Dijkstra et al., 2018).

1.3. Motivation and thesis outline

Over the past two decades, in-situ studies have aimed to accelerate landfill stabilization and reduce long-term monitoring by increasing moisture or enhancing aerobic degradation through oxygen supply (Brandstätter et al., 2020; Chung et al., 2015; Reinhart, 1996; Ritzkowski et al., 2006). However, landfills remain complex systems, and key knowledge gaps persist regarding the physical, chemical, and biological processes involved (Brandstätter et al., 2015b, 2015a; Ritzkowski, 2021). Deeper insights into these interactions are essential to optimize stabilization strategies.

To address these gaps, this thesis adopts a structured, stepwise approach. It begins by characterizing the physical and operational conditions of the landfills under study, followed by an assessment of spatial variability in gas-phase stabilization. It then evaluates carbon transformation, waste heterogeneity, and stabilization performance, culminating in an integrated carbon and nitrogen mass balance at field-scale. This framework allows for a comprehensive evaluation of in-situ stabilization as a viable method to reduce landfill aftercare requirements.

This thesis investigates the effectiveness of in-situ stabilization techniques, specifically landfill aeration and water recirculation, applied at BRA, WIE, and KRA sites. The overarching goal is to understand how these methods influence the physical, chemical, and biological stabilization of landfills over time, with a focus on carbon and nitrogen transformation, and long-term aftercare needs.

Chapter 2 provides a detailed description of the study sites, including historical context, waste composition, moisture content, and temperature in the waste body over time during the stabilization period. This chapter sets the foundation for interpreting stabilization behavior by establishing key site-specific characteristics. The research objective of this chapter was to characterize the physical properties, operational conditions, and baseline parameters of the three Dutch landfill compartments (BRA, WIE, and KRA) undergoing in-situ stabilization.

Chapter 3 examines the spatial and temporal variability of landfill gas (LFG) generation under combi-aeration at BRA. It addresses the challenge of uneven air and gas flow distribution caused by heterogeneous waste and variable water tables and analyses its effect on biodegradation efficiency. The research questions of this chapter are:

RQ3.1. Which is the spatial variability of landfill gas composition and flow under the operational conditions of combi-aeration?

RQ3.2. How do operational challenges, such as spatial variability in gas flow and perched water tables, impact the efficiency of landfill?

RQ3.3. How does aeration efficiency influences biodegradation, carbon extraction, and settlement?

To address these questions, gas composition, flow, pressure, and temperature were manually measured at individual wells, while data from the bulk gas was continuously recorded. Spatial and temporal variability were assessed using software tools, and CH_4/CO_2 ratios were used to estimate aerobic and anaerobic activity. Carbon extraction efficiency was calculated using the ideal gas law, while temperature and settlement were monitored with fiber optics and settlement beacons.

Chapter 4 evaluates the progression of carbon stabilization across the three sites after five years of stabilization. It compares modelled anaerobic carbon emissions with measured carbon recovery from on-site monitoring and laboratory incubations. This chapter also assesses the role of waste heterogeneity in carbon release potential, linking stabilization performance to underlying waste characteristics. The research objective of this chapter was to assess the degree of stabilization achieved after five years of in-situ treatment by quantifying carbon generation (CO_2 and CH_4) under aerobic and anaerobic conditions, and to examine the role of waste heterogeneity in stabilization outcomes. The research questions of this chapter are:

RQ4.1. After five years of stabilization, what is the carbon potential under aerobic and anaerobic conditions in waste from the pilots? Are the aerated pilots more stable than the anaerobic pilot?

RQ4.2. How do different waste characteristics affect the kinetics of carbon generation by waste in the three pilots?

RQ4.3. To what extent do aerobic conditions increase carbon potential?

RQ4.4. How do the methane and carbon generation values predicted by the Afvalzorg multiphase model compare with those measured in laboratory and on-site extractions? How could any discrepancies be explained?

RQ4.5. To what extent do waste properties influence the biodegradability in waste from different pilots?

To address these questions, carbon generation was quantified using field gas measurements, modeling, and laboratory incubations. Recovered carbon normalized to dry waste weight was estimated using gas composition, flow, temperature, and pressure data from landfill gas extraction systems. Modeled carbon generation was calculated using the NV Afvalzorg Multiphase Landfill Gas Model (2022), which accounts for waste-specific decomposition rates. Waste samples were collected from various depths, characterized for organic content, and subjected to anaerobic and aerobic incubations. Gas production (CO_2, CH_4) was fitted to exponential decay models to determine carbon potential and degradation rates, expressed per dry weight and normalized to total organic carbon (TOC).

Chapter 5 integrates carbon and nitrogen mass balances to explore how aerobic and anaerobic conditions influence the coupling of these two biogeochemical cycles. It combines long-term monitoring data with laboratory analyses to evaluate the effects of in-situ stabilization on carbon and nitrogen dynamics across solid, aqueous and gas phases. Specifically, the key research questions of this chapter are:

RQ5.1. Can carbon and nitrogen balances be established for full-scale landfills under both aerobic and anaerobic conditions?

RQ5.2. How do these balances improve understanding of in-situ processes and the partitioning of carbon and nitrogen between solid, aqueous, and gaseous phases?

RQ5.3. Do carbon and nitrogen balances provide insight into the long-term stabilization of waste and the potential for compliance with emission targets?

To answer these questions, gas, leachate, and solid-phase data from 2017 to 2024 were integrated. Gas and leachate monitoring included frequent sampling and flow measurements to quantify emissions and establish carbon and nitrogen mass balances over a seven-year period. Solid waste samples were analyzed for elemental composition. Gas production data from Chapter 4 informed assessments of degradable organic carbon (DOC_S), and nitrogen extractability was determined through water and KCl extractions. Leachate and gas monitoring focused on dissolved carbon and nitrogen species, and gas-phase transformations were evaluated using aeration efficiency and net denitrification indicators.

Chapter 6 synthesizes the main findings, discussing the effectiveness of aeration and recirculation, and its implications for landfill stabilization. Finally, **Chapter 7** concludes the thesis, summarizing key insight and providing recommendations for implementation and further study.

These objectives support the overall aim of enhancing the understanding and practical application of in-situ stabilization through aeration and water recirculation, contributing to the reduction of long-term aftercare.

Note: Some repetition appears in the introduction and methods sections of individual chapters, as these were originally prepared as standalone journal articles.

Bibliography

1. Anex, R. P. (1996). Optimal waste decomposition-landfill as treatment process. Journal of Environmental Engineering, 122(11), 955–1048. https://doi.org/https://doi.org/10.1061/(ASCE)0733-9372(1996)122:11(964)
2. Brand, E., de Nijs, T. C. M., Dijkstra, J. J., & Comans, R. N. J. (2016). A novel approach in calculating site-specific aftercare completion criteria for landfills in The Netherlands: Policy developments. Waste Management, 56, 255–261. https://doi.org/10.1016/J.WASMAN.2016.07.038
3. Brand, E., de Nijs, T., Claessens, J., Dijkstra, J. J., Comans, R. N. J., & Lieste, R. (2014). Development of emission testing values to assess sustainable landfill management on pilot landfills. Phase 2 : Proposals for testing values. www.rivm.nl
4. Brandstätter, C., Laner, D., & Fellner, J. (2015a). Carbon pools and flows during lab-scale degradation of old landfilled waste under different oxygen and water regimes. Waste Management, 40, 100–111. https://doi.org/10.1016/J.WASMAN.2015.03.011
5. Brandstätter, C., Laner, D., & Fellner, J. (2015b). Nitrogen pools and flows during lab-scale degradation of old landfilled waste under different oxygen and water regimes. Biodegradation, 26(5), 399–414. https://doi.org/10.1007/s10532-015-9742-5
6. Brandstätter, C., Prantl, R., & Fellner, J. (2020). Performance assessment of landfill in-situ aeration – A case study. Waste Management, 101, 231–240. https://doi.org/10.1016/j.wasman.2019.10.022
7. Cao, L., Chen, N., Hu, Z., Liao, Z., & Chen, Z. (2016). Landfill: The world's largest ecological restoration case - A case study of the Jinkou Landfill in Wuhan. Urban Management & Technology. https://doi.org/10.16242/j.cnki.umst.2016.03.003
8. Chung, J., Kim, S., Baek, S., Lee, N. H., Park, S., Lee, J., Lee, H., & Bae, W. (2015). Acceleration of aged-landfill stabilization by combining partial nitrification and leachate recirculation: A field-scale study. Journal of Hazardous Materials, 285, 436–444. https://doi.org/10.1016/J.JHAZMAT.2014.12.013
9. Council of the European Union. (1999). Council Directive 1999/31/EC of 26 April 1999 on the landfill of waste (consolidated version 2024-08-04). In 1999. https://data.europa.eu/eli/dir/1999/31/2024-08-04
10. Dijkstra, J. J., van Zomeren, A., Brand, E., & Comans, R. N. J. (2018). Site-specific aftercare completion criteria for sustainable landfilling in the Netherlands: Geochemical modelling and sensitivity analysis. Waste Management, 75, 407–414. https://doi.org/10.1016/j.wasman.2016.07.038
11. Eurostat. (2025, February 13). Municipal waste by waste management operations (Online data code: env_wasmun). https://doi.org/https://doi.org/10.2908/ENV_WASMUN
12. Fei, X., Zekkos, D., & Raskin, L. (2016). Quantification of parameters influencing methane generation due to biodegradation of municipal solid waste in landfills and laboratory experiments. Waste Management, 55, 276–287. https://doi.org/10.1016/J.WASMAN.2015.10.015
13. Government of the Netherlands. (2024). Besluit stortplaatsen en stortverboden afvalstoffen [Decree on landfills and waste dumping bans]. Geldend van 01-01-2024 t/m heden. https://wetten.overheid.nl/jci1.3:c:BWBR0009094&z=2024-01-01&g=2024-01-01
14. Government of the Netherlands. (2025). Wet milieubeheer [Environmental Management Act]. Geldend van 01-01-2025 t/m heden. https://wetten.overheid.nl/jci1.3:c:BWBR0003245&z=2025-01-01&g=2025-01-01
15. Hrad, M., & Huber-Humer, M. (2017). Performance and completion assessment of an in-situ aerated municipal solid waste landfill – Final scientific documentation of an Austrian case study. Waste Management, 63, 397–409. https://doi.org/10.1016/j.wasman.2016.07.043
16. Lee, H., Coulon, F., Beriro, D. J., & Wagland, S. T. (2022). Recovering metal(loids) and rare earth elements from closed landfill sites without excavation: Leachate recirculation opportunities and challenges. Chemosphere, 292, 133418. https://doi.org/10.1016/J.CHEMOSPHERE.2021.133418
17. Lieten, S. H., & Dijcker, R. (2018). Landfill Management in the Netherlands (Final version, Report No. 107801/18-

006.894). https://projects2014-2020.interregeurope.eu/fileadmin/user_upload/tx_tevprojects/library/file_1534506068.pdf

18. Raga, R., Cossu, R., Heerenklage, J., Pivato, A., & Ritzkowski, M. (2015). Landfill aeration for emission control before and during landfill mining. Waste Management, 46, 420–429. https://doi.org/10.1016/j.wasman.2015.09.037
19. Reinhart, D. R. (1996). Full-Scale Experiences With Leachate Recirculating Landfills : Case Studies. 347–365.
20. Rich, C., Gronow, J., & Voulvoulis, N. (2008). The potential for aeration of MSW landfills to accelerate completion. Waste Management, 28(6), 1039–1048. https://doi.org/10.1016/J.WASMAN.2007.03.022
21. Ritzkowski, M. (2021). Landfill aeration - an important contribution towards landfill sustainability. Sardinia 2021, 18th International Symposium on Waste Management and Sustainable Landfilling.
22. Ritzkowski, M., Heyer, K. U., & Stegmann, R. (2006). Fundamental processes and implications during in situ aeration of old landfills. Waste Management, 26(4), 356–372. https://doi.org/10.1016/J.WASMAN.2005.11.009
23. Ritzkowski, M., & Stegmann, R. (2012). Landfill aeration worldwide: Concepts, indications and findings. Waste Management, 32(7), 1411–1419. https://doi.org/10.1016/j.wasman.2012.02.020
24. Ritzkowski, M., Walker, B., Kuchta, K., Raga, R., & Stegmann, R. (2016). Aeration of the teuftal landfill: Field scale concept and lab scale simulation. Waste Management, 55, 99–107. https://doi.org/10.1016/j.wasman.2016.06.004
25. Scharff, H. (2014). Landfill reduction experience in The Netherlands. Waste Management, 34(11), 2218–2224. https://doi.org/10.1016/j.wasman.2014.05.019
26. Stegmann, R., & Heyer, K. U. (2003). Discussion of criteria for the completion of landfill aftercare. Proceedings Sardinia, October. http://www.image.unipd.it/tetrawama/S2003/discussion%7B%5C_%7Dof%7B%5C_%7Dcriteria%7B%5C_%7Dfor%7B%5C_%7Dcompletion.pdf
27. Sustainable Landfill Foundation. (2010). Sustainable Landfill Management (iDS). https://www.duurzaamstortbeheer.nl/over-ids/
28. Tintner, J., Smidt, E., Böhm, K., & Matiasch, L. (2012). Risk assessment of an old landfill regarding the potential of gaseous emissions – A case study based on bioindication, FT-IR spectroscopy and thermal analysis. Waste Management, 32(12), 2418–2425. https://doi.org/10.1016/J.WASMAN.2012.07.022
29. United Nations Environment Programme. (2024). Global Waste Management Outlook 2024: Beyond an age of waste – Turning rubbish into a resource. https://wedocs.unep.org/20.500.11822/44939
30. van Turnhout, A. G., Brandstätter, C., Kleerebezem, R., Fellner, J., & Heimovaara, T. J. (2018). Theoretical analysis of municipal solid waste treatment by leachate recirculation under anaerobic and aerobic conditions. Waste Management, 71, 246–254. https://doi.org/10.1016/j.wasman.2017.09.034
31. Versluijs, C., Brand, E., Claessens, J., & Wezenbeek, J. (2011). Phase 1: An inventory Development of test values for pilot landfills for sustainable landfill management. https://www.rivm.nl/bibliotheek/rapporten/607710001.pdf
32. Werkgroep Afvalregistratie. (2024). Afvalverwerking in Nederland: gegevens 2022 [Waste processing in the Netherlands: data 2022]. www.afvalcirculair.nl
33. Zhang, G., Liu, K., Lv, L., Gao, W., Li, W., Ren, Z., Yan, W., Wang, P., Liu, X., & Sun, L. (2023). Enhanced landfill process based on leachate recirculation and micro-aeration: A comprehensive technical, environmental, and economic assessment. Science of The Total Environment, 857, 159535. https://doi.org/10.1016/J.SCITOTENV.2022.159535
34. Zhang, X., Jiang, C., Shan, Y., Zhang, X., & Zhao, Y. (2019). Influence of the void fraction and vertical gas vents on the waste decomposition in semi-aerobic landfill: Lab-scale tests. Waste Management, 100, 28–35. https://doi.org/10.1016/J.WASMAN.2019.08.039

2

Sites of investigation

2.1. General description

The description of the landfills, the in-situ stabilization pilots and the stabilization strategies are based on the feasibility studies (Brocker et al., 2011; Brocker & Kaiser, 2011; van Meeteren et al., 2009a, 2009b; van Vossen et al., 2009), project plans (Lammen & Scharff, 2018; Vereniging Afvalbedrijven, 2014a, 2014b, 2015a, 2015b, 2015c), and progress result reports (Gronert et al., 2014a, 2014b; A. C. Kanen & Kedzia, 2021; Lammen et al., 2020, 2021; Oonk, 2014) elaborated in the framework of the Dutch Sustainable Landfill Management program (iDS). All pilots have gas and leachate collection system and are not covered by an impermeable layer at the top.

The following table summarizes key characteristics of the in-situ stabilization landfill pilots BRA, WIE and KRA, which are part of the larger landfills Braambergen, Wieringermeer, and Kragge.

Table 2.1. Overview of in-situ stabilization landfill pilots characteristics

	BRA	WIE	KRA
Location	Southern Flevoland	Noord Holland	Bergen op Zoom
Landfill	Braambergen	Wieringermeer	Kragge
Compartment under stabilization	Compartments 11N, 11Z and 12	Compartment 6	Compartment 3
Area	10 ha	2.6 ha	5.6 ha
Landfilled waste	1.2 million tons of main-ly contaminated soils and residues (80.6%mass)	280,000 tons of mostly commercial waste (72%mass)	1 million tons of primarily household waste (29.2%mass)
Landfilling period	1999 to 2008	1992 to 2003	1993 to 1998
Landfilling height	~11 m	~12 m	~17 m
Top seal	Earth, bottom ash, jet grout (1-1.5 m)	Earth (1-1.5 m)	Earth and industrial de-bris (0.5-1 m)
Type of bottom seal	Combination of mineral (50 cm sand bentonite) and 2 mm HDPE-liner	2 mm HDPE-liner	2 mm HDPE-liner
Stabilization method	Aeration (combi-aeration and over-extraction) (since September 2017)	Aeration (over-extraction) (since August 2017)	Water recirculation (since March 2018)

2.2. Landfill pilots under in-situ aeration

The landfill compartments under in-situ aeration are operated by NV Afvalzorg Holding and consist of networks of aeration wells distributed across the areas under stabilization. Sonic Samp Drill technology was selected for borehole drilling due to its combined sonic vibration and rotational capabilities, which are well suited for penetrating heterogeneous waste layers. This method also enables simultaneous waste sampling during drilling.

Each borehole was fitted with HDPE pipes (32/24 mm), consisting of a 2-meter slotted bottom section and a 2-meter solid upper section. The slotted portion features 0.3 mm-wide slots spaced 10 mm apart over 175 cm, covering 60% of the pipe circumference, starting 12.5 cm from the base.

Two aeration strategies are employed: combi-aeration and over-extraction (Figure 2.1, top left).

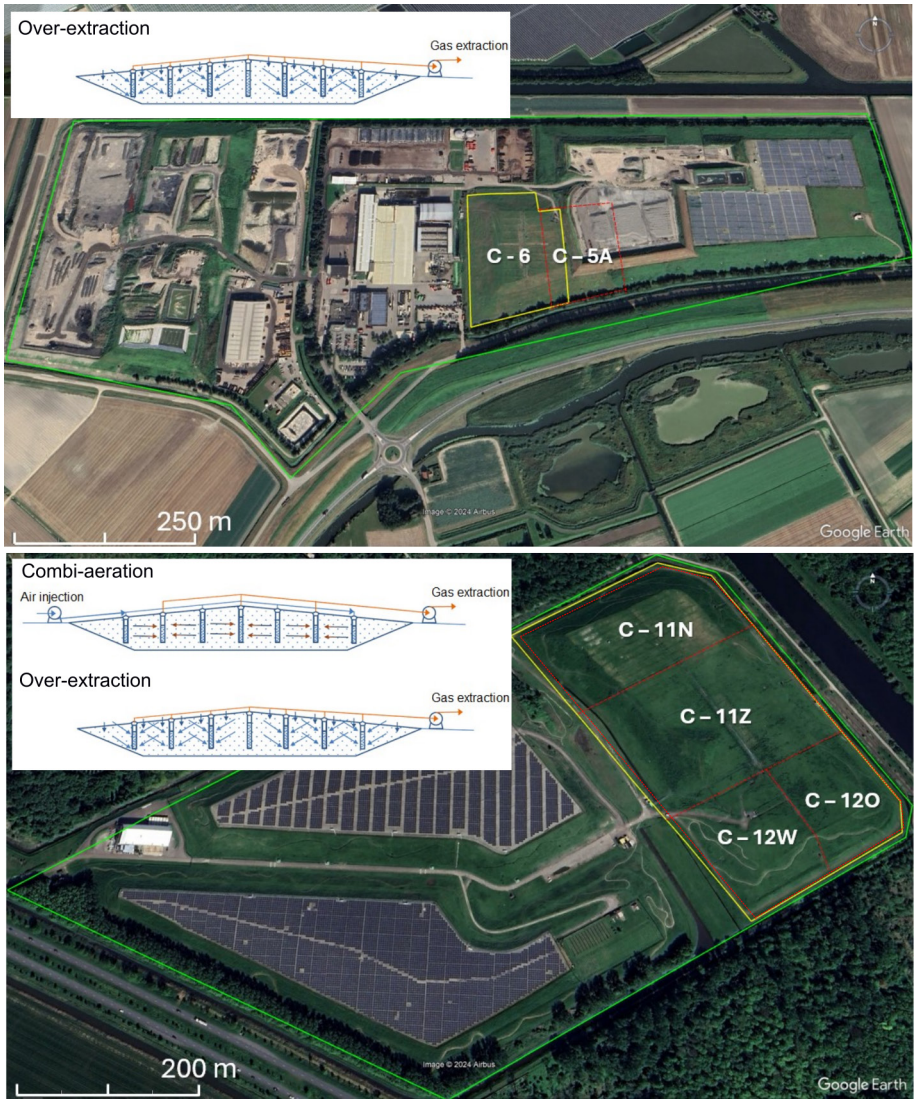

Figure 2.1. Aerial photograph (Google earth) of the landfill (green line), in-situ stabilization landfill pilot (yellow line), and compartments within it (red dotted line). Scheme of aeration strategies in the top left. Top: Braambergen; bottom: Wieringermeer.

- **Combi-aeration** combine air injection and gas extraction. Half of the wells are used to inject air, while the other half extract landfill gas. The system is designed such that the extracted volume always exceeds the injected volume, ensuring negative pressure and minimizing diffuse emissions. The injection flow is sized at half the extraction flow to maintain safe under pressure.

- **Over-extraction** involves applying negative pressure to extract landfill gas at a rate 5 to 10 times higher than the natural gas production rate. This induces the inflow of atmospheric air into the waste body. In both strategies, the exhaust air can be treated to reduce methane emissions and odor nuisance.

The monitoring of the landfill gas was done on individual aeration wells and in the bulk gas. On aeration wells, flow velocity and temperature (multifunctional handheld unit, Höntzsch U426, TA-10 probe), gas composition (Geotech Gas Analyzer GA2000; detection limit 0.1%), and the pressure (pressure gauge by Blue line S4600) were measured manually on a monthly interval. The bulk gas was monitored at the gas blower station. Bulk landfill gas flow rate (Proline Prosonic Flow B 200 Ultrasonic flowmeter for gas extraction, and Proline 65i T-mass flowmeter for air injection; both Endress+Hauser), pressure (PMC51-R8K2/0; Endress+Hausser), gas composition (CH_4, CO_2, and O_2, Biotech Gas Analyzer 3000), and temperature (iTEMP TMT181; Endress+Hauser) were continuously measured and recorded every fifteen minutes.

The system was originally designed for a maximum gas extraction flow of 1,000 m^3/h at each site, based on 2016 landfill gas production estimates. After approximately two years of flow rates below 700 m^3/h, extraction rates were increased, raising gas velocities from 80% to 100% of the target flow.

The leachate drainage system discharges into a leachate collection sump, where cumulative leachate volume (measured using an OPTIFLUX 2100, Krohne) was recorded every 15 minutes. Leachate samples were taken biweekly from 2017 onward to measure carbon, nitrogen, and other key components.

BRA – aeration pilot of Braambergen landfill:

BRA refers to compartments 11N/Z (north/south) and 12W/O (west/east) within the Braambergen landfill, located near the city of Almere in the central Netherlands. This area, situated in the northeastern part of the landfill (referential coordinates: 655936 m E, 5800962 m N), has been under in-situ aeration since September 2017 (Figure 2.1, top). The leachate drainage and collection system comprises three separate drainage systems for zones 11N, 11Z, and 12 (a combined drainage system for 12O and 12W).

To decide the wells distribution a test drilling and test extractions were carried out. The aeration system includes 230 wells (64 in 11N, 110 in 11Z, 25 in 12O, and 31 in 12W) connected via HDPE transport pipes (DN 50 mm) at ground level. The wells are spaced at standard intervals of 20 metres in compartments 11N and 12, whereas in compartment 11Z, the spacing is reduced to 15 metres. Wells were installed one meter above the drainage layer across a 10-hectare area. In 2022, an additional 98 wells were installed (Cruz & Lammen, 2023).

In 2017, a yearly mean flow rate of 680 m^3/h was reached. Thereafter, flow rates decreased and fluctuated between 270 and 504 m^3/h (Supplementary Information B, Table S5.4.1).

The aeration strategy at BRA followed this timeline:

- September 2017 to September 2019: Over-extraction
- September 2019 to April 2020: Combi-aeration
- April 2020 to May 2020: Over-extraction
- May 2020 to November 2020: Combi-aeration
- November 2020 to date: Over-extraction, with 15-30 minutes daily air injection implemented since March 2021

WIE – aeration pilot of Wieringermeer landfill:

WIE refers to Compartment 6 of the Wieringermeer landfill, located near the city of Medemblik in the north of the Netherlands (referential coordinates: 639801 m E, 5848699 m N). To reduce boundary effects, 20-25% of adjacent Compartment 5A is also included in the aerated area (Figure 2.1, bottom). A single leachate drainage and collection system services compartment 6.

Aeration at WIE began in August 2017 using over-extraction. The initial yearly mean flow rate was 595 m^3/h, after which it fluctuated between 380 m^3/h and 556 m^3/h (Supplementary Information B, Table S5.4.1).

The aeration system includes 109 wells, with 87 located in Compartment 6. Wells are positioned 1.4 meters above the drainage system, spaced 12.5 to 13.5 meters apart, and cover a 3.2-hectare area.

2.3. Landfill pilot under in-situ water recirculation

KRA refers to compartment 3 of Kragge landfill (referential coordinates: 593276 m E, 5707076 m N) which is operated by Attero BV. Water recirculation was selected for in-situ stabilization due to its higher content of degradable organic matter and the economic feasibility of this approach. Compared to aeration, water recirculation involves lower operational costs and allows for continued recovery of landfill gas, which remains economically viable (Vereniging Afvalbedrijven, 2015c). The water recirculation system began in March 2018.

The infiltration system includes trenches and drainage pipes embedded in gravel beds, allowing treated leachate to re-enter the waste mass. During the infiltration process, a portion of the released leachate undergoes purification before being reintroduced into the waste package. Infiltration rates have varied between 2 and 7 m^3/h since the commencement of recirculation. To mitigate chloride levels, part of the leachate is discharged into the sewer system (Figure 2.2, top left).

Approximately 90% of the leachate is treated via an Anammox water purification system, where ammonium (NH_4) is converted into nitrogen gas (N_2). A fraction of the leachate is

directed to a nitritation reactor, converting NH_4^+ to NO_2^-, with an efficiency of 20-40% (T. Kanen & Kedzia-Kowalski, 2021). The return of leachate containing NO_2^- to the landfill is intended to stimulate in-situ Anammox reaction. Since 2018, the average NO_2 concentration in the leachate has been 0.17 mg/L. Inert compounds like Cl^- are removed via venting and replaced by 1.2 to 4.8 m^3/h of clean water, both directly and via the nitritation reactor (Van Raffe et al., 2023).

The leachate drainage system is discharged into a leachate collection sump, where cumulative leachate volumes were recorded daily using the OPTIFLUX 2100 flowmeter. Leachate sampling for carbon, nitrogen, and other critical parameters was conducted biweekly from 2018 onward.

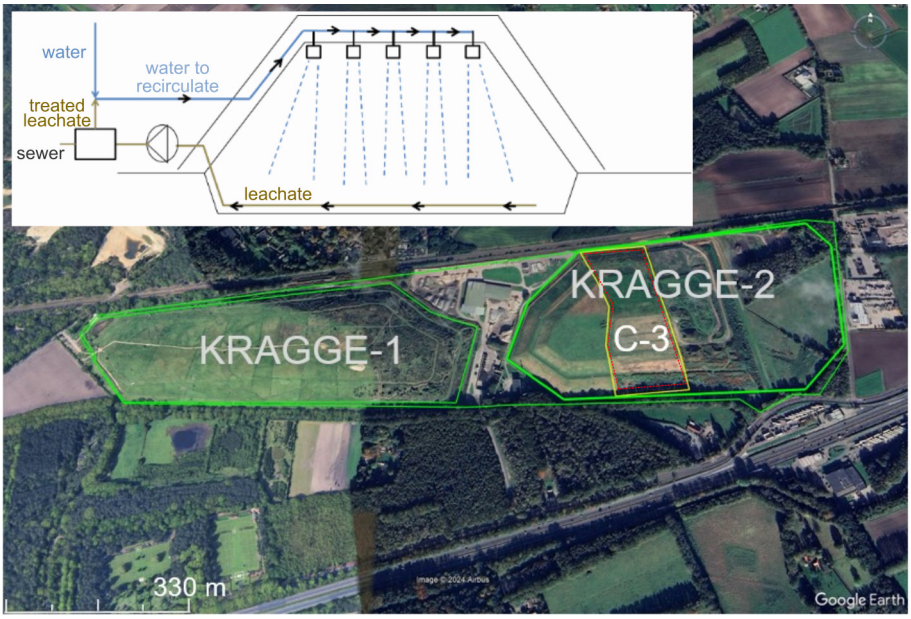

Figure 2.2. Aerial photographs (Google earth) of the Kragge landfill (green line), compartment 3 within the in-situ stabilization pilot (red and yellow line). Scheme of water recirculation in the top left.

Regarding the gas collection system, gas wells at Kragge landfill are grouped into collection points (CPs), which are connected to a single shared pipeline per hill (Kragge 1 and Kragge 2, Figure 2.2). Gas from both Kragge 1 and Kragge 2 is combined and used for cogeneration, producing both electricity and heat. Part of the electricity powers water treatment plants; the rest is fed into the grid. Heat is used to maintain the Anammox and Nitritation reactor temperatures between 25-30°C.

The gas extraction pressure (GGW150 A4-U2 and a Barksdale D1X-M3SS-ex) was measured only in the combined bulk gas, while gas flow (Prosonic Flow 200; Endress+Hauser) was monitored hourly in Kragge 1, Kragge 2, and the combined bulk gas. Gas composition (CH_4, CO_2, and O_2; Biotech Gas Analyzer 3000) was measured monthly at individual wells and CPs, and weekly in Kragge 1, Kragge 2, and the combined bulk gas. Gas velocity (KIMO VT-

100 handheld unit) was measured monthly at individual gas wells and CPs.

2.4. Waste composition

The aerated pilots had a more homogeneous waste composition with one dominant type of waste. BRA, the largest pilot, was landfilled with 1.2 million tons of mainly contaminated soils and residues (80.6%$_{mass}$) while WIE, the smallest pilot, was landfilled with 280,000 tons of mostly commercial waste (72%$_{mass}$). In contrast KRA was landfilled with 1 million tons of primarily household waste (29.2%$_{mass}$), but also construction and demolition waste (21.4%$_{mass}$), and commercial waste (21.3%$_{mass}$). Waste composition and landfilling periods are shown in Figure 2.3.

2.5. Baseline study (prior to in-situ stabilization)

An initial characterization of the waste was conducted in 2017, prior to the start of stabilization efforts at the three landfill pilots, serving as a reference for subsequent evaluations. A total of 12 waste cores were retrieved from each of the WIE and KRA pilots, and 24 from BRA (12 in BRA-11N, and 12 in BRA-11Z), using a 2-metre-long hollow tubes to depths from 11 to 16 m (Lammen & Scharff, 2018). At the WIE pilot, the top two meters were discarded as the cover layer, whereas no such distinction was made for the BRA or KRA pilots. Samples were divided into three-layer groups: top, middle, and bottom layer samples for further characterization.

The baseline measurements included measurements of dry matter, loss on ignition, asbestos content, respiration tests, total organic carbon and total nitrogen (Oonk, 2020). Additionally, the waste samples were characterized by a leaching study, during which a wide range of organic and inorganic parameters were measured (Dijkstra & Van Zomeren, 2019; van Raffe et al., 2025).

2.5.1. Water content, carbon and, nitrogen content

The water content was estimated from the average dry mass measured in the baseline study (Figure 2.4, top). The calculated average water content, expressed on a dry-weight basis, followed the order BRA-11N>KRA> BRA-11Z>WIE. This pattern aligns with the estimated initial water content at the time of deposition (Table 2.2), which was derived from waste composition and Dutch waste stream data (TAUW, 2011).

The average total organic carbon (TOC) and total Kjeldahl nitrogen (TN) concentrations in waste samples per depth group were lower in the top layer (Figure 2.4, middle and bottom). This is likely due to increased exposure to air, facilitating oxidation and aerobic degradation, as well as the downward percolation of rainwater flushing these substances into deeper layers (Dijkstra & Van Zomeren, 2019). The inclusion of the cover layer may also have affected the result for the top layer in BRA and KRA. Overall, the highest TOC and TN were observed in KRA, consistent with its higher proportion of organic waste compared

to the other pilots (Figure 2.3). Additionally, storage conditions may have influenced the nitrogen content of waste samples during the baseline study (Oonk, 2020).

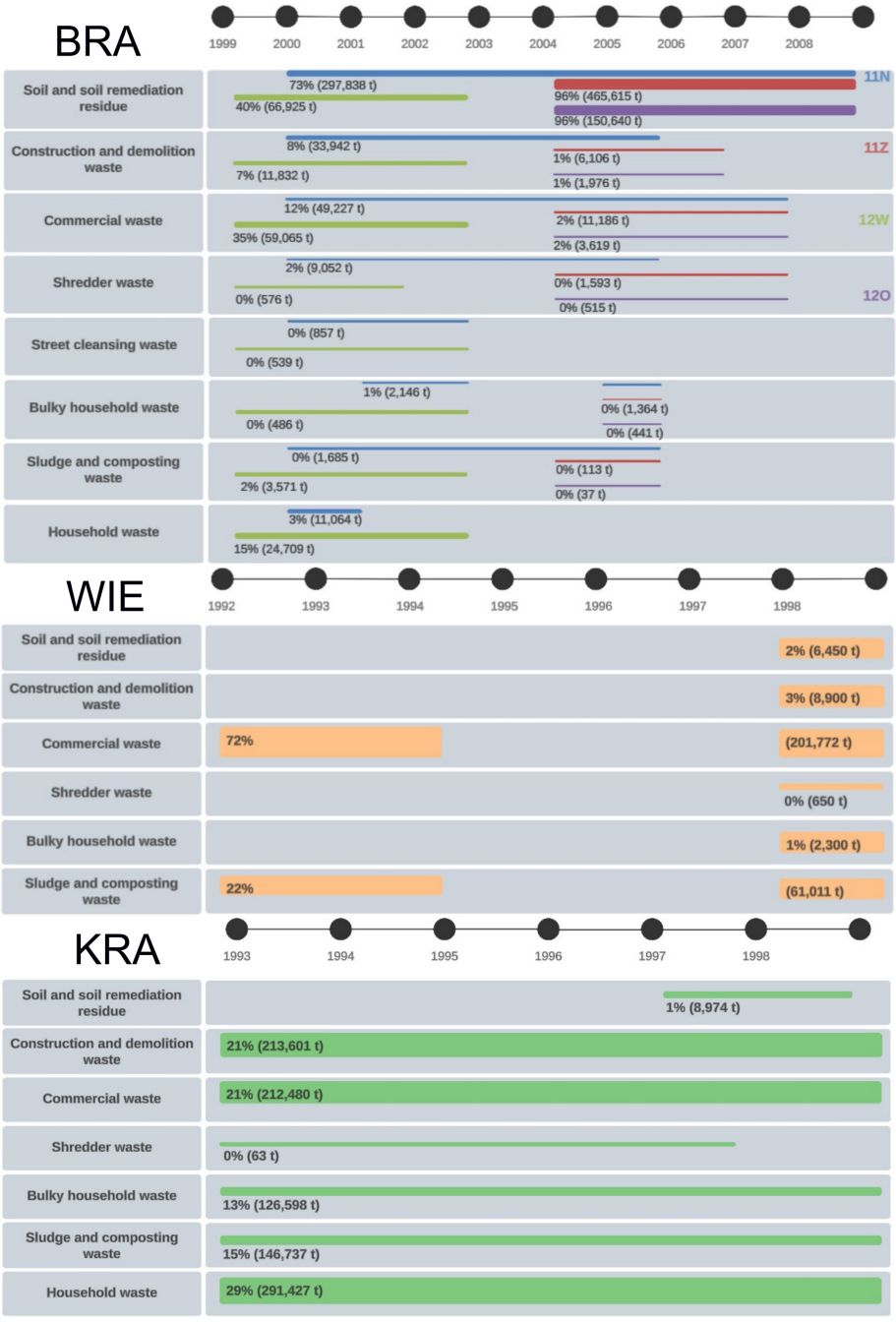

Figure 2.3. Waste composition in the stabilisation pilots over the landfilled period in BRA (compartments 11N, 11Z, 12W, and 12O), WIE (compartment 6), and KRA (compartment 3).

Table 2.2. Estimated water content at the time of deposition ($WC_{deposition}$) and measured at the baseline ($WC_{baseline}$), expressed on a dry-weight basis (%dw) in BRA, WIE and KRA pilots.

Pilot	WCdeposition	WCbaseline
BRA	$52\%_{dw}$	BRA-11N: $40\%_{dw}$ BRA-11Z: $32\%_{dw}$
WIE	$35\%_{dw}$	$29\%_{dw}$
KRA	$32\%_{dw}$	$34\%_{dw}$

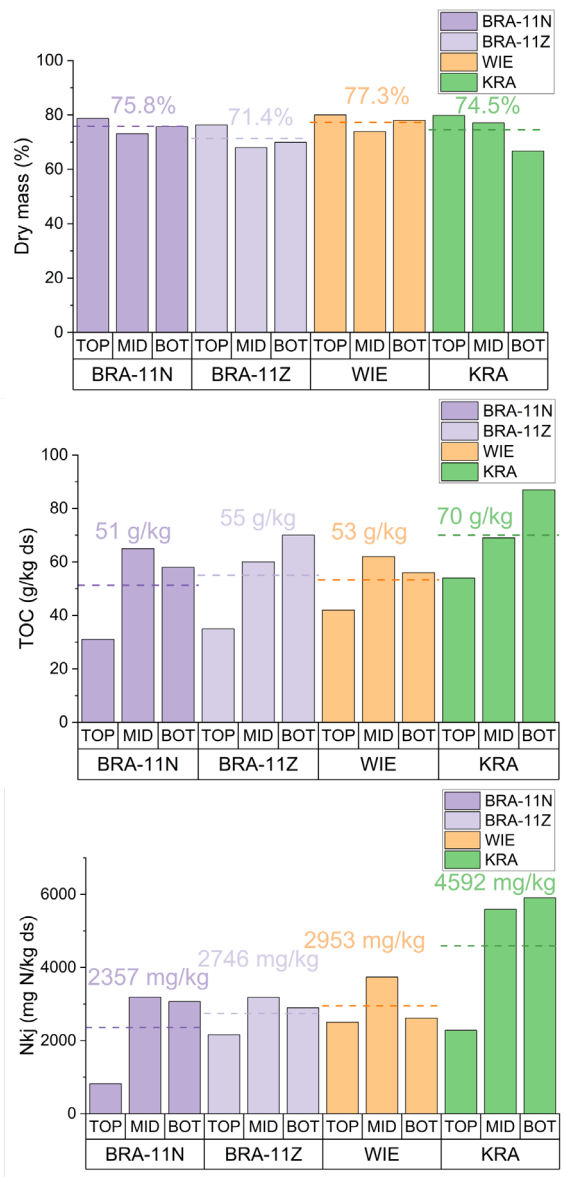

Figure 2.4. Average dry mass, total organic carbon (TOC) and nitrogen Kjeldahl (Nkj) per layer in waste samples from BRA, WIE and KRA. Average per pilot indicated by dotted lines.

2.5.2. Dissolved organic matter

A subset of samples was frozen for future analysis. Using the acid-base extraction method (Van Zomeren & Comans, 2007), organic matter was fractionated to quantify different carbon and nitrogen components (Oonk, 2020; van Raffe et al., 2025). These analyses were carried out at the chair group Soil Chemestry and Chemical Soil Quality (Prof. Rob Comans) at Wageningen University and Research (WUR).

Acid-base extracted dissolved organic nitrogen (DON) and carbon (DOC_L) concentrations in the baseline study showed distinct depth-related patterns across pilots (Figure 2. 5). In absolute terms, DON and DOC_L concentrations generally increase over depth. However, when expressed relative to total nitrogen (TN) and total organic carbon (TOC), their proportions decreased (Figure 2. 5, left), indicating a lower contribution of soluble organic matter to the overall carbon and nitrogen pools in deeper layers. In BRA and KRA, higher DON and DOC_L percentages in the top layers are likely influenced by the inclusion of cover soil, which introduces finer, more decomposed, and water-soluble organic compounds, as well as microbial activity that enhances degradation.

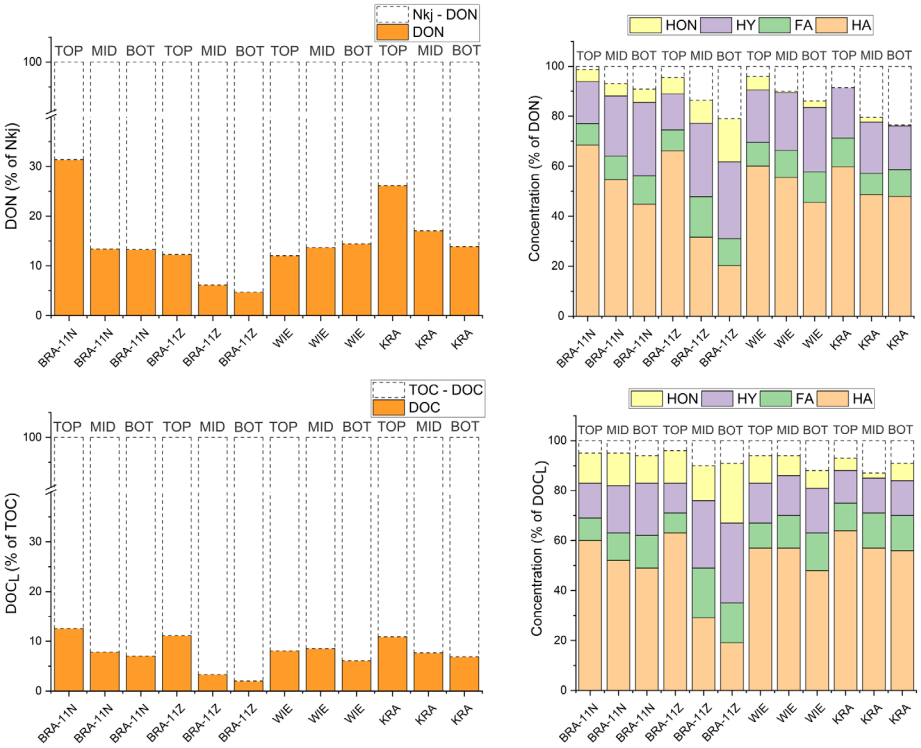

Figure 2.5. Acid-base extracted dissolved organic nitrogen (%DON) as a percentage of Kjeldahl nitrogen and dissolved organic carbon (%DOC_L) as a percentage of Total Organic Carbon (TOC) (left); and fractionation analysis (right) across the top, middle, and bottom layers of the three landfill pilots. DON figures calculated using data provided by F. van Raffe (18/11/2024).

Although TOC levels in the top layers were generally lower, indicating degradation and the loss of solid-phase organic matter, DOC_L and DON concentrations were higher specifically

in samples that retained the cover soil. This may be partially attributed to the decomposition of vegetation present in the cover layer, which can release soluble organic compounds and contribute to elevated DOC_L and DON despite a lower overall TOC content.

Fractionation analysis indicated that most DON and DOC_L were associated with humic acids (HA; Figure 2. 5, right) representing the relatively stable fraction of dissolved organic matter. As humic and fulvic acids (FA) are resistant by-products of biomass degradation and, being only partially leachable, contribute significantly to the long-term chemical oxygen demand in leachate (Morello et al., 2018). The proportion of DON and DOC_L in humic acids decreased with depth, particularly in the aerated pilots, although the extension of this decrease varied among sites. A higher proportion of HA-associated DON and DOC_L in the top layers, considered a proxy for organic matter stabilization, suggests that these layers are more degraded and biogeochemically stable than the middle and bottom layers. In BRA, the difference between compartments 11N and 11Z indicates greater stabilization in 11N, while the bottom layer of 11Z appears less stabilized. WIE exhibited a similar pattern to BRA-11N, with lower stabilization in the bottom layer, likely due to reduced aeration. In contrast, KRA showed almost no variation between the middle and bottom layers, probably because of the predominance of anaerobic conditions in both layers.

The FA fraction was consistently smaller than HA, ranging from 8% to 20% of DON and DOC_L across pilots. Interestingly, BRA-11Z exhibited the highest FA percentages in the middle layer, coinciding with elevated hydrophilic organic (HY) fractions, suggesting that intermediate degradation products are more abundant in this zone. The lowest percentages were found in the hydrophobic organic neutral (HON) fraction, generally below 5% of DON and 13% of DOC_L in most compartments. BRA-11Z was again an exception, with HON reaching up to 17% of DON and 24% of DOC_L. This likely reflects degradation of HA releasing intermediate-size compounds such as HON (Straathof et al., 2014). In fact, HON content was negatively correlated with HA in all samples ($r \geq |0.6|$).

The predominance of humic acid-associated DON and DOC_L highlights the relatively stable state of organic matter in these pilots, while variations in HY and HON indicate differing potentials for further degradation and mineralization. Some biodegradable carbon ultimately transforms into stable humic substances, contributing to long-term leachate pollution (Brandstätter et al., 2015; Morello et al., 2018).

2.5.3. pH-dependent leaching test

A pH-dependent leaching test conducted at the chair group Soil Chemistry and Chemical Soil Quality (Prof. Rob Comans) at Wageningen University and Research (WUR) revealed that over time NH_4-N concentrations increased significantly at extreme pH values, while remaining relatively stable around pH 7. This behaviour indicates that sorption processes largely control the solubility of ammonium (van Raffe et al., 2025).

The mechanism is linked to the pH-dependent surface charge and speciation of

ammonium. At low pH, protonation of mineral and organic surfaces reduces their negative charge, decreasing NH_4^+ sorption. As pH increases, surface deprotonation enhances cation adsorption until NH_4^+ begins to deprotonate to NH_3 at very high pH, again reducing sorption capacity. Thus, NH_4^+ solubility is minimal near neutral pH and increases toward both acidic and alkaline extremes.

The pH in the waste samples ranged between 7 and 7.8. NH_4-N concentrations were minimal near neutral pH and increased sharply under extreme pH conditions (van Raffe et al., 2025). For example:

- BRA: 390-fold increase at pH 11.8.
- WIE: 636-fold increase at pH 2.2.
- KRA: 36-fold increase at pH 2.9.

2.6. Temperature in the waste body

Temperature in the landfill pilots was monitored using a Silixa Ultima XT-DTS distributed temperature sensor, which performs double-ended measurements every 0.5 m along a glass fibre cable installed throughout each pilot area. Between 2021 and 2023, the sensor was rotated among the three sites, recording temperatures at depths of up to 12 m, with measurements taken at intervals of one, four, or six hours. For the data analysis, the top 2m were discarded as cover layer.

Aerobic degradation is an exothermic process that releases significantly more heat than anaerobic degradation. In contrast, water recirculation can help moderate or reduce internal temperatures within the landfill (Reinhart et al., 2020; Wu et al., 2023). This difference is reflected in the maximum temperatures recorded in the pilots: BRA (aerated) reached 67°C, WIE (aerated) reached 55°C, and KRA (anaerobic conditions with water recirculation) reached 37°C (Figure 2.6 and Table 2.3).

Despite the high maximum temperature, the median temperature in WIE was lower than in the other two pilots. This may be explained by the limited seasonal coverage of the DTS data for WIE, which includes only winter and spring months. In contrast, the monitoring period at KRA included both summer and winter seasons. BRA had the most varied seasonal coverage, including summer, autumn and winter.

Seasonal variation is expected to influence temperatures primarily in the top layers of the pilot, while temperatures in the middle and bottom layers are largely governed by heat generated through biological degradation processes (Meza et al., 2022). However, the temperature within the waste body may also be affected by the intake of warm or cold atmospheric air during the over-extraction process. This effect is likely to be more pronounced at WIE, where over-extraction has been employed as the main aeration strategy since the beginning of the stabilization process.

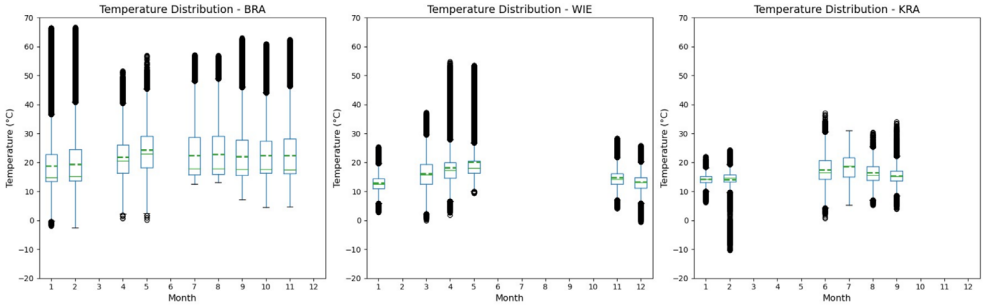

Figure 2.6: Temperature per month in the landfill pilots KRA, BRA and WIE.

Table 2.3. Minimum, maximum, mean and median temperatures in BRA, WIE and KRA landfill pilots.

Landfill pilot	Period	Temperature (°C)			
	Months	Min	Max	Mean	Median
BRA	Jan-Feb, Apr-May, Jul-Nov	-2 to 13	52 to 67	19 to 24	15 to 23
WIE	Jan, Mar-May, Nov-Dec	-1 to 9	25 to 55	13 to 20	13 to 18
KRA	Jan-Feb, Jun-Sep	-10 to 6	22 to 37	14 to 19	14 to 19

Bibliography

1. Brandstätter, C., Laner, D., & Fellner, J. (2015). Carbon pools and flows during lab-scale degradation of old landfilled waste under different oxygen and water regimes. Waste Management, 40, 100–111. https://doi.org/10.1016/J.WASMAN.2015.03.011
2. Brocker, C., & Kaiser, W. (2011). Feasibility study on sustainable emission reduction at the existing Braambergen landfill in the Netherlands. Specific report: Current status of the Braambergen landfill.
3. Brocker, C., Kaiser, W., Jurgen, K., & Ulrich, K. (2011). Feasibility study on sustainable emission reduction at the existing Braambergen landfill in the Netherlands. Specific report: Preliminary design and cost- estimate of the techni cal measures to enhance stabilisation with the DEPO+ process at the Braamberg.
4. Cruz, C., & Lammen, H. (2023). Landfill gas stabilization by aeration: initial insights following design and operational adjustments. www.cisapublisher.com
5. Cruz, C., Lammen, H., & Oonk, H. (2021). Sustainable landfill management: carbon removal in two aerated landfills.
6. Dijkstra, J. J., & Van Zomeren, A. (2019). Geochemische Karakterisering IDS stortplaatsen: Locaties Kragge, Braambergen en Wieringermeer [Geochemical Characterization of IDS landfills: Locations Kragge, Braambergen and Wieringermeer].
7. Gronert, R., Meijer, L. M. G., & Oonk, H. (2014a). Voortgangsresultaten nulonderzoek introductie duurzaam stortbeheer (IDS): Stortlocatie Braambergen [Progress results of the baseline study on the introduction of sustainable landfill management (IDS): Braambergen landfill site] (Issue November).
8. Gronert, R., Meijer, L. M. G., & Oonk, H. (2014b). Voortgangsresultaten nulonderzoek introductie duurzaam stortbeheer (IDS): Stortlocatie Wieringermeer [Progress results of the baseline study on the introduction of sustainable landfill management (IDS): Wieringermeer landfill site] (Issue November). https://www.duurzaamstortbeheer.nl/projectstukken/
9. Kanen, A. C., & Kedzia, S. (2021). Voortgangsrapportage iDS Kragge [Progress report iDS Kragge]. https://www.duurzaamstortbeheer.nl/projectstukken/
10. Lammen, H., & Scharff, H. (2018). Addendum deelplannen van aanpak iDS pilots Braambergen , Kragge en Wieringermeer. Monstername, voorbehandeling en analyse van vast afval [Addendum to the sub-plans for the iDS pilot projects in Braambergen, Kragge, and Wieringermeer. Sampling, pretreatment, and analysis of solid waste].
11. Lammen, H., Scharff, H., Oonk, H., Heimovaara, T., & Comans, R. (2021). Voortgangsrapportage Braambergen September 2017 - Mei 2020 [Progress report Braambergen Septembre 2017 - March 2021] (Vol. 2, Issue October 2020). https://www.duurzaamstortbeheer.nl/projectstukken/
12. Lammen, H., Scharff, H., Oonk, H., Heimovaara, T. J., & Comans, R. N. J. (2020). Voortgangsrapportage Wieringermeer Augustus 2017 - Mei 2020 [Progress report Wieringermeer August 2017 - March 2021] (Vol. 2). https://www.duurzaamstortbeheer.nl/projectstukken/
13. Meza, N., Lammen, H., Cruz, C., Heimovaara, T., & Gebert, J. (2022). Spatial Variability of Gas Composition and Flow in a Landfill Under in-Situ Aeration. Detritus, 19, 104–113. https://doi.org/10.31025/2611-4135/2022.15191
14. Morello, L., Raga, R., Sgarbossa, P., Rosson, E., & Cossu, R. (2018). Storage potential and residual emissions from fresh and stabilized waste samples from a landfill simulation experiment. Waste Management, 75, 372–383. https://doi.org/10.1016/J.WASMAN.2018.01.026
15. Oonk, H. (2014). Voortgangsresultaten Nulonderzoek Ids De Kragge 2 [Progress results baseline survey De Kragge 2] (Issue June).
16. Oonk, H. (2020). Afvalmonstername en analyse bij de nulmeting van de iDS-pilots [Waste sampling and analysis during the baseline measurement of the iDS pilots].
17. Reinhart, D., Joslyn, R., & Emrich, C. T. (2020). Characterization of Florida, U.S. landfills with elevated temperatures. Waste Management, 118, 55–61. https://doi.org/10.1016/j.wasman.2020.08.031
18. Straathof, A. L., Chincarini, R., Comans, R. N. J., & Hoffland, E. (2014). Dynamics of soil dissolved organic carbon

pools reveal both hydrophobic and hydrophilic compounds sustain microbial respiration. Soil Biology and Biochemistry, 79, 109–116. https://doi.org/10.1016/j.soilbio.2014.09.004

19. TAUW. (2011). Validatie van het nationale stortgas emissiemodel (Issue april).
20. van Meeteren, M., van Vossen, W., & Heyer, K. U. (2009a). Feasibility study pilot project sustainable emission reduction at the existing landfills in the Netherlands. Preliminary design and cost-estimate of the technical measures infiltration and aeration to enhance stabilization at the landfill Kragge. (Issue March). http://duurzaamstorten.nl/wawcs0122291/Publications.html
21. van Meeteren, M., van Vossen, W. J., & Heyer, K. U. (2009b). Feasibility study sustainable emission reduction at he existing landfills in the Netherlands, specific report: Preliminary design and cost-estimate of the technical measures infiltration and aeration to enhance stabilization at the landfill Wieringermeer (Issue March). http://duurzaamstorten.nl/wawcs0122291/Publications.html
22. Van Raffe, F., Dijkstra, J. J., & Comans, R. N. J. (2025). Mechanisms controlling the release of inorganic contaminants, organic matter fractions, and ammonium from solid landfill waste: pH dependent leaching experiments and geochemical modelling. Applied Geochemistry, 190. https://doi.org/10.1016/j.apgeochem.2025.106503
23. Van Raffe, F., Quist, N., Kanen, T., & Comans, R. N. J. (2023). Sustainable landfill management in the Netherlands: Long term changes in landfill leachate quality during (an)aerobic in-situ stabilization. 19Th International Symposium on Waste Management, Resource Recovery and Sustainable Landfilling, 2023.
24. van Vossen, W., van Meeteren, M., Timens, D., & Heyer, K. U. (2009). Feasibility study sustainable emission reduction at the existing landfills Kragge and Wieringermeer in the Netherlands. Specific report: Current state of the landfill Kragge. (Issue March). http://duurzaamstorten.nl/wawcs0122291/Publications.html
25. Van Zomeren, A., & Comans, R. N. J. (2007). Measurement of humic and fulvic acid concentrations and dissolution properties by a rapid ratch procedure. Environmental Science and Technology, 41(19), 6755–6761. https://doi.org/10.1021/es0709223
26. Vereniging Afvalbedrijven. (2014a). Deelplan van Aanpak verduurzamingspilot op stortplaats Braambergen [Subplan of approach sustainability pilot at Braambergen landfill] (Issue December). https://www.duurzaamstortbeheer.nl/projectstukken/
27. Vereniging Afvalbedrijven. (2014b). Deelplan van Aanpak verduurzamingspilot op stortplaats Wieringermeer (Issue December).
28. Vereniging Afvalbedrijven. (2015a). Deelplan van aanpak verduurzamingspilot op stortplaats De Kragge 2 [Partial plan of approach for sustainability pilot at the De Kragge 2 landfill] (Issue April). https://www.duurzaamstortbeheer.nl/projectstukken/
29. Vereniging Afvalbedrijven. (2015b). Project plan Sustainable Landfill Management Braambergen (Issue November).
30. Vereniging Afvalbedrijven. (2015c). Project plan Sustainable Landfill Management De Kragge 2. (Issue November). https://www.duurzaamstortbeheer.nl/projectstukken/
31. Wu, S. J., Zheng, Q. T., Zhao, Y., & Feng, S. J. (2023). Prediction and control of elevated temperatures within landfills under aeration and recirculation based on the thermal non-equilibrium model. Journal of Environmental Management, 345, 118873. https://doi.org/10.1016/J.JENVMAN.2023.118873

3

Spatial Variability of Gas Composition and Flow in a Landfill Under In-Situ Aeration

Abstract

In-situ aeration of landfills accelerates biodegradation of waste organic matter and hence advances waste stabilization. The spatial outreach of aeration greatly affects stabilization efficiency. This study analyzed the spatial variability of gas composition and flow in 230 wells spread over four compartments of a Dutch landfill which is under in situ aeration since 2017, as well as the carbon extraction efficiency, temperature, and settlement. Flow rates and gas composition in the extraction wells varied strongly. The highest variability was observed in the compartment with the highest water tables with submerged filter screens for most wells, with low flow rates, and elevated ratios of CH_4 to CO_2, indicating predominance of anaerobic processes (compartment 11Z). The compartment with the most uniform distribution of gas flow rates, composition and lower ratios of CH_4 to CO_2, suggesting a significant share of aerobic carbon mineralization, also showed higher temperatures, a carbon extraction efficiency, and larger cumulative settlement, all indicative of enhanced microbial activity (compartment 11N). In this compartment, the amount of extracted carbon exceeded the carbon generation predicted from landfill gas modeling by the factor of 2 over the hitherto four years aeration. The effect of water tables on gas flow and the correlation between the flow, and the ratio of CH_4 to CO_2 appeared weak, indicating that also other factors than water tables influence gas concentration and flow. Future work includes stable isotope probing to analyze the significance of microbial respiration and microbial CH_4 oxidation for the composition of the final extracted gas mixture.

This chapter was published in Meza et al. (2022)

3.1. Introduction

In-situ aeration is considered a possible method for the stabilization of landfills, reducing waste reactivity and the landfill's emission potential faster than under anaerobic conditions and therefore also reducing the time for monitoring during aftercare (Erses et al., 2008; Grossule & Stegmann, 2020; Ritzkowski et al., 2006). On a field scale, an important factor for the efficacy of treatment by in-situ aeration is the spatial distribution of air and gas throughout the waste body (van Turnhout et al., 2020), controlling (a) the reduction of the remaining methane production potential, (b) the desired increase in organic matter decay by microbial respiration and (c) the extent of methane oxidation within the landfill fulfill. However, homogeneous aeration on a field scale is a challenge not easy to reach (Ritzkowski & Stegmann, 2012), and is mainly limited by zones of water saturation and preferential liquid flow paths (Fellner & Brunner, 2010; Hrad et al., 2013). The spatial distribution of gas flow also depends on the operational conditions of aeration. For example, a model developed to find an optimal aeration strategy in a landfill indicated that air injection reaches a larger volume fraction of waste with higher airflow, but extraction appears to achieve a more homogeneous distribution of oxygen throughout the waste body (van Turnhout et al., 2020). Most of the in-situ aeration strategies use low-pressure aeration, which usually considers pressure within the range of 20-80 mbar (Ritzkowski & Stegmann, 2012). For optimal performance of in-situ aeration, the permeability of the waste body to both gas and water has to be considered (Ritzkowski & Stegmann, 2012; Xu et al., 2020).

Within the Dutch sustainable landfilling program iDS (Sustainable Landfill Foundation, n.d.), four compartments of the landfill Braambergen located near the city of Almere (The Netherlands), have been aerated since September 2017 (Cruz et al., 2021; Lammen et al., 2019, 2021). The waste comprises mainly soil and soil decontamination residues and around 15% of organic waste (more detail in Chapter 2, Section 2.4). Two different aeration strategies were employed: over-extraction and combi-aeration (low-pressure aeration). The over-extraction method creates a suction pressure by extracting more gas than gas produced, thereby causing ambient air to intrude into the landfill. Low-pressure aeration combines air injection and gas extraction considering lower pressure for injected air than extracted gas (Vereniging Afvalbedrijven, 2015). This paper researches the spatial variability of landfill gas composition and flow under the operational conditions of combi-aeration. It was hypothesized that based on the variability of the water tables detected in the injection-extraction wells (Gebert et al., this issue), neither the flow of the extracted gas nor the flow of the injected air is distributed uniformly. Consequently, the enhancement of biodegradation would differ spatially, and this would be reflected in the landfill gas (LFG) composition. To better understand which factors cause this spatial variability, data on gas composition was combined with data on gas flow rates and water columns in all compartments. The ratio of CH_4 to CO_2 was used to assess the spatial variability of the impact of aerobic and anaerobic processes on the measured gas composition. Further, this study analyzes the temporal variability of carbon extraction efficiency, temperature, and settlement for the

period 2017-2020. It was hypothesized that compartments with higher aeration efficiency would show a higher carbon extraction efficiency, higher temperatures in relation to higher biodegradation rates, and higher settlement rates.

3.2. Materials and Methods

3.2.1 Description of site and aeration system

The Braambergen landfill is located near the city of Almere in the northern part of the Netherlands, with the four pilot compartments 11North (11N) and South (11Z) and 12 East (12O) and West (12W) in operation from 1999 to 2008 on a surface area of approximately 10 ha. The pilot compartments contain around 1,200,000 tons of waste, mainly composed of soil and soil decontamination residues (80.6%) (Cruz et al., 2021; Lammen et al., 2019). Figure 3.1 shows a timeline of landfilling considering the different compartments and the main waste components, including soil and soil decontamination residues, construction and demolition waste, commercial waste, shredder, street cleansing waste, coarse household waste, sludge, and household waste. Compartments 12O and 11Z comprise mainly soil and soil decontamination residues (95.8%) and are approximately the same age. The oldest compartment is 12W and has the lowest percentage of soil and soil decontamination residues. This compartment together with compartment 11N are the ones that were filled with commercial waste and household waste (2.7% for compartment 11N). Compartment 11N is also the one with the longest active landfilling period.

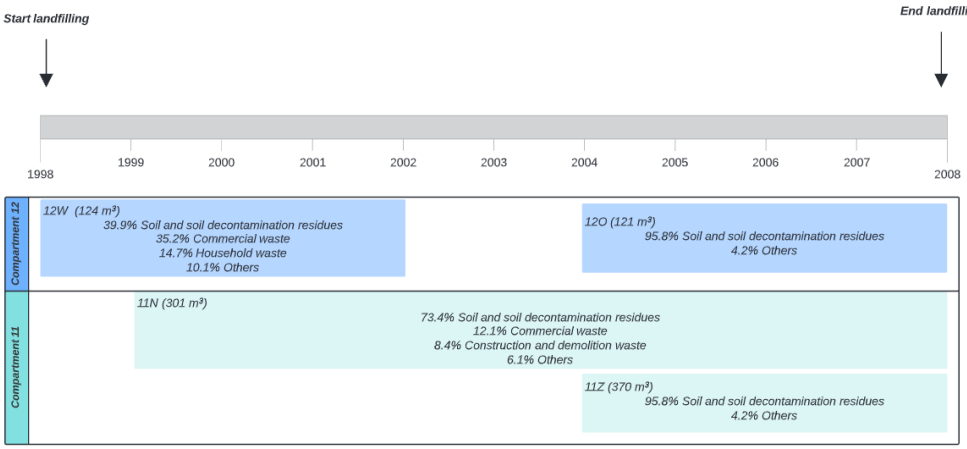

Figure 3. 1. Timeline of waste landfilling per compartment.

Landfill stabilization through in-situ aeration is carried out since September 2017. A network of 230 wells spaced at 15 to 20 m distance over the four compartments (Figure 3.2, left) can be operated in an over-extraction or combi-aeration mode (Figure 3.2, lower right). From north to south, each aeration line is denoted by a letter (A to W), and from west to east, each well by a number (1 to 8-11) (Figure 3.2, top right). All wells are deep filtered with the

filter screen over a height of 1.8 m from the bottom of the well, which has been inserted to a total depth of up to 10-12 m below the landfill surface, corresponding to approximately 2 m below the Amsterdam Ordnance Datum (NAP) into the waste body.

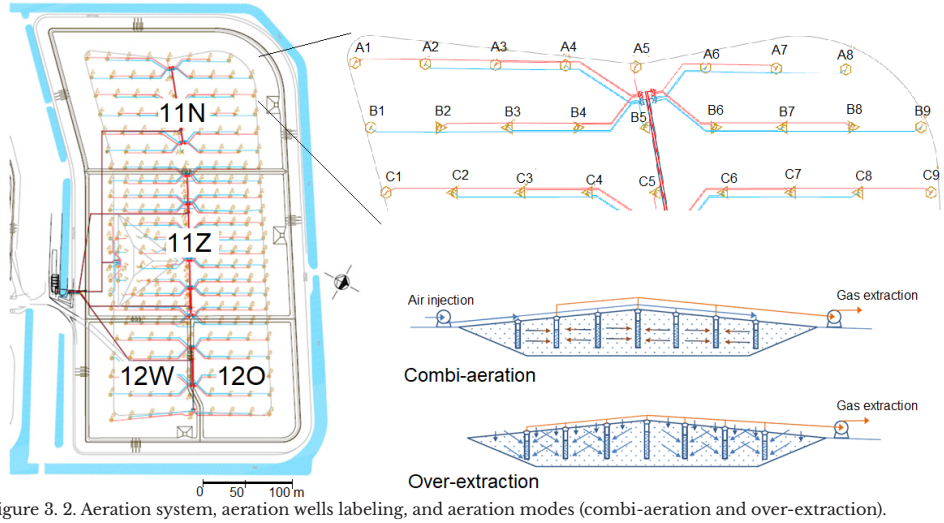

Figure 3. 2. Aeration system, aeration wells labeling, and aeration modes (combi-aeration and over-extraction).

3.2.2 Data acquisition, selection and processing

Flow velocity and temperature (multifunctional handheld unit, Höntzsch U426, TA-10 probe), gas composition (Geotech Gas Analyzer GA2000; detection limit 0.1%), and the pressure (pressure gauge by Blue line S4600) were measured manually on a monthly interval. At the gas blower station, landfill gas (LFG) flow rate (Proline Prosonic Flow B 200 Ultrasonic flowmeter for gas extraction, and Proline 65i T-mass flowmeter for air injection; both Endress+Hauser), pressure (PMC51-R8K2/0; Endress+Hausser), gas composition (CH_4, CO_2, and O_2, Biotech Gas Analyzer 3000), and temperature (iTEMP TMT181; Endress+Hauser) were continuously measured and recorded every fifteen minutes. The data from the gas blower station with the same collection time as the individual well sampling was selected for analysis. To obtain the flow rate for each well, the normalized flow (at standard temperature and pressure) from the gas extraction blower were averaged over the period in which the manual measurements were carried out, then divided by the individual wells in proportion to the velocity measured at each well. This study presents data from March 2020.

Using Python, MS Excel, and Origin software packages, the spatial variability of gas composition, flow, and water columns were visualized and analyzed. Based on the gas composition and the ratio of CH_4 to CO_2, the percentage of anaerobic activity (PAA) was calculated for each well (Yazdani et al., 2010) as follows:

$$PAA=(2[CH_4])/(2[CH_4]+([CO_2]-[CH_4])) \times 100 \quad (1)$$

Where $[CH_4]$ and $[CO_2]$ are the measured concentrations (% v/v) of CH_4 and CO_2. PAA was

then normalized to the maximum observed value to obtain the normalized anaerobic activity. The difference of 1 was considered as the normalized aerobic activity (NAA, Eq. 2):

$$NAA = 1- PAA/PAA_{max} \quad (2)$$

Where PAA_{max} is the highest percentage of anaerobic activity.

The coefficient of variation for gas composition and flow was calculated by dividing the standard deviation and the mean for all the datasets in each compartment. The spatial variability was analyzed using the Rijks-Driehoek (RD) coordinate system from the Dutch Geographical service in EPSG projection 28992 (Amersfoort datum). The relationship between the individual parameters was tested using Pearson's coefficient r. The number of observations, the variability of the parameters, and the confidence level determined the significance of this correlation.

Using the ideal gas law, the gas concentration, flow, pressure, and temperature, the extracted carbon in kilograms of carbon per hour was calculated. The carbon extraction efficiency was calculated using the amount of extracted carbon normalized to the number of wells and tons of waste in each compartment.

The temperature in compartments 11N and 11Z was obtained using a Silixa Ultima XT-DTS distributed temperature sensor which performed a double-ended measurement every 0.5 m using a long section of glass fiber distributed over 12 wells in each compartment (11N and 11Z) between -2 m and 9 m with respect to the NAP. For data configuration and collection, Silixa software was used. The height of the landfill surface and hence landfill settlement was measured twice per year on a network of 43 settlement beacons distributed over the four compartments using a TRIMBLE R8-2 rover GNSS Receiver.

3.3. Results and Discussion

The following sections present the spatial variability of CH_4 concentrations, the ratios between CO_2 and CH_4, methane and total gas flow rates, and temperature in the individual wells. Gas-related parameters are only taken into account for the 110 wells that are operating in extraction mode during simultaneous air injection and gas extraction on alternative wells (combi-aeration) in March 2020.

3.3.1 Variability of gas composition

The CH_4 concentration in aeration wells of the compartments 11N, 11Z, 12W, and 12O of Braambergen landfill in March 2020 was not spatially uniform, with the largest range observed in compartments 11N, 11Z, and 12O (Figure 3.3). In those three compartments, CH_4 concentration varied between close to zero and higher than 40%. High CH_4 concentrations are related to anaerobic waste degradation processes, whereas low CH_4 concentrations are related to CH_4 oxidation processes, as well as to non-existent or reduced (anaerobic) landfill gas formation, for example as a result of aeration. Little information is available from the

literature regarding the variability of CH_4 concentrations in waste bodies. However, high variability in CH_4 concentrations in 90 cm depth of an old municipal solid waste landfill (Röwer et al., 2011) have been reported, and the high variability of surface CH_4 emissions is well known (Giani et al., 2002; Mønster et al., 2019; Rachor et al., 2013; Spokas et al., 2003). As the spatial patterns in surface CH_4 emissions are not only impacted by the heterogeneity of waste composition and flow paths within the waste, but also by the variability of cover soil permeability. The comparability between the dynamics of the waste body's gas phase and surface emission is limited.

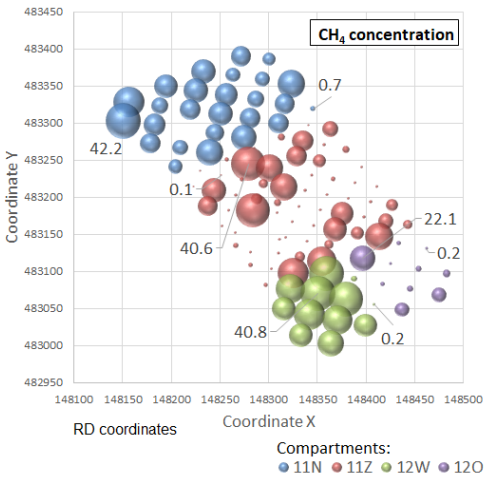

Figure 3.3. Spatial distribution of CH_4 concentration (vol.%) in the extraction wells - March 2020. The size of the symbol is indicative of CH_4 concentration. Data in graph = exemplary CH_4 concentration.

The ratio of CH_4 to CO_2 and the normalized aerobic activity (NAA) in the extracted gas (Figure 3.4) provides information about the share of aerobic to anaerobic processes occurring in the waste body. In compartment 11N most of the wells produced more CO_2 than CH_4 (ratios CH_4:CO_2 below 1), indicating the dominance of aerobic activity in most of its wells compared to the other compartments. Aeration in this compartment is likely to be more efficient due to the lower water tables (Gebert et al., this issue), allowing for an increased level of aeration and therefore increased CO_2 production from both, respiration of waste organic matter and CH_4 oxidation. For an old municipal solid waste landfill, it showed that the onset of aeration led to a decline of the ratio of CH_4 to CO_2 to values below 1 in most of the control wells. However, in many of the monitoring wells, especially those intercepting the deeper layers, this ratio increased again after the three year aeration period was terminated, suggesting that the effect of aeration on waste stabilization was limited by the vertical distribution of the injected air and that therefore stabilization had not been completed (Hrad & Huber-Humer, 2017).

Compartment 11Z had the highest water tables and the largest spread with the ratios of CH_4 to CO_2 ranging between 0 and 7, and the NAA varied between 0 and 0.8, as was also

observed in compartment 12O. In compartment 12W most wells produced the same or higher concentration of CH_4 than CO_2, indicating a predominance of anaerobic waste degradation. This was consistent with the low aerobic activity found in 8 out of 12 wells (NAA<0.5, Figure 3.4 right). Overall aeration appeared to be most effective and uniform (Figure 3.5) in compartment 11N.

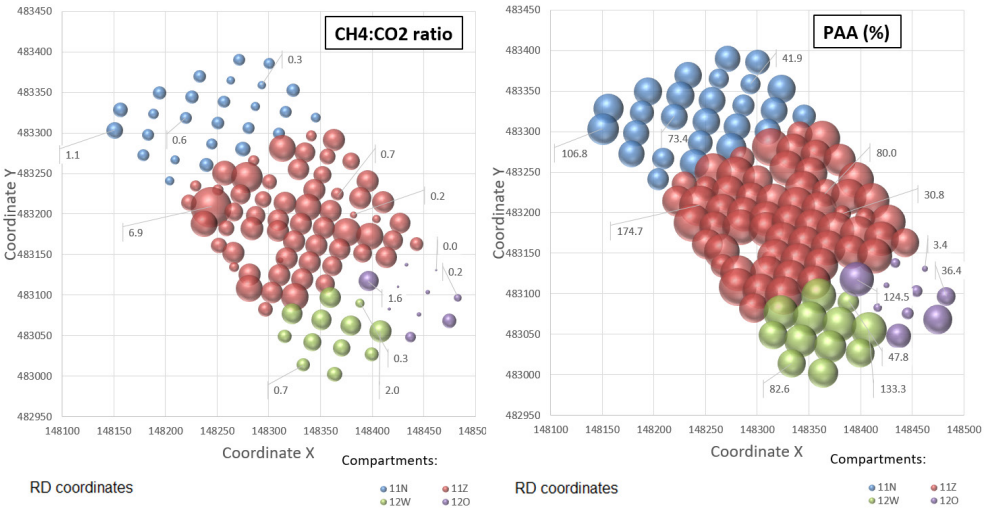

Figure 3.4. Spatial distribution of the ratio CH_4 to CO_2 in the extraction wells (left) and percent of anaerobic activity (right) - March 2020. The size of the symbol is indicative of the ratio CH_4 to CO_2. Data in graph = exemplary ratio CH_4 to CO_2.

The spatial distribution of CO_2 follows a similar behavior, with the highest variability in compartment 11Z (Figure 3.5). The fraction of CO_2 increases under conditions of aerobic waste degradation (respiration) compared to anaerobic conditions when also CH_4 is produced besides CO_2. On the other hand, the O_2 concentration in compartment 11Z was more homogeneous than other compartments, with a coefficient of variability of 0.3. Higher O_2 concentrations were found in compartment 11Z, with most of the values close to 21%, reflecting near-atmospheric concentrations. The fact that the extracted gas has a similar percentage of O_2 as the injected air suggests short-circuiting of atmospheric air along with the wells and consequently a reduced extent of aeration of the waste body in the area of influence of the well, likely maintaining the anaerobic conditions. In general, the N_2 concentration varies the least, in line with the fact that N_2 is non-reactive and therefore only affected by variability in transport processes. The observed spatial variability in the gas composition is likely to be closely related to water content and water tables in the landfill, increasing the resistivity to the airflow, hence limiting the aeration efficiency (Hrad et al., 2013).

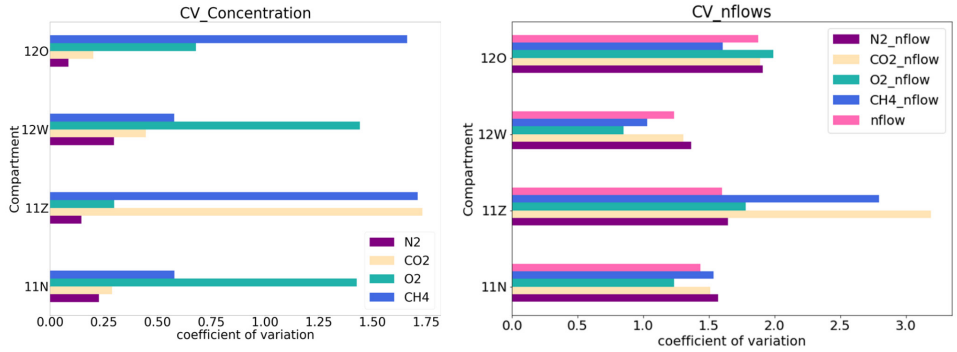

Figure 3.5. Coefficient of variation for the concentration of CH_4, CO_2, O_2, and N_2, and normalized aerobic activity (NAA) (left) and for flow rate, and flow rates of CH_4, CO_2, O_2, and N_2 in the gas extraction wells - March 2020.

Although the CH_4-CO_2-ratio and the calculated share of aerobic activity (NAA) give an estimation of aerobic activity, the contribution of the individual processes (respiration, CH_4 oxidation) to the final value is unclear and shall be further investigated using stable isotope probing that could elucidate the significance of anaerobic and aerobic processes for gas composition in the wells. Those wells producing a mixture significantly impacted by CH_4 oxidation should show enrichment in ^{13}C (Cabral et al., 2010; Chanton et al., 2008; Gebert & Streese-Kleeberg, 2017), whereas wells with low gas generation, or in wells where LFG is diluted by air short-circuiting, the isotopic signature of CH_4 should be similar to that of the original landfill gas.

3.3.2 Variability of gas flow

Compartment 11N showed both higher total flow rates and higher CH_4 flow rates (Figure 3.6). Gas flow rates in compartment 11Z were significantly lower, with 35 out of 64 wells showing no flow, presumably in connection with high water tables (Gebert et al., this issue). Compartments 12W and 12O seem to be more homogeneous despite the outliers in wells W2, W4, and S8. The spatial pattern of total flow rate and CH_4 flow rate is similar for compartments 11N and 11Z, but similarities are less for compartments 12W and 12O, in which some wells produce a high total flow rate at low CH_4 concentration and vice versa.

The variability of CH_4 flow rates was similar to the gas concentration variability in each compartment, i.e. compartments 11N and 12W showing a lower variability and compartments 11Z and 12O a higher variability (Figure 3.5). Considering the waste composition and age, the similarity in gas composition and flow between 11N and 12W and between 12O and 11Z was expected. The highest values for the variability of CH_4 and CO_2 flow rates and concentrations were found in compartment 11Z.

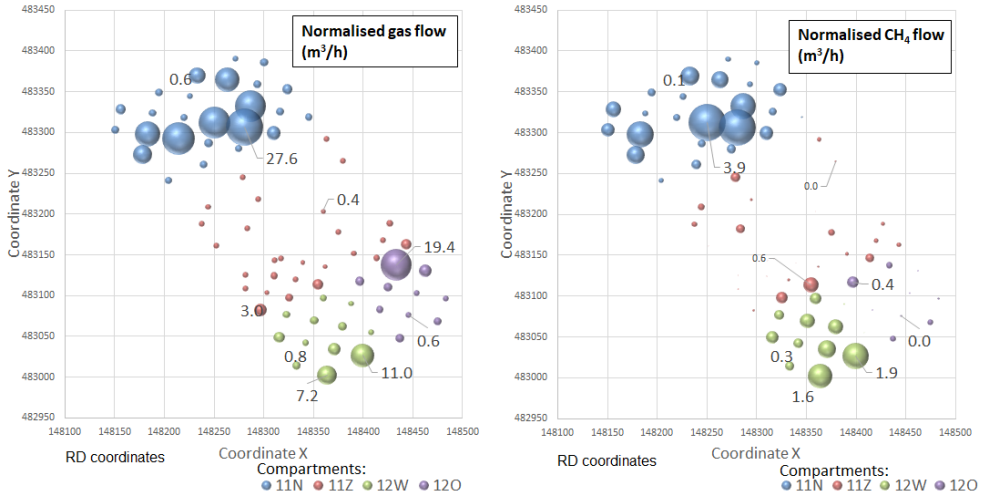

Figure 3.6. Spatial distribution of normalized flow rates (m³/h) (left) and CH_4 flow rates (right) - March 2020. The size of the symbol is indicative of (CH_4) flow rate. Data in graph = exemplary flow rates and CH_4 flow rates.

To analyze possible correlations between the flow rate (for conditions of flow > 0) and the ratio of CH_4 to CO_2 in the extraction wells, Pearson's coefficient was calculated. In the case of airflow limiting the aerobic processes, an inverse correlation should be visible, i.e. higher flow rates correlating with higher CO_2 concentrations and therefore a lower ratio of CH_4 to CO_2 in extracted gas. On a confidence level of 99.95%, the flow and the ratio of CH_4 to CO_2 for the total dataset (n=73) were indeed negatively correlated (-0.23), albeit on a low level. With some variation between the compartments (12W: n=12, -0.74; 12O: n=10, 0.01; 11N: n=24, -0.29; 11Z: n=27, -0.10) indicating that the relationship between the two parameters is confounded, for example, by short-circuiting or near-well differences in waste permeability and hence efficiency of aeration.

The gas prognosis for the aeration pilot (total of all four compartments), carried out with the Afvalzorg Multiphase Model (available from https://www.afvalzorg.com/landfill-gas/lfg-models), estimated the total carbon generation (CH_4-C + CO_2-C) of ~1010 t C for the years 2017 to 2020 if the compartments would not have been aerated (Table 3.1). Overall compartments, the extracted C exceeded this estimate by a factor of 1.5. A more detailed look at predicted C generation versus realized C extraction reveals that for the wells aerated in compartment 11N, showed the highest C extraction efficiency and highest cumulative settlement, 436 t C more were extracted than predicted to be generated, increasing the factor to > 2, while C extraction in the other compartments remained more or less in the order of magnitude of predicted (anaerobic) C generation. C generation was only modeled for compartment 12 as a whole; hence it is possible that the higher C extraction efficiency calculated for 12W was masked by the less efficient compartment 12O.

While the measured C extraction is deemed accurate, gas generation modeling is subject to

high uncertainty (e.g., Scharff & Jacobs, 2006). For example, due to often insufficient data on the waste composition and/or model assumptions on the degradable fraction or kinetic parameters that do not match the deposited waste. The comparison of absolute differences between predicted C generation and extracted C should thus be undertaken with caution. Further, the extracted carbon relates strictly to the gas phase and does not include carbon released from waste biodegradation that leaves the waste body as dissolved organic or inorganic carbon with the leachate. Adding this fraction would increase the share of carbon released in comparison to the predicted carbon generation (landfill gas modeling).

Table 3.1: Predicted average landfill gas generation and measured average landfill gas extraction for 2017-2020.

Compartment	Predicted cumulative carbon generation (CH_4-C + CO_2-C) 2017-2020 (tons C)	Measured cumulative carbon extraction (CH_4-C + CO_2-C) 2017-2020 (tons C)
11N	382.36	817.82
11Z	193.01	291.60
12W + 12O	435.12	398.87
Total	1010.48	1508.29

3.3.2.1 Effect of water tables on gas flow

Analysis of the spatial distribution of water tables over the four compartments showed that most of the wells in compartment 11Z have water tables over the screened part of the aeration well (1.8 m; Gebert et al., this issue). Compartment 11Z is also the one with lower flow rates, higher variability in CH_4 concentrations, and higher ratios of CH_4 to CO_2 (Figures 3.3 to 3.6), the latter two suggesting a higher share of anaerobic processes.

The water tables in the waste impede landfill gas and airflow through the wells. It is expected to have a decrease in the flow while the water table gets closer to the top of the screening part of the aeration well. Figure 3.7 on the far right shows the theoretical relationship between gas flow and height of the water table in the wells, given the location of the filter screen in the lower 1.8 m. For all compartments, the outer boundary of the data approximates this relationship. However, in all compartments also lower gas flow rates were measured than would have been expected from the observed water table, indicating that other factors than the height of the water table, such as the (variable) permeability of the surrounding waste body (Gebert et al., this issue; Xu et al., 2020) also impact aeration efficiency. This was especially pronounced for compartment 11Z in which a high number (98 out of 132 wells) of 'no flow' wells were detected. It can also be seen that the magnitude of gas flow varied per compartment, with at comparable pressures compartment 11N achieving the highest gas velocities.

3.3.3 Temporal variability of carbon extraction efficiency, temperature and settlement

As seen from Figure 3.6 (data for March 2020), compartment 11N showed higher carbon flow rates than the other three compartments. To analyze whether this enhanced performance is consistent over time, the carbon extraction efficiency (carbon flux per compartment

normalized to the number of wells and waste volume), waste temperature, and cumulative settlement were analyzed. The carbon extraction efficiency was calculated for the four compartments from the beginning of the aeration in 2017 to 2020 (Figure 3.8). It is seen that, plausibly, the compartment with the higher aeration efficiency, i.e. the higher share of aerobic processes (PAA, Figure 3.4) also showed by far the highest carbon extraction efficiency. Compartment 12W showed the second highest carbon extraction efficiency, followed by 11Z and 12O, reflecting the order already seen from the CH_4 flow (Figure 3.6, right). The differences between the compartments were consistent over the four years since the onset of aeration in 2017.

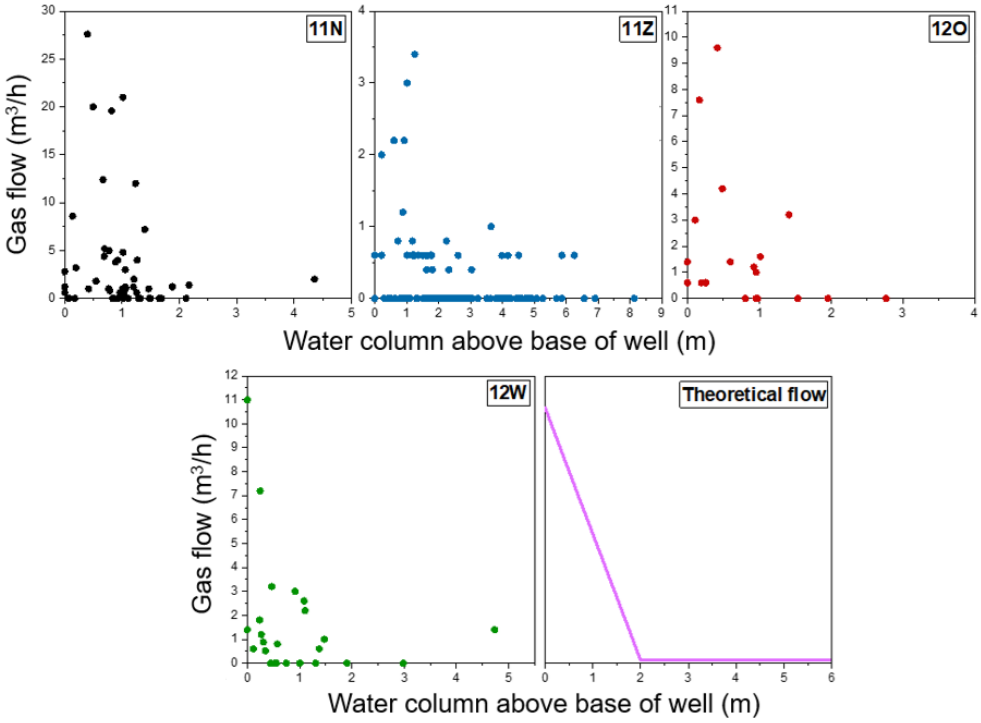

Figure 3.7. Measured normalized gas flow in relation to the height of the water table above the base of the well for compartments 11N, 11Z, 12O, and 12W, expected relationship (far right).

Figure 3.9 shows the temperature in compartments 11N and 11Z at +9 m, +6 m, +2 m, and -2 m with respect to the NAP. The landfill surface is between +8 m to +10 m NAP, hence the temperature at +9 m NAP reflects near-surface effects in the landfill, showing the expected seasonal variability with lower temperatures at the beginning of the year and higher temperatures during summer (Figure 3.9, top left). In the underlying layers, the temperature is influenced by processes within the waste body. The higher aeration efficiency and hence the higher carbon removal efficiency in compartment 11N, as discussed above, reflects clearly the higher waste temperatures due to enhanced biodegradation rates, releasing more heat. Although both compartments are filled with approximately the same

amount of waste (11N: 300,637 m³, 11Z: 370,110 m³), they differ slightly with respect to waste composition: 11N contains almost 20% of waste with potential organic material in it, compared to the only 2.93% in 11Z. This waste body includes commercial waste (11N: 12.1%; 11Z: 2.3%), shredded waste (11N: 2.2%; 11Z: 0.33%), street waste (11N: 0.2%; 11Z: 0.0%), coarse household waste (11N: 0.5%; 11Z: 0.28%), sludge (11N: 0.4%; 11Z: 0.02%) and household waste (11N: 2.7%; ; 11Z: 0.0%), suggesting a higher potential for microbial degradation of waste organic matter. It is likely, however, that the difference in aeration efficiency and therefore the difference in temperature is due to the differences in water tables (Figure 3.7), limiting aeration efficiency in compartment 11Z.

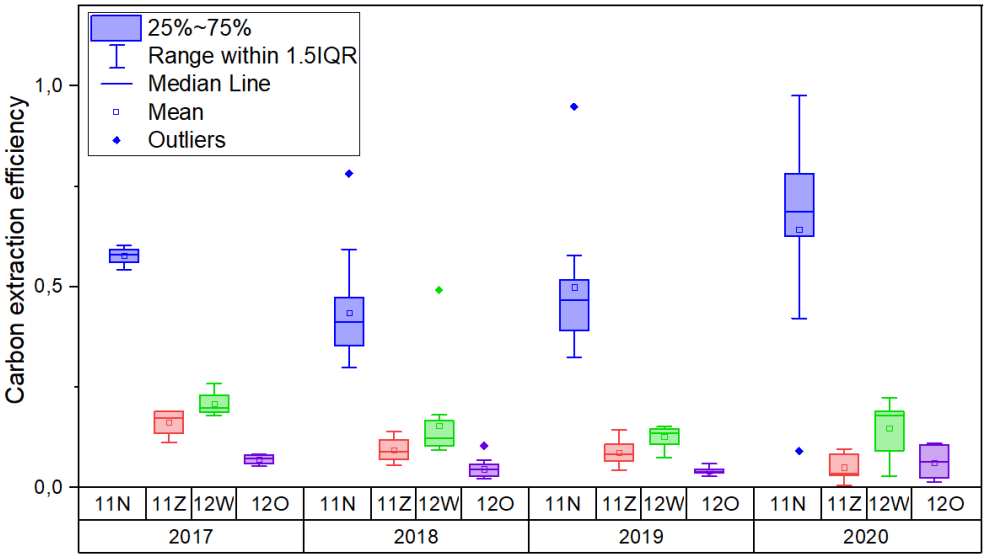

Figure 3.8. Carbon extraction efficiency for compartments 11N, 11Z, 12O, and 12W over the years 2017- 2020.

The cumulative settlement with respect to the first measurement (2017) until 2020 is shown in Figure 3.10. In line with the increased extent of aeration and increased carbon extraction efficiency, compartment 11N stood out with the highest cumulative settlement of on average 0.3 m in the period 2017-2020. Also, the range of cumulative settlement in 11N increased over time, indicating that individual areas are subject to higher biodegradation rates than others.

The higher carbon extraction efficiency, temperature, and cumulative settlement suggest a higher microbial activity in compartment 11N, which corroborates the better performance of the aeration system, evidenced by a higher share of CO_2 in the extracted gas compared to CH_4, higher flow rates, lower water tables and higher amount of organic waste.

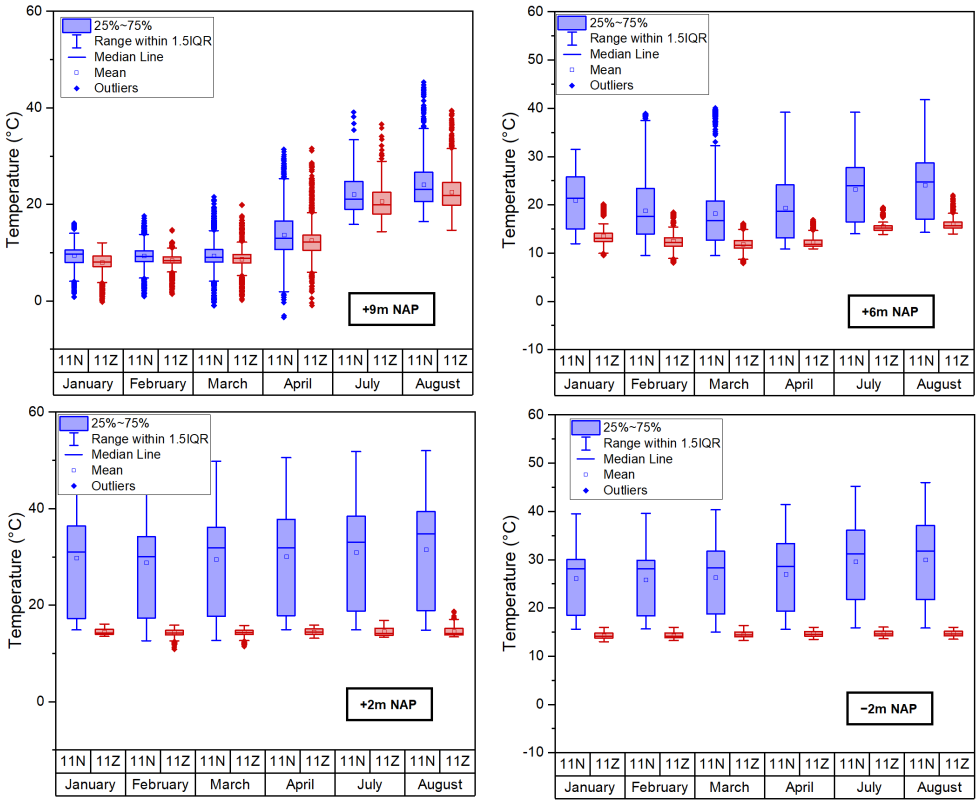

Figure 3.9. Temporal variability in temperature at +9m NAP (top left), +6m NAP (top right), +2m NAP (down left), -2m NAP (down right) – January-August 2020.

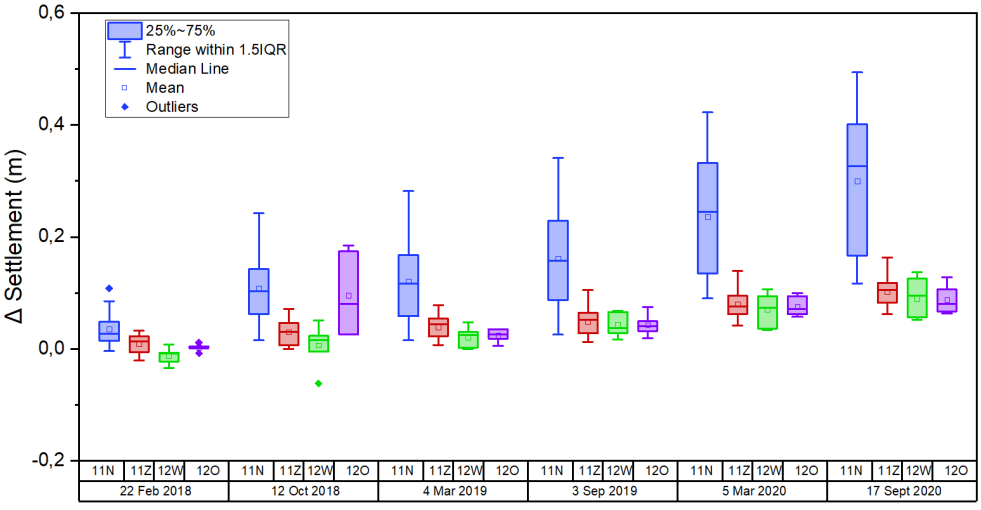

Figure 3.10. Cumulative settlement for compartments 11N, 11Z, 12O, and 12W over the years 2017 to 2020.

3.4. Conclusion & Outlook

The dense network of wells installed for in-situ aeration of four compartments of the Braambergen landfill provided a unique opportunity to study the small-scale spatial variability of gas flow, composition, and water columns in the wells. So far, the following conclusions can be drawn:

- Gas composition and gas flow rates are subject to high spatial variability, both within one compartment and between compartments.
- Particularly in compartment 11Z, considerable perched water tables, impede gas flow and hence aeration efficiency, as also from high ratios of CH_4 to CO_2, indicating predominantly anaerobic conditions. This is consistent with the estimated low aerobic activity. However, high water columns alone can not explain the difference in flow rates. Other factors need also to be considered such as the spatial variability of the gas permeability within the waste body.
- The detected short-circuiting of atmospheric air along wells will limit the efficient aeration of the zone of influence of the respective well.
- The highest difference between the measured cumulative C extraction and the predicted cumulative C generation (by landfill gas modeling) between 2017 and 2020 was found in compartment 11N, with more than double the extracted carbon with respect to the predicted value.

Higher aeration efficiency (11N) enables higher organic matter degradation, evidenced by higher carbon extraction efficiency, higher temperature, and higher cumulative settlement. Future investigations will include liquid and gas tracer tests to analyze the spatial variability of permeability within the waste package and the sphere of influence of the aeration wells. Further, stable isotope probing of the gas in the aeration wells will be carried out to identify wells influenced by processes of CH_4 oxidation, respiration, anaerobic landfill gas production, and dilution.

Bibliography

1. Cabral, A. R., Capanema, M. A., Gebert, J., Moreira, J. F., & Jugnia, L. B. (2010). Quantifying microbial methane oxidation efficiencies in two experimental landfill biocovers using stable isotopes. Water, Air, and Soil Pollution, 209(1–4), 157–172. https://doi.org/10.1007/s11270-009-0188-4
2. Chanton, J. P., Powelson, D. K., Abichou, T., & Hater, G. (2008). Improved field methods to quantify methane oxidation in landfill cover materials using stable carbon isotopes. Environmental Science and Technology, 42(3), 665–670. https://doi.org/10.1021/es0710757
3. Cruz, C., Lammen, H., & Oonk, H. (2021). Sustainable landfill management: carbon removal in two aerated landfills.
4. Erses, A. S., Onay, T. T., & Yenigun, O. (2008). Comparison of aerobic and anaerobic degradation of municipal solid waste in bioreactor landfills. Bioresource Technology, 99(13), 5418–5426. https://doi.org/10.1016/j.biortech.2007.11.008
5. Fellner, J., & Brunner, P. H. (2010). Modeling of leachate generation from MSW landfills by a 2-dimensional 2-domain approach. Waste Management (New York, N.Y.), 30(11), 2084–2095. https://doi.org/10.1016/j.wasman.2010.03.020
6. Gebert, J., Jong, T. De, Rees-white, T., Beaven, R., & Lammen, H. (2021). Spatial Variability of Leachate Tables , Leachate Composition and Hydraulic Conductivity in a Landfill Stabilized By in Situ Aeration.
7. Gebert, J., & Streese-Kleeberg, J. (2017). Coupling Stable Isotope Analysis with Gas Push-Pull Tests to Derive In Situ Values for the Fractionation Factor α_{ox} Associated with the Microbial Oxidation of Methane in Soils . Soil Science Society of America Journal, 81(5), 1107–1114. https://doi.org/10.2136/sssaj2016.11.0387
8. Giani, L., Bredenkamp, J., & Eden, I. (2002). Temporal and spatial variability of the CH4 dynamics of landfill cover soils. Journal of Plant Nutrition and Soil Science, 165(2), 205–210. https://doi.org/10.1002/1522-2624(200204)165:2<205::AID-JPLN205>3.0.CO;2-T
9. Grossule, V., & Stegmann, R. (2020). Problems in traditional landfilling and proposals for solutions based on sustainability. Detritus, 12, 78–91. https://doi.org/10.31025/2611-4135/2020.14000
10. Hrad, M., Gamperling, O., & Huber-Humer, M. (2013). Comparison between lab- and full-scale applications of in situ aeration of an old landfill and assessment of long-term emission development after completion. Waste Management, 33(10), 2061–2073. https://doi.org/10.1016/j.wasman.2013.01.027
11. Hrad, M., & Huber-Humer, M. (2017). Performance and completion assessment of an in-situ aerated municipal solid waste landfill – Final scientific documentation of an Austrian case study. Waste Management, 63, 397–409. https://doi.org/10.1016/J.WASMAN.2016.07.043
12. Lammen, H., Cruz, C., & Scharff, H. (2021). Sustainable landfill management : leachate development in two aerated landfills.
13. Lammen, H., Van Zomeren, A., Dijkstra, J. J., & Comans, R. N. J. (2019). Sustainable landfill management: solid waste sampling and geochemical characterization prior to (an)aerobic stabilization of three old landfills. Proceedings Sardinia 2019, Seventeenth International Waste Management and Landfill Symposium, 11 pp.-11 pp.
14. Mønster, J., Kjeldsen, P., & Scheutz, C. (2019). Methodologies for measuring fugitive methane emissions from landfills – A review. Waste Management, 87, 835–859. https://doi.org/10.1016/J.WASMAN.2018.12.047
15. Rachor, I. M., Gebert, J., Gröngröft, A., & Pfeiffer, E. M. (2013). Variability of methane emissions from an old landfill over different time-scales. European Journal of Soil Science, 64(1), 16–26. https://doi.org/10.1111/ejss.12004
16. Ritzkowski, M., Heyer, K.-U., & Stegmann, R. (2006). Fundamental processes and implications during in situ aeration of old landfills. Waste Management (New York, N.Y.), 26(4), 356–372. https://doi.org/10.1016/j.wasman.2005.11.009
17. Ritzkowski, M., & Stegmann, R. (2012). Landfill aeration worldwide: Concepts, indications and findings. Waste Management, 32(7), 1411–1419. https://doi.org/10.1016/j.wasman.2012.02.020
18. Röwer, I. U., Geck, C., Gebert, J., & Pfeiffer, E. M. (2011). Spatial variability of soil gas concentration and methane oxidation capacity in landfill covers. Waste Management, 31(5), 926–934. https://doi.org/10.1016/J.WASMAN.2010.09.013

19. Scharff, H., & Jacobs, J. (2006). Applying guidance for methane emission estimation for landfills. Waste Management (New York, N.Y.), 26(4), 417–429. https://doi.org/10.1016/j.wasman.2005.11.015
20. Spokas, K., Graff, C., Morcet, M., & Aran, C. (2003). Implications of the spatial variability of landfill emission rates on geospatial analyses. Waste Management, 23(7), 599–607. https://doi.org/10.1016/S0956-053X(03)00102-8
21. Sustainable Landfill Foundation. (n.d.). Introducing Sustainable Landfill programme (iDS). Retrieved February 24, 2021, from https://duurzaamstorten.nl/en/
22. van Turnhout, A. G., Oonk, H., Scharff, H., & Heimovaara, T. J. (2020). Optimizing landfill aeration strategy with a 3-D multiphase model. Waste Management, 102, 499–509. https://doi.org/10.1016/j.wasman.2019.10.051
23. Vereniging Afvalbedrijven. (2015). Project plan Sustainable Landfill Management Braambergen (Issue November).
24. Xu, X. B., Powrie, W., Zhang, W. J., Holmes, D. S., Xu, H., & Beaven, R. (2020). Experimental study of the intrinsic permeability of municipal solid waste. Waste Management, 102, 304–311. https://doi.org/10.1016/j.wasman.2019.10.039
25. Yazdani, R., Mostafid, M. E., Han, B., Imhoff, P. T., Chiu, P., Augenstein, D., Kayhanian, M., & Tchobanoglous, G. (2010). Quantifying factors limiting aerobic degradation during aerobic bioreactor landfilling. Environmental Science and Technology, 44(16), 6215–6220. https://doi.org/10.1021/es1022398

4

Comparing modelled, recovered and generated carbon in three landfill pilots under in-situ stabilization

Abstract

Stabilization of landfilled waste can be enhanced by water recirculation, which re-moisturizes waste and stimulates microbial activity, or by aeration, which supplies oxygen and accelerates aerobic degradation. This chapter evaluates the effectiveness of these in-situ strategies in three Dutch landfill pilots: Kragge (KRA; water recirculation), Braambergen (BRA; aeration) and Wieringermeer (WIE; aeration). Carbon generation predicted by the 2022 NV Afvalzorg Multiphase Landfill Gas Model was compared with on-site carbon extraction and with laboratory gas production (anaerobic) and respiration (aerobic) tests.

Parallel incubations showed that aerobic carbon generation exceeded anaerobic generation by a factor of 4 in KRA, 7 in BRA and 8 in WIE, demonstrating the strong potential of aeration for accelerating stabilization. Sequential tests, in which aerobic conditions followed anaerobic degradation, further re-activated carbon release by 59–750%. After five years of stabilization, almost all anaerobically degradable organic carbon had been depleted in all pilots (carbon potential<10%). Aerated sites (BRA, WIE) also showed much lower aerobic carbon potential, indicating advanced stabilization, whereas KRA retained substantial amounts of aerobically degradable material.

Laboratory carbon generation far exceeded model predictions and on-site extraction, up to 20-fold higher than modelled and more than 80-fold higher than extracted in KRA, revealing large unrealized degradation potential in the field. In contrast, extracted carbon in the aerated pilots exceeded the modelled anaerobic baseline (BRA: 195%, WIE: 525%), highlighting the higher degradation efficiency of aeration. Short-term laboratory tests proved useful for predicting long-term carbon generation, though correlations were affected by waste heterogeneity and stabilization state.

The content of this chapter is based on a manuscript in preparation for publication in a peer-reviewed journal with coauthors Hans Lammen, Twan Kanen, Timo Heimovaara and Julia Gebert.

4.1. Introduction

Under aerobic conditions, microbial degradation of organic matter is enhanced by the availability of oxygen, leading to a faster breakdown of organic material and the production of carbon dioxide (CO_2) as the terminal carbon product. In contrast, anaerobic conditions result in the release of both methane (CH_4) and CO_2, with landfill gas typically composed of 55-60% CH_4 and 40-45% CO_2. Under anaerobic conditions, processes such as sulphate reduction can also generate gases. However, their contribution is negligible, as they occur at a much lower order of magnitude. In MSW landfills, average H_2S concentrations are typically below 50 ppb (Nunes et al., 2021; Yilmaz et al., 2021).

Methane can be recovered and used as an energy source (Kamalan et al., 2011), providing economic benefits for landfill operators. One method to assess the potential for recovering landfill gas is through a landfill gas model (Toha & Rahman, 2023), which utilizes site-specific information on waste inventory and deposition to estimate gas generation over time (Afvalzorg, 2022). Alternatively, laboratory incubation can be used to directly assess gas generation from waste and estimate the gas potential. Several studies have quantified gas production under aerobic and anaerobic conditions using both fresh waste and natural materials such as sediments (Brandstätter et al., 2020; Gebert et al., 2006, 2011, 2019; Ritzkowski et al., 2016; Zander et al., 2022).

The landfill pilots at Braambergen (BRA) and Wieringermeer (WIE) have been aerated since the end of 2017, while Kragge (KRA) has been treated by water recirculation since early 2018. After five years of stabilization, with an additional five years anticipated, it was of interest to assess the degree of stabilization in terms of carbon (CO_2-C and CH_4-C) generation. This chapter compares modelled carbon generation, reflecting the anaerobic base case (i.e., without the effects of aeration or water recirculation) with the carbon recovered on site and with carbon generation measured in laboratory incubations. Furthermore, we investigate the heterogeneity of the waste's carbon potential, defined as the total cumulative carbon released when time approaches to infinity, and its relation to various waste properties. This chapter is guided by the following questions:

RQ4.1. After five years of stabilization, what is the carbon potential under aerobic and anaerobic conditions in waste from the pilots? Are the aerated pilots more stable than the anaerobic pilot?

RQ4.2. How do different waste characteristics affect the kinetics of carbon generation by waste in the three pilots?

RQ4.3. To what extent do aerobic conditions increase carbon potential?

RQ4.4. How do the gas generation values predicted by the Afvalzorg multiphase model compare with those measured in laboratory and on-site extractions? How could any discrepancies be explained?

RQ4.5. To what extent do waste properties influence the biodegradability in waste from different pilots?

Guided by the research questions presented above, this chapter describes the degradation or mineralization of waste organic matter using various terms and parameters. While it is the organic matter that is microbially degraded, resulting in degradation or release of carbon as CO_2, CH_4 (gas phase) and as dissolved species, in this research the process is synonymously also referred to as "degradation of organic matter", with subsequent use of the terms "degradable organic carbon" or "degradability of organic carbon".

4.2. Materials, methods and boundary conditions

The description of the pilots can be found in Chapter 2. For comparison purposes, all carbon (CH_4-C, CO_2-C) generation using field measurements (recovered carbon), a model (modelled carbon) and measured in the laboratory (generated carbon) were normalised to dry waste weight. The water content considered for the recovered and modelled carbon was based on the measurements performed before the start of the stabilization (Chapter 2) with an average of $36\%_{dw}$ in BRA, $29\%_{dw}$ in WIE and $34\%_{dw}$ in KRA. The water content considered for the generated carbon measured in the laboratory was measured using a sub-sample of each incubation batch.

4.2.1. Estimation of carbon recovery using field gas measurements

At Kragge, the gas composition (CH_4, CO_2, and O_2, Biotech Gas Analyzer 3000) and gas velocity (handheld unit from KIMO, VT-100) in all compartments, including compartment 3, is measured monthly on individual gas wells. These gas wells are grouped into collection points (CPs), which are connected to a single pipe (Kragge 2). A similar system is used in Kragge 1 and the bulk gas from both is combined (Kragge) (Chapter 2, Figure 2.2). The mixed gas from each hill is routed to the gas station where the gas composition (CH_4, CO_2, and O_2, Biotech Gas Analyzer 3000) and flow (Prosonic Flow 200 from Endress +Hauser) are monitored and data stored every hour. The gas extraction pressure (GGW150 A4-U2 and a Barksdale D1X-M3SS-ex) is measured only in the combined bulk gas originating from the hills Kragge 1 and Kragge 2 (Table 4.1).

To calculate the landfill gas recovered from the specific section of the stabilization pilot KRA, the monthly measurements of gas composition and gas velocity on individual gas wells in the hill Kragge 2 for the year 2021 were used. To derive gas flow rates from the velocities measured on individual wells, the recovered bulk gas flow from the hill Kragge 2 was divided proportionally to the gas velocities in all the measured CPs and wells in the hill Kragge 2. Finally, 13 gas wells located in compartment 3 were selected and the number of moles was calculated as follow:

$$n_{An}=V \times ([G_{LFG}])/100 \times 1/MV \quad \text{(Eq. 1)}$$

Where n_{An} is the number of moles of gas in the anaerobic pilot (compartment 3), V the

landfill gas (LFG) volume (m^3) in the pilot, [G_{LFG}] is the average gas concentration (vol.%) of CH_4 or CO_2 measured in the LFG, and MV is the molar volume (L/mol) at 20°C.

The gas wells in the aerated pilots BRA and WIE are connected to a gas collection system exclusively extracting from the stabilization pilot compartments. Extraction lines from the individual wells are grouped and ultimately connected to a single extraction pipe leading to the gas blower station, where bulk gas flow (Proline Prosonic Flow B 200 Ultrasonic flowmeter for gas extraction, and Proline 65i T-mass flowmeter for air injection; both Endress+Hauser), pressure (PMC51-R8K2/0; Endress+Hauser), temperature (iTEMP TMT181; Endress+Hauser), and gas composition (CH_4, CO_2, and O_2, Biotech Gas Analyzer 3000) are monitored and the data stored every 15 minutes (Table 4.1). The number of moles of extracted CH_4 and CO_2 in both aerated pilots for the year 2023 was calculated based on the ideal gas law:

$$n = PV / RT \quad \text{(Eq. 2)}$$

Where n is the number of moles of CH_4 or CO_2 present in the gas phase, P is the pressure (Pa), V the LFG volume (m^3), R the universal gas constant (8.314463 m^3 Pa / K mol) and T is the temperature (K).

Using the number of moles (Eq. 1 and 2), the molar masses, the data on gas composition and the estimated landfill pilot water content (dry weight) the amount of carbon recovered (CH_4 + CO_2) per dry weight (dw) over the time were calculated.

Table 4.1. Yearly median pressure, flow rate and gas composition (CH_4, CO_2, and O_2) in three landfill pilots.

Landfill pilot	Measurement period	Median				
		Pressure (hPa)	Flow rate (m^3/h)	CH_4 (% Vol.)	CO_2 (% Vol.)	O_2 (% Vol.)
KRA	2021	-6.85*	*53.5***	43.4	27.4	0.8
BRA	2023	-33.6	*487.5*	4.3	13.9	*6.5*
WIE	2023	-38.3	*505.5*	7.2	15.6	*6.5*

*Measured in the bulk gas of Kragge
** Measured in the bulk gas in Kragge 2

4.2.2. Estimation of carbon generation using a model (anaerobic base case)

The NV Afvalzorg Multiphase Landfill Gas Model (Afvalzorg, 2022) is a first-order decay model developed by the Agricultural University of Wageningen in 1996 (Scharff & Jacobs, 2006). This model uses information such as the type and amount of waste that was landfilled over the years calculating the methane generation for a period of 100 years since the first year of disposal. It holds datasets for different low-organic waste categories such as mixed bulky waste (unrecyclable and incombustible), construction and demolition (C&D) waste, soil (contaminated with oil and other residues), shredder (shredded pieces of end-of-life vehicles or machines) waste, street cleansing (residues from street cleansing) waste, and refuse derived fuel (RDF).

The model is based on the TNO first-order model which estimates landfill gas production by modelling the degradation of organic carbon in waste. The Afvalzorg Multiphase Landfill Gas Model accounts for different degradable organic carbon (DOC_S) content across different waste types, recognizing that they degrade at different rates (Afvalzorg, 2022; Scharff & Jacobs, 2006). It applies IPCC mathematical principles and standard parameters to estimate annual carbon degradation, which is then used to calculate methane generation, recovery, oxidation, and emissions over time. The decay rate constants (k-values) are derived from default IPCC values but have been adjusted using field measurements from three Dutch landfills. Additionally, DOC_S values were refined based on Dutch waste composition analyses.

The latest version of the NV Afvalzorg Multiphase Landfill Gas Model (version 2022) aligns with the 2019 IPCC recommendations (IPCC, 2019) and incorporates three distinct fractions of degradable organic carbon dissimilation (DOCf) for low, moderately, and highly decomposable waste. These fractions reflect limitations to organic matter degradability due to (unfavourable) landfill conditions. In contrast, previous versions of the model used a single DOCf value (0.7). This update results in lower estimated methane generation compared to earlier models. The DOCf and k-values used in the 2022 NV Afvalzorg Multiphase Landfill Gas Model are provided in Table 4.2. This study utilizes this latest version of the model to estimate methane generation for the three pilots.

Table 4.2. Afvalzorg multi-phase model fractions of degradable organic carbon dissimilation (DOCf) and decay rate constants (k-values) per waste decomposability category (Afvalzorg, 2022).

Decomposability (-)	DOCf (-)	k-value (y^{-1})
High	0.7	0.187
Moderate	0.5	0.099
Low	0.1	0.030

The degraded carbon (kg C) for the year 2021 (KRA) and 2023 (BRA and WIE), along with the total waste mass and average water content per pilot, was used to express modelled carbon emissions (CH_4-C, CO_2-C) expressed in kg $C/t_{dw.}$

4.2.3. Waste sampling, pre-treatment and characterization

4.2.3.1. Waste sampling

Several drillings were conducted at the pilot KRA to install piezometers and a pumping well. Waste samples were retrieved during these activities (Table 4.3). After removing the top layer, primarily landfill cover soil, the waste was mixed across several meters of depth (Figure 4.1, top). A total of 19 samples from different layers and boreholes were collected in 10 L and 20 L buckets.

For pilots BRA and WIE, asbestos presence necessitated additional safety measures during sampling (details in S4.2.1). A total of 36 waste samples in BRA and 16 waste samples in WIE weighing 4–28 kg were collected (Figure 4.1, middle and bottom) and placed in heavy-duty

asbestos removal bags for transport and processing.

Table 4.3. Overview of waste samples.

Landfill pilot	Drilling (s)	Date	Storage conditions	Experiment
KRA	Four drillings (A3 to A4-3)	November 2020	Samples divided into two sub-samples, one stored under freezing conditions and the other under cooling conditions	Pre-test and Sequential anaerobic and aerobic incu-bation
	One drilling (A4-4)	January 2022		Pre-test
	Eight drillings (PZ9.8 to PZ19.19)	March 2023	Cooling conditions	Parallel anaerobic and aerobic incu-bation
BRA	Eight drillings (An2, An-6, Cn2, Cn-6, En2, En4, En-6, Ln6)	September 2022	Cooling conditions	
WIE	Three drillings (1, 2, 3)	October 2022	Cooling conditions	

4.2.3.2. Waste pre-treatment

Samples from the 2020 and 2022 drillings at the KRA pilot, weighing 1–14 kg each, were not sieved. By contrast, samples from the BRA, WIE, and KRA (KRA-25, 2023) pilots, which weighed 4–28 kg each, were sieved through a 3.6 cm grid for sorting. From these, approximately 2 kg per sample were retained for characterization and gas production and respiration experiments (Table 4.3).

The BRA and WIE samples were analysed by an external laboratory (Eurofins Analytico B.V.) for asbestos content (European Committee for Standardization (CEN), 2016). Asbestos was detected in four BRA samples and two WIE samples. These samples were discarded, and the remaining waste, including KRA-25, was sieved further through a 4 mm mesh and then mixed to create composite samples per layer group: top (BRA: 2 to 4 mbs, WIE: 2 to 6 mbs, KRA: 1 to 6 mbs), middle (BRA: 4 to 8 mbs, WIE: 6 to 10 mbs, KRA: 6 to 12 mbs), and bottom (BRA: 8 to 12 mbs, WIE: 10 to 14 mbs, KRA: 12 to 18 mbs). After taking a sample to measure carbon and organic matter content, the waste from the three layers were combined to create the mixed samples for each pilot (KRA-25, BRA-139, and WIE-216).

Approximately 100 g of all KRA samples were dried in a soil drying oven (SDO) at 105 °C for 24 hours to determine water content (European Committee for Standardization (CEN), 2014). Non-asbestos samples from BRA and WIE were dried in aluminium dishes with paper covers clipped on as a safety measure to prevent the dissipation of fibrous particles. These samples were dried in an oven until their weight stabilized to within ±1 g. Values for dry matter content of asbestos-contaminated BRA and WIE samples was obtained from the external laboratory.

The dried KRA samples that had not been sieved (drillings 2020, 2022) were milled using the Retsch SM 2000 miller and the Herzog HSM 100 P disk mill. Details of these procedures can be found in the supplementary information A (S4.2.2). Dried non-asbestos samples from BRA and WIE, which had been sieved through a 3.6 cm grid, were milled using a Jaw Crusher (Retsch) to reduce particle sizes to 4 mm. These samples, along with the mixed

samples (KRA-25, BRA-139, and WIE-216) that had already been sieved through a 4 mm mesh, were further milled using a VWR ball mill. Milling was conducted at 18 shakes per second for two minutes, divided into four 30-second intervals.

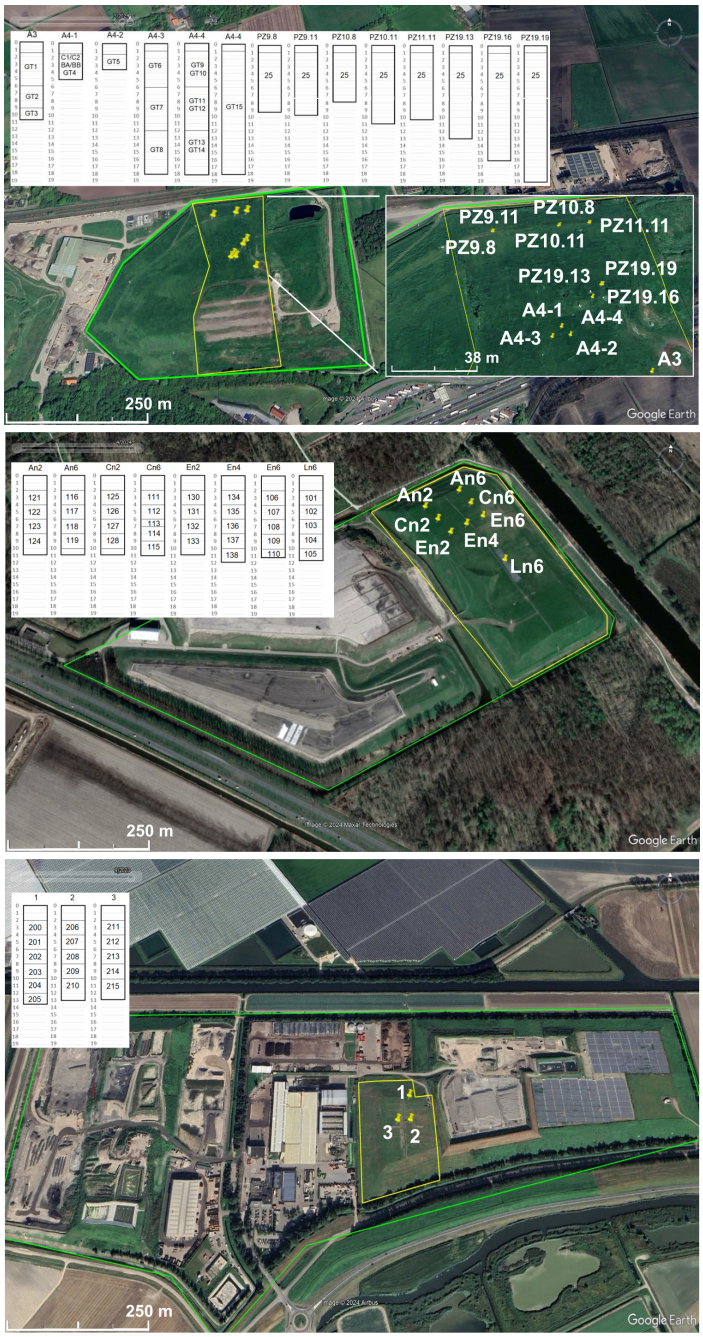

Figure 4.1: Aerial photographs (Google earth) of the pilots (green line), in situ stabilization landfill pilots (yellow line), and schematic (top left in each subfigure) showing the waste samples depth. Top: Kragge II; middle: Braambergen; bottom: Wieringermeer.

4.2.3.3. Waste characterization

The analysis of the waste characterization includes all samples from KRA, samples from one drilling well per compartment in BRA and WIE (Ln6, En6, and 2, Table 4.3 and Figure 4.1, middle and bottom), and the mixed samples from all pilots (KRA-25, BRA-139, WIE-216, and composite samples per layer group). The selection of the drilling well per compartment in BRA and WIE was based on the gas generation tests, further detail in section 4.2.4.

4.2.3.3.1. Sorting

Sorting was performed on all fresh samples from the BRA, WIE, and KRA pilots and results were expressed in percentage fresh weight (%fw). For the 2020 and 2022 KRA samples, manual sorting into seven fractions (fines, soft plastics, hard plastics, wood, stones, metal, and residual materials) was conducted without pre-treatment. All samples from BRA, and WIE pilots, and sample KRA-25, were sorted after being retained by the 3.6 cm sieve grid. The average composition for each pilot was used to characterize the mixed samples (KRA-25, BRA-139, and WIE-216) and the sorted waste was discarded afterwards.

4.2.3.3.2. pH and electrical conductivity (EC)

For pH and EC measurements of non-asbestos samples from the BRA and WIE pilots, as well as the mixed KRA-25 sample, 10 g of fresh waste sample was suspended in 25 ml of demineralized water and allowed to sit for one hour before measurement at 25 °C (European Committee for Standardization, 2011; Food and Agriculture Organization of the United Nations, 2021; International Organization for Standardization, 2021).

4.2.3.3.3. Carbon and organic matter content

The carbon and organic matter content were measured in the KRA samples and non-asbestos samples from the BRA and WIE pilots. The methods included dry combustion for total carbon (TC), Rock Eval S7 pyrolysis and loss-on-ignition (LOI) for organic matter content (Table 4.4).

The soil-specific program in the Rock Eval S7 quantifies soil organic matter (SOM) fractions by detecting hydrocarbons, CO and CO_2 released during pyrolysis and oxidation over a temperature ramp (Carrie et al., 2012; Disnar et al., 2003; Sebag et al., 2016). Using powdered samples (20-100 mg), pyrolysis occurs in an inert N_2 atmosphere from 125°C to 650°C, followed by oxidation in an oxygen-rich atmosphere from 300°C to 850°C. The Hydrogen Index (HI) reflects the share of hydrogen-rich labile organic matter, while the I-index and R-index assess thermally labile immature organic fractions and thermally stable refractory fractions, respectively (Sebag et al., 2016). The oxygen index (OI) indicates the relative abundance of oxygen-rich compounds in organic matter and, when used alongside HI, can help assess the degree of organic matter decomposition (Gregorich et al., 2015). Total organic carbon (TOC), total inorganic carbon (TIC) expressed as total mineral carbon (%), HI, OI were measured, and the R-index and I-index were calculated in all samples (data

provided by N. Quist). More detail in the Rock Eval parameters, including formulas, can be found in the supplementary information A (S4.2.3).

For the LOI, oven-dried samples (Heraeus UT6120, 105 °C) were heated in a muffle furnace (Nabertherm L15/12/P330) at a rate of 10 °C/min until reaching 550 °C, with a baking time of three hours. LOI was performed for KRA (all samples), BRA and WIE (samples per group layer - top, middle, bottom- as well as mixed samples). Detailed procedures are provided in the supplementary information A (S4.2.4).

Table 4.4. Overview of analyses to quantify carbon and organic matter species and fractions.

Parameter	Method/instrument	Standard/Reference
Total carbon (TC)	Dry combustion/ UNICUBE (Elemen-tar) and LECO	ISO 10694:1995 / (International Organization for Standardization, 1995)
Total organic carbon (TOC) Total inorganic carbon (TIC) Hydrogen index (HI) Oxygen index (OI) R-index I-index	Soil program / Rock Eval S7	(Carrie et al., 2012; Disnar et al., 2003; Sebag et al., 2016)
Organic matter content*	Loss on ignition (LOI)/ muffle furnace (Nabertherm L15/12/P330)	NEN 5754:2005 /Supplementary information A (S4.2.3), (European Committee for Standardization, 2020)

*Measured in KRA (all samples), BRA and WIE (samples per group layer- top, middle, bottom- as well as mixed samples).

4.2.4. Analysis of carbon generation in laboratory bench-top incubations

The laboratory experiments were designed to quantify CH_4 and CO_2 generation under anaerobic (gas production, referred to as GT) and aerobic (respiration, referred to as RT) conditions using waste samples retrieved from various depths. A pre-test to define the container size and temperature storage conditions is described in the supplementary information A (S4.3.5). Two experimental approaches were applied: parallel anaerobic and aerobic incubation and sequential anaerobic-aerobic incubation.

Parallel anaerobic and aerobic incubation: This experiment assessed carbon release under parallel respiration (RT) and gas production (GT) tests using sieved (3.6 cm) samples stored under cooling from the three pilots (BRA, WIE, and KRA). For RT, two sub-samples of ~25 g were placed in 1 L glass bottles (e.g., 25_RT_A and 25_RT_B), and for GT, two sub-samples of ~50 g were placed in 500 mL glass bottles (e.g., 25_GT_A and 25_GT_B). All bottles were sealed with butyl rubber stoppers. All samples from BRA and WIE (48 samples) were tested in parallel anaerobic and aerobic incubation for at least 30 days. For long-term testing, CH_4 and CO_2 concentrations were normalized to 21 days, and the carbon content (sum of CH_4 and CO_2) was categorized as high, medium, or low. From these, one drilling well per compartment containing high, medium and low carbon content (Ln6, En6, 2, Table 4.3 and Figure 4.1, middle and bottom) were selected for the characterization analysis and longer incubation lasting at least 1.2 years. In addition, one mixed sample from each pilot (BRA-139, WIE-216, and KRA-25) was included and measured for nearly one year.

Sequential anaerobic-aerobic incubation: This experiment focused on carbon release in a sequential test consisting of an anaerobic incubation (GT) for 1.6 years followed by an aerobic incubation (RT) for an additional 1.2 years. Sixteen frozen, non-sieved samples from KRA (GT1-GT8) were used. The samples (1.2 kg to 10.2 kg each) were defrosted overnight at 10 °C, after which two ~250 g sub-samples were placed in 1 L glass bottles (e.g., GT1.1 and GT1.2) and sealed with butyl rubber stoppers.

4.2.4.1. Experimental setup and measurement procedure

To establish anaerobic conditions in the gas production test (GT), the bottles were flushed with 100% N_2 over a period of 5 minutes. In the case of the aerobic conditions in the respiration test (RT), bottles were closed after weigh-in and pressurized with 100 ml of laboratory air to prevent the development of under pressure due to volume removal for analysis. Thereafter, samples were incubated in the dark at 20 °C.

Gas generation over time was monitored by measuring the pressure and the composition of the bottle headspace. For both measurements (GT and RT), a syringe with a needle that passed through the rubber stopper was used to withdraw gas samples for gas chromatographic analysis of headspace CH_4, CO_2, N_2 and O_2 concentration. Approximately 3 ml of headspace gas mixture was injected into a gas chromatograph (Agilent 490-PRO micro GC, Da Vinci). CH_4 and CO_2 were analysed using a 1m Cox Heated Injector Backflush column, operated at an initial temperature of 120 °C and and a pressure of 200 kPa. N_2 and O_2 were analysed using a heated BF column (5 m PBQ+10 m MS5A), operated at 80 °C and 200 kPa. Helium was used as a carrier gas and a thermal conductivity detector (TCD) for signal detection.

The pressure was measured before and after gas sampling by connecting the needle to a digital manometer (LEX1, Keller) and to calculate the gas generation between measurements. To prevent excessive pressure buildup inside the GT bottles, the pressure was released upon reaching 1500 hPa. In the case of the RT bottles, the inhibition of organic matter degradation due to high CO_2 levels was controlled by flushing the headspace of the bottle with atmospheric air once CO_2 concentrations reached three volume percent in the gas phase, after which measurements recommenced. Initially, the gas composition and pressure were measured twice a week, and thereafter, depending on the reactivity of the sample, the measurement frequency was adjusted.

All experiments were carried out in duplicate. The procedure for the gas production and respiration measurements on BRA and WIE samples had additional safety measures because of potential asbestos content and is described in the supplementary information A (S4.2.1).

4.2.4.2. Data analysis

For both aerobic and anaerobic conditions, it was assumed that the headspace consisted only of CH_4, CO_2, N_2 and O_2, as these were the dominant gases produced.

The number of CH_4 and CO_2 moles were calculated using the ideal gas law previously described (Eq. 2), where pressure corresponds to bottle pressure, volume to the headspace volume of CH_4 and CO_2, and temperature to the incubation temperature (20 °C). The amount of degraded carbon was calculated as follows:

$$C = ((n_{CH_4} + n_{CO_2}) \times MM_C)/dw \times 1000 \quad \text{(Eq. 3)}$$

Where C is the amount of degraded carbon in kg C/t_{dw}, n_{CH_4} and n_{CO_2} are the number of CH_4 and CO_2 moles respectively, MM_C is the carbon molar mass (12,01 g/mol), and dw the sample dry weight (g).

The cumulative degraded carbon, represented as carbon generation ($C\text{-}CH_4$ + $C\text{-}CO_2$) per dry weight over the time, was fitted to either a one-phase or two-phase exponential decay model, know as G-model (Arndt et al., 2013; Jorgensen, 1978; Westrich & Berner, 1984). This was done using the ExpDec1, ExpDecay1, ExpDec2 and ExpDecay2 functions in OriginLab software (Origin 2022). Model fitting was based on statistical analysis, including the number of data points, degrees of freedom, reduced Chi-square, residual sum of squares, R-square and adjusted R-square. A maximum of 400 iterations was used to ensure convergence.

Data were fitted using a Levenberg Marquardt Iteration Algorithm with one-phase exponential function (ExpDec1: eq. 4, ExpDecay1: eq. 5) or two-phase exponential function (ExpDec2: eq. 6, ExpDecay1: eq. 7) which are described by the following equations:

$$Y = Y_0 + A_1 * e^{(-k_1 t)} \quad \text{(Eq. 4)}$$

$$Y = Y_0 + A_1 * e^{(-k_1 (t-t_0))} \quad \text{(Eq. 5)}$$

$$Y = Y_0 + A_1 * e^{(-k_1 t)} + A_2 * e^{(-k_2 t)} \quad \text{(Eq. 6)}$$

$$Y = Y_0 + A_1 * e^{(-k_1 (t-t_0))} + A_2 * e^{(-k_2 (t-t_0))} \quad \text{(Eq. 7)}$$

Where Y is the cumulative amount of carbon released in kg C/t_{dw}, t is the time in days, Y_0 is the value to which the measurement decays representing the total cumulative carbon released when t approaches to infinity, in this research defined as the carbon potential, A_1 and A_2 are the amplitude representing the initial value in each phase, t_0 is the time at which the decay process starts, and k_1 and k_2 are the individual decay rate constant (k-value) for each phase.

The final model selection was based on the highest coefficient of determination (R^2), and a carbon potential (Y_0) and gas generation for 21 and 365 days that follows the trend observed in the experimental data. This means that a sample with a lower slope and carbon generation to its parallel should not have a higher Y_0. Model fitting for samples that did not reach the plateau (high uncertainty) were evaluated individually, negative k-values (k_1, k_2) and carbon potential (Y_0) were discarded (Supplementary information A, S4.3.3). The discarded Y_0 was extrapolated from the correlation between Y_0 and Y_{365} in each pilot (Supplementary information A, S4.3.4).

Cumulative carbon generation was normalised to dry weight and to total organic carbon (TOC). For asbestos-containing samples, the TOC from the corresponding layer group was used, as these samples were not milled and TOC measurements were unavailable. The following table summarizes the parameters obtained during the laboratory experiment:

Table 4.5. Overview of parameters directly measured or derived from laboratory incubations of landfilled waste.

Term	Parameter	Description	Units
GT GT_{21} GT_{365} GT_d	Gas generation test	Cumulative carbon generation under anaerobic conditions. Carbon originates from CH_4 and CO_2. Suffix "d" indicate time in the unit of days. 21 and 365 days were used to compare short-term carbon generation with yearly carbon generation.	Normalised to dry weight: kg C/t_{dw}
RT RT_{21} RT_{365} RT_d	Respiration test	Cumulative carbon generation under aerobic conditions. Carbon originates from CO_2. Suffix "d" indicate time in the unit of days. 21 and 365 days were used to compare short-term carbon generation with yearly carbon generation.	Normalised to dry weight: kg C/t_{dw}
Y_0 GT_{Y_0} RT_{Y_0}	Carbon potential, anaerobic or aerobic	Cumulative carbon generation when time approaches infinity. This parameter describes the absolute amount of degradable carbon in the sample.	Normalised to dry weight: kg C/t_{dw}
$GT_{d\text{-}TOC}$ $RT_{d\text{-}TOC}$ $GT_{Y_0\text{-}TOC}$ $RT_{Y_0\text{-}TOC}$	Degradable organic carbon, anaerobic or aerobic	Cumulative carbon generation relative to total organic carbon at specific day or when time approaches infinity. This parameter expresses the amount of degradable carbon in the sample as a percentage or a fraction of the total organic carbon (TOC) present at the beginning of laboratory incubation. It therefore indicates degradability of the organic material.	Normalised to total organic carbon: %
k1 k2	Individual decay rate	Derived parameter that indicates the waste decay rate in each degradation phase.	$year^{-1}$

The follow exemplary long-term cumulative curve of carbon generation under anaerobic conditions (Figure 4.2) fit better with a two-phase exponential decay model. This model showed a lower reduced Chi-sqr (X^2) value and a higher R-square (R^2) value after discarding the initial lag-phase (10 days). The fitted equation (Eq. 5) was used to determine the carbon potential, and their fitted parameters were used to calculate the individual decay rates and gas generation parameters normalized to dry weight. To estimate the degradable organic carbon, the carbon generation was normalized to the total organic carbon, which was 9.79%$_{dw}$ in this sample. The results are shown in Table 4.6.

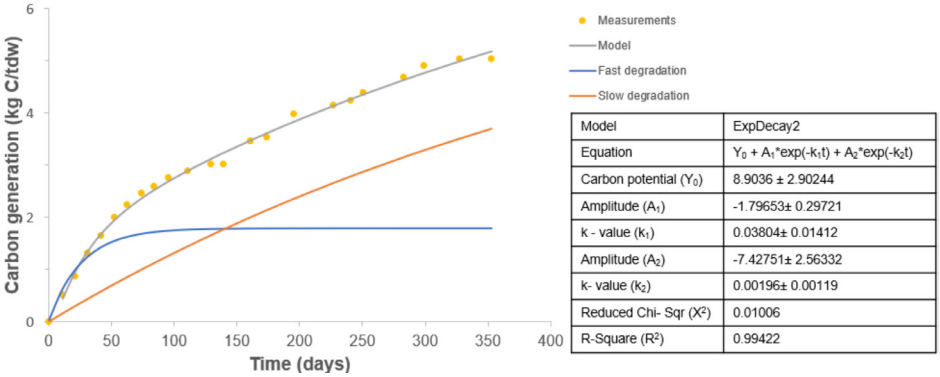

Model	ExpDecay2
Equation	$Y_0 + A_1*exp(-k_1t) + A_2*exp(-k_2t)$
Carbon potential (Y_0)	8.9036 ± 2.90244
Amplitude (A_1)	-1.79653± 0.29721
k - value (k_1)	0.03804± 0.01412
Amplitude (A_2)	-7.42751± 2.56332
k- value (k_2)	0.00196± 0.00119
Reduced Chi- Sqr (X^2)	0.01006
R-Square (R^2)	0.99422

Figure 4.2. Exemplary long term cumulative curve fitted with a two-phase exponential decay model.

Table 4.6. Laboratory parameters in exemplary cumulative curve.

Parameter	Term	Value
Gas generation test in 21 days	GT_{21}	0.97 kg C/t_{dw}
Gas generation test in 365 days	GT_{365}	5.27 kg C/t_{dw}
Anaerobic degradable organic carbon in 365 days	$GT_{365\text{-}TOC}$	5.38 %
Anaerobic carbon potential	GT_{Y_0}	8.90 kg C/t_{dw}
Anaerobic degradable organic carbon potential	$GT_{Y_0\text{-}TOC}$	9.09 %
Individual decay rate- phase 1	k_1	13.88 $year^{-1}$
Individual decay rate- phase 2	k_2	0.71 $year^{-1}$

4.3. Results and discussion

4.3.1. Waste characterization

4.3.1. 1. Waste composition

The waste composition in the KRA samples (2020 and 2022 drillings), revealed a significant presence of plastics, particularly in sample KRA-1, where plastics accounted for nearly 70%$_{fw}$ (percentage of the fresh weight) (Figure 4.3, top). Samples KRA-5 and KRA-14 had the highest percentages of residual materials, including fines, glass, ceramics, textiles, rubber, shells, and other miscellaneous items. The high plastic content in the pilot may encase other waste materials, potentially hindering their degradation. Notably, samples KRA-4 and KRA-8 exhibited free water, as indicated by their high water contents of 127%$_{dw}$ (percentage of the dry weight) and 116%$_{dw}$, respectively.

The majority of the waste from BRA and WIE pilots, including those containing asbestos, and sample KRA-25, passed through the 3.6 cm sieve grid and was not sorted (Figure 4.3, bottom). The waste retained by the 3.6 cm sieve grid constituted up to 25%$_{fw}$ in BRA, 17%$_{fw}$ in WIE, and 19%$_{fw}$ in KRA, primarily consisted of wood (4-5%$_{fw}$) and residual waste (4%$_{fw}$) in the aerated pilots (BRA and WIE), as well as wood (4%$_{fw}$) and plastic waste (7%$_{fw}$) in KRA.

4.3.1. 2. Water content and organic matter

The water content and organic matter was measured in mixed samples from each group layer (top, middle, bottom), as well as in samples used for the pre-tests and sequential and parallel incubation experiments.

The water content varied considerably across the samples (Figure 4.4, top left). The KRA pilot samples exhibited the highest water levels, with both sieved (4 mm sieve) and non-sieved waste samples ranging from 43%$_{dw}$ to 127%$_{dw}$, which was found in the top layer. The middle layer was the driest layer with the lowest variability among layers (54%$_{dw}$ - 102%$_{dw}$). This elevated water content could be related to the practice of water recirculation and/or ponding against impermeable materials, such as plastic sheets (see elevated plastic contents

shown in section 3.1.1). Drier zones in the middle layer of KRA as well as wet pockets throughout the pilot were visualized by electrical resistivity measurements in KRA (Ren, 2021). No significant difference was observed between the water content of sieved and non-sieved samples: the non-sieved mixed sample (KRA-15) had a water content of 80%$_{dw}$, while the sieved sample (KRA-25) had 72%$_{dw}$.

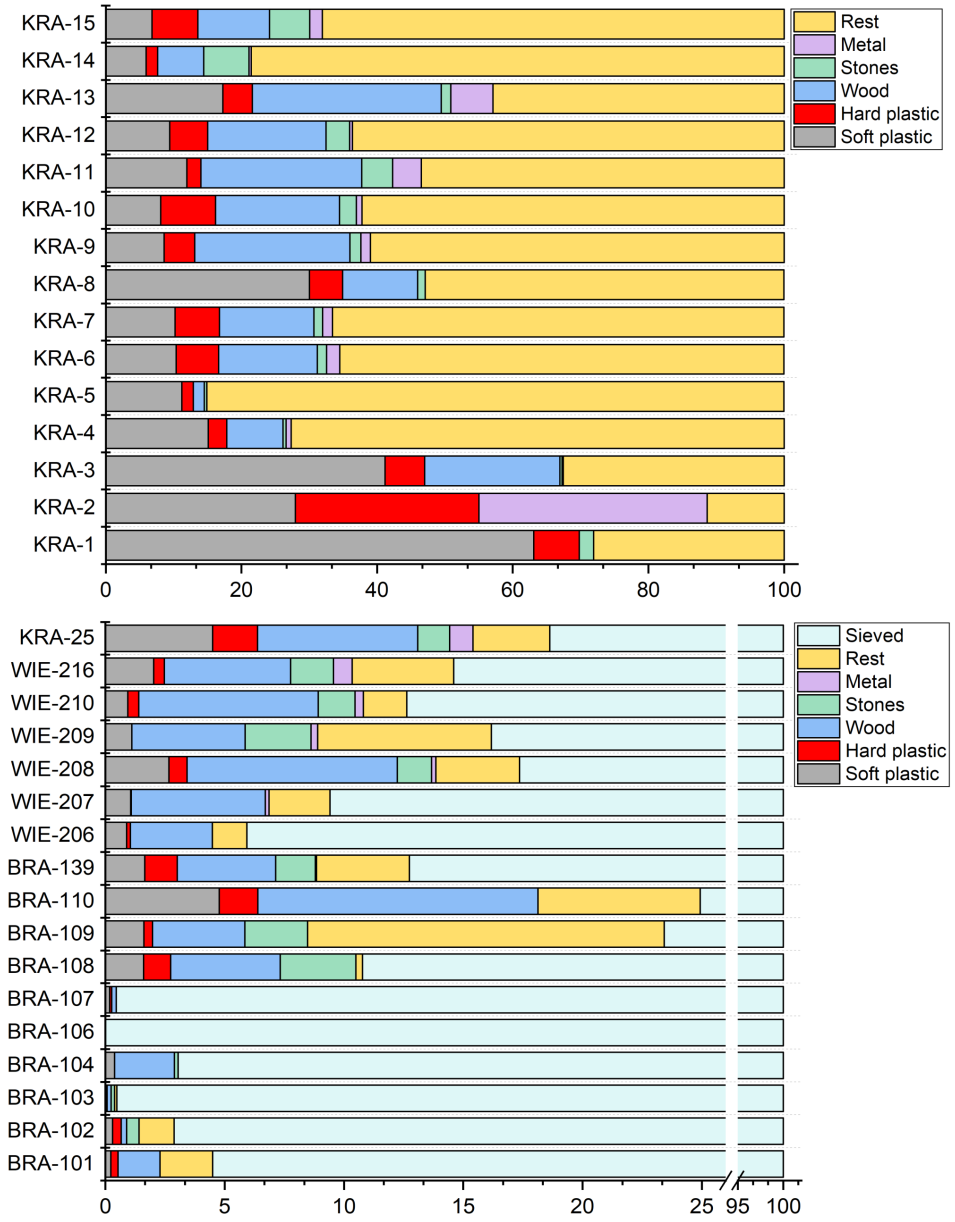

Figure 4.3. Waste composition in percentage of fresh weight (%$_{fw}$) on un-sieved waste from KRA landfill pilot (top) and the waste retained by the 3.6 cm sieve grid in BRA, WIE and KRA landfill pilots (bottom).

Among the aerated pilots, samples from BRA displayed water contents ranging from 34%$_{dw}$ to 72%$_{dw}$, with increasing water content over depth and the mixed sample measuring 37%$_{dw}$. Samples from WIE exhibited slightly lower water contents (27%$_{dw}$ to 59%$_{dw}$), with the highest water content in the middle layer and the mixed sample measuring 35%$_{dw}$. All samples in these pilots were sieved to 3.6 cm and the mixed samples to 4 mm. Previous studies have reported water contents between 18%$_{dw}$ and 79%$_{dw}$ for MSW (Eck, 2000; Fricko et al., 2021; Maciel & Jucá, 2011; Puyuelo et al., 2011; Themelis & Ulloa, 2007). Figure S4.3.1 (supplementary information A) shows the water content per group layer in the three pilots.

The carbon content and organic matter in the samples from the aerated pilots were similar and lower than those in KRA (Figure 4.4, top middle and Table 4.7). This was expected, since household waste, which is higher in organic content, was a major component of KRA, whereas BRA primarily received polluted soils and WIE mainly contained commercial waste (Chapter 2, Figure 2.3). Low contents of degradable organic matter is a prerequisite for applying aeration as a stabilization method as it provides a safe, efficient, and controlled method for reducing residual emissions and enhancing long-term stability without causing excessive biological reactions, increasing the risk of excessive heating and settlement (Grossule & Stegmann, 2020; Ritzkowski, 2021; Ritzkowski & Stegmann, 2012). On the other hand, in landfills with high organic matter content an anaerobic stabilization is preferred as the extracted landfill gas can be used to generate energy reducing the costs of stabilization (Benson et al., 2007; Heyer et al., 2003; Ritzkowski et al., 2006).

The high TOC heterogeneity in KRA (Table 4.7) was driven by the first sampling event in 2020, where samples from wells A3, A4-1, A4-2 and A4-3 (Figure 4.4, top) had a TOC ranging 4-30%$_{dw}$ with an average TOC of 18%$_{dw}$. Fourteen months later, a second sampling from well A4-4 showed an unchanged TOC average with lower variability (12-26%$_{dw}$), while the mixed sample KRA-15 had a TOC of 14 %$_{dw}$. Another 14 months later, a final sampling from nine wells (PZ9.8 to PZ19.19) was conducted, where mixed samples from different depth layers (top, bottom, middle) had similar TOC values (12%$_{dw}$), and the mixed sample KRA-25 had an average TOC of 10%$_{dw}$. Waste samples from old German landfills also showed a broad TOC range with the initial TOC ranging <1-29%$_{dw}$ (Gebert et al., 2011; Ritzkowski et al., 2006).

Within the KRA samples, the lowest content in Total Organic Carbon (TOC, 4%) was observed in sample KRA-5, retrieved from the shallowest layer (1.5-3.5 mbs). Most other samples showed a TOC values between 10% and 30%. For comparison, TOC in an Austrian MSW landfill from the 1970s ranged between 13% and 14% (Fricko et al., 2021), while the TOC in an Italian landfill ranged from 10% to 15% (Raga & Cossu, 2013). Interestingly, the mixed sample from one drilling well (sample KRA-15, 1-18 mbs, used in the pre-test) had a TOC of 14% while the mixed sample from eight drilling wells (sample KRA-25, used in the parallel incubation), with most waste retrieved from the top and middle layers (up to 12 mbs), had a TOC of 10%. In both cases, the TOC values of the mixed samples were consistent with those reported in the literature, suggesting that the organic matter content of KRA is typical of

long-established MSW landfills.

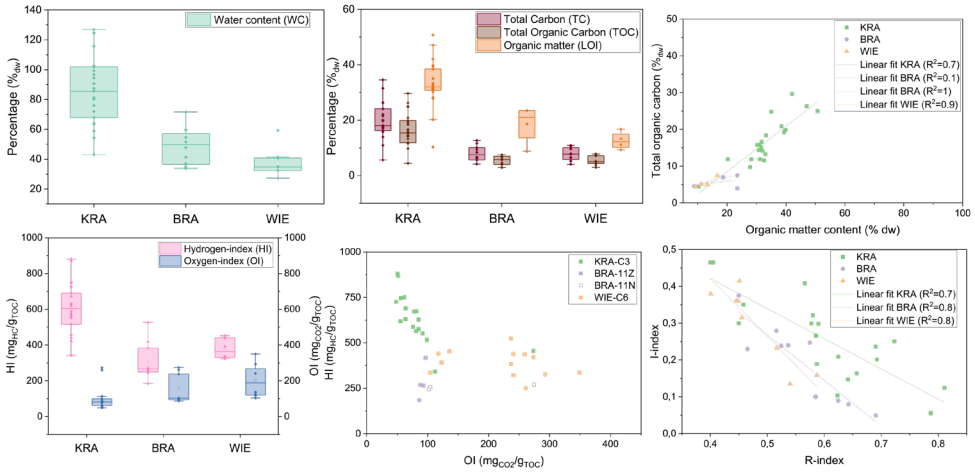

Figure 4.4. Water content ($\%_{dw}$) (top left); Total Carbon (TC), Total Organic Carbon (TOC) and organic matter (LOI) (top middle); LOI versus TOC (top right); Hydrogen index and Oxygen index (bottom left and middle); and R-index versus I-index (bottom right) in waste from the three pilots. Box plots: box = 25th-75th percentile, line = median, whiskers = 1.5 IQR, circle symbol = mean, rhombus symbol outside whiskers = outliers.

The correlation between the TOC and the LOI (Figure 4.4, top right) was higher for WIE (R^2=0.9, slope=0.4) than for KRA (R^2 >0.7, slope=0.6). In both pilots the correlation was significant (Supplementary information A, Table S4.3.9.2 and Table S4.3.9.6). A similar correlation to KRA was found in three old German MSW landfills (R^2>0.9, slope=0.6) (Gebert et al., 2011). In BRA, the correlation coefficient dropped significantly (R^2=0.1, slope=0.08) when including sample BRA-top, a mixed sample from the top layer (2 to 4 mbs) in compartment 11N. This sample likely contains a higher proportion of volatile components, which may have increased LOI without a proportional increase in TOC. Excluding this sample increased the correlation to R^2=1 (slope=0.2), indicating that the remaining samples followed a consistent TOC-LOI relationship. Overall, these results suggest that the nature of organic matter differs between the aerated pilots (BRA, WIE) and pilot KRA, non-carbon volatile matter decreasing in the order BRA > WIE > KRA. The total inorganic carbon (TIC) expressed as total mineral carbon (%), averaged 1% across all pilots (Table 4.7, and Supplementary Information A, Figure S4.3.1).

Rock-Eval pyrolysis revealed two distinct clusters with KRA waste showing a high Hydrogen Index (HI) but a low Oxygen-Index (OI), while the waste from aerated pilots WIE and BRA had a consistently lower HI but spanned a wider range of OI (Figure 4.4, bottom left and middle, Table 4.7). Higher HI values indicate more easily degradable organic matter (Sebag et al., 2016; Zander et al., 2023). This aligns with both the waste composition, with KRA containing a higher fraction of household waste than BRA and WIE (Chapter 2, section 2.4), and the fact that the aerated pilots were already in a late methanogenic phase prior to the onset of aeration (Vereniging Afvalbedrijven, 2014, 2015a). Among the aerated pilots, WIE samples showed slightly higher HI values than BRA (Figure 4.4, bottom left, and Table 4.7),

suggesting presence of more easily degradable organic matter in WIE waste.

Table 4.7. Mean, median and standard deviation of Total Carbon (TC), Total Organic Carbon (TOC); Total Inorganic Carbon (TIC) as MINC (total mineral carbon); organic matter (LOI); Hydrogen index (HI); Oxygen index (OI); R-index; I-index in waste from the three pilots.

Landfill pilot	TC ($\%_{dw}$)			TOC ($\%_{dw}$)			IC (MINC%) ($\%_{dw}$)			LOI ($\%_{dw}$)		
	Mean	Median	Stdv	Mean	Median	Stdv	Mean	Median	Stdv	Mean	Median	Stdv
KRA	20.16	18.04	6.92	16.66	15.45	6.06	0.94	0.93	0.21	33.16	32.02	8.46
BRA	8.05	7.51	2.75	5.24	5.12	1.5	1.29	1.23	0.3	18.58	21.05	6.41
WIE	7.81	7.79	2.37	5.46	5.04	1.74	1.11	1.01	0.3	12.62	12.22	2.95
Landfill pilot	HI (mg HC/gTOC)			OI (mg CO_2/g_{TOC})			R-index			I-index		
	Mean	Median	Stdv	Mean	Median	Stdv	Mean	Median	Stdv	Mean	Median	Stdv
KRA	602.75	603.5	141.48	111.21	81.25	79.73	0.62	0.62	0.12	0.22	0.24	0.17
BRA	306.65	267.25	99.94	157.9	103	80	0.56	0.56	0.08	0.19	0.23	0.1
WIE	380.52	363.58	54.6	200.54	188.5	89.64	0.48	0.45	0.06	0.29	0.34	0.1

In a study using a variety of pure biochemicals and biological standards, Carrie et al. (2012) found that the Oxygen Index (OI), as defined by Lafargue et al. (1998), was positively correlated with residual carbon (RC), which consists of strongly resistant and refractory organic components. In this chapter, higher OI values were observed in samples from the aerated pilots, with WIE showing the highest OI, suggesting a more advanced level of organic matter stabilization in WIE compared to the other sites. According to Rock-Eval theory and previous studies (e.g., Gregorich et al., 2015), an inverse relationship between the Hydrogen Index (HI) and OI is typically expected along gradients of organic matter degradation or maturation, with decreasing HI and increasing OI reflecting progressive oxidation and stabilization (personal communication Maarten van Hoef, Wageningen University and Research). This pattern was observed in KRA compared to the aerated pilots, but the relationship between HI and OI within the aerated pilots (WIE and BRA) was less straightforward. WIE exhibited both slightly higher HI and the highest OI among the aerated sites, possibly reflecting the coexistence of residual labile organic matter alongside a more oxygen-rich, refractory carbon pool formed through prolonged aeration. The difference in OI between WIE and BRA (mean OI: 200 vs. 158; median OI: 189 vs. 103) further supports the interpretation of more extensive oxidative transformation in WIE, despite its marginally higher HI values.

Interestingly, OI values were more than twice as high in the mixed samples per layer (top, middle, bottom) and in the overall mixed samples from each pilot (KRA-25, BRA-139, and WIE-216) compared to individual samples. This contributed to greater variability in the aerated pilots, which had fewer total samples (Figure 4.4, bottom left). Within BRA, compartment-level differences were also evident: samples from compartment 11N showed higher OI and lower HI values than those from compartment 11Z, indicating more stabilized organic matter. The mixed sample from compartment 11N had the highest OI of

all BRA samples (Figure 4.4, bottom middle). These differences likely reflect variations in waste composition and age: while both compartments primarily contained polluted soils (≥73%mass), 11N also included commercial waste (12%mass) and construction and demolition waste (8%mass), whereas 11Z consisted of 96%mass polluted soils and was filled four years later, making it the younger of the two (Chapter 2, Section 2.4). The combination of higher organic matter content and older waste in 11N likely contributed to faster stabilization, resulting in a more refractory organic matter composition compared to 11Z. Overall, these results highlight the heterogeneity of the samples, showing that degradation varies considerably across the site, that mixed samples combine wastes with different degrees of prior degradation, and that waste composition and age play a role in shaping the degree of organic matter maturity in aerated pilots.

The inverse linear relationship between the R-index and I-index (R^2>0.7) in the pilots (Figure 4.4, bottom right) suggest organic matter stabilization processes (Sebag et al., 2016) as the R-index increases (indicating more refractory and stable matter) while the I-index decreases (indicating lower transformation of labile organic matter). A steeper slope (more negative) implies a faster decline in the I-index relative to the increase in the R-index. This means that at in KRA (slope=-0.8) the transformation of labile organic matter is slower suggesting an earlier stage of organic matter transformation. While in WIE (slope=-1.6) and BRA (slope=-1.2) the organic matter transformation (I-index) decreases more sharply as the refractory fraction (R-index) suggesting more advance degradation processes. This points to the highest extent of organic matter stability in WIE compared to the other pilots.
Considering the results on waste characterization, the activity in the gas production and respiration tests would be expected to be higher in KRA than in the aerated pilots.

4.3.2. Gas generation of excavated wastes

The course of carbon generation over time in the gas production and respiration tests for all samples, is provided in the supplementary information A (S4.3.5 - S4.3.7).

4.3.2.1. Carbon generation in parallel anaerobic and aerobic incubation

This experiment compared long-term carbon generation in parallel gas production (anaerobic) and respiration (aerobic) tests (Table 4.8 and Supplementary Information A, S4.3.6). Most carbon was mineralized under aerobic conditions (RT/GT > 4), with the highest ratios in the aerated pilots (mixed samples, Table 4.8). The notably high mean ratio in BRA was driven by sample BRA-106 (Supplementary Information A, Figure S4.3.6.2), which exhibited the highest OI, one of the highest R-index values, and one of the lowest I-index values among the BRA samples. These characteristics indicate a more stabilized organic matter composition, with a higher share of strongly resistant and refractory compounds (Sebag et al., 2016), which likely required aerobic conditions for further degradation, while remaining largely undegraded under anaerobic conditions. Furthermore, the anaerobic degradation of waste samples from the aerated pilots were less than a quarter compared

to the samples from the anaerobic pilot (mixed samples, Table 4.8), indicating very little anaerobic potential in those samples.

Table 4.8. Mean and standard deviation of gas generation under aerobic and anaerobic conditions and the ratio RT to GT per landfill pilot and layer group.

Landfill pilot	Layer group	Experimental data								
		Days GT	GT (kg C/t_{dw})		Days RT	RT (kg C/t_{dw})		RT/GT		
		mean	mean	std	mean	mean	std	mean	median	std
BRA	top	553,0	0,3	0,2	516,6	3,7	0,5	28,2	25,2	24,8
	mid	555,8	1,5	1,1	555,6	8,4	2,8	7,8	8,2	4,0
	bot	543,4	2,8	4,1	556,1	8,9	2,8	17,2	14,5	17,1
WIE	top	512,1	1,7	1,4	512,1	7,7	3,9	9,2	4,8	9,5
	mid	512,1	2,8	0,9	512,1	17,2	1,3	6,7	6,4	2,1
	bot	513,1	1,3	0,2	513,1	8,8	1,3	7,1	7,1	1,9
KRA	mix	352,7	4,9	0,2	352,6	21,1	2,3	4,3	4,3	0,6
BRA	mix	352,7	1,2	0,0	347,2	8,0	0,4	6,7	6,7	0,2
WIE	mix	352,6	1,3	0,2	352,6	10,4	0,3	8,2	8,2	0,8

For comparison purposes, the carbon generation over 365 days for anaerobic (GT_{365}) and aerobic (RT_{365}) incubation was estimated using the fitting parameters from single- or dual-phase exponential decay models. Excluding the results from the incubation of the mixed samples (KRA-25, BRA-139, WIE-216), which were tested for nearly a year, samples from the WIE pilot released a higher percentage (80% to 90%) of the total carbon generated than BRA (75% to 83%) by the end of the experiment within the first year of anaerobic and aerobic incubation respectively (Table 4.9).

During the first year, the carbon released in the mixed sample from KRA (sample KRA-25) was more than double compared to the mixed samples from the aerated pilots (samples BRA-139 and WIE-216), for both anaerobic (GT_{365}) and aerobic (RT_{365}) conditions (Table 4.9). The higher carbon release in KRA compared to the aerated pilots is likely due to its greater organic content (Figure 4.4, top middle) and its higher share of easily degradable organic matter, evidenced by higher HI and lower OI (Table 4.7).

The combination of high organic content and the associated costs of aeration in a pilot with an average landfill height of 17 m which would require a high energy input made water recirculation the preferred initial in-situ stabilization strategy for the KRA pilot (Vereniging Afvalbedrijven, 2015b). The risk of potentially explosive mixtures with the combination of methane and air in aerated landfills with high organic matter content (Wu et al., 2023) aligns with the recommendation to prioritize anaerobic treatment before introducing aeration in landfill stabilization in landfills with high carbon content since methane valorisation is still an option (Rich et al., 2008; Ritzkowski, 2021).

Table 4.9. Mean and standard deviation of gas generation under aerobic and anaerobic conditions per landfill pilot and layer group. Experimental data, fitted data for one year and carbon released during first year of experiment.

Landfill pilot	Layer group	Experimental data (end of experiment)		Fitted data				Released during first year of experiment			
		GT (kg C/t_{dw})	RT (kg C/t_{dw})	GT_{365} (kg C/t_{dw})		RT_{365} (kg C/t_{dw})		GT (%)		RT (%)	
		mean	mean	mean	std	mean	std	mean	std	mean	std
BRA	top	0,3	3,7	0,2	0,2	3,0	0,4	79,2	5,2	82,9	9,2
	mid	1,5	8,4	1,2	0,9	6,9	2,5	79,7	5,3	81,2	3,9
	bot	2,8	8,9	2,2	3,4	6,7	2,0	78,3	10,2	75,4	3,6
WIE	top	1,7	7,7	1,5	1,3	6,5	3,4	80,1	15,6	83,9	1,6
	mid	2,8	17,2	2,2	0,8	15,2	1,1	80,5	5,3	88,5	3,5
	bot	1,3	8,8	1,0	0,1	7,9	1,1	83,0	0,7	90,2	0,1
KRA	mix	--	--	5,1	0,2	21,9	3,0	--	--	--	--
BRA	mix	--	--	1,3	0,1	8,0	0,2	--	--	--	--
WIE	mix	--	--	1,3	0,2	10,2	0,2	--	--	--	--

The samples from the aerated pilots BRA and WIE also showed greater organic matter degradation under aerobic incubation than under anaerobic conditions (Supplementary Information A, Figure S4.3.6.2). A Spanish study that used a wide variety of organic samples to determine carbon to nitrogen ratios using biodegradable fractions, found that in general, raw wastes, such as municipal solid waste, had higher aerobic biodegradable carbon compared to the anaerobically biodegradable carbon (Puyuelo et al., 2011). Under anaerobic conditions, organic matter degrades more slowly and to a lesser extent due to the lower energy yield available to heterotrophic bacteria and the inhibition of primary substrate degradation by oxygenases, which are only active under oxic conditions (Bastviken et al., 2004; Gebert & Zander, 2024; Zehnder & Svensson, 1986). Anaerobic conditions limit both the rate of hydrolysis and fermentation of complex organic matter, while complete mineralization of larger molecules like lignin is only possible under aerobic conditions (Blume et al., 2015; Stinson & Ham, 1995; H. Xu et al., 2024). Previous studies using landfilled MSW had also shown that aerobic conditions are more effective at mineralizing organic matter in waste, with 18 g TOC/kg DM reported in aerobic reactors compared to 10 g TOC/kg DM in anaerobic reactors (MSW, Fricko et al., 2021); and carbon release in aerobic reactors exceeding that in anaerobic reactors by more than a factor of three (Ritzkowski et al., 2016). These findings are consistent with the results of this study.

Stabilisation in the aerated pilots was expected to progress from the top downward, as oxygen enters from the surface. This was especially anticipated at WIE, which has been under over-extraction since the start of aeration. In WIE (drilling well 2, Figure 4.1, bottom), the top layer sample (WIE-206) exhibited one of the lowest organic matter degraded for one year of incubation, both in the gas production test and in the respiration test. Degradation rates increased with depth but then declined again in the bottom layer (Supplementary Information A, Figure S4.3.6.3). This was also observed in the carbon generation per layer

group (Table 4.8 and Table 4.9). A similar trend was observed in samples from compartment 11Z of BRA (BRA-101 to BRA-104, drilling well Ln6, Figure 4.1, middle). In contrast, samples from compartment 11N (drilling well En6; BRA-106 to BRA-109.5) showed a different pattern: degradation increased with depth under anaerobic conditions, while under aerobic conditions, degradation decreased to the middle layer and then increased again in the bottom layer (Supplementary Information A, Figure S4.3.6.2).

These variations suggest that waste heterogeneity may obscure consistent depth-related patterns of stabilization. For KRA, only mixed samples (KRA-25) were tested in the parallel incubation experiment, preventing depth-based comparisons.

4.3.2.2. Effect of sequential anaerobic – aerobic degradation

Cumulative gas production under anaerobic conditions in KRA waste over nearly 600 days ranged from 0.6 kg C/t_{dw} to 22.2 kg C/t_{dw} (Figure 4.5 and Supplementary Information A, Figure S4.3.7). High small-scale heterogeneity within parallels persisted with three out of nine samples, showing a different gas production over time. For example, sample KRA-3 showed the highest gas production among KRA samples. However, one of its two parallels released only two thirds of the carbon released bu the other parallel within 365 days. This heterogeneity suggests treating each parallel as an individual experiment.

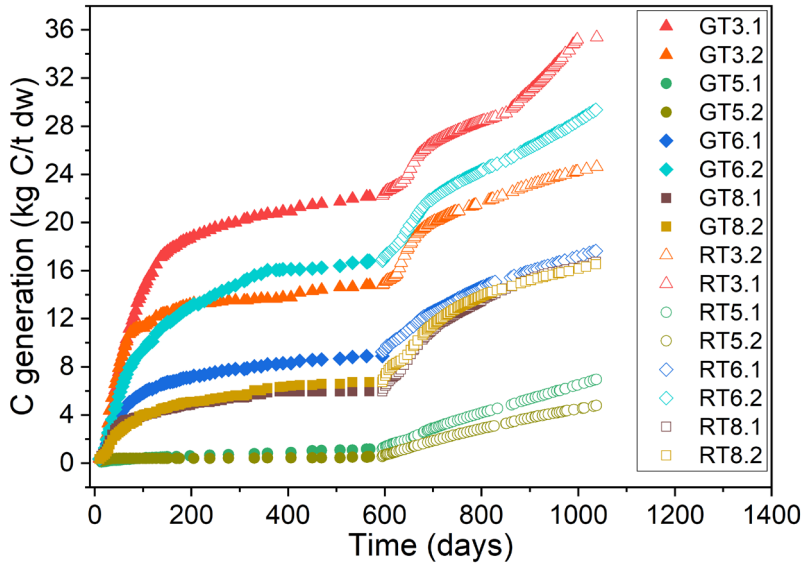

Figure 4.5. Pilot KRA. Course of carbon generation over time in laboratory experiment under anaerobic and sequential aerobic conditions.

After anaerobic degradability was exhausted, introducing oxygen as a terminal electron acceptor reactivated carbon generation, releasing an additional 59% to 750% of the carbon released under the previous anaerobic conditions . Interestingly, the samples with the lowest and highest gas production (GT5.2 and GT3.1) showed the highest and lowest additional release of carbon after changeover to aerobic conditions (750% and 59%, respectively)

(Figure 4.5). This suggests that most of the organic matter in sample KRA-3 was degradable under anaerobic conditions, whereas sample KRA-5 required aerobic conditions to achieve higher carbon generation. Sample KRA-3 showed the lowest R-index and the highest I-index, suggesting the presence of more immature organic matter with less refractory content (Sebag et al., 2016), which reflected in a significant share being degraded under anaerobic conditions. While sample KRA-5 had the highest OI and lowest HI compared to the rest of the samples in this experiment, indicating a lower share of easily degradable organic matter and a higher share of strongly resistant and refractory compounds (Carrie et al., 2012; Zander et al., 2023).

Other studies have observed significant additional carbon release when anaerobically degraded organic matter was exposed to aerobic conditions, with mineralization rates of 33% to 42% of the anaerobically degraded carbon occurring within 100 days after the transition to aerobic conditions (Gebert & Zander, 2024). A sequential anoxic–oxic degradation study using organic matter from a humic lake found that initial anoxic conditions enhanced the subsequent oxic degradation phase, enabling the system to reach the same total mineralization as a fully oxic treatment over the same period (Bastviken et al., 2004). Although overall mineralization did not increase, the anoxic pre-treatment appeared to prime the organic matter for more rapid oxidation once oxygen became available.

The depth from which the waste was sampled did not appear to significantly influence its activity (Figure 4.6). The high heterogeneity was reflected in its high standard deviation (Supplementary information A, Table S4.3.7) with exception of the bottom layer, which only had two samples.

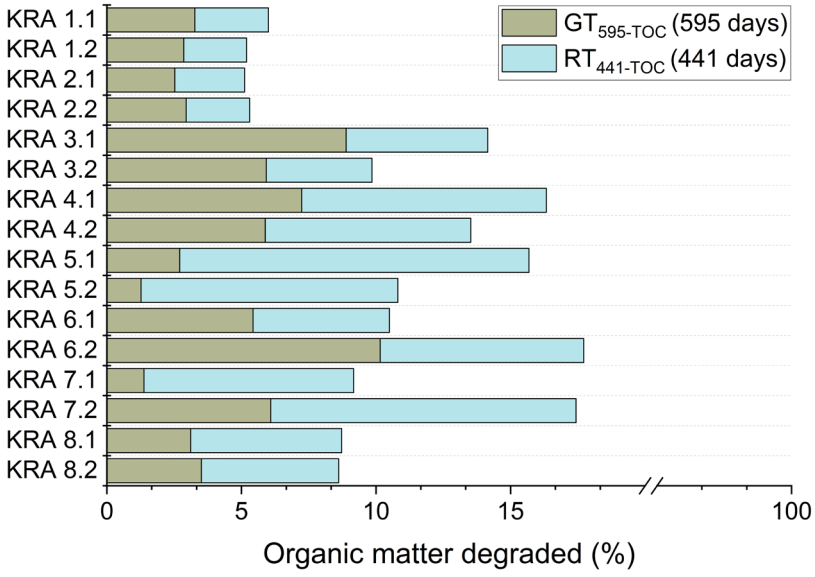

Figure 4.6. Pilot KRA. Organic matter degraded (expressed as % of TOC) in laboratory experiment under anaerobic and sequential aerobic conditions.

For all the samples, the amount of degraded organic matter (expressed as % of TOC) was estimated (Figure 4.6). By the end of the experiment, after 595 days of anaerobic incubation, on average 5% of the organic matter had degraded, while another 6% of the originally present organic matter were degraded during the subsequent 441-day aerobic incubation ($GT_{595\text{-}TOC}$, $RT_{441\text{-}TOC}$, Table 4.10). Most of the organic matter degraded during the first year of incubation ($GT_{365\text{-}TOC}$, $RT_{365\text{-}TOC}$, Table 4.10). The results suggest that a significant portion of the carbon would only be released under aerobic conditions (Figure 4.6), highlighting the importance of incorporating aeration into the pilot's long-term stabilization plan.

Table 4.10. Mean, median, maximum, minimum and standard deviation of gas generation under anaerobic and sequential aerobic conditions in Kragge.

	Parameter	Mean	Median	Max	Min	Std
Experimental data	GT_{595} (kg C/t_{dw})	9	9	22	1	6
	RT_{441} (kg C/t_{dw})	10	10	17	4	4
	Additional carbon released (%)	200	114	750	59	207
	$GT_{595\text{-}TOC}$ (% of TOC)	5	3	10	1	3
	$RT_{441\text{-}TOC}$ (% of TOC)	6	5	13	2	3
Fitted data	GT_{365} (kg C/t_{dw})	8	8	21	0	5
	RT_{365} (kg C/t_{dw})	8	8	15	4	3
	GT_{21} (kg C/t_{dw})	1	1	2	0	1
	$GT_{365\text{-}TOC}$ (% of TOC)	4	3	9	1	2
	$RT_{365\text{-}TOC}$ (% of TOC)	5	5	11	2	3

A laboratory-scale degradation experiment using a 60 L landfill simulation reactor (LSR) with sieved waste from an old municipal solid waste landfill under anaerobic conditions released 7.6% of the initial TOC pool (13%-14%) over 699 days. The LSR incorporated leachate recirculation per circulation sequence and was conducted at 34.5 ± 1.2 °C (Fricko et al., 2021). Differences in experiment scale (60L vs. 1L), temperature (35 °C vs. 20 °C), moisturizing control (included vs. not included), waste size (sieved vs. non-sieved) and the heterogeneity in the initial TOC (13%-14% vs 4%-30%) make direct comparison difficult. However, the TOC degradation in the LSR experiment (7.6%) falls within the range observed for anaerobic incubation of MSW (pilot KRA) in this study (1%-10%). The results also highlight the high heterogeneity of landfill waste.

A 21-day incubation period is commonly used to assess the short-term degradability of organic matter, as standardized in various studies and regulations (Gebert et al., 2011; Gebert & Zander, 2024; Hrad et al., 2013; Laner et al., 2012; Puyuelo et al., 2011; Ritzkowski et al., 2006; Zander et al., 2020). The German landfill ordinance (DepV, 2009) formalized this approach by setting a threshold of 20 L/kg for gas formation after 21 days at 35°C, based on the DIN 38414-8 method (DIN, 1985). To compare this limit with results from the present study conducted at lower temperatures, a temperature correction must be applied.

Temperature sensitivity of microbial activity is typically described using the Q10 value,

which quantifies the rate increase per 10°C rise in temperature. A Q10 of 2 is commonly used in soil studies (Fan et al., 2022; Q. Xu et al., 2024), implying that a reaction rate at 35°C is about double that at 25°C and approximately 2.8 times higher that at 20°C. Applying this correction, gas production of 7 L/kg at 20°C corresponds to approximately 20 L/kg at 35°C. Similarly, anaerobic carbon release in sediments has been shown to be 3.4 times higher at 35°C than at 20°C (Zander, 2022), and methanogenic activity in UASB reactors drops to one-third at 11°C compared to 22–24°C (Kettunen & Rintala, 1997a).

In this study, the highest 21 days gas release was 2.34 L/kg_{dw}. Applying a temperature correction factor of 3.4 yields an estimated 7.96 L/kg_{dw} at 35 °C. Although this remains below the 20 L/kg threshold of the German ordinance, the comparison primarly ilustrates the importance of temperature normalization when evaluating gas formation. An external laboratory test using the DIN 38414-8 method at 38 °C reported 11.3 L/kg_{dw} for the mixed KRA-25 sample (Ritzkowski, 2024), highlighting the strong influence of methodological and temperature differences on measured gas generation.

4.3.2.3. Kinetics of carbon generation

The carbon generation in most of the samples exhibited a non-linear trend over time (Figure 4.5, and Supplementary Information A, S4.3.5 to S4.3.7). The degradation rate remains constant in time, but the decay is non-linear, because the mass present is continuously decreasing. For most gas production experiments involving KRA samples, a two-phase exponential decay function discarding the initial lag-phase (up to 14 days) provided the best fit, indicating the presence of waste with different decay constants (Arndt et al., 2013; Li et al., 2024; Westrich & Berner, 1984). This pattern suggests that the initial phase involved the rapid consumption of easily degradable organic matter, followed by a slower phase as the less degradable organic matter became predominant (Gebert & Zander, 2024). In contrast, a one-phase exponential decay function best described most of the respiration tests on KRA samples, as well as most of the gas production and respiration tests for the BRA and WIE samples. In this case, the lag-phase at the beginning of the experiment did not appear to affect the short-term analysis (21 days), with better model fitting achieved when the lag-phase data was included. The fitting was not possible for two samples in KRA during the respiration test (RT3.1 and RT4.1, supplementary information A, Table S4.3.2.2), which showed an increasing activity after more than 50 days of reduced activity. The high statistical significance of the exponential decay models (Supplementary information A, Tables S4.3.2.1 - S4.3.2.6) indicates an accurate representation of carbon generation kinetics.

4.3.2.3.1. Carbon potential (Y_0)

For most samples (97%), it was possible to extrapolate the total carbon potential (Y_0, see section 2.4.2) using exponential fitting. Some fitted samples, however, produced unrealistic results, e.g. negative Y_0 values, likely due to very low reactivity (< 0.5 g C/kg_{DW}) or excessively high Y_0 values, probably reflecting the higher uncertainty in samples that did not reach a

plateau (e.g. sample WIE-216, Supplementary information A, Figure S4.3.6.3). In such cases, Y_0 was estimated using linear correlation between the carbon released over 365 days (GT_{365}, RT_{365}) and Y_0 (GT_{Y0}, RT_{Y0}) for each pilot and experiment (Supplementary information A, Section S4.3.4). The potentially degradable organic matter normalised to TOC ($GT_{Y0\text{-}TOC}$ and $RT_{Y0\text{-}TOC}$; Table 4.5 and Figure 4.2) was then calculated for all samples (Figure 4.7 and Table 4.11).

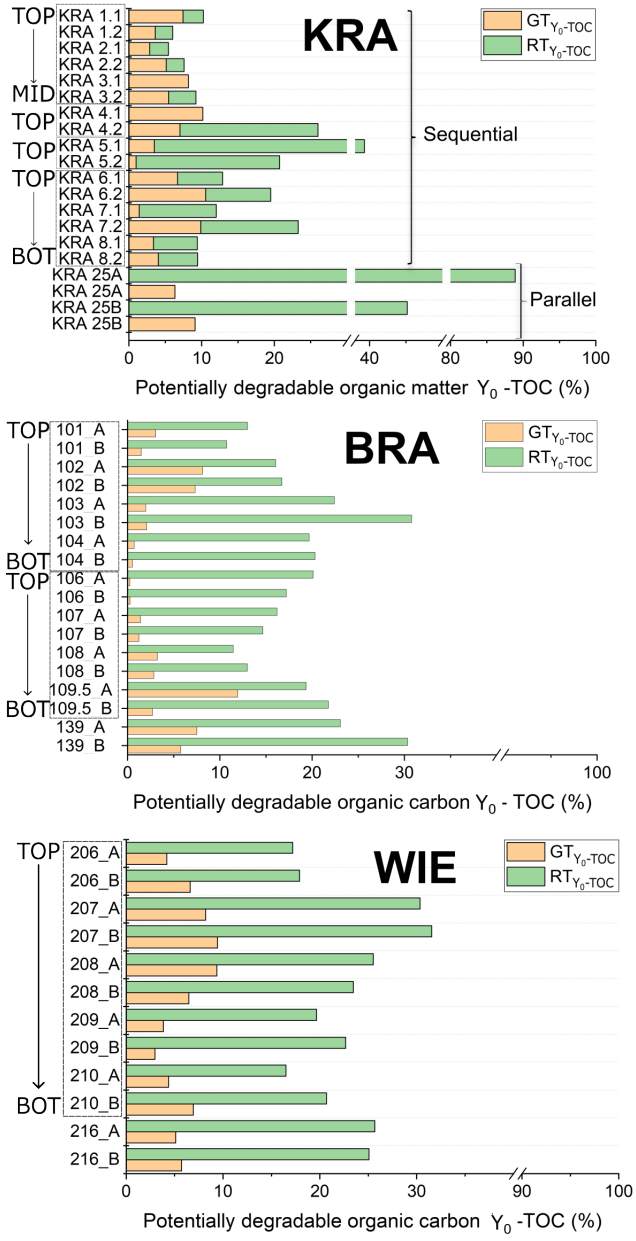

Figure 4.7. Potentially degradable organic matter during the gas production ($GT_{Y0\text{-}TOC}$) and respiration ($RT_{Y0\text{-}TOC}$) in KRA (fitting not possible for RT-3.1 and RT-4.1, left), BRA (middle), and WIE (right) pilots.

As discussed in the parallel incubation experiment, aerobic degradation generally enhanced the breakdown of organic matter by providing higher energy yields for microorganisms and enabling oxygenase-driven reactions, which accelerate the mineralization of complex compounds like lignin. This was reflected in higher $RT_{Y0\text{-}TOC}$ compared to anaerobic $GT_{Y0\text{-}TOC}$ across all pilots (Table 4.11 and Figure 4.7). In KRA, aerobic degradation (parallel experiment, sample KRA-25) released ten times the carbon released under anaerobic degradation ($RT_{Y0\text{-}TOC}$/ $GT_{Y0\text{-}TOC}$, Table 4.11). Although KRA-25 did not reach a plateau during the respiration test, indicating greater uncertainty, the results nonetheless suggest that this pilot, currently under mainly anaerobic conditions, holds significant potential for enhanced degradation under future aeration. In the aerated pilots, BRA and WIE, $RT_{Y0\text{-}TOC}$ values were also higher than $GT_{Y0\text{-}TOC}$, but the differences were smaller than in KRA (factor 4 and 5 respectively) (mixed samples, Table 4.11).

Table 4.11. Mean of carbon degraded during laboratory experiment and carbon potentially degradable per pilot and experiment. Standard deviation in brackets.

Landfill pilot	KRA		BRA	WIE
Experiment	Parallel	Sequential	Parallel	Parallel
$GT_{Y0\text{-}TOC}$ (% of TOC)	8 (2)	6 (3)	4 (3)	6 (2)
$RT_{Y0\text{-}TOC}$ (% of TOC)	67 (31)	10 (9)	19 (6)	23 (5)
$GT_{365\text{-}TOC}$ + $RT_{365\text{-}TOC}$ (% of TOC)	-	9 (4)	-	-
$GT_{595\text{-}TOC}$ + $RT_{441\text{-}TOC}$ (% of TOC)	-	11 (4)	-	-
$GT_{Y0\text{-}TOC}$ + $RT_{Y0\text{-}TOC}$ (% of TOC)	-	15 (10)	-	-
$RT_{Y0\text{-}TOC}$ / $GT_{Y0\text{-}TOC}$ (all samples)	10 (6)	4 (6)	16 (22)	4 (1)
$RT_{Y0\text{-}TOC}$ / $GT_{Y0\text{-}TOC}$ (mixed samples)	10 (6)	-	4 (1)	5 (0)
% of the potentially degradable organic matter mineralized during the experiment ($GT_{595\text{-}TOC}$ + $RT_{441\text{-}TOC}$)	-	76 (19)	-	-
% of the potentially degradable organic matter mineralized during the 1st year of experiment (GT)	70 (15)	76 (19)	58 (18)	49 (20)
% of the potentially degradable organic matter mineralized during the 1st year of experiment (RT)	36 (12)	73 (22)	61 (11)	82 (8)

When comparing pilots, the anaerobic pilot (KRA) showed a higher fraction of potentially degradable organic matter mineralized during the first year of anaerobic incubation (GT) than the aerated pilots, while the aerated pilots showed a higher fraction degraded during aerobic incubation (RT). Moreover, both $RT_{Y0\text{-}TOC}$ and $GT_{Y0\text{-}TOC}$ where higher in KRA than in the aerated pilots, suggesting greater availability of degradable waste in KRA. This indicates that KRA still retains substantial long term degradation potential, whereas the aerated pilots appear more stabilized.

In the sequential experiment (KRA), the sum of potentially degradable organic matter normalized to TOC during anaerobic and sequent aerobic incubation ($GT_{Y0\text{-}TOC}$+$RT_{Y0\text{-}TOC}$) averaged 15% (Table 4.11) ranging from 5% in sample KRA 2.1 to 39% in sample KRA 5.1 (Figure 4.7, left). Comparing the total organic matter degraded at the end of the experiment (GT_{595}+RT_{441}; Figure 4.5) with the estimated potential (GT_{Y0} +RT_{Y0} ; Figure 4.7) revealed

strong variability: in sample KRA 3.2, more than 100% of the potentially degradable organic matter was mineralized (indicating complete degradation), while in sample KRA 5.1, only 40% was degraded. The low degradability of KRA 5.1 aligns with its higher share of strongly resistant and refractory compounds, as also indicated by its high OI (112 mg CO_2/g TOC) and low I-index (0.27) compared to other samples (Figure 4.4, bottom middle and right). On average, 76% of the potentially degradable organic matter was mineralized during this experiment (Table 4.11).

In KRA, sequential degradation also revealed higher mineralization under aerobic conditions (73%) compared to parallel aerobic degradation (36%) during the first year of incubation (Table 4.11), highlighting the enhancement effect of a preceding anaerobic stage. However, extrapolated RT_{y0} values appeared higher in the parallel experiment than in the sequential experiment, thought this may be influenced by the high uncertainty of the parallel samples, which did not reach a plateau. The higher ratio of aerobic to anaerobic degradation observed in KRA during the parallel incubation, compared to the sequential setup, suggests that a significant portion of the organic matter was already degraded anaerobically before the onset of aerobic conditions.

4.3.2.3.2. Degradation rate constants (k values)

In laboratory experiments, the k value is mainly influenced by the amount and availability of biodegradable waste. In contrast, the large scale and less favourable conditions for degradation in landfills often lead to lower k values (Fei et al., 2016). A review of available MSW biodegradation data from 49 laboratory experiments and 57 landfill studies demonstrated that decay rates constant (k values) observed in laboratory experiments were, on average, 31 times higher than those measured in landfills or recommended by LandGEM for waste with similar composition and methane generation potential (Fei et al., 2016).

The k values from the laboratory tests exceeded even the k value for rapidly degradable waste in the Afvalzorg multi-phase model (0.187 y^{-1}, Figure 4.8). This difference was especially pronounced in the KRA pilot, where the average k value during the first phase of degradation in gas production (GT, sequential experiment) was 9.2 y^{-1}, 49 times higher than the model value. These elevated values suggest shorter half-lives for the organic waste fractions, likely due to waste disturbance during drilling and sampling, which enhanced surface accessibility and exposed previously enclosed easily degradable organic matter. They also indicate that the waste in KRA is inherently more degradable than average, while the lower in-situ rates observed in the field are likely due to unfavourable conditions (e.g. dryness, low pH, or inhibition). Although Afvalzorg's k values are broadly consistent with IPCC recommendations, the model accounts for reduced field degradation efficiency by adjusting the degradable organic carbon fraction (DOCf) and the DOC_S percentage (%DOC) per waste category, thereby compensating for the discrepancy between laboratory and field behaviour.

In most samples, carbon generation levelled off or ceased within one year, indicating that the total carbon potential was largely exhausted during this period. This is supported by the good correlation between the carbon potential (Y_0) and carbon generated within one year (GT_{365} and RT_{365}; see Supplementary information A, Figure S4.3.4). The rapid depletion of easily degradable organic matter was also reflected in lower k values during subsequent aerobic respiration (RT) compared to the parallel test (Figure 4.8).

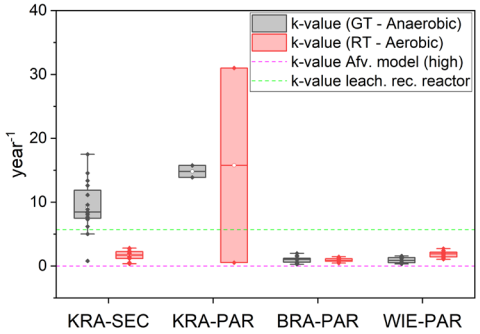

Pilot	KRA		BRA	WIE
Exp.	Parallel	Sequential	Parallel	Parallel
k_1 - GT	14.8 (1.3)	9.2 (4)	1,0 (0.5)	0,9 (0.5)
k_2 - GT	1.1 (0.5)	0.9 (0.6)	-	-
k_1 - RT	15.8 (21.5)	1.6 (0.8)	1,0 (0.3)	1,8 (0.5)
k_2 - RT	0.3 (-)	-	-	-

Figure 4.8. Degradation rate constants (k values) for the fast degradation rate (k1) in waste samples from KRA, BRA, and WIE under anaerobic (GT) and aerobic (RT) conditions, compared to the Afvalzorg multi-phase model for highly decomposable waste and a referential water recirculation reactor k value (Bilgili et al., 2007) (left). Mean k-values and standar deviation values in brackets for the three pilots (right). For box plots: box = 25th-75th percentile, line = median, whiskers = 1.5 IQR, circle symbol = mean, rhombus symbol outside whiskers = outliers.

In the parallel experiments, k values for RT were up to twice as high as those for GT because oxygen availability allowed faster consumption of readily degradable substrates, leading to a rapid initial reaction followed by earlier stabilization. However, the two RT samples from KRA showed high variability (Figure 4.8, left), likely due to greater uncertainty as they had not reached a plateau. The aerated pilots BRA and WIE, which had lower organic content, exhibited lower k values than KRA (Figure 4.8, left). On average, the k value in KRA was up to 16 times the ones for BRA and WIE (Figure 4.8, right), indicating a greater presence of easily degradable organic matter in KRA. In BRA, k values were similar for GT and RT, suggesting little advantage of aerobic over anaerobic conditions in terms of degradation rates, though the total amount of carbon degraded differed. In contrast, WIE, showed k values during RT that were twice as high as during GT (Figure 4.8). The k values from anaerobic tests (GT) were closer to default values from various first-order decay models, which typically range between 0.1 y^{-1} and 0.7 y^{-1}, as well as the values reported in the literature for different waste or landfill categories (Mou et al., 2015; Scharff & Jacobs, 2006).

For comparison, a Turkish study evaluating the biochemical methane potential of landfilled solid waste, where organic waste comprised 44% of the waste composition, reported k-values of 5.7 y^{-1} for a leachate-recirculated reactor, and 4.4 y^{-1} for a non-recirculated reactor (Bilgili et al., 2009). Despite the similar organic waste composition in KRA (~44%) and its use of water recirculation, KRA showed a mean k value of 15 y^{-1} (GT: 0.8-17.5 y^{-1}), suggesting higher degradability than average. The wide variability in KRA may be linked to waste composition, as the samples were neither sieved nor homogenised, introducing heterogeneity and

fractions with higher organic carbon content and water content (Figure 4.4).

4.3.3. Comparison of carbon generation with model predictions and field recovery

In KRA, the anaerobic pilot, carbon generation over 365 days from anaerobic incubation (GT_{365}) was compared to both the carbon recovered from the pilot and the modelled carbon generation using the NV Afvalzorg Multiphase Landfill Gas Model (version 2022) for the year 2021. For the aerated pilots, BRA and WIE, GT_{365} was compared to the model's estimates for the year 2023, while carbon generation from aerobic incubation (RT_{365}) was compared to the carbon recovered from the pilots in 2023 (Figure 4.9).

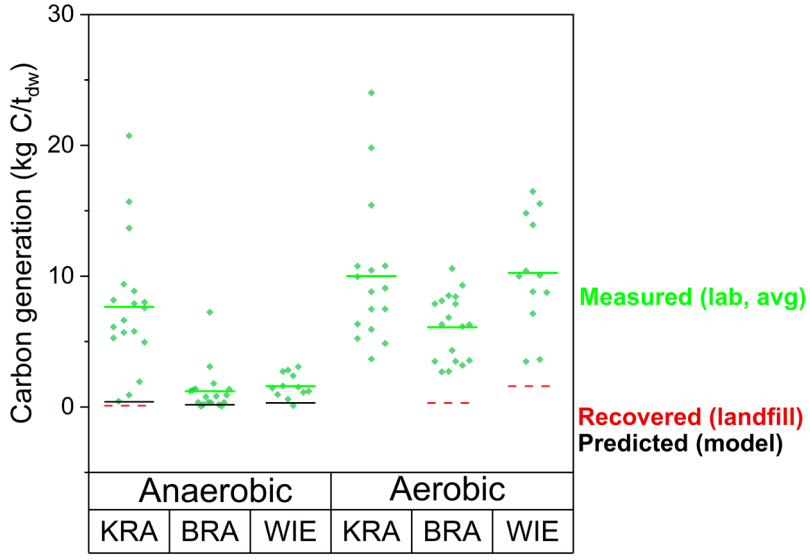

Figure 4.9. Carbon generation under anaerobic and aerobic conditions measured for 365 days (GT_{365} and RT_{365}) in the laboratory (average in green line) and comparison with the predicted (black line) and extracted carbon (red dotted line) for 1 year in KRA, BRA and WIE.

In all pilots, the average cumulative carbon generation under anaerobic laboratory conditions in one year (GT_{365}) was significantly higher the model predictions, specially at KRA (Table 4.12, Figure 4.9). This difference was primarily due to the lower GT_{365} values in the aerated pilots compared to KRA, indicating greater stability of waste in the aerated sites.

In the aerated pilots, the recovered carbon was closer to the carbon generated under aerobic laboratory conditions (RT_{365}, Table 4.12, Figure 4.9). These findings suggest that although the overall reactivity of the waste is low, there remains untapped gas potential in the landfilled waste under in-situ conditions.

The predicted carbon generation for KRA was four times higher than the recovered carbon (Table 4.12), indicating a nominal recovery efficiency of only 24%. This aligns with previous findings for Kragge II (Vereniging Afvalbedrijven, 2015b) and a study of 23 Danish low-organic content landfills, where gas collection efficiencies ranged from 13% to 86% (Duan

et al., 2022). In that study, a reference from other countries was included, one of them was the Netherlands with a gas collection efficiency of 36%. The recovery efficiency was estimated based on the methane collection rate relative to the sum of collection, emission, and oxidation rates, rather than the ratio of recovered to modelled gas generation, due to high model uncertainties (Duan et al., 2022). In contrast, the carbon recovered from both aerated pilots exceeded the anaerobic base-case model predictions by far (Table 4.12, Figure 4.9). This outcome was expected since the model does not account for the higher carbon release as a result of aeration but rather represents a strictly anaerobic scenario.

Table 4.12. Mean of carbon generation during laboratory experiment, recovered and modelled for one year per pilot and experiment. Units are in kg C/t_{dw}.

Mode	Pilot	KRA		BRA	WIE
	Experiment	Parallel	Sequential	Parallel	Parallel
Anaerobic	Laboratory (GT_{365})	5,1	8,0	1,2	1,6
	Recovered (2021 or 2023)	0,1	0,1	-	-
	Modelled (2021 or 2023)	0,4	0,4	0,2	0,3
Aerobic	Laboratory (RT_{365})	21,9	8,3	6,1	10,3
	Recovered (2021 or 2023)	-	-	0,3	1,6

Model uncertainty must also be considered, particularly regarding the type and quantity of landfilled waste (Chapter 2, section 2.4). Additionally, the Afvalzorg model is partially based on the IPCC waste model, which was developed to help countries estimate methane emissions from solid waste disposal sites and ensure comparability. The default parameters in this model represent expert best estimates under average conditions but were not intended to fully capture site-specific landfill conditions (Scharff & Jacobs, 2006). Methane emissions from three Dutch landfills using six different models were between 40% and 570% of the measured whole-site emissions. One of the used models was the Afvalzorg multi-phase model and results suggested an underestimation of methane emissions with respect to the measurements (Scharff & Jacobs, 2006).

Another important consideration for the aerated pilots is that, while controlling aerobic and anaerobic conditions in laboratory experiments is relatively straightforward due to the smaller scale, aerated pilots persistently contain anaerobic zones where methane concentrations are higher (Meza et al., 2022). A laboratory-scale lysimeter experiment using municipal solid waste found that, with O_2 injection, the proportion of CH_4 oxidation gradually exceeded that of aerobic waste degradation, with a maximum of 21.4% CO_2 produced by CH_4 oxidation compared to approximately 16.0% CO_2 produced by aerobic degradation (Ma et al., 2023). This suggests that although oxygen is primarily used for aerobic waste degradation in the laboratory, methane oxidation may be the dominant process in the field.

Further uncertainty is introduced by the technical limitation of gas extraction and aeration systems. The number and distribution of gas wells within a landfill significantly influence

the volume of gas that can be extracted relative to the total gas produced (Themelis & Ulloa, 2007; van Turnhout et al., 2020). For instance, in KRA, three out of the thirteen gas wells showed no gas flow, while in BRA, gas extraction in compartment 11Z was particularly limited, with 35 out of 64 wells showing no flow at all (Meza et al., 2022).

Water content in the sampled waste varied significantly, especially in the KRA pilot (Figure 4.4, top left) which showed the highest water levels in the top layer, a decrease in the middle layer, and an increase in the bottom layer (Supplementary information A, Figure S4.3.1). This pattern suggests large variations in water content caused by a large heterogeneity in hydraulic conductive properties and the presence of dry pockets. Controlling and monitoring water distribution in landfills with water recirculation remains a major challenge. In many cases, the added water is insufficient to reach field capacity (Benson et al., 2007). Field capacity refers to the amount of water that remains after draining due to gravity with a specific pressure head boundary (He & Hu, 2022; Zotarelli et al., 2010). Several studies have measured water retention capacity in MSW under varying conditions. Results showed that water content decreased with increasing suction and that the water content varies between 21 and 60 percent wet weight ($\%_{ww}$) (He & Hu, 2022). These differences likely stem from variations in factors such as waste composition, age, the diameter of the compression cell, and applied stress. In general, landfill field capacity is approximately $45\%_{ww}$ (equivalent to $82\%_{dw}$) and is necessary for optimal biodegradation across the entire waste mass (Benson et al., 2007). In KRA, the highest gas production was observed in a sample with a water content of $81\%_{dw}$, while the sample with the lowest water content ($43\%_{dw}$) also exhibited the lowest gas and respiration rates. Again, our results fall within the range measured by others.

The limited degradability of waste in the landfills may be attributed to several factors, including water and temperature constraints (Fei et al., 2016; Kettunen & Rintala, 1997a), substrate type and microbial adaptation (Kettunen & Rintala, 1997b), inhibition due to the accumulation of metabolic products, or the intrinsic degradability of the waste organic matter itself. One of the main differences between laboratory scale and full-scale degradation processes is caused by temperature (Ritzkowski & Stegmann, 2012). Although maximum temperatures in the pilots can reach 37°C to 67°C, the mean temperature (2m to 12 m depth from the surface) ranged from 13°C to 24°C over the year (Chapter 2, Figure 2.6 and Table 2.1). The higher hydrolysis in the areas with higher temperature was expected to compensate areas with lower temperature to not represent a significative difference with the incubation temperature of the laboratory experiment (20°C). In any case, temperature differences alone do not explain the large difference (factor 87) between GT_{365} and the carbon recovered via active gas extraction in KRA. A pilot-scale UASB reactor used to study treatment of municipal landfill leachate at low temperatures (13-23 °C) and in on-site conditions for 226 days found that the specific methanogenic activity at 11°C remained one third of that at 22-24°C (Kettunen & Rintala, 1997a).

4.3.4. Correlation of carbon generation with waste properties

The relationships between waste properties and carbon generation were explored for both short- and long-term anaerobic gas production (GT) and aerobic respiration (RT). All available samples, including pre-test and mixed pilot layer samples, were included in the analysis. Significant correlations ($p < 0.0001$) are presented in Table 4.13, while pilot-specific results and sample sizes are detailed in the supplementary material (Tables S4.3.9.1–S4.3.9.7).

Water content (WC)

Water is essential for hydrolysis and provides the medium for microbial activity, yet excessive (immobile) water can inhibit degradation. This complexity makes direct correlations difficult, as multiple factors interact. WC was significantly correlated with several indicators of carbon generation, including anaerobic carbon potential (GT_{Y0}), short- and long-term respiration (RT_{21}, RT_{365}), and gas production (GT_{21}, GT_{365}) (Table 4.13). The strongest associations were observed in WIE, where higher WC supported aerobic biodegradation, particularly RT_{365} (Figure 4.10, top left). This may partly reflect correlations between WC and total organic carbon (TOC), and TOC and RT_{365} (Supplementary information A, Table S4.3.9.6).

In KRA, overall correlations between WC and gas production were weak, but the bottom layer exhibited both the lowest median WC (Supplementary information A, Figure S4.3.1) and the lowest median carbon potential (Supplementary information A, Figure S4.3.9.1). Similarly, in BRA and WIE, the top layers showed both the lowest WC and the lowest carbon potential, suggesting WC was a limiting factor. Anaerobic bacteria generally require water contents above $67\%_{dw}$ for optimal activity (Themelis & Ulloa, 2007), and no water was added during the experiments. Overall, correlations between WC and carbon generation were limited and varied strongly among samples (Figure 4.10).

WC correlated strongly with TOC, loss on ignition (LOI), and hydrogen index (HI) (Table 4.13), which indicate immature, easily degradable organic matter. This confirms the role of organic matter in supporting water retention and microbial activity. However, the relationship between WC and biodegradation remains highly context-dependent, influenced by stratification, waste composition, and hydrophobic materials (e.g. plastics in KRA), which disrupt water distribution and lead to heterogeneous outcomes.

Electrical conductivity (EC)

At the overall level, electrical conductivity (EC) was strongly and positively correlated with the Oxygen Index (OI), indicating that more oxidized or humified organic matter is associated with higher ionic mobility. This relationship was most pronounced in the aerated pilots (BRA and WIE), where oxidative processes likely enhanced both EC and OI (Supplementary information A, Table S4.3.9.4 and Table S4.3.9.6). EC reflects ion mobility in pore water or along surfaces, and in porous systems is largely governed by water content and connectivity. Stabilized organic matter is more hydrophilic than fresh waste, which

may explain the stronger association of water with oxidized OM.

EC also correlated with carbon generation metrics. In BRA, EC was significantly linked to gas generation, while in WIE the correlations were weaker and not significant, possibly due to differences in ionic composition or water transport. No correlation was found in KRA, likely due to limited sample numbers.

Organic matter quality (TOC and LOI)

TOC and LOI were strongly correlated with HI, confirming their role as indicators of immature organic matter. Both parameters were negatively correlated with OI (a marker of refractory material) but positively correlated with the refractory index (R-ind) in KRA samples. The aerated pilots, however, showed the opposite trend, with TOC and LOI negatively correlated with R-ind (Supplementary information A, Table S4.3.9.4 and Table S4.3.9.6).

TOC and LOI also correlated well with carbon generation (Table 4.13), underscoring the central role of organic matter in driving microbial degradation. Within pilots, TOC was positively correlated with GT_{365} and GT_{Y0} in KRA and with RT_{365} and RT_{Y0} in BRA and WIE (Figure 4.10, top left), suggesting that higher organic content supports long-term carbon turnover under anaerobic and aerobic conditions.

Rock-Eval parameters

As discussed in Section 3.1.2, HI (labile organic matter) and OI (refractory, oxidized compounds) showed the expected negative correlation, as did I-index (immature OM) and R-index (refractory OM). However, in KRA, HI also correlated positively with R-ind, possibly due to some form of inhibition or limiting microbial access to both labile and stable OM. By contrast, the aerated pilots showed the expected negative correlation. This deviation in KRA highlights how physical barriers, such as encapsulation, can override chemical indicators of biodegradability.

HI was positively correlated with gas production and respiration outcomes, confirming its predictive value for identifying reactive waste. This was especially clear in WIE, where HI strongly correlated with both RT_{365} and RT_{Y0}. In contrast, R-ind in WIE correlated negatively with carbon generation indicators, particularly RT_{Y0}, and GT_{365}, reflecting the inhibitory role of refractory materials, especially under aerobic conditions. Similar negative effects of R-ind were also observed in BRA.

Table 4.13. Pearson's coefficient r for correlations between material characteristics and gas production (GT) and respiration test (RT) related to dry weight for 21 days and 365 days in BRA, WIE and KRA pilots. WC = water content related to dry weight ($\%_{dw}$), EC = electroconductivity, TOC = total organic carbon ($\%_{dw}$), HI = Hydrogen index, OI = Oxygen index, R-ind = R-index, LOI = organic matter content, Y_0 = carbon potential. Bold = Pearson's coefficient r significant on a confidence level of 99.99%, two-sided test.

	WC	EC	TOC	HI	OI	R-ind	LOI	GT_{Y_0}	GT_{365}	GT_{21}	RT_{Y_0}	RT_{365}	RT_{21}
WC	1.00	0.44	0.66	0.62	-0.39	0.33	0.65	0.54	0.44	0.46	0.57*	0.50*	0.49*
EC	--	1.00	0.50	0.09	0.88	-0.25	0.95	0.48	0.58	0.82	0.71*	0.54*	0.86*
TOC	--	--	1.00	0.92	-0.51	0.56	0.90	0.68	0.64	0.63	0.74*	0.87*	0.70*
HI	--	--	--	1.00	-0.51	0.58	0.82	0.63	0.56	0.57	0.44*	0.61*	0.37*
OI	--	--	--	--	1.00	-0.70	-0.71	-0.29	-0.23	-0.19	0.49*	0.49*	0.73*
R-ind	--	--	--	--	--	1.00	0.54	0.27	0.17	0.28	-0.47*	-0.81*	-0.49*
LOI	--	--	--	--	--	--	1.00	0.49	0.52	0.43	0.89*	0.98*	0.98*
GT_{Y_0}	--	--	--	--	--	--	--	1.00	0.87	0.80	0.53*	0.64*	0.54*
GT_{365}	--	--	--	--	--	--	--	--	1.00	0.88	0.60*	0.62*	0.58*
GT_{21}	--	--	--	--	--	--	--	--	--	1.00	0.74*	0.56*	0.72*
RT_{Y_0}	--	--	--	--	--	--	--	--	--	--	1.00	0.79	0.85
RT_{365}	--	--	--	--	--	--	--	--	--	--	--	1.00	0.77
RT_{21}	--	--	--	--	--	--	--	--	--	--	--	--	1.00

* Correlation does not include sequential experiment

Predictive value of short-term tests

Short-term carbon generation tests (GT_{21}, RT_{21}) were generally good predictors of long-term outcomes (Table 4.13). Strong correlations were observed across the dataset between short- and long-term gas production and respiration, confirming that early-phase respiration tests can be used to estimate aerobic stability over longer timescales.

However, predictive strength varied by pilot (Figure 4.10, bottom left and right). BRA showed the highest consistency, particularly between GT_{365} and GT_{Y0}, while WIE showed weaker relationships, likely due to low anaerobic reactivity and reduced accessibility of labile carbon. This demonstrates that while short-term tests are valuable screening tools, their reliability depends on waste composition, degradation potential, and degree of stabilization. Similar findings have been reported previously: Gebert et al. (2011) observed strong correlations between gas production at 21 days and over seven months in MSW from German landfills, although the relationship weakened at low reactivity (<10 L/kgdw). Gebert et al. (2019) also found high predictive power ($R^2 > 0.9$) over a two-year incubation of dredged sediments but cautioned against over-reliance in low-reactivity materials.

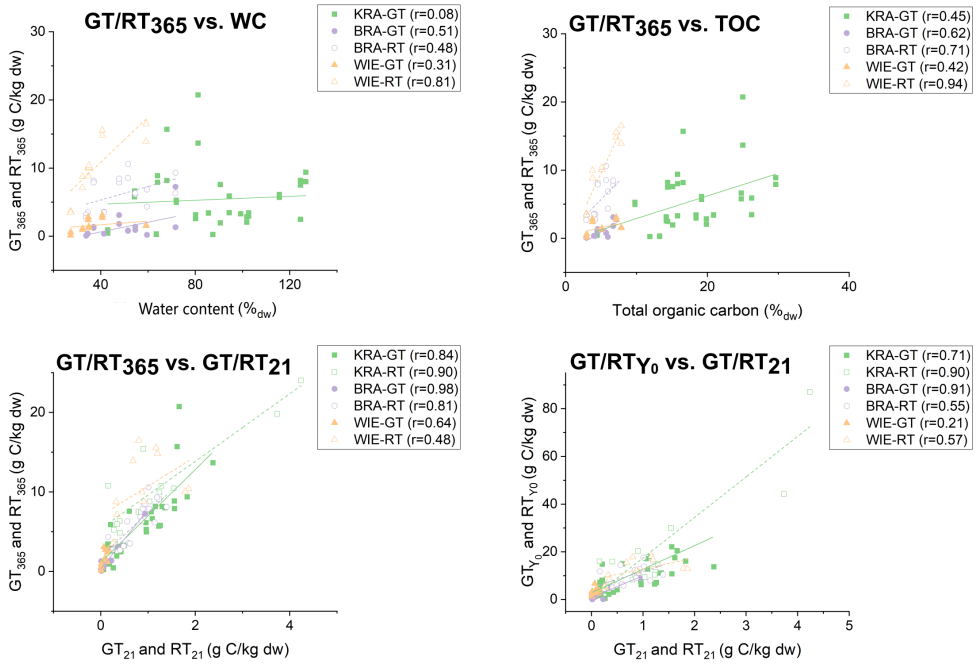

Figure 4.10. Relationship between water content and carbon generation at 365 days (GT_{365} and RT_{365}) (top left), total organic carbon and carbon generation at 365 days (GT_{365} and RT_{365}) (top right), carbon generation at 21 days (GT_{21} and RT_{21}) and 365 days (GT_{365} and RT_{365}) (bottom left), and carbon generation at 21 days (GT_{21} and RT_{21}) and carbon potential Y_0 (GT_{Y0} and RT_{Y0}) (bottom right).

4.4. Summary and conclusions

This study provides a comprehensive analysis of landfill waste characterization and gas generation kinetics. Carbon potential and decay rate constants (k-values) vary significantly across different pilot samples. Wastes from the anaerobic pilot (KRA) showed higher water content and organic content, along with a greater share of easily degradable and less refractory organic matter. These characteristics were reflected in faster degradation kinetics compared to the aerated pilots (BRA and WIE) samples.

Aerobic conditions consistently led to significantly higher carbon generation than anaerobic conditions in the parallel incubation. Across all pilots, respiration tests released at least four times more carbon, demonstrating the effectiveness of aeration in enhancing waste breakdown. Notably, in the sequential experiment, the introduction of aerobic conditions after anaerobic degradability was exhausted substantially reactivated carbon generation. An additional 59-750% of carbon was released during the sequential aerobic phase compared to the preceding anaerobic phase. This underscores the potential of aeration in accelerating waste stabilization and confirms presence of organic matter that cannot be further degraded under anaerobic conditions but requires oxygen as a terminal electron acceptor to be further mineralized.

After five years of stabilization, almost all anaerobically degradable organic carbon had been depleted in all three pilots, with anaerobic carbon potentials ($GT_{Y0\text{-}TOC}$) in the excavated wastes falling below 10% of the total organic carbon present in the sample. The aerated pilots (BRA and WIE) showed significantly lower carbon potential under aerobic conditions ($RT_{Y0\text{-}TOC}$), averaging 19% in BRA and 23% in WIE, indicating an enhanced level of stabilization. In contrast, the anaerobic pilot (KRA) still contained considerable amounts of aerobically degradable organic matter in the excavated wastes. However, degradation in the anaerobic pilot could be limited by low waste permeability reducing waste accessibility and impeding gas and water flow.

Laboratory tests consistently produced carbon generation values that exceeded both model predictions and estimates based on on-site extractions. This highlights the presence of untapped gas potential, which may be released through further physical breakdown and increased surface exposure of waste. Furthermore, strong correlations between short-term and long-term carbon generation suggest that short-term tests can be useful predictors of long-term gas potential. Total gas generation is largely governed by the quantity of easily degradable carbon consumed in the early incubation phase, though waste heterogeneity and site-specific factors, such as water content and the presence of non-degradable materials, modulate these relationships.

The data generated in this study provide robust, site-specific insights into carbon degradation dynamics, enabling refinement of key model parameters such as the degradation rate constant (k) and the degradable organic carbon fraction (DOCf). By bridging the gap between laboratory findings and in-situ landfill conditions, the results support more accurate calibration of predictive models like the Afvalzorg multi-phase model.

Bibliography

1. Afvalzorg. (2022). Multiphase landfill gas generation model. Version 2022. https://www.afvalzorg.com/landfill-gas/lfg-models/multiphase-landfill-gas-generation-model
2. Arndt, S., Jørgensen, B. B., LaRowe, D. E., Middelburg, J. J., Pancost, R. D., & Regnier, P. (2013). Quantifying the degradation of organic matter in marine sediments: A review and synthesis. Earth-Science Reviews, 123, 53–86. https://doi.org/10.1016/J.EARSCIREV.2013.02.008
3. Bastviken, D., Persson, L., Odham, G., & Tranvik, L. (2004). Degradation of dissolved organic matter in oxic and anoxic lake water. Limnology and Oceanography, 49(1), 109–116. https://doi.org/10.4319/lo.2004.49.1.0109
4. Benson, C. H., Barlaz, M. A., Lane, D. T., & Rawe, J. M. (2007). Practice review of five bioreactor/recirculation landfills. Waste Management, 27(1), 13–29. https://doi.org/10.1016/J.WASMAN.2006.04.005
5. Bilgili, M. S., Demir, A., & Özkaya, B. (2007). Influence of leachate recirculation on aerobic and anaerobic decomposition of solid wastes. Journal of Hazardous Materials, 143(1–2), 177–183. https://doi.org/10.1016/J.JHAZMAT.2006.09.012
6. Bilgili, M. S., Demir, A., & Varank, G. (2009). Evaluation and modeling of biochemical methane potential (BMP) of landfilled solid waste: A pilot scale study. Bioresource Technology, 100(21), 4976–4980. https://doi.org/10.1016/j.biortech.2009.05.012
7. Blume, H. P., Brümmer, G. W., Fleige, H., Horn, R., Kandeler, E., Kögel-Knabner, I., Kretzschmar, R., Stahr, K., & Wilke, B. M. (2015). Scheffer/schachtschabel soil science. In Scheffer/Schachtschabel Soil Science. https://doi.org/10.1007/978-3-642-30942-7
8. Brandstätter, C., Prantl, R., & Fellner, J. (2020). Performance assessment of landfill in-situ aeration – A case study. Waste Management, 101, 231–240. https://doi.org/10.1016/j.wasman.2019.10.022
9. Carrie, J., Sanei, H., & Stern, G. (2012). Standardisation of Rock–Eval pyrolysis for the analysis of recent sediments and soils. Organic Geochemistry, 46, 38–53. https://doi.org/10.1016/J.ORGGEOCHEM.2012.01.011
10. DepV. (2009). DepV – Deponieverordnung. Verordnung über Deponien und Langzeitlager. BGBl. I, Nr. 22. (pp. 1–64).
11. DIN. (1985). German standard methods for the examination of water, waste water and sludge; sludge and sediments (group S); determination of the amenability to anaerobic digestion (S 8).
12. Disnar, J. R., Guillet, B., Keravis, D., Di-Giovanni, C., & Sebag, D. (2003). Soil organic matter (SOM) characterization by Rock-Eval pyrolysis: scope and limitations. Organic Geochemistry, 34(3), 327–343. https://doi.org/10.1016/S0146-6380(02)00239-5
13. Duan, Z., Kjeldsen, P., & Scheutz, C. (2022). Efficiency of gas collection systems at Danish landfills and implications for regulations. Waste Management, 139, 269–278. https://doi.org/10.1016/J.WASMAN.2021.12.023
14. Eck, C. P. (2000). Effects of moisture content in solid waste landfills. Air Force Institute of Technology.
15. European Committee for Standardization. (2011). Soil improvers and growing media – Determination of electrical conductivity (EN 13038:2011).
16. European Committee for Standardization. (2020). Soil - Determination of organic matter content on a mass basis in soil and sediment as loss-on-ignition (NEN 5754:2005 nl).
17. European Committee for Standardization (CEN). (2014). Geotechnical investigation and testing - Laboratory testing of soil - Part 1: Determination of water content (NEN-EN-ISO 17892-1).
18. European Committee for Standardization (CEN). (2016). Determination of the content of asbestos in soil, sediment, waste materials and demolition waste (NEN 5898:2016).
19. Fan, L., Dippold, M. A., Thiel, V., Ge, T., Wu, J., Kuzyakov, Y., & Dorodnikov, M. (2022). Temperature sensitivity of anaerobic methane oxidation versus methanogenesis in paddy soil: Implications for the CH_4 balance under global warming. Global Change Biology, 28(2), 654–664. https://doi.org/10.1111/gcb.15935
20. Fei, X., Zekkos, D., & Raskin, L. (2016). Quantification of parameters influencing methane generation due to

biodegradation of municipal solid waste in landfills and laboratory experiments. Waste Management, *55*, 276–287. https://doi.org/10.1016/J.WASMAN.2015.10.015

21. Food and Agriculture Organization of the United Nations. (2021). Standard operating procedure for soil pH determination. In International Organization. https://doi.org/10.1017/S0020818300006160
22. Fricko, N., Brandstätter, C., & Fellner, J. (2021). Enduring reduction of carbon and nitrogen emissions from landfills due to aeration? Waste Management, 135(June), 457–466. https://doi.org/10.1016/j.wasman.2021.09.024
23. Gebert, J., Hanke, N., Bohn, S., Smidt, E., & Streese-Kleeberg, J. (2011). Gas Potential of Old Landfills. Proceedings Sardinia 2011, 13th International Waste Management and Landfill Symposium, 10.
24. Gebert, J., Knoblauch, C., & Gröngröft, A. (2019). Gas production from dredged sediment. Waste Management, 85, 82–89. https://doi.org/10.1016/j.wasman.2018.12.009
25. Gebert, J., Köthe, H., & Gröngröft, A. (2006). Prognosis of methane formation by river sediments. Journal of Soils and Sediments, 6(2), 75–83. https://doi.org/10.1065/jss2006.04.153
26. Gebert, J., & Zander, F. (2024). Aerobic and anaerobic mineralisation of sediment organic matter in the tidal River Elbe. Journal of Soils and Sediments, 24(7), 2874–2886. https://doi.org/10.1007/s11368-024-03799-6
27. Gregorich, E. G., Gillespie, A. W., Beare, M. H., Curtin, D., Sanei, H., & Yanni, S. F. (2015). Evaluating biodegradability of soil organic matter by its thermal stability and chemical composition. Soil Biology and Biochemistry, 91, 182–191. https://doi.org/10.1016/j.soilbio.2015.08.032
28. Grossule, V., & Stegmann, R. (2020). Problems in traditional landfilling and proposals for solutions based on sustainability. Detritus, 12, 78–91. https://doi.org/10.31025/2611-4135/2020.14000
29. He, H. J., & Hu, J. (2022). Leachate drainage volume of municipal solid waste landfills: field testing and hydro-mechanical modeling. Environmental Science and Pollution Research, 29(43), 64680–64691. https://doi.org/10.1007/s11356-022-20413-9
30. Heyer, K.-U., Hupe, K., Koop, A., Ritzkowski, M., & Stegmann, R. (2003). The low pressure aeration of landfills: experience, operation and costs. Proceedings Sardinia 2003, Ninth International Waste Management and Landfill Symposium, 9. http://ifas-hamburg.de/pdf/aeration03.pdf
31. Hrad, M., Gamperling, O., & Huber-Humer, M. (2013). Comparison between lab- and full-scale applications of in situ aeration of an old landfill and assessment of long-term emission development after completion. Waste Management, 33(10), 2061–2073. https://doi.org/10.1016/J.WASMAN.2013.01.027
32. International Organization for Standardization. (1995). Soil quality — Determination of organic and total carbon after dry combustion (elementary analysis), ISO 10694:1995.
33. International Organization for Standardization. (2021). Soil, treated biowaste and sludge - Determination of pH (ISO 10390:2021).
34. IPCC. (2019). 2019 Refinement to the 2006 IPCC Guidelines for National Greenhouse Gas Inventories. Volume 5 Waste. 2019 Refinement to the 2006 IPCC Guidelines for National Greenhouse Gas Inventories. Volume 5 Waste. https://www.ipcc-nggip.iges.or.jp/public/2019rf/vol5.html
35. JØrgensen, B. B. (1978). A comparison of methods for the quantification of bacterial sulfate reduction in coastal marine sediments. II. Calculation from mathematical models. Geomicrobiology Journal. https://doi.org/https://doi.org/10.1080/01490457809377722
36. Kamalan, H., Sabour, M., & Shariatmadari, N. (2011). A review on available landfill gas models. Journal of Environmental Science and Technology, 4, 79–92.
37. Kettunen, R. H., & Rintala, J. A. (1997a). Performance of an on-site uasb reactor treating leachate at low temperature. https://doi.org/https://doi.org/10.1016/S0043-1354(97)00319-9
38. Kettunen, R. H., & Rintala, J. a. (1997b). The effect of low temperature (5-29 degrees C) and adaptation on the methanogenic activity of biomass. Applied Microbiology and Biotechnology, 48(4), 570–576. http://www.ncbi.nlm.nih.gov/pubmed/9445540
39. Lafargue, E., Marquis, F., & Pillot, D. (1998). Rock-eval 6 applications in hydrocarbon exploration, production, and soil contamination studies (Vol. 53).

40. Laner, D., Crest, M., Scharff, H., Morris, J. W. F., & Barlaz, M. A. (2012). A review of approaches for the long-term management of municipal solid waste landfills. Waste Management, 32(3), 498–512. https://doi.org/10.1016/j.wasman.2011.11.010
41. Li, J., Haeckel, M., Dale, A. W., & Wallmann, K. (2024). Degradation and accumulation of organic matter in euxinic surface sediments. Geochimica et Cosmochimica Acta, 370, 128–143. https://doi.org/10.1016/j.gca.2023.12.030
42. Ma, J., Gu, Y., Liu, L., Zhang, Y., Wei, M., Jiang, A., Liu, X., & He, C. (2023). Study on the effect of landfill gas on aerobic municipal solid waste degradation: Lab-scale model and tests. Science of the Total Environment, 869. https://doi.org/10.1016/j.scitotenv.2023.161875
43. Maciel, F. J., & Jucá, J. F. T. (2011). Evaluation of landfill gas production and emissions in a MSW large-scale Experimental Cell in Brazil. Waste Management, 31(5), 966–977. https://doi.org/10.1016/J.WASMAN.2011.01.030
44. Meza, N., Lammen, H., Cruz, C., Heimovaara, T., & Gebert, J. (2022). Spatial Variability of Gas Composition and Flow in a Landfill Under in-Situ Aeration. Detritus, 19, 104–113. https://doi.org/10.31025/2611-4135/2022.15191
45. Mou, Z., Scheutz, C., & Kjeldsen, P. (2015). Evaluating the methane generation rate constant (k value) of low-organic waste at Danish landfills. Waste Management, 35, 170–176. https://doi.org/10.1016/J.WASMAN.2014.10.003
46. Nunes, M. I., Kalinowski, C., Godoi, A. F. L., Gomes, A. P., & Cerqueira, M. (2021). Hydrogen sulfide levels in the ambient air of municipal solid waste management facilities: A case study in Portugal. Case Studies in Chemical and Environmental Engineering, 4, 100152. https://doi.org/10.1016/J.CSCEE.2021.100152
47. Puyuelo, B., Ponsá, S., Gea, T., & Sánchez, A. (2011). Determining C/N ratios for typical organic wastes using biodegradable fractions. Chemosphere, 85(4), 653–659. https://doi.org/10.1016/J.CHEMOSPHERE.2011.07.014
48. Raga, R., & Cossu, R. (2013). Bioreactor tests preliminary to landfill in situ aeration: A case study. Waste Management, 33(4), 871–880. https://doi.org/10.1016/j.wasman.2012.11.014
49. Ren, Z. (2021). Visualizing Water Distribution in the Landfill Using Electrical Resistivity Tomography. Delft University of Technology.
50. Rich, C., Gronow, J., & Voulvoulis, N. (2008). The potential for aeration of MSW landfills to accelerate completion. Waste Management (New York, N.Y.), 28(6), 1039–1048. https://doi.org/10.1016/j.wasman.2007.03.022
51. Ritzkowski, M. (2021). Landfill aeration - an important contribution towards landfill sustainability. Sardinia 2021, 18th International Symposium on Waste Management and Sustainable Landfilling.
52. Ritzkowski, M. (2024). Analyses of waste solid samples [Analysen von Abfallfeststoffproben]. www.hiicce.de
53. Ritzkowski, M., Heyer, K. U., & Stegmann, R. (2006). Fundamental processes and implications during in situ aeration of old landfills. Waste Management, 26(4), 356–372. https://doi.org/10.1016/J.WASMAN.2005.11.009
54. Ritzkowski, M., & Stegmann, R. (2012). Landfill aeration worldwide: concepts, indications and findings. Waste Management (New York, N.Y.), 32(7), 1411–1419. https://doi.org/10.1016/j.wasman.2012.02.020
55. Ritzkowski, M., Walker, B., Kuchta, K., Raga, R., & Stegmann, R. (2016). Aeration of the teuftal landfill: Field scale concept and lab scale simulation. Waste Management, 55, 99–107. https://doi.org/10.1016/j.wasman.2016.06.004
56. Scharff, H., & Jacobs, J. (2006). Applying guidance for methane emission estimation for landfills. Waste Management, 26(4), 417–429. https://doi.org/10.1016/j.wasman.2005.11.015
57. Sebag, D., Verrecchia, E. P., Cécillon, L., Adatte, T., Albrecht, R., Aubert, M., Bureau, F., Cailleau, G., Copard, Y., Decaens, T., Disnar, J. R., Hetényi, M., Nyilas, T., & Trombino, L. (2016). Dynamics of soil organic matter based on new Rock-Eval indices. Geoderma, 284, 185–203. https://doi.org/10.1016/j.geoderma.2016.08.025
58. Stinson, J. A., & Ham, R. K. (1995). Effect of Lignin on the Anaerobic Decomposition of Cellulose As Determined through the Use of a Diochemical Methane Potential Method. In Environ. Sci. Technol (Vol. 29). https://pubs.acs.org/sharingguidelines
59. Themelis, N. J., & Ulloa, P. A. (2007). Methane generation in landfills. Renewable Energy, 32(7), 1243–1257. https://doi.org/10.1016/j.renene.2006.04.020
60. Toha, M., & Rahman, M. M. (2023). Estimation and prediction of methane gas generation from landfill sites in Dhaka city, Bangladesh. Case Studies in Chemical and Environmental Engineering, 7, 100302. https://doi.org/10.1016/J.CSCEE.2023.100302

61. van Turnhout, A. G., Oonk, H., Scharff, H., & Heimovaara, T. J. (2020). Optimizing landfill aeration strategy with a 3-D multiphase model. Waste Management, 102, 499–509. https://doi.org/10.1016/j.wasman.2019.10.051
62. Vereniging Afvalbedrijven. (2014). Deelplan van Aanpak verduurzamingspilot op stortplaats Wieringermeer (Issue December).
63. Vereniging Afvalbedrijven. (2015a). Project plan Sustainable Landfill Management Braambergen (Issue November).
64. Vereniging Afvalbedrijven. (2015b). Project plan Sustainable Landfill Management De Kragge 2. (Issue November).
65. Westrich, J. T., & Berner, R. A. (1984). The role of sedimentary organic matter in bacterial sulfate reduction: The G model tested. Limnology and Oceanography, 29(2), 236–249. https://doi.org/10.4319/lo.1984.29.2.0236
66. Wu, S. J., Zheng, Q. T., Zhao, Y., & Feng, S. J. (2023). Prediction and control of elevated temperatures within landfills under aeration and recirculation based on the thermal non-equilibrium model. Journal of Environmental Management, 345, 118873. https://doi.org/10.1016/J.JENVMAN.2023.118873
67. Xu, H., Chen, T. H., Zhu, G., Peng, M. Q., & Zhan, L. T. (2024). Semi-quantitative study on the secondary compression characteristics of municipal solid waste in aerobic and anaerobic bioreactors. Waste Management, 176, 74–84. https://doi.org/10.1016/j.wasman.2023.12.058
68. Xu, Q., Du, Z., Wang, L., Zhao, L., Chen, D., Yan, F., Zhu, X., Wei, Z., Zhang, G., Zhang, B., Chen, T., Liu, Y., & Xiao, C. (2024). Temperature sensitivity of methanogenesis and anaerobic methane oxidation in thermokarst lakes modulated by surrounding vegetation on the Qinghai-Tibet Plateau. Science of The Total Environment, 907, 167962. https://doi.org/10.1016/J.SCITOTENV.2023.167962
69. Yilmaz, M., Tinjum, J. M., Acker, C., & Marten, B. (2021). Transport mechanisms and emission of landfill gas through various cover soil configurations in an MSW landfill using a static flux chamber technique. Journal of Environmental Management, 280, 111677. https://doi.org/10.1016/J.JENVMAN.2020.111677
70. Zander, F. (2022). Turnover of Suspended and Settled Organic Matter in Ports and Waterways. Delft University of Technology.
71. Zander, F., Comans, R. N. J., & Gebert, J. (2023). Linking patterns of physical and chemical organic matter fractions to its lability in sediments of the tidal Elbe river. Applied Geochemistry, 156, 105760. https://doi.org/10.1016/J.APGEOCHEM.2023.105760
72. Zander, F., Groengroeft, A., Eschenbach, A., Heimovaara, T. J., & Gebert, J. (2022). Organic matter pools in sediments of the tidal Elbe river. Limnologica, 96(June), 125997. https://doi.org/10.1016/j.limno.2022.125997
73. Zander, F., Heimovaara, T., & Gebert, J. (2020). Spatial variability of organic matter degradability in tidal Elbe sediments. Journal of Soils and Sediments, 20(6), 2573–2587. https://doi.org/10.1007/s11368-020-02569-4
74. Zehnder, A. J. B., & Svensson, B. H. (1986). Life without oxygen: what can and what cannot? Experientia, 42(11–12), 1197–1205. https://doi.org/10.1007/BF01946391
75. Zotarelli, L., Dukes, M. D., & Morgan, K. T. (2010). Interpretation of Soil Moisture Content to Determine Soil Field Capacity and Avoid Over-Irrigating Sandy Soils Using Soil Moisture Sensors 1. EDIS. http://edis.ifas.ufl.edu/AE266

5

Carbon and nitrogen balancing to identify processes and assess progress of landfill in-situ stabilization

Abstract

Carbon and nitrogen mass balances provide a framework to identify key transformation processes and assess the progress of in-situ landfill stabilization. While such balances have been widely studied at the laboratory scale, they have not yet been applied at full scale using long-term monitoring data and integrated assessment of the solid, aqueous, and gas phases. This study addresses this gap by establishing carbon and nitrogen balances for three landfill pilot sites over a seven-year period.

At a general level, the results show that aeration accelerates organic matter degradation, enhances carbon and nitrogen release through the gas phase, and leads to more stable total organic carbon (TOC) and total nitrogen (TN) levels in waste. In contrast, anaerobic conditions result in greater nitrogen release through leachate. Across all sites, carbon leaching through the aqueous phase was minimal (<1% TOC), while poorly mobilizable nitrogen pools (KCl extractable and microbial nitrogen) represent a substantial long-term sink that may delay compliance with emission targets.

The aerated pilots (BRA and WIE) released up to 23% of the initial TOC and most to all of the initial TN through the gas phase, with WIE showing apparent nitrogen releases exceeding 100% (177–253%) due to uncertainties in the initial TN estimates. In contrast, the anaerobic pilot (KRA) released less than 1% of the initial TOC through both gas and leachate. KRA showed the highest nitrogen release through leachate (8% TN) and evidence of nitrogen fixation. Poorly mobilizable nitrogen accounted for ~16% of TN in the aerated pilots and ~35% in KRA.

By integrating long-term monitoring with laboratory analyses, this study demonstrates that full-scale carbon and nitrogen balances can effectively distinguish aerobic and anaerobic stabilization pathways, reveal persistent nitrogen constraints, and serve as a robust tool to evaluate and guide landfill in-situ stabilization.

The content of this chapter is based on a manuscript in preparation for publication in a peer-reviewed journal with Julia Gebert. Other coauthors include Hans Lammen and Timo Heimovaara.

5.1. Introduction

Sanitary landfills are essential components of waste management, designed to minimize environmental impacts using impermeable barriers that prevent leachate infiltration and protect soil and groundwater. However, these barriers also hinder stabilization processes by creating anaerobic conditions and limiting water availability and solute transport required for organic matter degradation. As a result, waste decomposition is significantly prolonged, requiring decades to centuries of monitoring and posing long-term environmental risks.

Over the past two decades, various in-situ studies have sought to accelerate landfill stabilization and reduce the monitoring period by increasing the water content within the waste through water addition (Chung et al., 2015; Reinhart, 1996) and/or enhancing oxygen availability to promote aerobic degradation (Brandstätter et al., 2020; Hrad et al., 2013; Ritzkowski et al., 2006; Ritzkowski & Stegmann, 2012). These studies highlight the technical challenges associated with full-scale implementation (Ritzkowski & Stegmann, 2012). Despite advancements in aeration and water recirculation, significant knowledge gaps remain in understanding the processes governing in-situ landfill stabilization. Landfills are inherently complex systems with numerous physical, chemical, and biological interactions. A deeper understanding of carbon and nitrogen dynamics, key factors in waste stabilization, is necessary to optimize these processes (Brandstätter et al., 2015b, 2015a; Ritzkowski, 2021). Carbon and nitrogen transformation in landfills occurs across solid, dissolved, and gaseous phases, with waste being the primary source of both elements (Brandstätter et al., 2015a, 2015b; Dang et al., 2023). These elements exist in degradable or recalcitrant forms (Morello et al., 2018). While some degradable compounds break down readily, others become less accessible to microbial degradation due to process such as adsorption onto solid materials (Fricko et al., 2021; Kim, 2002; Puyuelo et al., 2011; Thompson et al., 2009) or co-precipitation with oxidised organic matter. In addition, physical isolation of waste (e.g. organic matter trapped in plastic bags or large wood fragments) can further limit decomposition. These mechanisms illustrate just a few of the many processes that contribute to the persistence of organic matter in landfills.

The decomposition of waste organic matter (WOM) involves a series of complex, parallel, and/or sequential reactions. Degradation begins with hydrolysis, breaking down WOM into simpler compounds such as sugars, amino acids and fatty acids. During the carbon cycle in a landfill (Figure 5.1, left), hydrolysis of degradable organic carbon (DOC_S) produces soluble compounds summarized as dissolved organic carbon (DOC_L), which may be released in leachate (L), assimilated by microbial biomass or further degraded.

Under anaerobic conditions, hydrolysis products undergo acidogenesis, acetogenesis and ultimately methanogenesis, leading to the production of methane (CH_4) and bicarbonate (HCO_3^-), which can be released as carbon dioxide (CO_2). Anaerobic oxidation of organic compounds can also yield CO_2, with electron acceptors such as nitrate, sulphate, or ferric iron in place of oxygen. In aerobic zones, organic matter degrades via respiration,

producing CO_2. Methane produced in methanogenic zones can be oxidized to CO_2 at oxic-anoxic interfaces, although this process competes with aerobic respiration for the available oxygen. Carbon species such as CO_2 and CH_4 either emit as gas or leave the landfill dissolved in leachate (as DIC).

From the nitrogen cycle perspective (Figure 5.1, right), the nitrogen fraction of dissolved organic matter is referred to as dissolved organic nitrogen (DON). Hydrolysis also releases ammonium (NH_4^+), which can be present as free ions in pore water (PW), adsorbed to solids, or fixed in the solid matrix. Water-soluble ammonium (NW) is weakly adsorbed through van der Waals forces and hydrogen bonds, while exchangeable ammonium (NK) binds through electrostatic interactions via ion exchange. Fixed nitrogen, incorporated into mineral structures, is considered stable and would not represent a significant harm to the environment (Ouyang et al., 2023; Wang et al., 2025). Extraction methods using KCl or $CaCl_2$ are employed to quantify ion-exchangeable ammonium (Kodithuwakku et al., 2024). Both, DON and NH_4^+ may be released through the leachate, assimilated by microorganisms or further transformed.

Under aerobic conditions, nitrification converts NH_4^+ to nitrite (NO_2^-) and subsequently to nitrate (NO_3^-). In anaerobic zones, denitrification reduces NO_3^- and NO_2^- to nitrogen gas (N_2), while the anammox process converts NH_4^+ and NO_2^- into N_2. Nitrogen gas can be emitted into the gas phase (G, Figure 5.1). In addition, biological nitrogen fixation may reintroduce N_2 (atmospheric or produced within the landfill body) as ammonia (NH_3), which can then re-enter the nitrification cycle.

Carbon and nitrogen can remain within the waste body, either adsorbed onto solids, assimilated into microbial biomass, or bound in non-degraded organic matter. Total organic carbon (TOC) and total nitrogen (TN) include both the biomass-associated and solid phase fractions.

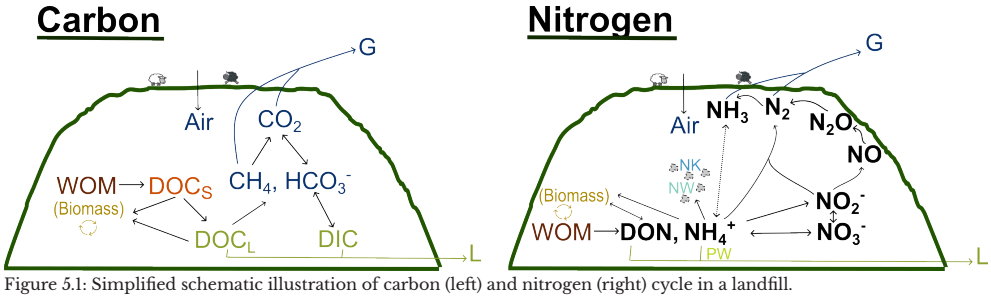

Figure 5.1: Simplified schematic illustration of carbon (left) and nitrogen (right) cycle in a landfill.

The transformation and release of carbon and nitrogen are central to landfill stabilization, as solid waste provides large pools of both elements, while leachate and gas act as their main release pathways. However, quantifying these processes remains challenging. Landfill waste bodies are physically and chemically heterogeneous due to the disposal of mixed wastes, and long-term monitoring data are scarce (Ritzkowski & Stegmann, 2012; Zhao et al., 2024).

While carbon and nitrogen balances have been extensively studied at the laboratory scale (Brandstätter et al., 2015b, 2015a; Cossu et al., 2016; Fricko et al., 2021; Zhang et al., 2023), no carbon and nitrogen balance was so far attempted at field-scale. As shown in Chapter 3 and 4, landfill waste bodies exhibit high spatial variability in gas composition, flow and waste characteristics. The contrasting conditions in the pilot sites BRA, WIE and KRA illustrates how this variability complicates extrapolating localized measurements to the scale of an entire landfill.

This chapter addresses these gaps by stablishing carbon and nitrogen mass balances at the field scale, integrating monitoring data with laboratory analyses. The objective is twofold: first, to evaluate how carbon and nitrogen are partitioned across solid, liquid, and gaseous phases under aerobic and anaerobic conditions; and second, to assess whether in-situ stabilization can realistically achieve environmental protection criteria, such as the 50 mg/L ammonium target for leachate (Brand et al., 2014; Dijkstra et al., 2018). Because many processes act simultaneously and large pools of carbon and nitrogen remain in the waste body, quantifying their transformation and projecting future emissions is a critical challenge. Mass balance approaches provide a framework to address this complexity and to evaluate the effectiveness of stabilization strategies.

Research questions addressed in this chapter are:

RQ5.1. Can carbon and nitrogen balances be established for full-scale landfills under both aerobic and anaerobic conditions?

RQ5.2. How do these balances improve understanding of in-situ processes and the partitioning of carbon and nitrogen between solid, aqueous, and gaseous phases?

RQ5.3. Do carbon and nitrogen balances provide insight into the long-term stabilization of waste and the potential for compliance with emission targets?

To address these questions, this chapter analysed carbon and nitrogen across the solid, aqueous and gas phases employing a comprehensive methodology:

- Solid phase: Elemental analyses of excavated waste quantified organic carbon and total nitrogen. These results were compared with baseline conditions before stabilization (Chapter 2). Degradable organic carbon (DOC_S) was estimated (Afvalzorg, 2022) and validated against carbon potential results from laboratory experiments (Chapter 4). Ammonium adsorption to depth-specific waste was measured through water (H_2O) and potassium chloride (KCl) extractions, while microbial biomass contributions were estimated from literature data.
- Aqueous phase: Leachate composition was analysed to quantify the release of carbon and nitrogen through the leachate.
- Gas phase: carbon and nitrogen release were quantified using gas composition data, aerobic efficiency calculations, and the net nitrification or nitrogen consumption

estimates. Comparisons with non-aerated conditions provided insights into the effects of aeration and leachate recirculation on stabilization.

- Mass balance: A carbon and nitrogen mass balance are presented for the three landfill pilots.

By integrating mass balance techniques with depth-specific and site-specific analyses, this study aims to advance the understanding of in-situ landfill stabilization processes and inform the development of aeration and leachate recirculation strategies.

5.2. Methods

The presented data pertain to the landfill pilots Braambergen (BRA), Wieringermeer (WIE) and Kragge (KRA). The description of the sites can be found in Chapter 2.

5.2.1. Field data on landfill gas and leachate

Data on gas flow rate, pressure, temperature and composition and on leachate composition used in this chapter were collected and made available by the operators of the landfill pilots (Chapter 2). Gas data in the aerated pilots were collected and stored in a 15 minutes interval and in a weekly frequency at the anaerobic pilot. This was done on site at the blower station. Leachate samples were collected biweekly and analysed in a commercial laboratory. Unless stated otherwise, we used data from the time periods listed in Table 5.1.

Table 5.1. Time periods on landfill gas and leachate field data in Braambergen (BRA), Wieringermeer (WIE) and Kragge (KRA).

Site	Data type	From	To
BRA	Gas	2017-09-08	2024-09-08
	Leachate	2017-09-08	2024-04-16
WIE	Gas	2017-08-15	2024-04-16
	Leachate	2017-08-15	2024-07-11
KRA	Gas	2018-03-01	2024-01-01
	Leachate	2018-03-09	2023-12-01

5.2.2. Carbon and nitrogen in the solid phase

The carbon and nitrogen pools within each pilot were derived from the total organic carbon (TOC) and nitrogen Kjeldahl (TN) measured in waste samples from different depth layers at the start of stabilization in BRA, WIE and KRA (Chapter 2, Section 2.5.1).

5.2.2.1. Waste sampling and analysis during in-situ stabilization

Waste sampling was performed between 2020 and 2023. The waste was characterized, and the degradability of waste organic matter under aerobic and anaerobic conditions analysed for at least 352 days (Chapter 4). The characterization process included pre-treatment, sorting and the measurement of water content, pH, electrical conductivity (EC), total carbon (TC), total organic carbon (TOC), loss on ignition (LOI), and the Rock-Eval

pyrolysis parameters hydrogen index (HI), oxygen index (OI), R-index, I-index, among others (Chapter 4). Rock-Eval pyrolysis was carried out at the chair group Soil Chemestry and Chemical Soil Quality (Prof. Rob Comans) at Wageningen University and Research (WUR). Total nitrogen (TN) content was measured together with total carbon (TC) through dry combustion in accordance with ISO 10694:1995, using a UNICUBE elemental analyser (Elementar) and a LECO 828 CN analyzer. To determine the carbon and nitrogen content in the waste for each pilot, all samples collected between 2020 and 2023 were considered.

5.2.2.2. Degradable organic carbon (DOC_S)

The amount of degradable organic carbon present in the waste bodies (DOC_S) was estimated using the NV Afvalzorg Multiphase Landfill Gas Model 2022 (Afvalzorg, 2022). Although the primary purpose of this model is to predict CH_4 and CO_2 emissions over time, it is also parametrized with data on the amount and composition of the deposited waste. Organic matter content is calculated using predefined values for each waste type, resulting in a DOC_S content expressed as kilograms of carbon per tonne of wet waste (kg C/t wet waste). DOC_S is further partitioned into high, medium, and low degradability fractions (Chapter 4, Section 4.2.2).

The model calculates carbon degradation from the onset of landfilling by applying k-values to determine the fraction of DOC_S degraded annually. The remaining DOC_S at the start of the stabilization was calculated by subtracting the cumulative degraded carbon from the initial estimated DOC_S, accounting for the time elapsed since deposition.

Laboratory gas generation and respiration tests (Chapter 4) showed that aerobic conditions enhanced organic carbon degradation compared with anaerobic conditions. In BRA, the mixed sample from seven wells degraded on average 4.2 times as much carbon under aerobic conditions as under anaerobic conditions. In WIE, the mixed sample from three wells degraded 4.7 times as much. These ratios were used to calculate the remaining DOC_S at the start of stabilization under fully aerobic conditions. No additional correction was made for KRA, which was considered under anaerobic conditions.

For partially aerobic conditions, aeration efficiency (AE, defined in Section 5.2.4.1) was included in the calculation of remaining DOC_S at the start of stabilization. The calculation followed Equation 1:

$$DOC_R=(DOC_T-DOC_D)\ x\ R_{A\text{-}An}\ x\ AE \qquad \text{(Eq. 1)}$$

Where DOC_R (t) is the remaining DOC_S at the start of aeration under partially aerobic conditions, DOC_T (t) is the total DOC_S deposited since landfilling began, DOC_D (t) is the degraded DOC_S under anaerobic conditions from the start of landfilling to the start of aeration, the $R_{A\text{-}An}$ is the ratio aerobic to anaerobic carbon degraded, and AE (%) is the aeration efficiency. DOC_R was normalized to dry waste at the beginning of the stabilization.

5.2.2.3. Quantification of mobile and adsorbed ammonium

After exhaustive organic matter degradation under anaerobic conditions in the laboratory (Chapter 4), 42 bottles were selected (Supplementary information B, section S5.1) to measure NH_4^+ adsorption characteristics (mobile, water-extractable and KCl-extractable NH_4^+).

Two parallel samples were used for the NH_4^+ extraction: one parallel was used for H_2O extraction (including pore water) and the other for the KCl extraction. All liquid-to-solid ratios were weight-to-weight, based on dry solid weight.

The water content in the waste was used to calculate the dry waste (g) and the amount of H_2O or KCl solution to be added for each extraction. The experimental densities used were 1.04 g/mL for the KCl solution and 0.99 g/mL for the demineralized water. The volume of supernatant (mL) in each extraction included the initial water content in the waste plus the added H_2O or KCl.

Pore water (Bottle A): Demineralized water was added to the sample at a 12:1 liquid-to-solid ratio. The bottle was briefly (~5 seconds) hand-shaken, and a portion of the supernatant (2:1 liquid-to-solid ratio) was centrifuged (Megafuge 1.0S, Heraeus) at 3000 RPM for 10 minutes to analyse pore water.

Water extraction (Bottle A): For the remaining supernatant (10:1 liquid-to-solid), the bottle was shaken on an overhead shaker (Reax 20, Heidolph) at 5 RPM for 60 minutes and centrifuged at 3000 RPM to obtain water-extractable ammonium.

KCl extraction (Bottle B): A 10:1 ratio of 1 M KCl solution was added, followed by 60 minutes of overhead shaking at 5 RPM and centrifugation at 3000 RPM to extract KCl-extractable ammonium.

The centrifuged supernatants from all extractions were filtered using GF/F 0.7 µm filters and analysed for ammonium nitrogen (NH_4-N) content via a discrete colorimetric analyser.

The NH_4^+-based nitrogen concentration in the pore water (NP_L) was calculated as follows:

$$NP_L = (NH_4\text{-}N)_{ml} \times (WC_S + H_2O\ added)/WC_S \quad \text{(Eq. 2)}$$

Where NP_L was the nitrogen in the pore water, in mg NH_4-N/L; $(NH_4\text{-}N)_{ml}$ was the average ammonium-nitrogen concentration measured in the first supernatant, in mg NH_4-N/L; WC_S was the water content in the sample, in mL; H_2O *added* was the volume of water added in mL, which was equivalent to 12 times the dry waste weight in bottle A.

The NP_L was expressed in mg NH_4-N/kg dry weight (dw) by:

$$NP = (NP_L \times WC_S)/(sample\ dry) \quad \text{(Eq. 3)}$$

Where NP was the nitrogen in the pore water expressed in mg NH_4-N/kg_{dw}, NP_L was the nitrogen in the pore water, in mg NH_4-N/L; WC_S was the water content in the sample, in mL; and *sample dry* was the weight of the dry sample in g.

The H_2O-extractable nitrogen (NW) and the KCl-extractable nitrogen (NK) were calculated as follows:

$$NW=(NH_4\text{-}N)_{m2} \text{ x } ((WC_S+H_2\,0\ \textit{remaining})/(\textit{sample dry})) \text{ - NP} \quad \text{(Eq. 4)}$$

Where NW was the H_2O-extractable nitrogen, in mg NH_4-N/kg_{dw}; $(NH_4\text{-}N)_{m2}$ is the average concentration of ammonium-nitrogen measured in the second supernatant (bottle A), in mg NH_4-N/L; WC_S was the water content in the sample, in mL; the H_2O remaining was 10 times the dry waste weight in bottle A and was expressed in mL; sample dry was the weight of the dry sample in g; and NP was the nitrogen in the pore water expressed in mg NH_4-N/kg_{dw}

$$NK=(NH_4\text{-}N)_{m3} \text{ x } ((WC_S+KCl\ \textit{added}))/(\textit{sample dry}) \text{ - NW} \quad \text{(Eq. 5)}$$

Where NK was the KCl-extractable nitrogen, in mg NH_4-N/kg_{dw}; $(NH_4\text{-}N)_{m3}$ was the average concentration of ammonium-nitrogen in the supernatant (bottle B) in mg NH_4-N/L; WC_S was the water content in the sample, in mL; the KCl added was the volume of 1M KCl solution added, which was 10 times the dry waste weight in bottle B; sample dry was the weight of the dry sample in g; and NW was the H_2O-extractable nitrogen, expressed in mg NH_4-N/kg_{dw}.

Results were extrapolated to the pilots considering the weighted average percentage of NP, NW, NK and water content (e.g. sample BRA-139 counted as 7) and the amount of wet waste landfilled. Free (NP) and adsorbed (NW and NK) were assumed to be the same for the seven years balance.

4.2.3. Carbon and nitrogen in the aqueous phase (landfill leachate)

4.2.3.1. Leachate monitoring

At BRA, the leachate drainage and collection system consist of three separate drainage networks: compartments 11N, 11Z, and 12 (with a combined drainage system for 12O and 12W). For WIE, a single drainage system services compartment 6. Cumulative leachate volumes were recorded every 15 minutes at each drainage system's collection sump using an OPTIFLUX 2100 flowmeter (Krohne).

At KRA, the water recirculation pilot involved an infiltration system with an Anammox water purification system, and a nitritation reactor (Chapter 2, Section 2.3). Inert components, such as chloride (Cl^-), were removed from the waste package by discharging treated leachate to the sewage system. This discharged leachate was replaced with 1.2 to 4.8 m^3/h of clean water, introduced either directly or via the nitritation reactor (Van Raffe et al., 2023). The leachate composition of the reinfiltrated leachate was not monitored, making difficult the asses of mass balance.

Each drainage system at KRA discharged into a leachate collection sump, where cumulative leachate volumes were also recorded daily using the OPTIFLUX 2100 flowmeter.

Biweekly leachate samples were collected in the three pilots from the start of stabilization onward to analyse carbon, nitrogen, and other key components.

4.2.3.2. Carbon and nitrogen in the leachate

The quantification of carbon and nitrogen released through the leachate considered the following:

- **Carbon:** Dissolved inorganic carbon (DIC) concentrations were calculated as the sum of bicarbonate (HCO_3^-) and carbonate (CO_3^{2-}) concentrations, with results reported in mg C/L. Dissolved organic carbon (DOC_L), total inorganic carbon (TIC), chloride, and pH values were also monitored over time to assess carbon dynamics in the leachate. Because the leachate samples were collected directly from the landfill drainage system and not equilibrated with atmospheric CO_2, partial degassing during sampling or storage may have occurred. No correction was applied, but potential effects of degassing are considered in the discussion. DOC_L was normalized to chloride to assess the change in DOC_L independently of dilution.
- **Nitrogen:** Total nitrogen was determined by summing the concentrations of Kjeldahl nitrogen, nitrate nitrogen (NO_3-N), and nitrite nitrogen (NO_2-N). Results were reported in mg N/L. Ammonium nitrogen (NH_4-N) was also monitored to track nitrogen cycling and transformations within the landfill system. The dissolved organic nitrogen (DON) percentage per layer group and pilot before the start of the stabilization was calculated using the nitrogen Kjeldahl (Chapter 2, Figure 2.4) and the acid-base extracted DON concentration per depth layer group (Chapter 2, Figure 2.5). The DON average percentage of BRA-11N and BRA-11Z per layer group was considered for BRA-12.

The carbon and nitrogen released through the leachate was expressed in tonnes per year (t/a), and the balance for seven years was normalized to dry waste at the beginning of the stabilization.

5.2.4. Carbon and nitrogen in the gas phase

5.2.4.1. Landfill gas monitoring

In the aeration landfill projects at BRA and WIE, gas flow velocity and temperature (multifunctional handheld unit, Höntzsch U426, TA-10 probe), gas composition (Geotech Gas Analyzer GA2000; detection limit 0.1%), and pressure (pressure gauge by Blue line S4600) were manually measured at individual wells bimonthly in 2017 and monthly from 2018 to 2024. These individual gas wells were grouped and connected to a single extraction pipe, leading to a gas blower station.

At the blower station, bulk gas flow (Proline Prosonic Flow B 200 Ultrasonic flowmeter for gas extraction, and Proline 65i T-mass flowmeter for air injection; both from Endress+Hauser), pressure (PMC51-R8K2/0; Endress+Hauser), temperature (iTEMP TMT181; Endress+Hauser), and gas composition (CH_4, CO_2, and O_2, monitored by Biotech

Gas Analyzer 3000) were measured and stored every 15 minutes.

At Kragge, gas wells are grouped into collection points (CPs), which are connected to a single pipe (Kragge 2). A similar system is used in Kragge 1 and the bulk gas from both is combined (Kragge) (Chapter 2, Figure 2.1). The gas extraction pressure (GGW150 A4-U2 and a Barksdale D1X-M3SS-ex) was measured only in the combined bulk gas, while gas flow (Prosonic Flow 200; Endress+Hauser) was monitored hourly in Kragge 1, Kragge 2, and the combined bulk gas. Gas composition (CH_4, CO_2, and O_2; Biotech Gas Analyzer 3000) was measured monthly at individual wells and CPs, and weekly in Kragge 1, Kragge 2, and the combined bulk gas. Gas velocity (KIMO VT-100 handheld unit) was measured monthly at individual gas wells and CPs.

5.2.4.2. Carbon and nitrogen in the extracted landfill gas

To estimate the gas originating specifically from compartment 6 at WIE, the bulk landfill gas data were corrected using the relative contribution of wells located within that compartment. Gas velocities from wells in compartment 6 were compared with the total gas velocity across all wells, and the resulting share was expressed as a percentage (%) and averaged monthly. This percentage was then used to adjust the bulk gas flow, thereby estimating the fraction of landfill gas attributable to compartment 6. Gas composition and pressure measured in the bulk gas were assumed to be representative for the compartment. The corrected gas flow was subsequently used to calculate the carbon and nitrogen released from compartment 6 in the mass balance.

Similarly, the gas originating from compartment 3 in the bulk gas mixture at Kragge 2 was estimated by analysing the contributions of gas wells located in compartment 3 to the total gas recovery. Prior to infiltration, approximately one-third of the gas formed originated from compartment 3 (Vereniging Afvalbedrijven, 2015). In 2021, gas velocities measured at individual wells and CPs indicated that 34% of the bulk gas mixture at Kragge 2 originated from compartment 3 (Chapter 4). The gas flow in compartment 3 was estimated as one-third of the bulk gas flow in Kragge 2, and its gas composition was averaged from the wells located in compartment 3.

Calculations

Carbon and nitrogen released through the gas phase was calculated according to equations 6-8:

Anaerobic landfill pilot KRA:

$$n_{An} = V \times ([G_{LFG}]/100) \times (1/MV) \quad \text{(Eq. 6)}$$

Where n_{An} is the number of moles of gas in KRA's compartment 3, V the extracted landfill gas (LFG) volume (m^3), $[G_{LFG}]$ is the average gas concentration of CH_4, CO_2 or N_2 measured in the LFG (vol.%), and MV is the molar volume at 20°C (L/mol).

Aerated landfill pilots BRA and WIE:

$$n_A=(PV\,[G_{LFG}])/RT \quad \text{(Eq. 7)}$$

Where n_A is the number of moles in the extracted gas, P is the pressure (Pa), R the universal gas constant 8.314463 m^3 Pa / (K mol) and T is the LFG temperature (K).

Carbon released through the landfill gas

Using equations 6 and 7, the number of moles of CH_4, and CO_2 in the LFG was calculated and the total carbon released through the gas phase was calculated as follows:

$$TC = ([n_{CH_4}+n_{CO_2}]\ x\ mmC)/1000 \quad \text{(Eq. 8)}$$

Where TC is the total carbon (t), n_{CH_4} is the number of CH_4 moles, n_{CO_2} is the number of CO_2 moles, and mmC is the carbon molecular mass (kg/mol).

Aeration efficiency

The extent of partial aerobic conditions of the aerated pilots was assessed using the aeration efficiency (AE), defined as the percentage of aerobically produced CO_2 relative to the total CO_2 and CH_4 concentrations in the extracted gas mixture (Gebert et al., 2023; Yazdani et al., 2010). AE and the carbon derived from aerobic processes (AC) were calculated as follows:

$$AE=([CO_{2\_LFG}]-[CO_{2\_AN}])/([CO_{2\_LFG}]+[CH_{4\_LFG}])\ x\,100 \quad \text{(Eq. 9)}$$

$$AC=TC\ x\ AE/100 \quad \text{(Eq. 10)}$$

Where AE is the aeration efficiency (%), CO_{2_LFG} is the concentration of total CO_2 measured in the extracted landfill gas mixture (vol.%), CO_{2_AN} is the concentration of anaerobically produced CO_2 (vol.%), which is assumed to be equal to the concentration of CH_4 (vol.%), CH_{4_LFG} is the concentration of CH_4 measured in the extracted landfill gas mixture (vol.%), AC is the aerobic carbon (t), and TC is the total carbon (t).

To compare the carbon released through the gas phase with respect to a scenario without stabilization (anaerobic scenario), the previously described Afvalzorg Multiphase model 2022 was used.

Denitrification and nitrogen fixation

Nitrogen release (denitrification) and uptake (fixation) were estimated using the noble gas argon (Ar), which originates exclusively from atmospheric air, to distinguish between atmospheric N_2 and N_2 produced or consumed by microbial transformations (denitrification and nitrogen fixation, respectively; Nagamori et al., 2016; Shigemitsu et al., 2016). The balance between the N_2 that comes from the atmosphere and the N_2 produced or consumed in the landfill was defined as N_{2_Excess}. Gas analyses and computation of the parameter N_{2_Excess} and methods are described in Yi et al. (2025). Using equations 6 and 7, the number of N_2 moles was calculated and the total N_2 released through the gas phase or fixed was calculated as follows:

$$TN=([n_{N2}\ ]\ x\ mmN_2)/1000\ x\ N_{2\_Excess} \quad \text{(Eq. 11)}$$

Where TN is the total nitrogen (t), n_{N2} is the number of N_2 moles, and mmN_2 is the nitrogen molecular mass (kg/mol) and the N_{2_Excess} is the net denitrification or nitrogen uptake (% of total N_2 measured in the extracted landfill gas).

Data for the N_{2_Excess} from August 2022 to February 2024 were used for all three pilots (provided by Dr. Yi). Mean and median values from the overall dataset and from bulk gas samples were used to define the lower and upper bounds of the N_{2_Excess} range per pilot. Because KRA lacks a dedicated sampling point for bulk landfill gas originating from all the stabilization compartment, its range was defined using the mean and median of the overall dataset for individual wells. These N_{2_Excess} values were then interpreted as net denitrification or fixation and incorporated into the nitrogen balance for each pilot.

5.3. Results and discussion

5.3.1. Total carbon and nitrogen in the solid phase

5.3.1.1. Carbon and nitrogen in the waste

Carbon and nitrogen pool at the beginning of stabilization

The experimentally determined amount of degradable carbon (carbon potential) showed large variation among samples (Chapter 4, Table 4.10 and Figure 4.7), reflecting the heterogeneity of the waste. Nevertheless, the degradable organic carbon (DOC_S) values estimated by the 2022 Afvalzorg Multiphase model fell within the range of anaerobic carbon potentials for KRA and aerobic carbon potentials for BRA and WIE (Table 5.2).

Baseline TOC and TN values corresponded to mixed samples from each landfill pilot (Chapter 2, section 2.5). Although the aerated pilots had lower initial total organic carbon (TOC) and total nitrogen (TN) than the anaerobic pilot before stabilization, the model estimated a higher proportion of remaining DOC_S (as a percentage of baseline TOC) at the start of stabilization in the aerated sites (Table 5.2). This pattern was consistent with the estimated laboratory carbon potential in waste samples excavated after five years of stabilization (Chapter 4).

Table 5.2. Waste characterization before the start of stabilization in Braambergen (BRA), Wieringermeer (WIE) and Kragge (KRA). Degradable organic carbon (DOC_S), total organic carbon (TOC), and total nitrogen (TN).

	Carbon potential	DOC_S at the start of stabilization	DOC_S at the start of stabilization	TOC baseline	TN baseline	T O C / T N baseline	DOC_S/TN
	% of baseline TOC		t	t	t	[-]	[-]
BRA	19 (11-31)*	12	5645	47575	2288	23	2,5
WIE	23 (17-32)*	23	2661	11581	642	18	4,1
KRA	6 (1-11)**	10	5040	52144	3420	17	1,5

*Aerobic carbon potential
**Anaerobic carbon potential

The estimates indicate that under aerobic conditions, waste degrades a higher fraction of degradable carbon than KRA, which remained under anaerobic conditions.
As a result, TOC/TN and DOC_S/TN ratios were higher in the aerated pilots (Table 5.2) than in KRA. All ratios were comparable to values reported for mature or stabilized municipal solid waste, which typically show biodegradable carbon-to-nitrogen ratios below 4 (Puyuelo et al., 2011).

Carbon and nitrogen content after five years of stabilization

Five years into the stabilization process, TOC levels in most BRA samples remained within the same range as in the baseline study (Figure 5.2, top right). In WIE, the TOC range was slightly broader than the baseline, yet the TOC from the mixed sample and the average TOC remained stable (Table 5.3). BRA and WIE were mainly landfilled with hardly degradable waste (Chapter 2, Figure 2.3) which can explain the stable TOC content in the waste. Similarly, a study on an Austrian MSW landfill from the 1970s found no significant TOC decrease in the waste samples composed with many hardly degradable substances after five years of in-situ aeration (Brandstätter et al., 2020). In contrast, the TOC decrease in an LSR experiment using waste from the same landfill resulted in 32% decrease for the aerobic LSR and 17% for the anaerobic ones after 2.2 years of experiment (Brandstätter et al., 2015a).

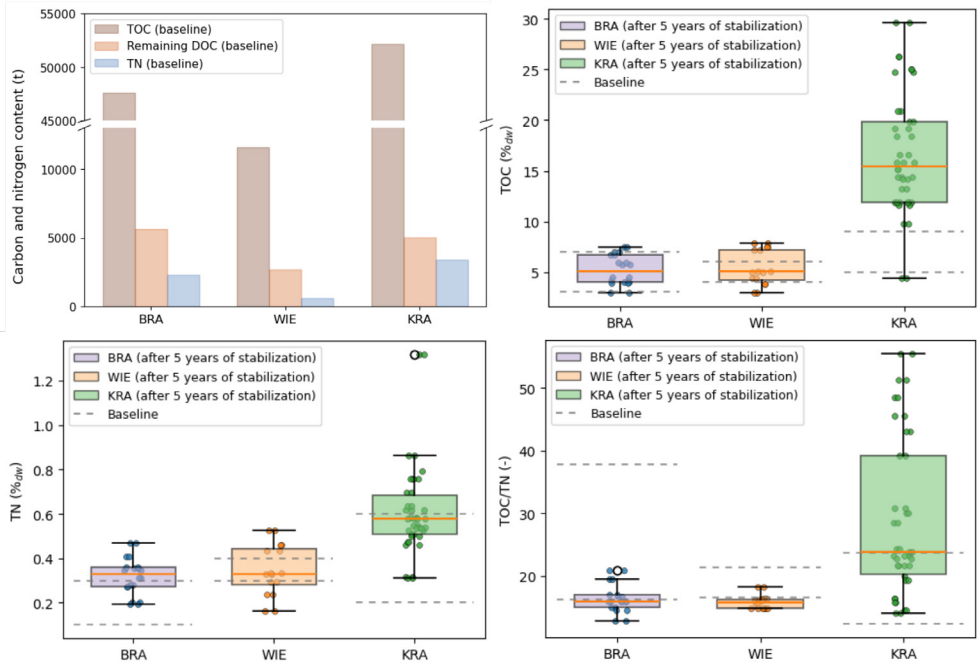

Figure 5.2: Carbon and nitrogen content (top left), total organic carbon (TOC, top right), total nitrogen (TN, bottom left), and total organic carbon to total nitrogen ratios (TOC/TN, bottom right) in samples from BRA, WIE and KRA landfill pilots.

Table 5.3. Waste characterization (mean values) after five years of stabilization in Braambergen (BRA), Wieringermeer (WIE) and Kragge (KRA). Total organic carbon (TOC), total carbon (TC), total nitrogen (TN).

Landfill	Compartment	Drill	Water content ($\%_{dw}$)	TOC (%)	TC Mean (%)	TN Mean (%)	TOC/TN	TC/TN
BRA	11Z	LN6	47.9	5.5	8.1	0.3	18.4	26.8
BRA	11N	Mixed	45.6	5.3	8.3	0.3	16.0	24.5
WIE	C6	Mixed	35.2	5.4	8.0	0.3	15.5	23.2
KRA	C3	Mixed	74.6	10.8	14.9	0.6	19.9	27.7

KRA, the pilot landfilled with more easily degradable waste compared with the aerated pilots (Chapter 2, Figure 2.3) exhibited a significantly higher TOC range in the waste samples retrieved after three to five years of stabilization compared with the baseline study (Figure 5.2, top right). However, the mixed sample retrieved after five years of stabilization was more similar to the baseline values. The high heterogeneity of individual samples in this pilot may have contributed to this difference. At the landfill scale, such heterogeneity masks measurable TOC reductions that would be evident under controlled LSR conditions, where degradation is assessed in homogeneous samples. This effect is most pronounced in KRA, the most heterogeneous of the three pilots.

The higher carbon content observed in KRA with respect to the baseline was also reflected in TN values compared with the baseline range (Figure 5.2, bottom left). In the aerated pilots, TN values were slightly higher than in the baseline study. In addition to a probable underestimation of nitrogen content in the baseline waste samples (Oonk, 2020), these differences may reflect natural landfill heterogeneity or potential nitrogen fixation, which was clearly observed in KRA and occasionally in the aerated pilots (Yi et al., 2025). Similar TN contents ($0.3\%_{dw}$ - $0.5\%_{dw}$) were found in Austrian MSW landfill waste samples (Fricko et al., 2021; Hrad et al., 2013), while MSW from old German landfills showed a wider range between $0.03\%_{dw}$ and $2.3\%_{dw}$ (Gebert et al., 2011).

As a result, TOC/TN ratios decreased in the aerated pilots, with the most significant change occurring in compartment 11N, where the baseline average TOC/TN ratio of 26 dropped to 16 in the mixed samples (Table 5.3). In KRA, the average TOC/TN ratio increased in the mixed samples (Table 5.2 and Table 5.3), while its high heterogeneity was reflected on individual samples (Figure 5.2, bottom right). Waste samples from Austrian MSW landfills had TOC/TN ratios of 21-26 (Fricko et al., 2021; Hrad et al., 2013; Mellendorf et al., 2010). Higher TOC/TN ratios were reported for a Spanish MSW samples (34) (Puyuelo et al., 2011) and Italian MSW samples (38) (Cossu et al., 2016) before landfilling.

Biological waste degradation is primarily carried out by microorganisms with high nitrogen demand, leading to slower nitrogen loss compared to carbon and a progressive decrease in C/N ratios over time (Manzoni et al., 2008). Although a TOC/TN decrease was observed in the aerated pilots, the results suggest that this change was not due to carbon degradation but rather an increase in nitrogen content relative to the baseline. An LSR experiment using

waste from an old MSW German landfill did not show a significative decrease in TOC and neither TN in the waste samples after 1.6 years of experiment under aerobic conditions, however, considering the carbon load through the gas and leachate, a degradation of ~32% of the initial carbon content was estimated, suggesting that TOC in the waste samples alone would not describe the stabilization process (Ritzkowski et al., 2006).

C/N ratios in all pilots (Table 5.3) falls within the optimal range for both aerobic an anaerobic microbial metabolism (15-30) (Brust, 2019; Huang et al., 2004; Kumar et al., 2010; Puyuelo et al., 2011). This suggests that while carbon and nitrogen content in the waste would not limit microbial activity, the biodegradability of organic matter may be a more critical factor.

5.3.1.2. Carbon and nitrogen in the microbial biomass

The carbon and nitrogen content in microbial biomass was not directly measured in this study. However, previous research on soils has estimated that microbial carbon accounts for less than 1% to 5% of soil organic carbon (Miltner et al., 2012; Setia et al., 2012; Xu et al., 2013) while microbial nitrogen comprises approximately 2% to 6% of total soil nitrogen (Xu et al., 2013). In sediments, microbial biomass has been reported to contain approximately 8% of total organic carbon (TOC) and 3.5% of total nitrogen (TN) (Gebert, 2024).

In waste degradation studies, a study on beech leaf litter decomposition over eight weeks found that microbial carbon accounted for less than 1% of total carbon, while microbial nitrogen represented less than 5% of total nitrogen in the litter (Brandstätter et al., 2013). However, in municipal solid waste (MSW), the share of microbial nitrogen content in relation to total nitrogen appears to be significantly higher. For example, a study on MSW decomposition in landfill simulation reactors found that microbial carbon accounted for an average of 3.7% of TOC, while microbial nitrogen accounted for 25.5% of TN (Fricko et al., 2021). Thus, while the share of microbial carbon in waste is of the same order of magnitude as soils, sediments and beech leaf litter, microbial nitrogen is one order of magnitude higher. This is expected because MSW contains substantial amounts of non-degradable carbon-rich materials such as plastics, as shown in the KRA characterization (Chapter 4, Figure 4.3), which increase TOC withouth contributing to nitrogen. As a result, the relative contribution of microbial nitrogen to the total nitrogen pool becomes larger. Another study compared microbial carbon and nitrogen in soil and soil treated with farmyard manure or MSW mature compost at two different application rates. Three years after organic matter application, microbial carbon and nitrogen in the treated soils with MSW mature compost was at least three times that of untreated soil (Bouzaiane et al., 2007).

Based on the above and the type and composition of the landfilled wastes, microbial biomass in the MSW landfill pilot (KRA) was assumed to contribute to TOC with 4% and to TN with 26%. For the aerated landfill pilots, microbial carbon and nitrogen were assumed to contribute with 1.3% and 9%, respectively, hence approximately one third of the shares assumed for KRA.

5.3.1.3. Adsorption of NH_4^+-based nitrogen to the solid phase

Two extraction media (water and KCl) were used to assess the strength of NH_4^+ binding to the solid surface. Additionally, these fractions were differentiated from mobile ammonium freely present in the waste pore water (see section 5.2.2.3). NH_4-N concentrations (pore water [NP], water-extractable [NW], and KCl-extractable [NK]) generally increased with depth within the same well, likely reflecting higher exposure to atmospheric oxygen at the top layers and precipitation-driven redistribution of solutes.

This trend was particularly pronounced in KRA, where NP increased nearly fourfold between the top and bottom layers. NW concentrations in KRA increased over 800 times with depth compared with the top layer (Figure 5.3, top), and NK concentrations increased nearly 62 times. The pattern may be influenced by active water recirculation in KRA, which enhances leachate movement and solute transport. However, since hydraulic conductivity in landfills is strongly anisotropic, most flow likely occurs laterally within permeable layers. Vertical flushing may still contribute locally, particularly near recirculation points, but the observed depth patterns likely reflect a combination of lateral transport and vertical redistribution. Similar solute transport behaviour was reported in landfill simulation reactor (LSR) studies (Bae et al., 2019; Purcell et al., 1999; Sohoo et al., 2021).

Across most samples, water-extractable ammonium was higher than pore water concentrations, while KCl-extractable ammonium consistently constituting the largest of the three fractions. This means that most of the mobile and adsorbed nitrogen resides in the poorly mobilizable KCl-fraction, delaying compliance with the emission target value (ETV) for ammonium in leachate (50 mg/L, Chapter 1). As pore water (NP) ammonium concentrations decline and more fresh water flushes the waste, desorption of the water-soluble fraction (NW) occurs until a new solid-liquid equilibrium is reached. Water-extractable ammonium is mobilized by flushing, which disrupts van der Waals forces and hydrogen bonds, whereas the KCl-fraction (NK) requires cation exchange to break electrostatic bonds (S. Yang & Yang, 2024).

Next to the nature of bonding to the solid phase (e.g. van der Waals forces, hydrogen bonds, cation exchange), NH_4^+ solubility is strongly pH-dependent (Chapter 2, numeral 2.5.3). As shown by van Raffe et al. (2025), at low pH, positive surface charge limits sorption; at neutral pH, sorption is strongest; and at high pH, deprotonation to NH_3 reduces sorption again. This pH-dependent behavior confirms that sorption–desorption reactions play a major role in controlling ammonium mobility in the landfill waste matrix.

Additional statistical analyses exploring correlations between free and adsorbed ammonium and waste characteristics are presented in the Supplementary Information B (Section S5.2). These correlations confirm that ammonium mobility is closely linked to water content, organic matter lability, and microbial activity, supporting the interpretation that sorption–desorption and ammonification processes jointly control NH_4^+ distribution in the waste

matrix.

Expressed as a percentage of total nitrogen (TN) present in the waste at the moment of extraction (Figure 5.3, bottom and Table 5.4), KRA showed a higher percentage of TN adsorbed in the waste than the aerated pilots.

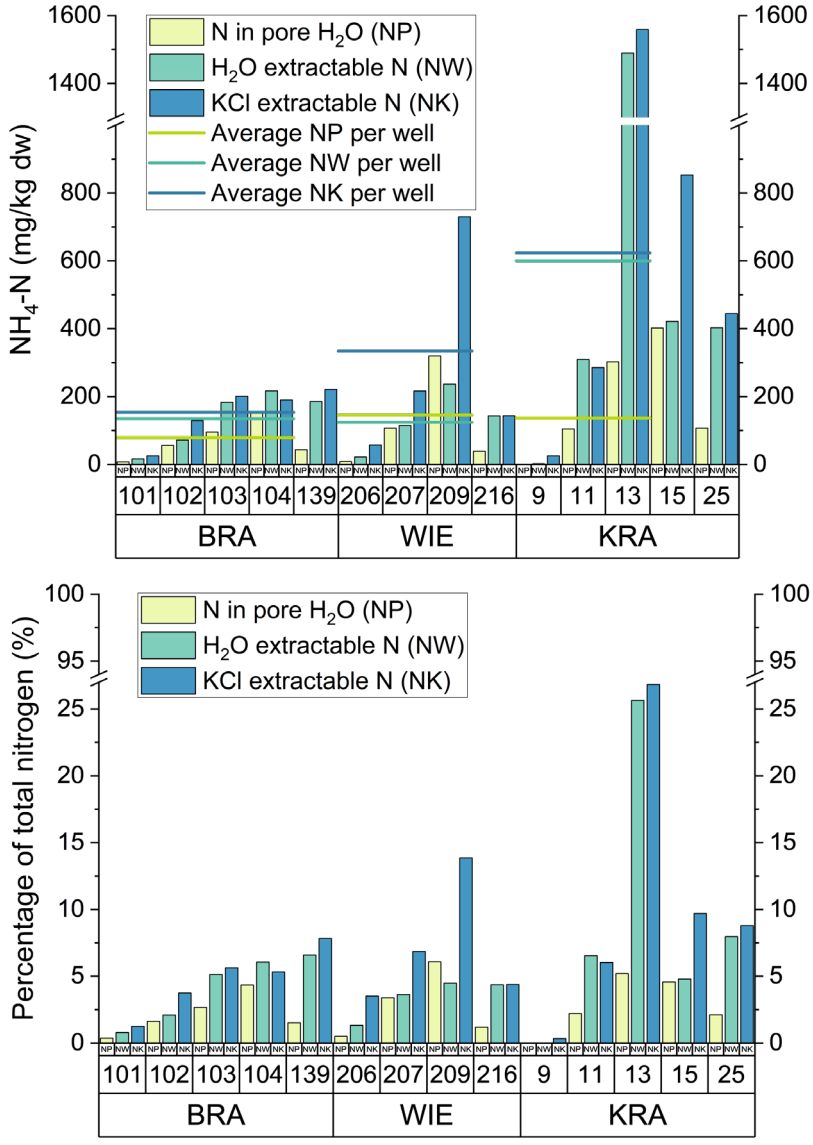

Figure 5.3: NH_4-N concentrations in the pore water (NP), water-extractable (NW), and KCl-extractable (NK) fractions (top); and the percentage contributions of NP, NW, and NK to total nitrogen (TN) in in waste samples from BRA, WIE, and KRA landfill pilots (bottom).

Table 5.4. Percentage contributions of NP, NW, and NK to total nitrogen (TN) in waste samples from BRA, WIE, and KRA landfill pilots.

Pilot (compartment)	Drilling well (s)	Sample (s)	NP (%)	NW (%)	NK (%)	Sum (%)
BRA (11N)	An2, An6, Cn2, Cn6, En2, En4, En6	Mixed sample (BRA-139)	1.5	6.6	6.7	15.9
BRA (11Z)	Ln6	BRA-101 to BRA-105	2.3	3.5	3.8	9.5
WIE (6)	WIE-2	WIE-206 to WIE-209	4.3	3.8	10.1	18.8
WIE (6)	WIE-1 to WIE-3	Mixed sample (WIE-216)	1.2	4.4	4.4	9.9
KRA (3)	A4-4	GT9, GT11, GT13	2.5	10.7	11.1	24.3
KRA (3)	A4-4	Mixed sample (GT15)	4.7	4.9	9.9	19.5
KRA (3)	PZ9.8 to PZ19,19	Mixed sample (KRA-25)	2.1	8.0	8.8	18.8

Extrapolating these results to the pilots (weight average), the nitrogen bound to the solid phase followed this order: KRA>BRA>WIE. The mobile nitrogen represented by the nitrogen in the pore water was up to 2%TN while the mobilizable nitrogen represented by the adsorbed nitrogen (H_2O and KCl) was up to 17%TN (Figure 5.4, left). This would mean that 83-90%TN is left in solid organic matter and biomass.

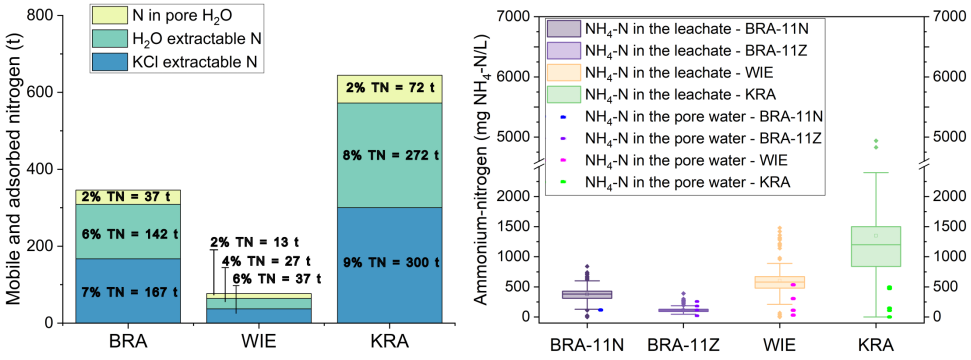

Figure 5.4: Average ammonium nitrogen (NH_4-N) in the pore water, H_2O- and the KCl-extractable fractions (left) and NH_4-N concentrations in the pore water and leachate (right) of BRA, WIE, and KRA landfill pilots.

Ammonium-nitrogen (NH_4-N) concentrations in pore water were comparable to those in the bulk leachate from the same compartment (Figure 5.4, right). In compartment BRA-11Z, a study of 132 wells sampled in 2020 reported NH_4-N concentrations within the same range (Gebert et al., 2022). In other compartments and pilots, NH_4-N concentrations in the pore water were typically at the lower end of the ranges observed in leachates (Figure 5.4, right).

NH_4-N concentrations in leachates were highest in KRA, likely due to the higher organic matter content, which provides a larger nitrogen source for ammonification. Anaerobic conditions promote the accumulation of NH_4-N due to the lack of degradation pathways for ammonia-nitrogen. Consequently, even after depletion of organic matter, ammonium levels remain elevated (Berge et al., 2005). Leachate recirculation likely enhanced the redistribution and flushing of ammonium within the waste body, as reflected by the increasing concentrations with depth (Figure 5.3, top). Elevated NH_4 concentrations also

persisted in the well-aerated compartments BRA-11N and WIE, indicating faster organic matter degradation, resulting in ammonium production exceeding its local oxidation.

5.3.2. Carbon and nitrogen in the aqueous phase

5.3.2.1. Carbon in the bulk leachate

Under aerobic conditions, carbon is primarily oxidized to CO_2, whereas under anaerobic conditions, it is released as both CH_4 and CO_2. The higher organic content in KRA (Figure 5.2), combined with its anaerobic conditions, resulted in higher dissolved organic carbon (DOC_L) and dissolved inorganic carbon (DIC) compared with the aerated pilots (Figure 5.5).

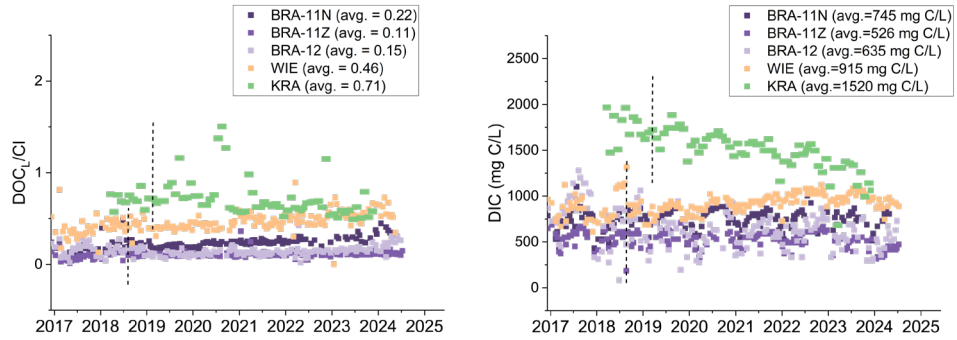

Figure 5.5. Dissolved organic carbon normalized to chloride (DOC_L / Chloride) (left), dissolved inorganic carbon (DIC) (right) over time in the leachate of BRA, WIE and KRA landfill pilots. Aeration started in August-September 2017 (left vertical dashed line) and leachate recirculation started in March 2018 (right vertical dashed line)

Leachate recirculation and aeration are expected to enhance organic matter reactivity, initially increasing DOC_L concentrations before declining as the easily degradable carbon is consumed. Once most of this labile carbon is degraded, the remaining DOC_L decomposes slowly and accumulates as bacteria continue to release dissolved organic matter (Dittmar, 2015). The decline in DOC_L is typically more pronounced under aerobic conditions than under anaerobic conditions (Bastviken et al., 2004). Moreover, the biodegradability of organic matter decreases with landfill age (Huo et al., 2008) as well as following aeration (He et al., 2006).

This trend was observed in KRA, were DOC_L normalized to chloride (DOC_L/Cl) increased until 2020 before declining steadily (Figure 5.5, left; and Supplementary information B, Section S5.3). In contrast, the aerated pilots showed less consistent patterns. At BRA-11Z, DOC_L/Cl remained relatively stable, whereas 11N displayed a clear rise after 2022. The additional aeration wells installed that year appears to have had a positive effect in 11N, but the impact in 11Z is less evident (Chapter 3, Figures 3.8-3.10), consistent with its lower aeration efficiency. Compartment 12 showed a marked increase in DOC_L/Cl from 2019 onwards, while WIE exhibited a steady rise from the start of aeration. These differences likely reflect variations in waste composition and the varying ages of the landfilled waste (Chapter 2, Table 2.1 and Figure 2.3). Overall, the results suggest enhanced degradation

under aeration, with lower DOC_L concentrations in the aerated pilots indicating a higher degree of stabilization compared with the anaerobic KRA pilot.

DIC levels are driven by CO_2 dissolution and its conversion to bicarbonates and carbonates (St-Jean, 2003). Since the start of the stabilization, DIC increased in the aerated pilots but declined in KRA (Supplementary information B, Section S5.3), likely due to contaminant flushing during water recirculation. DIC normalized to chloride (data not shown) followed similar trends across all pilots but with smaller slopes, especially in KRA, indicating that dilution effects partly influence the observed concentrations. It should be noted that leachate samples were not equilibrated with the atmosphere during sampling, and CO_2 degassing may have occurred. This process could lead to locally lower measured DIC concentrations, particularly in aerated zones where pressure fluctuations and gas exchange are more pronounced. Nevertheless, the observed differences between pilots are large enough that the general trends are not expected to be significantly affected.

The overall hierarchy in DOC_L and DIC (KRA > WIE > BRA-11N > BRA-12 > BRA-11Z) aligns with the DOC_L patterns measured in waste samples during the baseline study, which showed BRA-11Z as the compartment with the lowest DOC_L (Chapter 2, Figure 2.5). It also agrees with waste characterization results, which higher carbon content in KRA compared with the aerated pilots (Chapter 2, Figure 2.4; Chapter 4, Figure 4.4), and highlighted differences within BRA, with the highest carbon extraction efficiency in 11N (Chapter 3, Figures 3.8).

Seasonal variation was also evident, especially at KRA (Figure 5.6, left). Concentrations were higher in summer, likely due to greater evapotranspiration and reduced precipitation, and lower in winter when infiltration increased. The fact that this pattern was also observed under active recirculation indicates that natural precipitation remains an important driver of flushing, even when water is artificially added. This was confirmed by a recent study that estimated that rain and evapotranspiration were approximately one third of the recirculated water (T. Heimovaara, personal communication, August 2025).

5.3.2.2. Nitrogen in the bulk leachate

The nitrogen content in the leachate is predominantly in the form of ammonium-nitrogen (NH_4-N). Reported concentrations range between 500-5000 mg/L in MSW landfills in Asia, Africa and Latin America (Vaccari et al., 2019), and 300-2000 mg/L in the Netherlands (Valencia et al., 2011; Van Breukelen et al., 2003). In the sites under investigation, leachate nitrogen was also dominated by NH_4-N with yearly mean concentrations of 80-600 mg/L in BRA, 300-1000 mg/L in WIE, and 800-1400 mg/L in KRA. In contrast, nitrate and nitrite nitrogen (NO_3-N + NO_2-N) remained consistently low, averaging below 1 mg N/L across all pilots (Figure 5.6, right).

In this study, total nitrogen was defined as the sum of Kjeldahl nitrogen (Nkj, which includes organic nitrogen) and NO_3-N + NO_2-N. In KRA, at least 70% of Nkj was present as NH_4-N, while in the aerated pilots it was at least 47%. Nkj normalized to chloride (Nkj/Cl) followed

the same trend to carbon (KRA > WIE > BRA-11N > BRA-12 > BRA-11Z) (Figure 5.6, left), consistent with the positive correlation between ammonium and dissolved organic matter in KRA leachate (Van Raffe et al., 2023). This pattern can be attributed to differences in waste composition (Chapter 2, Figure 2.3), which is the primary source of nitrogen (Brandstätter et al., 2015b; Dang et al., 2023; Yang et al., 2012). Waste with higher organic matter degrades faster and anaerobic microbial decomposition forms ammonium (Figure 5.1). For KRA, and occasionally for BRA and WIE, nitrogen fixation is another source: up to 28% of nitrogen in the extracted LFG may originate from this process (Yi et al., 2025).

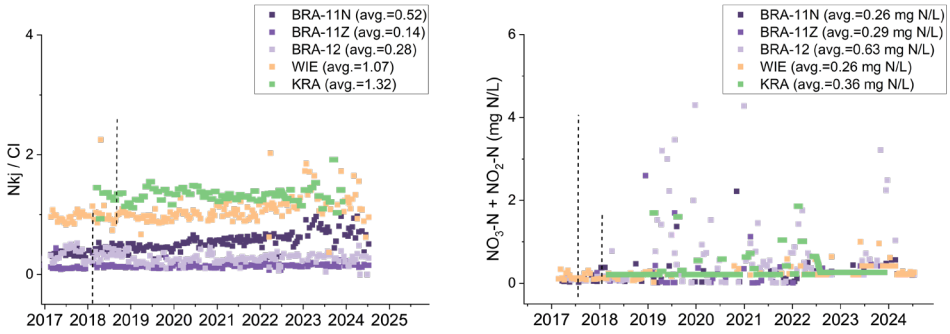

Figure 5.6. Kjeldahl nitrogen normalized to chloride (Nkj/Cl) (left) and nitrate plus nitrite nitrogen (NO_3-N + NO_2-N) (right) over time in the leachate of BRA, WIE and KRA landfill pilots. Aeration started in August-September 2017 (left vertical dashed line) and leachate recirculation started in March 2018 (right vertical dashed line).

Within the aerated pilots, limited oxygen availability may restrict ammonium oxidation (Ritzkowski et al., 2016). Although WIE exhibited higher Nkj concentrations than BRA, this likely reflects enhanced nitrogen release due to enhanced organic matter degradation rather than oxygen limitation. In BRA, higher aeration efficiency in compartment 11N compared with 11Z suggests greater organic matter degradation in 11N (Meza et al., 2022). Anaerobic pockets, however, would still maintain nitrogen release in the form of ammonium.

In KRA, Nkj concentrations decreased clearly over time (Supplementary information B, Section S5.3), as ammonium was flushed out with recirculated treated in Anammox and nitritation reactors. A similar decline in NH_4-N has been reported in pilot-scale landfills where recirculation of nitrified leachate reduced concentrations progressively (Bae et al., 2019). In contrast, Nkj/Cl in KRA showed a slight increase over time (Supplementary information B, Section S5.3), suggesting enhanced organic matter degradation.

Numerous landfill simulation reactors (LSR) operated under aerobic conditions have also shown declines in NH_4 due to nitrification and denitrification (Brandstätter et al., 2015b; Fricko et al., 2021; Y. Yang et al., 2012). In the aerated pilots, Nkj increased clearly in WIE and BRA-11N, while the increases in BRA-11Z and BRA-12 were more moderate (Supplementary information B, Section S5.3). This increase may be attributed to the hydrolysis of organic nitrogen, a process previously observed in aerated reactors (Cossu et al., 2016).

5.3.2.3. Cumulative carbon and nitrogen released through the bulk leachate

Over seven years of stabilization, the cumulative amounts of carbon and nitrogen released through the leachate were significantly higher in the anaerobic pilot than the aerated pilots (Figure 5.7). These differences are influenced by landfill size, waste composition, and water recirculation (Chapter 2, Table 2.1). This is evident when normalized to dry waste: WIE released more carbon and nitrogen than BRA.

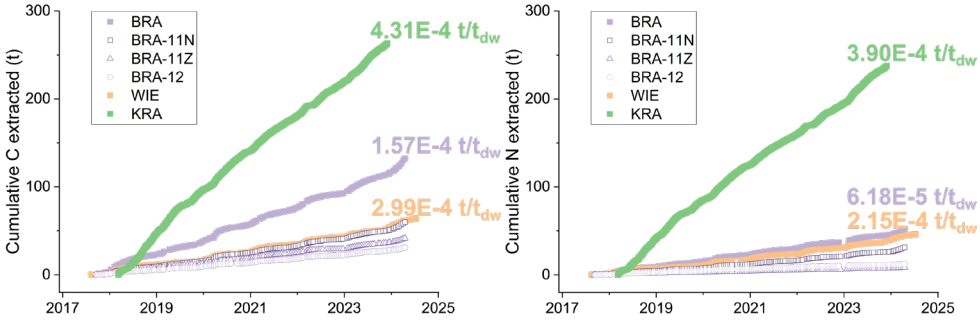

Figure 5.7. Cumulative mass of carbon (left) and nitrogen (right) released via the leachate pathway in BRA, WIE and KRA landfill pilots. Values are normalized to dry waste and indicated in the figure.

Overall, carbon release in KRA was 1.4 times higher than in WIE and 2.7 times higher than in BRA. Nitrogen release in KRA was almost twice that of WIE and more than six times that of BRA. This pattern likely reflects faster organic matter degradation to the gas phase in the aerated pilots, leaving less carbon and nitrogen in the leachate. Previous studies also reported up to twice as much carbon and nitrogen release through the leachate under anaerobic conditions compared with aerobic conditions (Brandstätter et al., 2015b, 2015a). Among the aerated pilots, compartment 11N in BRA showed a pattern similar to WIE, with higher carbon and nitrogen removal compared with compartments 11Z and 12.

The cumulative increase in carbon and nitrogen was approximately linear over time, indicating that a slowdown in the degradation process is not yet visible.

5.3.3. Carbon and nitrogen in the gas phase

In the aerated pilots, increasing O_2 concentrations coincided with decreasing CH_4 and CO_2 (Figure 5.8, top and middle left). The dominance of CO_2 over CH_4 after the onset of aeration indicates a shift from anaerobic methanogenesis to heterotrophic respiration. Microbial methane oxidation, another potential source of CO_2 generation and O_2 consumption, was considered negligible based on the isotopic composition of the gas (Supplementary information B, Figure S5.4.2). The inverse trend between O_2 and CH_4 + CO_2 reflects greater inflow of atmospheric air and dilution of the extracted landfill gas rather than reduced CO_2 generation.

In BRA, improved aeration following the 2022 installation of additional wells enhanced gas exchange, lowering CH_4 and CO_2 fractions. In WIE, the higher O_2 levels observed from 2022

onward resulted from operational changes: daily dewatering through brief air injection to improve condensate drainage and maintenance of the aeration system. A portion of the CO_2 produced by respiration likely dissolved in leachate as bicarbonate, further contributing to the observed decrease in gas-phase CO_2 and the increase in dissolved inorganic carbon (DIC, Figure 5.5).

In KRA, the yearly median CH_4 increased from 37%$_{vol}$ in 2018 to 43%$_{vol}$ in 2021 and then remained stable (Supplementary information B, Table S5.4.1) with higher CH_4 than CO_2 concentrations are consistent with its anaerobic conditions (Figure 5.8, bottom left).

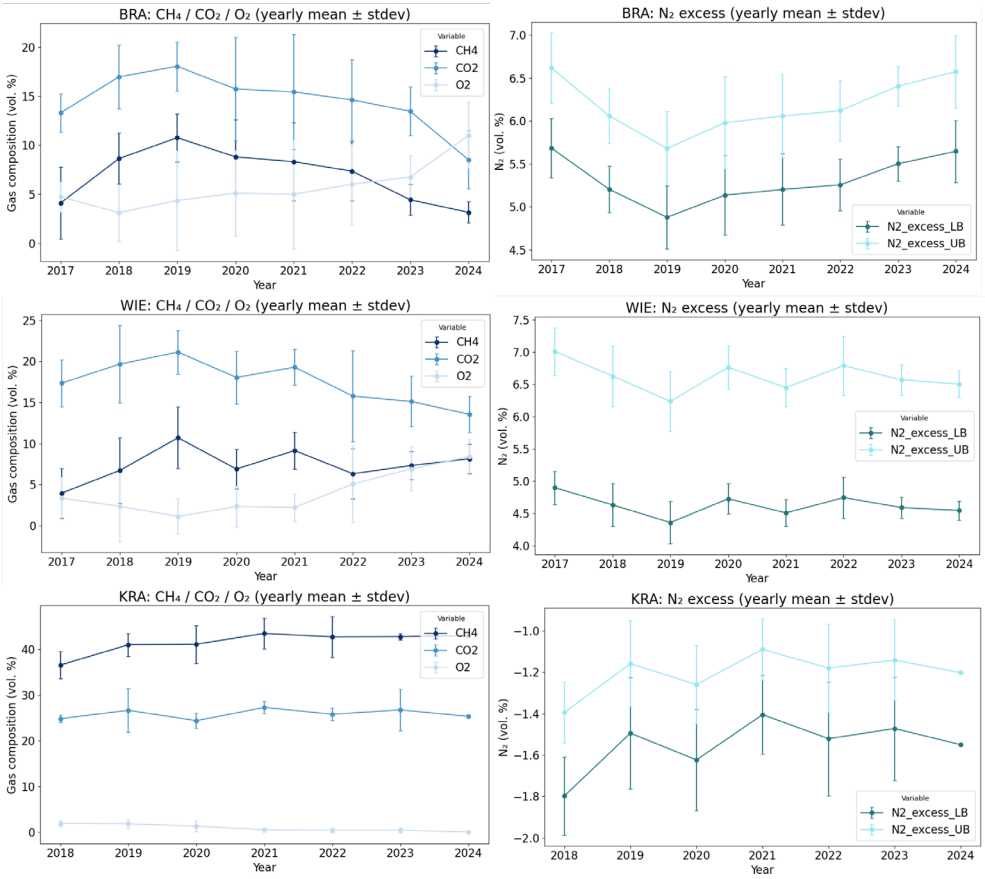

Figure 5.8. Yearly mean ± standard deviation of landfill gas (LFG) composition. Left: CH_4, CO_2, and O_2 concentrations in BRA (top), WIE (middle), and KRA (bottom). Right: estimated N_2 concentrations (N_{2_excess}) for the same pilots. $N_{2\_excess\_LB}$ and $N_{2\_excess\_UB}$ represent the lower and upper bounds derived from the bulk gas measurements.

Seasonal variations were also evident (Supplementary information B, Figure S5.4.1), with higher CH_4 and CO_2 concentrations during summer, likely due to greater cover-soil permeability and oxygen diffusion under drier conditions (Gebert et al., 2023). Cover soils with lower water content presents higher water-free porosity, which enhance diffusion of atmospheric air and advective air transport. Meaning that more oxygen is available to degrade organic matter and produce CO_2.

These aeration-induced shifts in gas composition also influenced nitrogen cycling. The introduction of atmospheric air and enhanced oxygen availability altered redox conditions within the waste, influencing both denitrification and nitrogen fixation. These processes are reflected in the estimated N_{2_Excess} and measured N_2O concentrations discussed below.

The mean N_{2_Excess} was used to estimate the N_2 production through denitrification and N_2 generation through fixation. When comparing the mean N_{2_Excess} from all samples (individual wells and bulk gas) with those from the bulk gas alone, the averages were similar (Supplementary information B, Table S5.4.2). However, the minimum and maximum differed, particularly in BRA, where the overall dataset indicated higher N_2 fixation than in WIE, a pattern not evident in the bulk gas. This discrepancy suggests a higher spatial variability of denitrification and nitrogen fixation processes within the landfill body at BRA. The mean N_2 released from the net denitrification in the aerated pilots was on average 5-6 $\%_{vol}$, whereas in KRA, N_2 consumption remained below 2$\%_{vol}$ (Figure 5.8, right).

Nitrous oxide (N_2O), produced when denitrification is incomplete, was detected only in trace amounts (Supplementary information B, Figure S5.4.3). Measurements from August 2022 to November 2024 (data provided by Susan Yi, 20/02/2025) showed a gradual increase in BRA, with an average 0.7 ppmv and the highest average concentration in compartment 11N (2.5 ppmv) compared with compartments 11Z and 12 (0.1 ppmv). This pattern indicates enhanced aeration in 11N, consistent with its higher aeration efficiency relative to 11Z and 12 (Meza et al., 2022), and with the increased aeration capacity following the installation of additional wells in 2022 (Chapter 2). In WIE, elevated N_2O concentrations observed in 2023 coincided with the highest denitrification rates and high median gas flow and O_2 concentration (Supplementary information B, Section S5.4), suggesting partial higher nitrification-fed denitrification. In contrast, KRA consistently showed no detectable N_2O, reflecting its persistently anaerobic conditions.

5.3.3.1. Cumulative carbon and nitrogen released through the gas phase

Although TOC and TN levels were similar in the aerated pilots, and higher in the anaerobic pilot KRA (Figure 5.2), WIE outperformed BRA, while KRA released the least carbon and nitrogen through the gas phase (Table 5.5, Figure 5.9). After seven years of stabilization, WIE released nearly five times as much carbon and nitrogen as BRA, and about 24 times as much carbon as KRA (Figure 5.9). The share of aerobic carbon, calculated using aeration efficiency (AE, Eq. 9), was higher in WIE than in BRA (43% and 36% respectively), and was 0% in KRA consistent with its anaerobic conditions (Table 5.5).

WIE's superior performance was also evident when compared with modelled carbon estimates (Afvalzorg, 2022). Cumulative carbon released in WIE was nearly five times the predicted under anaerobic conditions, and in BRA almost twice as high. In contrast, KRA released only one-fifth of its predicted carbon, suggesting inefficient carbon recovery and/or model overestimation. Gas tests demonstrated that anaerobically degradable carbon in

KRA waste samples ($GT_{Y0\text{-}TOC}$) was less than 10% of TOC (Chapter 4, Table 4.10), indicating that most anaerobically degradable organic carbon had already been depleted.

Table 5.5. Cumulative carbon and nitrogen released in seven years of stabilization through the gas phase in BRA, WIE and KRA pilots.

Cumulative mass (t)	BRA	WIE	KRA
Carbon	2244	2658	372
Aerobic carbon	814	1139	0
Nitrogen (Low boundary N_{2_excess})	1283	1136	-20
Nitrogen (Upper boundary N_{2_excess})	1494	1625	-16

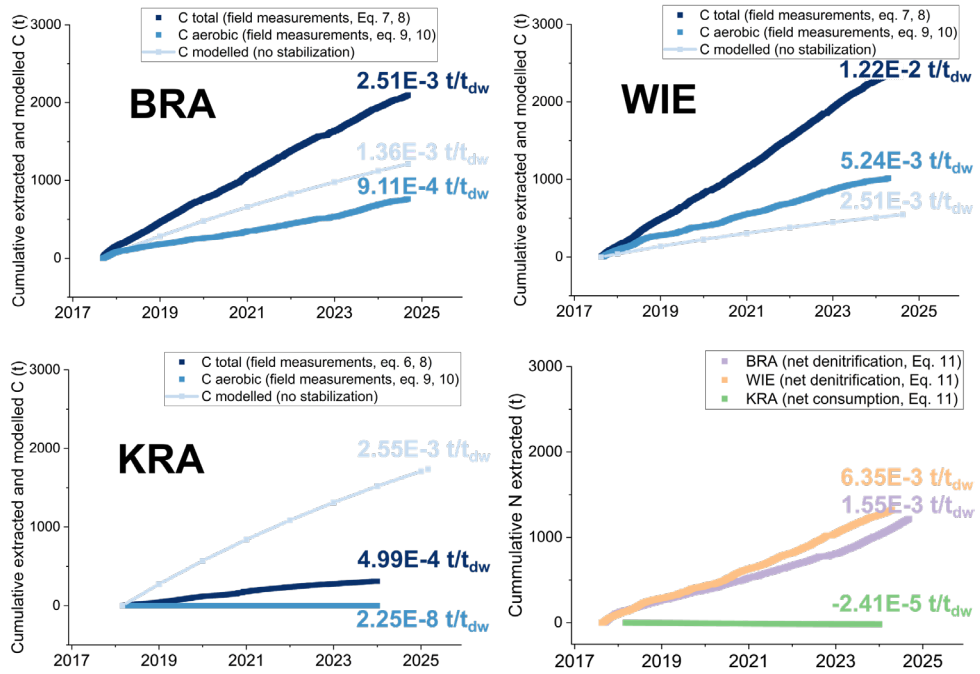

Figure 5.9. Cumulative carbon extraction from landfill pilots BRA (top left), WIE (top right), and KRA (bottom left), showing total carbon extracted (field measurements), the aerobic contribution, and the modeled carbon release without stabilization. The bottom-right panel shows cumulative nitrogen extraction for BRA, WIE, and KRA based on the average of lower and upper N_{2_excess} estimates. Values are normalized to dry waste and indicated in the figure.

Since KRA lacked bulk gas recovery data from only the recirculated pilot, gas velocity data from individual wells was used to estimate landfill gas (LFG) originating from the recirculated pilot. This analysis suggested that one-third of bulk LFG at Kragge II landfill originated from the pilot under recirculation, with a nominal recovery efficiency of 24% (Chapter 4). Yearly median pressure, flow and gas composition for the pilots are shown in the Supplementary information B (Table S5.4.1). The number of active gas wells also influence gas recovery (Themelis & Ulloa, 2007). Since the start of recirculation, only a maximum of nine out of thirteen gas wells has shown active gas flow.

The lower share of cumulative aerobic carbon in BRA compared with WIE (Figure 5.9, top) can be attributed to site-specific challenges, including low permeability, perched water

tables and high spatial variability in gas flow and waste permeability (Gebert et al., 2022; Meza et al., 2022). These factors limited aeration efficiency, particularly in areas like BRA-11Z, and resulted in higher CH_4 to CO_2 ratios, indicating persistent anaerobic conditions. The average CH_4 to CO_2 ratio was 0.5 in BRA and 0.4 in WIE.

Aerobic carbon estimates were derived by comparing measured gas compositions with an assumed anaerobic baseline in which CH_4 and CO_2 are produced in a 1:1 ratio through acetotrophic methanogenesis. In marine sediments, approximately two-thirds of methane production from organic matter decomposition originates from acetate (acetotrophic methanogenesis), while the remaining third results from CO_2 reduction (hydrogentrophic methanogenesis) (Ferry & Lessner, 2008). A study in a Chinese landfill found that acetotrophic and hydrogentrophic methanogenesis were the dominant methane production pathways (Dang et al., 2023), likely resulting in a higher CH_4 to CO_2 ratio than 1:1. Additionally, CO_2 produced during acetotrophic methanogenesis is in equilibrium with bicarbonate in the aqueous phase, meaning that factors such as pH and temperature can influence the proportion of CO_2 that remains dissolved in leachate versus that released as gas. Therefore, assuming a CH_4 to CO_2 ratio of 1:1 is a conservative estimate, suggesting that actual aerobic carbon levels in the landfills may be higher than estimated.

Cumulative carbon extraction from the aerated pilots (Figure 5.9, C total) exhibited a linear trend with no sign of plateauing, indicating the continued (non-limiting) presence of degradable organic matter and that degradation is constrained by O_2 ingress. This conclusion is further supported by the higher aeration efficiency in WIE during summer, as increased cover permeability allowed greater air inflow (Gebert et al., 2023). These findings highlight the role of cover soil hydrology in aeration performance, which was not fully considered in the experimental design.

Well spacing further influenced aeration effectiveness (Themelis & Ulloa, 2007; van Turnhout et al., 2020). Wider spacing reduces the waste volume receiving sufficient airflow. In BRA, well spacing ranged from 15-20 m, compared with 12.5-13.5 m in WIE. To address this, 98 additional aeration wells were installed in 2022 (Cruz & Lammen, 2023). This intervention seemed to have improvement aeration: the slope of cumulative carbon extraction increased from 0.28 to 0.36, and suction pressure slightly decreased, resulting in at least 1.5-fold increase in gas flow during 2023-2024. This suggests greater O_2 ingress (also saw in Figure 5.8, left), enhancing organic matter degradation and net denitrification (Figure 5.9, top left and bottom right).

5.3.4. Mass balance

The total organic carbon (TOC) and nitrogen (TN) in the solid phase before stabilization (baseline), extrapolated to each pilot, were used as the pool for degradation. In addition, degradable organic carbon (DOC_S), and the acid-base extracted dissolved organic nitrogen (DON) were included as carbon and nitrogen that can degrade or be released. Microbial

carbon and nitrogen were assumed to contribute up to 4%TOC and 26%TN, respectively.

At the beginning of the stabilization (baseline), DOC_S in the waste was estimated to be 10-23%TOC (Afvalzorg, 2022). In the aerated pilots, 9-21% of TN was present as acid-base extracted DON, compared with 14-26% in KRA (Figure 5.10). The high percentage is probably affected by the oxidation of ammonium during the storage of samples, leading to lower values of TN before the start of the stabilization (Figure 5.2). This can also explain the high percentage of nitrogen release through the gas phase with respect to the initial TN, especially in WIE (Figure 5.10, middle left).

Over seven years of stabilization, all DOC_S (~23%TOC) was released via gas and leachate in WIE, compared with ~40% DOC_S only (~5%TOC) in BRA, and only 7% DOC_S (<1%TOC) in the anaerobic pilot KRA (Figure 5.10, left). Earlier research using MSW bioreactors suggest that 47-52% of biogenic carbon may remain stored in the long term, with little leaching despite extensive flushing (Bolyard & Reinhart, 2016). DOC_S estimates remain uncertain due to model variability (see section 5.2.2.2) and high sample heterogeneity (Chapter 4, Figure 4.7). For instance, in WIE, the aerobic carbon potential averaged 23%TOC but ranged from 16-30%TOC across samples.

Carbon released was dominated by the gas phase in the aerobic pilots. After seven years, the gas to leachate carbon release ratio was 16-41 in the aerated pilots, while in KRA similar amounts were released through both phases. Landfill simulation reactor (LSR) experiments showed higher carbon released via gas compared to leachate. LSR studies also reported greater gas-phase release: Italian residual waste LSRs showed ratios of 5-9 in aerobic conditions and 2-3 under anaerobic (Cossu et al., 2016), while Austrian MSW LSRs reached ratios above 60 under aerobic conditions and about half that under anaerobic treatment (Fricko et al., 2021).

In our pilots, less than 1% TOC was removed via leachate. Gas phase removal was ≥ 5%TOC in the aerated pilots, compared with <1%TOC in KRA. Similar trends were observed in MSW LSRs, where aerobic degradation produced more than three times the carbon release of anaerobic degradation under optimal conditions (Ritzkowski et al., 2016).

For nitrogen, LSRs of landfilled MSW reported 73-93% of the initial nitrogen measured in the waste (TNinit) remained in the solid phase, with 2-4% released as N_2O in the aerobic reactors (Bolyard & Reinhart, 2016; Brandstätter et al., 2015b; Fricko et al., 2021). In our study, nitrogen release pathways differed by pilot. In the aerated pilots, the gas phase dominated, reaching over 100% of baseline TN. In contrast, in KRA the main pathway was leachate, releasing 8%TN. MSW LSR studies also found leachate to be the main N pathway in anaerobic reactors (8-9% TNinit), while gas phase dominated in aerobic reactors (Brandstätter et al., 2015b; Fricko et al., 2021). As with carbon (DOC_S), WIE released more nitrogen than was estimated to be present in the baseline waste samples.

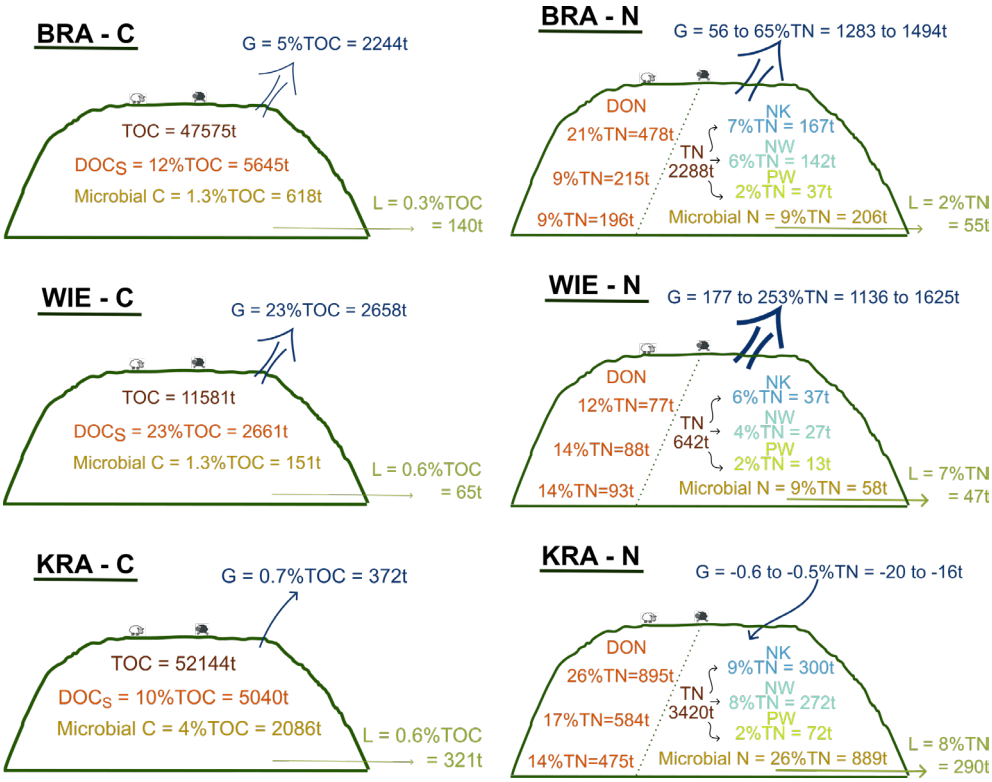

Figure 5.10. Carbon (left) and nitrogen (right) balance in BRA (top) and WIE (middle) and KRA (bottom) pilots. At the beginning of stabilization: TOC = total organic carbon, DOCs = estimated degradable organic carbon, DON = dissolved organic nitrogen, TN = total nitrogen; after seven years of stabilization: microbial C and N = assumed microbial carbon and nitrogen, NK = adsorbed nitrogen (KCl extractable), NW = adsorbed nitrogen (H_2O extractable), PW = dissolved nitrogen (pore water), L = leachate release, G = gas release.

The gas-to-leachate nitrogen release ratio was 23-24 in the aerated pilots. Net nitrogen release was affected by coupled nitrification-denitrification, caused by coexisting aerobic and anaerobic pockets (Yi et al., 2025). In KRA, by contrast, 290 t N were released through leachate, no nitrogen was released via gas, and 20 t were net consumed through nitrogen fixation, representing an additional nitrogen source.

5.3.4.1. Uncertainties in mass balancing

A number of factors contribute to uncertainty in the different carbon and nitrogen pools presented in the mass balance. Laboratory analyses showed high variability in waste sample composition, as discussed in the corresponding sections. All data related to the solid phase relied on waste excavated from a limited number of drillings, which, given the strong waste heterogeneity, cannot be regarded as fully representative. In addition, baseline measurements were affected by the inclusion of cover material and inappropriate sample storage, particularly influencing nitrogen content. As a result, the estimated carbon and nitrogen pools may not fully reflect true baseline conditions, especially for nitrogen.

Carbon released through the gas phase and carbon and nitrogen released through the leachate were calculated directly from field measurements of gas and leachate composition and flow. The main uncertainty in these calculations arises from short periods without measurements, which were not included in the cumulative carbon and nitrogen release. Consequently, these totals likely represent a conservative estimate. In contrast, nitrogen released through the gas phase was estimated using upper and lower boundaries of the N_{2_excess} range derived from gas composition data. The resulting values should therefore be regarded as estimates rather than direct measurements.

Uncertainties within the landfill itself remain significant, as the solid-phase pools depend on laboratory analyses of heterogeneous waste samples. Averaged data were used to approximate the carbon and nitrogen balances, but localized variability in moisture content and waste composition likely influenced the results.

Operational disruptions also affected the aeration process. At BRA, aeration was halted for two weeks in September 2022 due to well installations, reducing flow rates to below 50% for over a month. Similarly, WIE experienced a month-long maintenance shutdown starting in mid-October 2022, temporarily reducing gas extraction efficiency. However, these interruptions had a limited effect on the overall balance. For example, in BRA, a two-week stop in gas extraction corresponds to a reduction of only 0.03% TOC and 0.3% TN released via the gas phase.

Site configuration further contributed to uncertainty. BRA is located on an independent hill with separate leachate and gas systems, whereas WIE and KRA are situated near other actively managed landfill compartments. Although both have independent leachate collection systems, adjustments to the gas data were required to isolate the carbon and nitrogen released from the compartments under in-situ stabilization. In addition, ongoing degradation and settlement could have caused lateral waste displacement into adjacent compartments, complicating the mass balances.

In WIE, the aeration system included 20–25% of the adjacent compartment to minimize boundary effects (Chapter 2). This inclusion increased the effective waste volume and, consequently, the estimated carbon and nitrogen pools. To isolate the contribution from compartment 6, a correction factor was applied (see section 5.2.4).

At KRA, the absence of a dedicated gas extraction system capable of exclusively measuring gas flows from the stabilization compartment introduced additional uncertainty. As a result, estimates of carbon and nitrogen extracted through the gas phase are less reliable. Furthermore, nitrogen released via leachate did not account for the contribution of nitrogen reintroduced through recirculated treated leachate, since the quality of infiltrated leachate was not monitored regularly.

5.4. Conclusions

This chapter demonstrates that carbon and nitrogen balances can be established for full-scale landfills by integrating data from the solid, aqueous, and gaseous phases. Despite uncertainties arising from operational interruptions and incomplete monitoring, especially in KRA, the balances captured the main transformation and release pathways under both aerobic and anaerobic conditions.

Aeration enhanced organic matter stabilization and shifted carbon and nitrogen release toward the gas phase, whereas anaerobic conditions favored solute accumulation and leachate discharge. Carbon degradation in aerated pilots followed a linear trend, indicating that oxygen availability, rather than substrate limitation, controls the rate of stabilization. The balances also revealed that nitrogen cycling differs fundamentally between conditions: aerated landfills released nitrogen primarily via denitrification, while the anaerobic pilot retained nitrogen through fixation and adsorption.

After seven years of stabilization, aerated landfills exhibited more efficient organic matter stabilization, as indicated by the higher share of degraded DOC_S (degradable organic carbon) relative to total organic carbon (TOC), and a higher degree of nitrogen transformation than the anaerobic site. However, large nitrogen pools remained adsorbed or immobilized in the solid phase (up to 43% TN), which may delay compliance with the 50 mg/L ammonium target. Site-specific factors such as aeration efficiency, well spacing, and waste composition strongly influenced overall performance and balance uncertainties.

Overall, carbon and nitrogen balances proved to be powerful diagnostic tools to evaluate landfill stabilization, providing quantitative insight into degradation processes and emission dynamics under contrasting operational conditions.

Bibliography

1. Afvalzorg. (2022). Multiphase landfill gas generation model. Version 2022. https://www.afvalzorg.com/landfill-gas/lfg-models/multiphase-landfill-gas-generation-model
2. Bae, W., Kim, S., Lee, J., & Chung, J. (2019). Effect of leachate circulation with ex situ nitrification on waste decomposition and nitrogen removal for early stabilization of fresh refuse landfill. Journal of Hazardous Materials, 371, 721–727. https://doi.org/10.1016/j.jhazmat.2019.03.058
3. Bastviken, D., Persson, L., Odham, G., & Tranvik, L. (2004). Degradation of dissolved organic matter in oxic and anoxic lake water. Limnology and Oceanography, 49(1), 109–116. https://doi.org/10.4319/lo.2004.49.1.0109
4. Berge, N. D., Reinhart, D. R., & Townsend, T. G. (2005). The Fate of Nitrogen in Bioreactor Landfills. Critical Reviews in Environmental Science and Technology, 35(4), 365–399. https://doi.org/10.1080/10643380590945003
5. Bolyard, S. C., & Reinhart, D. R. (2016). Application of landfill treatment approaches for stabilization of municipal solid waste. Waste Management (New York, N.Y.). https://doi.org/10.1016/j.wasman.2016.01.024
6. Bouzaiane, O., Cherif, H., Ayari, F., Jedidi, N., & Hassen, A. (2007). Municipal solid waste compost dose effects on soil microbial biomass determined by chloroform fumigation-extraction and DNA methods. In Annals of Microbiology (Vol. 57, Issue 4).
7. Brand, E., de Nijs, T., Claessens, J., Dijkstra, J. J., Comans, R. N. J., & Lieste, R. (2014). Development of emission testing values to assess sustainable landfill management on pilot landfills. Phase 2 : Proposals for testing values. www.rivm.nl
8. Brandstätter, C., Keiblinger, K., Wanek, W., & Zechmeister-Boltenstern, S. (2013). A closeup study of early beech litter decomposition: Potential drivers and microbial interactions on a changing substrate. Plant and Soil, 371(1–2), 139–154. https://doi.org/10.1007/s11104-013-1671-7
9. Brandstätter, C., Laner, D., & Fellner, J. (2015a). Carbon pools and flows during lab-scale degradation of old landfilled waste under different oxygen and water regimes. Waste Management, 40, 100–111. https://doi.org/10.1016/J.WASMAN.2015.03.011
10. Brandstätter, C., Laner, D., & Fellner, J. (2015b). Nitrogen pools and flows during lab-scale degradation of old landfilled waste under different oxygen and water regimes. Biodegradation, 26(5), 399–414. https://doi.org/10.1007/s10532-015-9742-5
11. Brandstätter, C., Prantl, R., & Fellner, J. (2020). Performance assessment of landfill in-situ aeration – A case study. Waste Management, 101, 231–240. https://doi.org/10.1016/j.wasman.2019.10.022
12. Brust, G. E. (2019). Management strategies for organic vegetable fertility. In Safety and Practice for Organic Food (pp. 193–212). Elsevier. https://doi.org/10.1016/B978-0-12-812060-6.00009-X
13. Chung, J., Kim, S., Baek, S., Lee, N. H., Park, S., Lee, J., Lee, H., & Bae, W. (2015). Acceleration of aged-landfill stabilization by combining partial nitrification and leachate recirculation: A field-scale study. Journal of Hazardous Materials, 285, 436–444. https://doi.org/10.1016/J.JHAZMAT.2014.12.013
14. Cossu, R., Morello, L., Raga, R., & Cerminara, G. (2016). Biogas production enhancement using semi-aerobic pre-aeration in a hybrid bioreactor landfill. Waste Management, 55, 83–92. https://doi.org/10.1016/j.wasman.2015.10.025
15. Cruz, C., & Lammen, H. (2023). Landfill gas stabilization by aeration: initial insights following design and operational adjustments. www.cisapublisher.com
16. Dang, Q., Zhao, X., Li, Y., & Xi, B. (2023). Revisiting the biological pathway for methanogenesis in landfill from metagenomic perspective—A case study of county-level sanitary landfill of domestic waste in North China plain. Environmental Research, 222. https://doi.org/10.1016/j.envres.2022.115185
17. Dang, Q., Zhao, X., Xi, B., Zhang, C., & He, L. (2023). The key role of denitrification and dissimilatory nitrate reduction in nitrogen pollution along vertical landfill profiles from metagenomic perspective. Journal of Environmental Management, 342. https://doi.org/10.1016/j.jenvman.2023.118300
18. Dijkstra, J. J., van Zomeren, A., Brand, E., & Comans, R. N. J. (2018). Site-specific aftercare completion criteria for

sustainable landfilling in the Netherlands: Geochemical modelling and sensitivity analysis. Waste Management, 75, 407–414. https://doi.org/10.1016/j.wasman.2016.07.038

19. Dittmar, T. (2015). Reasons Behind the Long-Term Stability of Dissolved Organic Matter. In Biogeochemistry of Marine Dissolved Organic Matter: Second Edition (Second Edi). Elsevier Inc. https://doi.org/10.1016/B978-0-12-405940-5.00007-8
20. Ferry, J. G., & Lessner, D. J. (2008). Methanogenesis in marine sediments. Annals of the New York Academy of Sciences, 1125, 147–157. https://doi.org/10.1196/annals.1419.007
21. Fricko, N., Brandstätter, C., & Fellner, J. (2021). Enduring reduction of carbon and nitrogen emissions from landfills due to aeration? Waste Management, 135(June), 457–466. https://doi.org/10.1016/j.wasman.2021.09.024
22. Gebert, J. (2024). Distribution of carbon and nitrogen in the solid phase, aqueous phase and microbial biomass in fine-grained sediments and MSW.
23. Gebert, J., de Jong, T., Meza, N., Rees-White, T., Beaven, R. P., & Lammen, H. (2022). Spatial Variability of Leachate Tables, Leachate Composition and Hydraulic Conductivity in a Landfill Stabilized By in-Situ Aeration. Detritus, 19, 114–120. https://doi.org/10.31025/2611-4135/2022.15189
24. Gebert, J., Hanke, N., Bohn, S., Smidt, E., & Streese-Kleeberg, J. (2011). Gas Potential of Old Landfills. Proceedings Sardinia 2011, 13th International Waste Management and Landfill Symposium, 10.
25. Gebert, J., Meza, N., Cruz, C., & Lammen, H. (2023). Assessing the efficiency of landfill aeration with a carbon mass balance approach. Sardinia 2023, 19th International Symposium on Waste Management and Sustainable Landfilling, 1998.
26. He, P. J., Xue, J. F., Shao, L. M., Li, G. J., & Lee, D. J. (2006). Dissolved organic matter (DOM) in recycled leachate of bioreactor landfill. Water Research, 40(7), 1465–1473. https://doi.org/10.1016/j.watres.2006.01.048
27. Hrad, M., Gamperling, O., & Huber-Humer, M. (2013). Comparison between lab- and full-scale applications of in situ aeration of an old landfill and assessment of long-term emission development after completion. Waste Management, 33(10), 2061–2073. https://doi.org/10.1016/J.WASMAN.2013.01.027
28. Huang, G. F., Wong, J. W. C., Wu, Q. T., & Nagar, B. B. (2004). Effect of C/N on composting of pig manure with sawdust. Waste Management, 24(8), 805–813. https://doi.org/10.1016/j.wasman.2004.03.011
29. Huo, S., Xi, B., Yu, H., He, L., Fan, S., & Liu, H. (2008). Characteristics of dissolved organic matter (DOM) in leachate with different landfill ages. Journal of Environmental Sciences (China), 20(4), 492–498. http://www.ncbi.nlm.nih.gov/pubmed/23067547
30. Kanen, T., & Kedzia-Kowalski, S. (2021). Voortgangsrapportage iDS Kragge. september.
31. Kim, M. (2002). The study of landfill microbial communities using landfill gas and landfill gas condensate [Drexel University]. https://doi.org/10.17918/etd-152
32. Kodithuwakku, K., Huang, J., Doolette, C. L., Mason, S., Boland, J., Lehto, N. J., & Lombi, E. (2024). Plant responses to nitrate and ammonium availability in Australian soils as measured by diffusive gradients in thin-films (DGT) and KCl extraction. Geoderma, 449, 116997. https://doi.org/10.1016/J.GEODERMA.2024.116997
33. Kumar, M., Ou, Y. L., & Lin, J. G. (2010). Co-composting of green waste and food waste at low C/N ratio. Waste Management, 30(4), 602–609. https://doi.org/10.1016/J.WASMAN.2009.11.023
34. Manzoni, S., Jackson, R. B., Trofymow, J. A., & Porporato, A. (2008). The global stoichiometry of litter nitrogen mineralization. Science, 321(5889), 684–686. https://doi.org/10.1126/science.1159792
35. Mellendorf, M., Huber-Humer, M., Gamperling, O., Huber, P., Gerzabek, M. H., & Watzinger, A. (2010). Characterisation of microbial communities in relation to physical–chemical parameters during in situ aeration of waste material. Waste Management, 30(11), 2177–2184. https://doi.org/10.1016/J.WASMAN.2010.04.023
36. Meza, N., Lammen, H., Cruz, C., Heimovaara, T., & Gebert, J. (2022). Spatial Variability of Gas Composition and Flow in a Landfill Under in-Situ Aeration. Detritus, 19, 104–113. https://doi.org/10.31025/2611-4135/2022.15191
37. Miltner, A., Bombach, P., Schmidt-Brücken, B., & Kästner, M. (2012). SOM genesis: Microbial biomass as a significant source. Biogeochemistry, 111(1–3), 41–55. https://doi.org/10.1007/s10533-011-9658-z
38. Morello, L., Raga, R., Sgarbossa, P., Rosson, E., & Cossu, R. (2018). Storage potential and residual emissions from

fresh and stabilized waste samples from a landfill simulation experiment. Waste Management, 75, 372–383. https://doi.org/10.1016/J.WASMAN.2018.01.026

39. Nagamori, M., Mowjood, M. I. M., Watanabe, Y., Isobe, Y., Ishigaki, T., & Kawamoto, K. (2016). Characterization of temporal variations in landfill gas components inside an open solid waste dump site in Sri Lanka. Journal of the Air and Waste Management Association, 66(12), 1257–1267. https://doi.org/10.1080/10962247.2016.1212746
40. Oonk, H. (2020). Afvalmonstername en analyse bij de nulmeting van de iDS-pilots [Waste sampling and analysis during the baseline measurement of the iDS pilots].
41. Ouyang, Z., Yu, J., Li, X., Wei, N., Zhou, F., Li, X., & Chi, R. (2023). Dynamic elution of residual ion-exchangeable ammonium from weathered crust elution-deposited rare earth tailings. Colloids and Surfaces A: Physicochemical and Engineering Aspects, 679, 132658. https://doi.org/10.1016/J.COLSURFA.2023.132658
42. Purcell, B. E., Butler, A. P., Sollars, C. J., & Buss, S. E. (1999). Leachate ammonia flushing from landfill simulators. Water and Environment Journal, 13(2), 107–111. https://doi.org/10.1111/j.1747-6593.1999.tb01016.x
43. Puyuelo, B., Ponsá, S., Gea, T., & Sánchez, A. (2011). Determining C/N ratios for typical organic wastes using biodegradable fractions. Chemosphere, 85(4), 653–659. https://doi.org/10.1016/J.CHEMOSPHERE.2011.07.014
44. Reinhart, D. R. (1996). Full-Scale Experiences With Leachate Recirculating Landfills : Case Studies. 347–365.
45. Ritzkowski, M. (2021). Landfill aeration - an important contribution towards landfill sustainability. Sardinia 2021, 18th International Symposium on Waste Management and Sustainable Landfilling.
46. Ritzkowski, M., Heyer, K. U., & Stegmann, R. (2006). Fundamental processes and implications during in situ aeration of old landfills. Waste Management, 26(4), 356–372. https://doi.org/10.1016/J.WASMAN.2005.11.009
47. Ritzkowski, M., & Stegmann, R. (2012). Landfill aeration worldwide: Concepts, indications and findings. Waste Management, 32(7), 1411–1419. https://doi.org/10.1016/j.wasman.2012.02.020
48. Ritzkowski, M., Walker, B., Kuchta, K., Raga, R., & Stegmann, R. (2016). Aeration of the teuftal landfill: Field scale concept and lab scale simulation. Waste Management, 55, 99–107. https://doi.org/10.1016/j.wasman.2016.06.004
49. Sebag, D., Verrecchia, E. P., Cécillon, L., Adatte, T., Albrecht, R., Aubert, M., Bureau, F., Cailleau, G., Copard, Y., Decaens, T., Disnar, J. R., Hetényi, M., Nyilas, T., & Trombino, L. (2016). Dynamics of soil organic matter based on new Rock-Eval indices. Geoderma, 284, 185–203. https://doi.org/10.1016/j.geoderma.2016.08.025
50. Setia, R., Verma, S. L., & Marschner, P. (2012). Measuring microbial biomass carbon by direct extraction – Comparison with chloroform fumigation-extraction. European Journal of Soil Biology, 53, 103–106. https://doi.org/10.1016/J.EJSOBI.2012.09.005
51. Shigemitsu, M., Gruber, N., Oka, A., & Yamanaka, Y. (2016). Potential use of the N2/Ar ratio as a constraint on the oceanic fixed nitrogen loss. Global Biogeochemical Cycles, 30(4), 576–594. https://doi.org/10.1002/2015GB005297
52. Sohoo, I., Ritzkowski, M., & Kuchta, K. (2021). Influence of moisture content and leachate recirculation on oxygen consumption and waste stabilization in post aeration phase of landfill operation. Science of the Total Environment, 773. https://doi.org/10.1016/j.scitotenv.2021.145584
53. St-Jean, G. (2003). Automated quantitative and isotopic (13C) analysis of dissolved inorganic carbon and dissolved organic carbon in continuous-flow using a total organic carbon analyser. Rapid Communications in Mass Spectrometry, 17(5), 419–428. https://doi.org/10.1002/rcm.926
54. Themelis, N. J., & Ulloa, P. A. (2007). Methane generation in landfills. Renewable Energy, 32(7), 1243–1257. https://doi.org/10.1016/j.renene.2006.04.020
55. Thompson, S., Sawyer, J., Bonam, R., & Valdivia, J. E. (2009). Building a better methane generation model: Validating models with methane recovery rates from 35 Canadian landfills. Waste Management, 29(7), 2085–2091. https://doi.org/10.1016/j.wasman.2009.02.004
56. Vaccari, M., Tudor, T., & Vinti, G. (2019). Characteristics of leachate from landfills and dumpsites in Asia, Africa and Latin America: an overview. In Waste Management (Vol. 95, pp. 416–431). Elsevier Ltd. https://doi.org/10.1016/j.wasman.2019.06.032
57. Valencia, R., Zon, W. Van Der, Woelders, H., Lubberding, H. J., & Gijzen, H. J. (2011). Anammox: an option for ammonium removal in bioreactor landfills. Waste Management (New York, N.Y.), 31(11), 2287–2293. https://doi.

org/10.1016/j.wasman.2011.06.012

58. Van Breukelen, B. M., Röling, W. F. M., Groen, J., Griffioen, J., & Van Verseveld, H. W. (2003). Biogeochemistry and isotope geochemistry of a landfill leachate plume. Journal of Contaminant Hydrology, 65(3–4), 245–268. https://doi.org/10.1016/S0169-7722(03)00003-2
59. Van Raffe, F., Dijkstra, J. J., & Comans, R. N. J. (2025). Mechanisms controlling the release of inorganic contaminants, organic matter fractions, and ammonium from solid landfill waste: pH dependent leaching experiments and geochemical modelling. Applied Geochemistry, 190. https://doi.org/10.1016/j.apgeochem.2025.106503
60. Van Raffe, F., Quist, N., Kanen, T., & Comans, R. N. J. (2023). Sustainable landfill management in the Netherlands: Long term changes in landfill leachate quality during (an)aerobic in-situ stabilization. 19Th International Symposium on Waste Management, Resource Recovery and Sustainable Landfilling, 2023. www.cisapublisher.com
61. van Turnhout, A. G., Oonk, H., Scharff, H., & Heimovaara, T. J. (2020). Optimizing landfill aeration strategy with a 3-D multiphase model. Waste Management, 102, 499–509. https://doi.org/10.1016/j.wasman.2019.10.051
62. Vereniging Afvalbedrijven. (2015). Deelplan van aanpak verduurzamingspilot op stortplaats De Kragge 2 [Partial plan of approach for sustainability pilot at the De Kragge 2 landfill] (Issue April). https://www.duurzaamstortbeheer.nl/projectstukken/
63. Wang, R., Yu, J., Chen, Y., Li, X., Zhang, Z., Xiao, C., Fang, Z., & Chi, R. (2025). The adsorption mechanism of NH4+ on clay mineral surfaces: Experimental and theoretical studies. Separation and Purification Technology, 354, 128521. https://doi.org/10.1016/J.SEPPUR.2024.128521
64. Xu, X., Thornton, P. E., & Post, W. M. (2013). A global analysis of soil microbial biomass carbon, nitrogen and phosphorus in terrestrial ecosystems. Global Ecology and Biogeography, 22(6), 737–749. https://doi.org/10.1111/geb.12029
65. Yang, S., & Yang, G. (2024). Selective adsorption and release of the ammonium ion (NH4+) at smectites/water interfaces. Separation and Purification Technology, 339, 126662. https://doi.org/10.1016/J.SEPPUR.2024.126662
66. Yang, Y., Yue, B., Yang, Y., & Huang, Q. (2012). Influence of semi-aerobic and anaerobic landfill operation with leachate recirculation on stabilization processes. Waste Management and Research, 30(3), 255–265. https://doi.org/10.1177/0734242X11413328
67. Yazdani, R., Mostafid, M. E., Han, B., Imhoff, P. T., Chiu, P., Augenstein, D., Kayhanian, M., & Tchobanoglous, G. (2010). Quantifying factors limiting aerobic degradation during aerobic bioreactor landfilling. Environmental Science and Technology, 44(16), 6215–6220. https://doi.org/10.1021/es1022398
68. Yi, S., Meza, N., & Gebert, J. (2025). Application of the nitrogen-to-argon ratio to understand nitrogen transformation pathways in landfills under in-situ stabilization. Waste Management, 194, 13–23. https://doi.org/10.1016/j.wasman.2024.12.042
69. Zhang, G., Liu, K., Lv, L., Gao, W., Li, W., Ren, Z., Yan, W., Wang, P., Liu, X., & Sun, L. (2023). Enhanced landfill process based on leachate recirculation and micro-aeration: A comprehensive technical, environmental, and economic assessment. Science of The Total Environment, 857, 159535. https://doi.org/10.1016/J.SCITOTENV.2022.159535
70. Zhao, S., Zheng, Q., Wang, H., & Fan, X. (2024). Nitrogen in landfills: Sources, environmental impacts and novel treatment approaches. In Science of the Total Environment (Vol. 924). Elsevier B.V. https://doi.org/10.1016/j.scitotenv.2024.171725

6

Overarching discussion

Abstract

This discussion synthesizes the core findings of this thesis across all landfill pilots and experimental stages, focusing on how aeration and water recirculation influence carbon and nitrogen transformation during in-situ landfill stabilization. Field results are interpreted in light of baseline model expectations, operational implementation, and experimental validation.

Accelerated stabilization through aeration and water recirculation: effectiveness and constraints

All pilots share the same overall goal, that is, to accelerate waste decomposition and leachate contaminant reduction such that the respective site meets the Environmental Protection Criteria (EPCs; Brand et al., 2016) by the end of the active period. Aeration pilots (BRA and WIE) consistently demonstrated faster and more complete carbon mineralization than the anaerobic water recirculation pilot (KRA). This was evidenced by field gas extraction data and experimental degradation tests (Chapters 3–5).

Aeration led to a rapid reduction in methane concentrations in the extracted gas, from 20-30% to ~10%$_{vol}$, while CO_2 concentrations increased, indicating a shift from anaerobic methanogenesis to heterotrophic respiration (Chapter 5). Microbial methane oxidation, another possible source of CO_2 generation and O_2 consumption, was considered negligible based on the isotopic composition of the gas (Chapter 5, Supplementary information B, Figure S5.4.2). Organic matter degrades more slowly and incompletely under anaerobic conditions due to lower energy yields for microorganisms and the absence of oxygenase activity (Bastviken et al., 2004; Gebert & Zander, 2024; Zehnder & Svensson, 1986). Aerobic conditions enable faster hydrolysis and more complete breakdown of complex compounds like lignin (Stinson & Ham, 1995; Xu et al., 2024). Previous studies have consistently shown higher carbon mineralization of waste organic matter under aerobic conditions, with carbon release up to three times greater than in anaerobic systems (Fricko et al., 2021; Ritzkowski et al., 2016). Compartment 11N in BRA and WIE stood out for its high aeration efficiency, high carbon extraction efficiency, elevated waste temperature, high gas flow rates, and high cumulative settlement, typical indicators of active biodegradation (Chapters 2-5).

In contrast, site KRA was operated to maximize contaminant flushing and continued anaerobic decay of waste organic matter. Although water recirculation enhanced moisture content, as suggested by the increase in average water content in the mixed sample from 34%$_{dw}$ (Chapter 2) to 75%$_{dw}$ after five years of stabilization (Chapter 5), its effect on long-term stabilization was limited, as seen from gas generation studies of the excavated waste material (Chapter 4). Moisture distribution was uneven, with the middle waste layers remaining relatively dry (Chapter 4). Despite a reduction in N-Kj from 1600 mg/L to 1150mg/L between 2018–2023, this remains far above the EPC target of 50 mg NH_4^+/L. Overall gas recovery was poor (24% of modeled generation), and organic matter degradation was limited (Chapter 5). Laboratory tests confirmed that much of KRA's waste still contains high carbon potential, indicating that future aeration could unlock further degradation after anaerobic stabilization is reached.

However, the effectiveness of both aeration and water recirculation is strongly constrained by physical heterogeneities within the landfill. Uneven moisture distribution, as visualized through ERT measurements, revealed dry pockets particularly in the middle layers of KRA (Ren, 2021). Gas permeability tests in BRA demonstrated anisotropy, with horizontal gas

flow occurring 166 times more easily than vertical flow (Scott, 2025), limiting vertical oxygen penetration. Similarly, dilution tests at KRA revealed preferential leachate flow paths with vertical velocities far exceeding horizontal estimates, indicating hydraulic short-circuiting and inefficient wetting (Feenstra, 2022). These structural and hydraulic constraints reduce treatment uniformity and must be accounted for in the design and monitoring of in-situ stabilization systems.

Aeration enhances anaerobic decay

Surprisingly, aeration not only drove aerobic processes but appeared to enhance anaerobic degradation. In WIE, the anaerobic share in total gas extracted exceeded baseline expectations, suggesting that oxygen may have indirectly promoted microbial turnover in adjacent anaerobic niches (Chapter 5). One possible mechanism is that aerobic hydrolysis generates smaller, more bioavailable compounds that diffuse or are transported to anaerobic zones, where they fuel downstream processes like acidogenesis and methanogenesis. Similarly, sequential degradation tests in KRA showed that once anaerobic degradability was exhausted, introducing oxygen as a terminal electron acceptor reactivated carbon generation. Under aerobic conditions, this released an additional 59% to 750% of the carbon previously released under anaerobic conditions (Chapter 4). This aligns with findings by Bastviken et al. (2004), which showed that anoxic conditions promote fermentation, producing readily degradable intermediates such as volatile fatty acids and alcohols. When followed by oxic conditions, these compounds are rapidly mineralized, resulting in elevated aerobic degradation rates.

A sequential anoxic–oxic treatment strategy may offer a particularly effective approach for landfills like KRA that remain in the methanogenic phase. Beginning with anaerobic degradation (to maximize methane capture) and transitioning to aerobic treatment (to accelerate stabilization) leverages the strengths of both redox regimes. This strategy also supports coupled nitrification–denitrification, enhancing nitrogen removal. However, its implementation should consider operational constraints: initiating an aerobic phase may not be desirable when there is still potential for energetic recovery of the landfill gas. Additionally, in landfills with high organic matter content, aerobic activity can raise waste temperatures to levels that may inhibit microbial processes or damage infrastructure.

Carbon potential, kinetics, and modeling discrepancies

Experimental kinetics revealed higher degradation rate constants (k-values) in laboratory conditions than those assumed in field-scale models like Afvalzorg's (Afvalzorg, 2022). This discrepancy is consistent with broader findings from 49 laboratory studies and 57 landfill sites (Fei et al., 2016). In KRA, for instance, early-stage anaerobic degradation tests showed k-values up to 17.5 y^{-1}, nearly 49 times higher than Afvalzorg's standard value of 0.187 y^{-1} for rapidly degradable fractions (Chapter 4). This difference reflects the impact of waste disturbance during drilling and sample preparation, which exposes previously inaccessible

surfaces to microbial activity and water transport, enhancing degradation in the laboratory. In contrast, field conditions often feature restricted permeability, isolated anaerobic pockets, and non-uniform wetting, which can limit microbial access to degradable substrates, even under warm and moist conditions.

While Afvalzorg's model uses IPCC-aligned k-values, it compensates for slower field degradation by adjusting the degradable organic carbon fraction (DOCf and %DOC) per waste category. Despite the high lab-measured k-values, field data from KRA showed that only 24% of the modelled methane generation under anaerobic conditions was actually recovered (Chapter *5*). This low recovery does not necessarily indicate that large amounts of degradable carbon remain; it may also reflect inefficiencies in the gas collection system, including poor well coverage or gas migration outside the extraction network. Therefore, the observed gap between predicted and recovered carbon likely results from a combination of underperformance in gas capture and the conservative assumptions in model calibration.

Nitrogen dynamics: removal, fixation, and immobilization

Aeration not only accelerated carbon degradation but also influenced nitrogen cycling within the waste body. In BRA and WIE, gas-phase N_2 production (up to *5*–*6*$\%_{vol}$ of extracted gas) indicated active denitrification (Chapter *5*). This occurs because aeration promotes nitrification, converting ammonium (NH_4^+) into nitrate (NO_3^-), which can then diffuse into anaerobic zones where it serves as an electron acceptor for denitrifying microbes, ultimately being reduced to N_2. Across all pilots, nitrogen removal via the gas phase was significantly greater than through the leachate, especially in the aerated systems. This confirms that aerated waste bodies can function as bioreactors for nitrogen removal.

In WIE, the cumulative N_2 released in the gas phase even exceeded the estimated initial nitrogen pool in the waste. This suggests that the nitrogen available for denitrification must be continually replenished, either through continued mineralization of organic nitrogen or via microbial fixation. This interpretation is supported by the detection of nitrogen fixation at all sites, including BRA and WIE, where net N_2 consumption in the gas (lower in percentage terms than in KRA) suggests that atmospheric nitrogen is being biologically converted into reactive forms that can re-enter the nitrogen cycle and subsequently be denitrified. The nitrogen mass balance in WIE reinforces the need to consider fixation as a key process sustaining denitrification under aerated conditions (Chapter *5*). It may also indicate that the initial nitrogen pool in the waste was underestimated, as already discussed in Chapter 2 and *5*.

Nitrogen removal through the leachate showed compartment-specific patterns. In BRA-l1N, for example, nitrogen removal through denitrification was greater than in other compartments (Chapter *5*), likely reflecting more effective aeration and higher nitrification-denitrification activity. This may indicate more extensive microbial turnover or sustained aerobic-anaerobic cycling, which are consistent with advanced stage of microbial

degradation (Chapter 3). Across most pilots, chloride-normalized Kjeldahl nitrogen increased over time, possibly due to prolonged mineralization and/or equilibrium-driven sorption that delays nitrogen mobilization. In actively aerated zones, enhanced degradation can initially increase nitrogen release into leachate as organic nitrogen is mineralized. A decline in leachate ammonium is expected only after this release phase, once degradation slows and flushing begins to dominate.

Additionally, a large share of total nitrogen remains in immobile or poorly mobile forms. Upscaled ammonium extraction results indicated that only ~2% of total nitrogen accurs as freely dissolved ammonium in the mobile pore water, while up to 17% TN was adsorbed onto the solid phase. However, some individual samples, particularly in KRA, showed much higher adsorbed fractions, with over 50% of the total nitrogen bound to solid matter. This large, adsorbed pool suggests that nitrogen mobilization may be significantly delayed, and equilibrium-driven release could persist long after active treatment, complicating predictions of nitrogen flushing and the time needed to reach EPC targets.

Implications for design and aftercare

All pilots show that stabilization strategies must be tailored to site-specific waste characteristics and conditions. In KRA, the decision to begin the stabilization with water recirculation, rather than aeration, was based on its high organic content and anticipated anaerobic degradability (Vereniging Afvalbedrijven, 2015). In this context, early aeration was considered premature; the initial aim was to stimulate methane generation under bioreactor landfill conditions and recover energy through gas extraction. However, the effectiveness of water recirculation was constrained by system design and uneven moisture distribution. Field observations and drillings revealed that water infiltration was not uniform: while top and bottom layers were saturated, the middle layer remained relatively dry, indicating the presence of hydraulic breaks. This uneven profile likely limited microbial activity and substrate availability in key zones, thereby reducing overall degradation performance. Despite improvements in leachate handling, nitrogen removal remained modest, and carbon recovery through the gas reached only a fraction of predicted levels (Chapter 5).

Design of the aeration system at BRA and WIE benefitted from prior test drillings and gas extractions that informed aeration well placement. Previous modeling work using gas extraction data from WIE identified 20 m as the maximum effective spacing between aeration wells to ensure adequate oxygen distribution (van Turnhout et al., 2020). Based on this, in BRA, a denser well network was implemented in compartment 11Z (15 m spacing) compared to compartments 11N and 12 (20 m), anticipating more challenging conditions. Nevertheless, spatial heterogeneity in gas flow, perched water tables, and limited oxygen penetration continued to impact performance, reflected in contrasting outcomes between compartments 11N and 11Z (Chapter 3). Notably, expanding the well network in 11N and 11Z in 2022 led to improved aeration efficiency, evidenced by enhanced aerobic carbon degradation and net nitrogen release via denitrification between 2022 and 2024.

Bibliography

1. Afvalzorg. (2022). Multiphase landfill gas generation model. Version 2022. https://www.afvalzorg.com/landfill-gas/lfg-models/multiphase-landfill-gas-generation-model
2. Bastviken, D., Olsson, M., & Tranvik, L. (2003). Simultaneous measurements of organic carbon mineralization and bacterial production in oxic and anoxic lake sediments. Microbial Ecology, 46(1), 73–82. https://doi.org/10.1007/s00248-002-1061-9
3. Bastviken, D., Persson, L., Odham, G., & Tranvik, L. (2004). Degradation of dissolved organic matter in oxic and anoxic lake water. Limnology and Oceanography, 49(1), 109–116. https://doi.org/10.4319/lo.2004.49.1.0109
4. Brand, E., de Nijs, T. C. M., Dijkstra, J. J., & Comans, R. N. J. (2016). A novel approach in calculating site-specific aftercare completion criteria for landfills in The Netherlands: Policy developments. Waste Management, *56*, 255–261. https://doi.org/10.1016/J.WASMAN.2016.07.038
5. Feenstra, A. (2022). spatial variability of leachate flow and distribution in a landfill stabilized by leachate recirculation [Delft University of Technology]. https://resolver.tudelft.nl/uuid:3c415721-9744-46ac-ab5f-b7c76922ad19
6. Fei, X., Zekkos, D., & Raskin, L. (2016). Quantification of parameters influencing methane generation due to biodegradation of municipal solid waste in landfills and laboratory experiments. Waste Management, *55*, 276–287. https://doi.org/10.1016/J.WASMAN.2015.10.015
7. Fricko, N., Brandstätter, C., & Fellner, J. (2021). Enduring reduction of carbon and nitrogen emissions from landfills due to aeration? Waste Management, 135(June), 457–466. https://doi.org/10.1016/j.wasman.2021.09.024
8. Gebert, J., & Zander, F. (2024). Aerobic and anaerobic mineralisation of sediment organic matter in the tidal River Elbe. Journal of Soils and Sediments, 24(7), 2874–2886. https://doi.org/10.1007/s11368-024-03799-6
9. Ren, Z. (2021). Explanation of water distribution variations in the landfill using electrical resistivity tomography. Delft University of Technology.
10. Ritzkowski, M., Walker, B., Kuchta, K., Raga, R., & Stegmann, R. (2016). Aeration of the teuftal landfill: Field scale concept and lab scale simulation. Waste Management, *55*, 99–107. https://doi.org/10.1016/j.wasman.2016.06.004
11. Scott, S. P. (2025). Characterization of Gas Transport Pathways in an Aerated Landfill Using In-Situ Measurement Techniques [Delft University of Technology]. https://repository.tudelft.nl/record/uuid:08460d7d-887b-42e0-b8c7-77603326414a
12. Stinson, J. A., & Ham, R. K. (1995). Effect of Lignin on the Anaerobic Decomposition of Cellulose As Determined through the Use of a Diochemical Methane Potential Method. In Environ. Sci. Technol (Vol. 29). https://pubs.acs.org/sharingguidelines
13. van Turnhout, A. G., Oonk, H., Scharff, H., & Heimovaara, T. J. (2020). Optimizing landfill aeration strategy with a 3-D multiphase model. Waste Management, 102, 499–509. https://doi.org/10.1016/j.wasman.2019.10.051
14. Vereniging Afvalbedrijven. (2015). Project plan Sustainable Landfill Management De Kragge 2. (Issue November). https://www.duurzaamstortbeheer.nl/projectstukken/
15. Xu, H., Chen, T. H., Zhu, G., Peng, M. Q., & Zhan, L. T. (2024). Semi-quantitative study on the secondary compression characteristics of municipal solid waste in aerobic and anaerobic bioreactors. Waste Management, 176, 74–84. https://doi.org/10.1016/j.wasman.2023.12.058
16. Zehnder, A. J. B., & Svensson, B. H. (1986). Life without oxygen: what can and what cannot? Experientia, 42(11–12), 1197–1205. https://doi.org/10.1007/BF01946391

7

General conclussions, recommendations and outlook

General conclusions

This thesis presents an in-depth assessment of in-situ landfill stabilisation through a combination of field monitoring and laboratory experimentation across three landfill pilots subjected to different operational regimes: aeration (BRA and WIE) and water recirculation (KRA). The study explores the spatial and temporal variability of landfill gas (LFG) generation, the progression of carbon stabilisation, and the coupled dynamics of carbon and nitrogen over a seven-year period.

The findings confirm that aeration is a powerful driver of enhanced waste degradation. However, its success is closely tied to local conditions, including waste heterogeneity, permeability, perched water tables, and operational consistency. Aerated compartments exhibited significantly improved outcomes in terms of carbon extraction, organic matter stabilisation, and nitrogen transformation, whereas anaerobic environments showed slower, more variable degradation patterns and greater reliance on leachate pathways for pollutant release.

Gas flow and composition across aerated compartments revealed strong spatial variability, with some zones experiencing limited aeration due to a combination of perched water, potential short-circuiting of air, and heterogeneous waste properties affecting gas permeability. Compartment 11N, for instance, demonstrated high aeration efficiency, evidenced by elevated gas-phase carbon recovery, increased temperatures, and substantial waste settlement. In contrast, compartment 11Z remained largely anaerobic due to poor gas permeability and localised water accumulation, highlighting the importance of strategic well placement and system design.

The degree of carbon stabilisation achieved after six years of treatment varied significantly between sites. Aerated landfills consistently exhibited lower residual carbon potential under both aerobic and anaerobic conditions, confirming advanced stabilisation. Sequential aerobic treatment following anaerobic phases significantly boosted carbon release, underscoring the presence of residual degradable organic matter that can only be mineralised in the presence of oxygen. Laboratory incubations revealed higher gas generation than both field measurements and model predictions, indicating untapped degradation potential and the need for improved model calibration.

Waste characteristics such as moisture content and organic composition were key factors influencing degradation kinetics across the landfill sites. In the anaerobic pilot (KRA), limited permeability likely impeded gas and water flow, contributing to reduced carbon and nitrogen extraction. Plastic content may influence degradation behaviour, potentially by affecting waste accessibility or organic matter availability. Overall, the results highlight the importance of site-specific waste composition in shaping stabilisation outcomes and the need for tailored stabilisation strategies.

The integration of carbon and nitrogen mass balances revealed distinct patterns in how these biogeochemical cycles evolve under different stabilisation regimes. Although aerated landfills contain both aerobic and anaerobic zones, the introduction of oxygen promoted more effective organic matter degradation and supported nitrogen transformation, as reflected in relatively stable concentrations of dissolved organic and inorganic carbon in leachate and measurable gas-phase nitrogen emissions (e.g., N_2O). In contrast, the anaerobic landfill (KRA) exhibited more variable behaviour, with higher ammonium concentrations at depth and limited nitrogen release via the gas phase. Across all sites, the majority of nitrogen remained immobilised in the solid waste matrix, up to 43% of total nitrogen (TN), highlighting the dominant role of solid-phase retention in long-term nitrogen dynamics.

Operational challenges, such as low permeability, short-circuiting, and disruptions in gas flow, limited the potential benefits of aeration in some compartments. Nonetheless, overall carbon and nitrogen extraction via the gas phase was substantially higher in the aerated pilots, particularly WIE, which released over 22% of its total organic carbon and more than twice its initial total nitrogen through the gas phase. These findings highlight the critical role of oxygen availability, not just degradable carbon content, as the key limiting factor in landfill stabilisation.

Recommendations and outlook

The results of this study offer several important recommendations for improving the implementation of in-situ landfill aeration and highlight priorities for future research. As the pilots investigated are compartments within full-scale operational landfills, the findings have direct relevance for real-world waste management strategies.

To enhance stabilisation outcomes, aeration strategies should continue to be adapted to site-specific characteristics such as waste permeability, moisture distribution, and gas flow behaviour. Rather than assuming that increased well density universally improves performance, well spacing should be guided by preliminary extraction tests and operational feedback, as was done during the design and subsequent optimisation of the 11N and 11Z compartments. For example, the better performance of 11N, despite its wider well spacing compared to 11Z, illustrates that factors beyond well density, such as waste heterogeneity and water distribution, are critical in determining aeration efficiency.

Effective aeration does not necessarily imply fully aerobic conditions throughout the waste body. In fact, maintaining zones with anaerobic activity can be beneficial, particularly for promoting processes such as denitrification, which contribute to nitrogen removal. Therefore, the goal should be to manage oxygen distribution in a way that supports balanced degradation pathways, tailored to the functional and environmental objectives of stabilisation. Sequential treatment strategies, where aerobic phases follow anaerobic degradation, are also recommended to exploit the remaining biodegradation potential of organic matter that cannot be mineralised under anaerobic conditions.

Predictive models, such as the Afvalzorg multiphase landfill gas model, should be continuously recalibrated using empirical field and laboratory data. This study highlights the need to refine parameters such as the degradation rate constant and the degradable organic carbon fraction to improve model reliability for long-term forecasting. Stabilisation strategies must also be adapted to site-specific waste characteristics, particularly moisture content, organic composition, and the presence of plastics, which were found to correlate with carbon generation potential across all sites.

Future research should build on ongoing tracer studies already being conducted in the pilot compartments to further delineate gas and liquid transport dynamics and the effective sphere of influence of aeration wells. In addition, stable isotope probing offers a valuable tool for distinguishing overlapping microbial processes such as methane oxidation, aerobic respiration, and denitrification, especially in environments where aerobic and anaerobic zones coexist. To reduce uncertainty in carbon and nitrogen mass balance estimates, particularly in KRA, there is a need to improve monitoring infrastructure and address measurement gaps related to gas capture and the recirculation of treated leachate. Finally, extending field investigations to additional compartments or operational landfills will be essential for validating the long-term performance, scalability, and economic viability of the stabilisation strategies explored in this study.

A

Supplementary Information Chapter 4

Comparing modelled, recovered and generated carbon in three landfills under in-situ stabilization

S4.2.1. Procedure: Working with asbestos-containing waste material

Background

In a worldwide unique field trial, the NWO-funded CURE project researches the feasibility of in-situ stabilization of landfills by means of leachate recirculation and aeration. Most of the work was carried out in the field (on the landfills), but the project plan also included targeted experimental laboratory studies. For this purpose, waste was sampled from the three landfills under study. In two of these, the waste contained shares of asbestos. This procedure identified the related risks and explained which measures were taken to prevent exposure of researchers to these risks.

Risks from asbestos

Prolonged exposure to asbestos caused various forms of cancer and asbestosis of the lungs. Exposure of the human body to asbestos resulted from inhalation of very small asbestos particles. Inhalation could occur if asbestos dust or small fibres become airborne. This was only possible if the material was dry.

Sampling procedure and waste properties

The waste from landfills Braambergen and Wieringermeer were sampled from open drills in September and October 2022, respectively, following a strict decontamination protocol in line with instructions provided during a toolbox meeting by the landfill operator (BV Afvalzorg). This included defining areas of different contamination levels, wearing full hazardous material body suits, shoe covers, gloves, eye protection, and facial masks. At the end of each working day, all material was disposed of in asbestos-waste labelled bags which were landfilled at the operator's hazardous waste facility. The samples were double-bagged, tightly taped, and stored cool on site.

After all samples had been collected, the bags were opened again and the material was passed through 3.6 cm sieves in preparation for the experimental work. The full decontamination protocol described above was followed. Visual inspection of the waste during sampling and sieving confirmed that some samples contained larger chunks of asbestos, which were discarded and disposed of in labelled bags for hazardous waste. The sieved material was again double-bagged, taped and stored cool on site. Visual inspection during sieving confirmed that all samples were moist.

The samples were then sent to the laboratory for asbestos analysis, and any samples in which asbestos was detected were discarded.

Procedure: Gas production and respiration experiments

This procedure aimed to quantify the remaining gas production and respiration potential of sieved, moist landfill waste samples. It was designed to avoid exposing the researcher to

the waste during the experiment. All sampling and measurements were performed through rubber stopper without opening the bottles.

1. Sample preparation (in the landfill)

- The sieved, moist landfill waste was placed into 500 ml to 1000 ml borosilicate glass bottles, following the established decontamination protocol.
- Each bottle was sealed with a butyl rubber stopper and secured with a screw cap.
- To initiate anaerobic conditions for the gas production test, the headspace of each bottle was flushed with 100% nitrogen (N_2) using a mobile pressurized N_2 cylinder. This displaced oxygen and ensured anaerobic conditions.
- After sealing, bottles were not reopened until the experiments were completed.
- The sealed bottles were transported to the TU Delft laboratory under sealed conditions.

2. Sample preparation (in the laboratory)

- Upon arrival, an additional N_2 flush was performed on each bottle of the gas production test to further guarantee anaerobic conditions. This was conducted in a fume hood, with the outlet tube submerged in water to capture any potential fibres (Figure S4.2.1 a).
- Bottles for the respiration test were pressurized with 100 ml of laboratory air.
- All bottles were placed in dark closets at 20°C for incubation.

3. Gas production and respiration measurement

- The pressure in the bottle headspace was measured using a needle connected to a pressure gauge, inserted carefully through the rubber stopper.
- Approximately 3 ml of headspace gas was withdrawn using a syringe equipped with a 0.45µm filter (Figure S4.2.1 b).
- Gas samples were injected into the gas chromatograph for analysis.

4. Depressurization for gas production test (if needed)

- When depressurization was required, a needle connected to a tube leading to a water-filled bottle was inserted through the stopper. This ensured that released gases were safely captured.

5. Flushing for respiration test (if needed)

- When flushing with laboratory air was required, the pump's outlet (Figure S4.2.1 c) was connected to a tube leading to a water-filled bottle. This was also carried out in a fume hood to prevent any fibre release.

6. Safety Precautions

- The closet where bottles were stored was labelled with the necessary warnings so that the area was easily identifiable.
- All procedures involving potential fibre release, including flushing and depressurization, were performed in a fume hood.
- Strict adherence to the decontamination protocol was maintained at all times.
- Laboratory materials potentially contaminated with asbestos fibres, such as filters, were collected and labelled.
- At the end of the experiment, the waste inside the bottles and potentially contaminated materials were returned to the landfill for proper disposal.

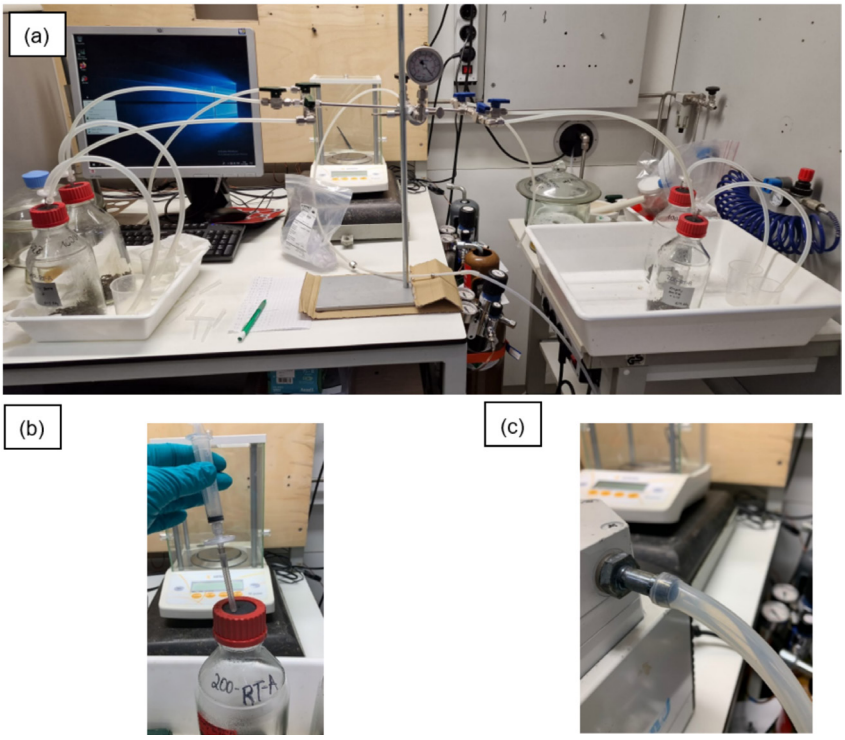

Figure S4.2.1. (a) Flushing with N_2 in the gas production test; (b) Gas sampling using a filter; (c) Pump outlet connected to a tube for the flushing with laboratory air in the respiration test

S4.2.2. Procedure: Shredding and milling waste samples

Purpose

Pulverizing the sample was essential for chemical characterization, including the analysis of carbon content.

Safety references

Particles smaller than 10 µm (PM10) could penetrate the respiratory system. To minimiza risk, protective gloves, a laboratory coat, and eye protection were worn. Air extractors were activated and positioned to the work area to capture airborne particles.

Instruments

- SDO soil drying oven
- Retsch SM 2000 miller
- Herzog HSM 100 P disk mill

Preparation of the samples

- Approximately 100 g of each waste sample was dried for 24 hours at 105 °C (NEN-EN-ISO 17892-1, 2014).
- Large stones, metal, or glass were separated, as they can damage the mill. In consultation with the laboratory technician, these separated material processed if deemed suitable.

Procedure

Milling 1: Retsch SM 2000

1. Milling began with the Retsch SM 2000 (Figure S4.2.2.1). The appropriate sieve/filter was installed, and air extractors were activated.

Figure S4.2.2.1: Retsch SM 2000 milling machine

2. The waste sample was inserted into the mill. Any coarse residue was collected, brushed out, and tranferres to an aluminium container (Figure S4.2.2.2)

Figure S4.2.2.2: Left: inserting sample into the milling machine. Right: collecting the sample with a brush

3. If necessary, coarse residues were milled a second time. Figure S4.2.2.3 illustrates sample GT6, milled to 0.5 mm and 0.125 mm, with remaining residue. All fractions were then combined for disk milling.

Figure S4.2.2.3: Sample GT6 after Retsch SM 2000 mill

Milling 2: Herzog HSM 100 P disk mill

1. The combine material was placed in the Herzog disk mill container.

2. Samples were milled for 30 seconds, with additional 10-20 seconds if required to achieve a fine powder (S4.2.2.4).

3. Milling was paused periodically to avoid overheating, which could cause clumping or partial melting.

Figure S4.2.2.4: Herzog HSM 100 P disk mill (left). Milled sample in the disk mill container (right)

S4.2.3. Parameters using Rock Eval data

Table S4.2.3. Overview of the parameters obtained from the Rock Eval that were used in this chapter (Sebag et al., 2016)

Parameter	Unit	Formula	Interpretation
Total organic carbon (TOC)	Weight percentage ((g TOC/g dry sample)%)	PC + RC Where PC is pyrolysable organic carbon and RC is the residual organic carbon	Carbon from organic matter. Indicates the potentially biodegradable carbon
Total mineral carbon (MINC)	Weight percentage ((g TOC/g dry sample)%)	PyroMinC + OxiMinC Where PyroMinC is pyrolisis mineral carbon and OxiMinC is oxidation mineral carbon	Total inorganic carbon (TIC). Carbon from inorganic minerals. Reflects non-biodegradable and stable carbon under most conditions.
Hydrogen index (HI)	mg HC/g TOC	S2 / TOC *100 Where S2 are the hydrocarbons released during pyrolysis (mg HC/g dry sample)	Indicates the amount of labile (easily degradable) organic matter
Oxygen index (OI)	mg CO_2/g TOC	OI = S3/TOC * 100 Where S3: CO + CO_2 released during pyrolysis (mg O_2/g dry sample)	Indicates the degree of oxidation of the organic matter. Higher values suggest more refractory, oxidized compounds
I-index	[-]	log10 ((A1+A2)/A3) Where A1: Area under the S2 pyrogram between 200–340 °C (labile biopolymers); A2: Area between 340–400 °C (resistant biopolymers); A3: Area between 400–460 °C (immature geopolymers)	Reflects the presence of thermally labile, immature SOM (e.g., fresh or undecomposed material). Higher I-index = more immature/labile organic matter.
R-index	[-]	A4 / (A1+A2+A3+A4) Where A4: Area under the S2 pyrogram after 460 °C (refractory geopolymers)	Reflects the thermal stability of the SOM. Higher R-index = more refractory, stable material

S4.2.4. Procedure: Loss on ignition in waste

Purpose

The loss on ignition (LOI) test provides an estimate of the amount of organic matter present in the sample. The procedure used in this study was based on NEN 5754:2005 (NEN 5754:2005), which describes the determination of loss on ignition in soil and sediment. It is important to note that the LOI value does not distinguish between different types of organic carbon or provide detailed information about its composition. Additionally, other volatile compounds, such as water and carbonates, may contribute to the weight loss observed during the LOI test.

Safety references

To determine LOI, the sample is incinerated at 550 °C after drying at 105 °C. Appropriate heat-resistant equipment and personal protective equipment should be used when handling the furnace and hot crucibles.

Instruments

- SDO soil drying oven
- Muffle furnace Nabertherm P330

Preparation of the samples

- Remove large particles from the milled sample
- Air dry the samples by drying at 105 °C for at least 2 hours
- Store the sample in the desiccator

Procedure

The LOI was expressed as a weight percentage of the dry mass.

Always use a crucible tong to handle the porcelain crucibles.

1. Zero the balance before weighing the empty crucible and record its weight.
2. Zero the balance again and weigh 5–10 g of sample (WS). To prevent incomplete combustion, the thickness of the sample layer in the crucible should not exceed 5 mm.
3. Weigh the crucible containing the sample. This corresponds to the total weight before ignition (WB).
4. Turn on the ventilation hood and the furnace.
5. Place the crucibles with the samples in the furnace using a crucible tong.
6. Select and verify the corresponding furnace program (P4). The furnace should be

programmed with a heating rate of 10 °C min^{-1} to 550 °C, followed by 3 hours at 550 °C. If a high organic matter content is expected, a heating rate of 5 °C min^{-1} may be used.

7. Once the furnace temperature has decreased to below 100 °C, remove the crucibles and place them immediately in a desiccator to cool to room temperature.

8. After cooling, weigh the crucible containing the sample again. This corresponds to the total weight after ignition (WA).

Calculation

The difference in weight before and after the ignition was used to calculate the loss on ignition.

LOI (%)= ((WB-WA))/WS

Where LOI (%) is the loss on ignition expressed in percentage, WB is the total weight before ignition, WA the total weight after ignition and WS is the weigh of the sample.

S4.3.1. Waste characterization

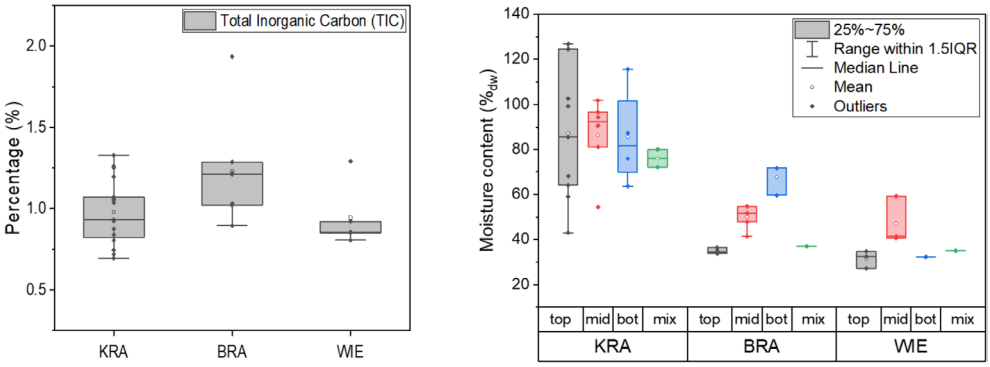

Figure S4.3.1: Total inorganic carbon (TIC, left) and moisture content per layer group (right) in waste from the three pilot landfills

S4.3.2. Statistical analysis exponential fitting

Table S4.3.2.1. Statistical data of the exponential decay models in gas production using KRA samples

Experiment	Sample	Number of Points	Degrees of Freedom	Reduced Chi-Sqr	Residual Sum of Squares	R-Square (COD)	Adj. R-Square	Fit Status
Pre-test	C1	88	85	0.01024	0.8702	0.98664	0.98633	Succeeded
	C2	76	73	0.00282	0.20603	0.99481	0.99467	Succeeded
	BA	129	126	0.05085	6.40652	0.9966	0.99654	Succeeded
	BB	126	123	0.04635	5.70087	0.99633	0.99627	Succeeded
	GT9.1	48	43	0.00395	0.16996	0.9992	0.99912	Succeeded
	GT9.2	49	46	0.00292	0.13445	0.99906	0.99902	Succeeded

Experiment	Sample	Number of Points	Degrees of Freedom	Reduced Chi-Sqr	Residual Sum of Squares	R-Square (COD)	Adj. R-Square	Fit Status
Pre-test	GT10.1	45	40	0.00485	0.19386	0.99833	0.99817	Succeeded
	GT10.2	45	40	0.00219	0.08753	0.99928	0.99921	Succeeded
	GT11.1	50	47	0.02083	0.97893	0.99078	0.99039	Succeeded
	GT11.2	57	54	0.0881	4.75718	0.98766	0.9872	Succeeded
Pre-test	GT12.1	44	39	0.02058	0.80256	0.97953	0.97743	Succeeded
	GT12.2	51	48	0.00865	0.41539	0.99626	0.9961	Succeeded
Pre-test	GT13.1	41	38	0.000422	0.01604	0.99043	0.98993	Succeeded
	GT13.2	41	38	0.000195	0.00742	0.99381	0.99349	Succeeded
	GT14.1	42	39	0.000989	0.03857	0.97171	0.97026	Succeeded
	GT14.2	42	39	0.000245	0.00956	0.99009	0.98958	Succeeded
	GT15.1	36	33	0.00646	0.21328	0.99531	0.99503	Succeeded
	GT15.2	33	28	0.0036	0.10077	0.9971	0.99669	Succeeded
Seq. experiment	GT1.1	86	81	0.01486	1.20394	0.99748	0.99735	Succeeded
	GT1.2	85	80	0.01217	0.97369	0.99751	0.99739	Succeeded
	GT2.1	81	76	0.01041	0.79147	0.99588	0.99566	Succeeded
	GT2.2	82	77	0.00639	0.4918	0.99828	0.99819	Succeeded
	GT3.1	102	97	0.12775	12.39166	0.99699	0.99686	Succeeded
	GT3.2	87	84	0.26997	22.67707	0.98291	0.98251	Succeeded
	GT4.1	84	79	0.00519	0.40976	0.99928	0.99924	Succeeded
	GT4.2	83	78	0.00358	0.27912	0.99937	0.99933	Succeeded
	GT5.1	51	48	0.000765	0.03673	0.99201	0.99168	Succeeded
	GT5.2	53	50	0.0015	0.07497	0.73917	0.72873	Succeeded
	GT6.1	85	80	0.01	0.80023	0.99822	0.99813	Succeeded
	GT6.2	110	105	0.04332	4.54908	0.99807	0.998	Succeeded
	GT7.1	56	51	0.000405	0.02063	0.99858	0.99847	Succeeded
	GT7.2	84	79	0.00647	0.51108	0.9989	0.99885	Succeeded
	GT8.1	74	69	0.02247	1.55041	0.99077	0.99023	Succeeded
	GT8.2	78	73	0.01034	0.75504	0.9968	0.99662	Succeeded
Parallel experiment	25_GT_B	23	18	0.01006	0.18102	0.99527	0.99422	Succeeded
	25_GT_A	21	16	0.0061	0.09757	0.99718	0.99648	Succeeded

Table S4.3.2.2. Statistical data of the exponential decay models in respiration test using KRA samples

Experiment	Sample	Number of Points	Degrees of Freedom	Reduced Chi-Sqr	Residual Sum of Squares	R-Square (COD)	Adj. R-Square	Fit Status
Seq. experiment	RT1.1	133	130	2.96E-02	3.85036	0.99452	0.99444	Succeeded
	RT1.2	164	161	1.38E-02	2.22308	0.99634	0.9963	Succeeded
	RT2.1	130	127	1.49E-02	1.89782	0.9957	0.99563	Succeeded
	RT2.2	110	107	0.03188	3.41108	0.9894	0.9892	Succeeded

Experiment	Sample	Number of Points	Degrees of Freedom	Reduced Chi-Sqr	Residual Sum of Squares	R-Square (COD)	Adj. R-Square	Fit Status
Seq. experiment	RT3.1	180	177	3.04E-01	53.82075	0.97398	0.97368	Failed
	RT3.2	136	133	1.34E-01	17.83013	0.98177	0.98149	Succeeded
	RT4.1	152	149	7.06E-02	10.52097	0.99613	0.99608	Failed
	RT4.2	164	161	1.13E-02	1.82228	0.99896	0.99895	Succeeded
	RT5.1	113	110	2.81E-03	0.30917	0.99899	0.99898	Succeeded
Seq. experiment	RT5.2	104	101	1.96E-04	0.01984	0.99988	0.99988	Succeeded
	RT6.1	147	144	0.00653	0.93989	0.99873	0.99871	Succeeded
	RT6.2	179	176	0.12176	21.42957	0.98948	0.98936	Succeeded
	RT7.1	161	158	1.21E-01	19.08831	0.98936	0.98923	Succeeded
	RT7.2	211	208	0.06418	13.34935	0.99722	0.99719	Succeeded
	RT8.1	150	147	0.02152	3.16355	0.99722	0.99718	Succeeded
	RT8.2	142	139	0.01607	2.23376	0.99736	0.99733	Succeeded
Parallel experiment	25_RT_B	33	30	0.11428	3.42839	0.99571	0.99542	Succeeded
	25_RT_A	34	31	0.18072	5.60237	0.99516	0.99484	Succeeded

Table S4.3.2.3. Statistical data of the exponential decay models in gas production using BRA samples

Experiment	Sample	Number of Points	Degrees of Freedom	Reduced Chi-Sqr	Residual Sum of Squares	R-Square (COD)	Adj. R-Square	Fit Status
Parallel experiment	101_GT_A	22	19	9.87E-05	0.00188	0.99479	0.99424	Succeeded
	101_GT_B	20	15	9.26E-04	0.01389	0.97253	0.9652	Succeeded
	102_GT_A	23	20	4.30E-03	8.61E-02	0.99354	0.99289	Succeeded
	102_GT_B	35	32	0.00619	0.19799	0.9956	0.99533	Succeeded
	103_GT_A	25	22	7.40E-04	0.01628	0.99337	0.99277	Succeeded
	103_GT_B	27	24	1.03E-03	0.02484	0.99144	0.99073	Succeeded
	104_GT_A	18	15	1.22E-04	0.00183	0.98684	0.98509	Succeeded
	104_GT_B	16	13	1.83E-04	0.00238	0.97478	0.9709	Succeeded
	106_GT_A	21	18	2.61E-05	4.70E-04	0.94594	0.93993	Succeeded
	106_GT_B	21	18	3.55E-05	6.39E-04	0.94419	0.93799	Succeeded
	107_GT_A	20	17	1.67E-04	0.00283	0.99383	0.9931	Succeeded
	107_GT_B	20	17	2.62E-04	0.00445	0.9892	0.98792	Succeeded
	108_GT_A	23	20	7.09E-04	0.01418	0.99815	0.99796	Succeeded
	108_GT_B	22	19	2.04E-04	0.00387	0.99894	0.99883	Succeeded
	109.5_GT_A	32	29	0.09942	2.8832	0.98618	0.98523	Succeeded
	109.5_GT_B	26	23	0.00379	0.08721	0.9931	0.9925	Succeeded
	139_GT_A	10	7	0.00127	0.00891	0.99324	0.99131	Succeeded
	139_GT_B	13	10	5.50E-04	0.0055	0.99703	0.99644	Succeeded

Table S4.3.2.4. Statistical data of the exponential decay models in respiration test using BRA samples

Experiment	Sample	Number of Points	Degrees of Freedom	Reduced Chi-Sqr	Residual Sum of Squares	R-Square (COD)	Adj. R-Square	Fit Status
Parallel experiment	101_RT_A	27	24	0.00474	0.11382	0.99735	0.99712	Succeeded
	101_RT_B	24	21	9.57E-04	0.0201	0.99917	0.99909	Succeeded
	102_RT_A	42	39	0.01849	0.7211	0.99805	0.99796	Succeeded
	102_RT_B	49	46	0.02468	1.13538	0.99745	0.99734	Succeeded
	103_RT_A	39	36	0.02105	0.75786	0.99814	0.99804	Succeeded
	103_RT_B	42	39	0.04056	1.58199	0.99775	0.99763	Succeeded
	104_RT_A	27	24	0.019	0.4559	0.99516	0.99476	Succeeded
	104_RT_B	33	30	0.01754	0.52611	0.99776	0.99761	Succeeded
	106_RT_A	33	30	0.00699	0.20968	0.99613	0.99587	Succeeded
	106_RT_B	33	30	0.00459	0.13784	0.99643	0.99619	Succeeded
	107_RT_A	31	28	0.01161	0.32495	0.9946	0.99422	Succeeded
	107_RT_B	29	26	0.01617	0.42037	0.99127	0.9906	Succeeded
	108_RT_A	39	36	0.04219	1.51901	0.99103	0.99053	Succeeded
	108_RT_B	39	36	0.00846	0.30458	0.9985	0.99842	Succeeded
	109.5_RT_A	43	40	0.00785	0.31393	0.99895	0.99889	Succeeded
	109.5_RT_B	44	41	0.01588	0.65123	0.9989	0.99885	Succeeded
	139_RT_A	21	18	0.06425	1.15648	0.98735	0.98594	Succeeded
	139_RT_B	14	11	0.02533	0.27863	0.99666	0.99606	Succeeded

Table S4.3.2.5. Statistical data of the exponential decay models in gas production using WIE samples

Experiment	Sample	Number of Points	Degrees of Freedom	Reduced Chi-Sqr	Residual Sum of Squares	R-Square (COD)	Adj. R-Square	Fit Status
Parallel experiment	206_GT_A	21	18	6.49E-05	0.00117	0.98233	0.98037	Succeeded
	206_GT_B	16	13	3.35E-04	0.00436	0.99618	0.99559	Succeeded
	207_GT_A	28	25	1.42E-02	0.35437	0.98615	0.98504	Succeeded
	207_GT_B	33	30	0.01651	0.49538	0.98671	0.98582	Succeeded
	208_GT_A	36	33	2.23E-02	0.73662	0.98696	0.98617	Succeeded
	208_GT_B	37	34	1.37E-02	0.46499	0.98865	0.98799	Succeeded
	209_GT_A	31	28	0.00198	0.05557	0.99508	0.99473	Succeeded
	209_GT_B	35	32	4.13E-03	0.13214	0.99031	0.9897	Succeeded
	210_GT_A	22	19	7.97E-04	0.01514	0.99541	0.99493	Succeeded
	210_GT_B	31	28	2.61E-03	7.31E-02	0.98543	0.98439	Succeeded
	216_GT_A	13	10	9.02E-04	0.00902	0.99517	0.9942	Succeeded
	216_GT_B	14	11	6.62E-04	0.00728	0.9973	0.99681	Succeeded

Table S4.3.2.6. Statistical data of the exponential decay models in respiration test using WIE samples

Experiment	Sample	Number of Points	Degrees of Freedom	Reduced Chi-Sqr	Residual Sum of Squares	R-Square (COD)	Adj. R-Square	Fit Status
Parallel experiment	206_RT_A	26	23	0.0047	0.10807	0.99811	0.99794	Succeeded
	206_RT_B	25	22	5.80E-03	0.12756	0.99748	0.99725	Succeeded
	207_RT_A	39	36	0.02877	1.03571	0.99745	0.99731	Succeeded
	207_RT_B	47	44	0.02831	1.24557	0.99776	0.99766	Succeeded
	208_RT_A	55	52	0.26314	13.68352	0.99135	0.99102	Succeeded
	208_RT_B	54	51	0.34026	17.35329	0.98746	0.98697	Succeeded
	209_RT_A	49	46	0.43704	20.10381	0.98275	0.982	Succeeded
	209_RT_B	47	44	0.95817	42.1593	0.97382	0.97263	Succeeded
	210_RT_A	40	37	0.09362	3.46402	0.9866	0.98587	Succeeded
	210_RT_B	43	40	0.19679	7.87149	0.98125	0.98032	Succeeded
	216_RT_A	25	22	0.06624	1.45729	0.99256	0.99189	Succeeded
	216_RT_B	26	23	0.07191	1.65399	0.99233	0.99166	Succeeded

S4.3.3. Fitting parameters

Table S4.3.3.1. Fitting parameters of the exponential decay models in gas production using KRA samples

Experiment	Sample	Y_0	Y_0	A1	A1	A2	A2	k1	k1	k2	k2	Comment
		Val.	Std E.	Val.	Std E.	Val.	Std E.	Val.	Std E.	Val.	Std E.	
Pre-test	C1	4,06443	0,05289	-3,90746	0,05158			0,00437	0,000148			--
	C2	3,0562	0,02653	-2,87919	0,02629			0,00436	9,77E-05			--
	BA	17,99046	0,23638	-17,4004	0,21423			0,00157	3,88E-05			--
	BB	17,10084	0,2528	-16,5427	0,23107			0,00149	4,02E-05			--
	GT9.1	42,56738	408,4514	-21,2835	--	-21,2789	--	0,000229	3,5626	0,000229	3,55906	Y_0 too high
	GT9.2	14,75092	0,8382	-14,7262	0,82846			6,09E-04	4,30E-05			--
	GT10.1	7,03635	1,01481	-3,56876	--	-3,55529	--	0,00183	4,42895	0,00183	4,44602	--
	GT10.2	8,09312	1,04434	-0,27887	1,26596	-7,87672	0,35845	0,00678	0,01768	0,00144	0,000544	--
	GT11.1	4,66238	0,08825	-4,88611	0,0827			0,00379	0,000173			--
	GT11.2	7,99307	0,14828	-8,42607	0,14236			0,00379	0,000185			--
	GT12.1	3,23427	0,57189	-1,70955	4637346	-1,79842	4637346	0,00295	5,15857	0,00295	4,90669	--
	GT12.2	7,20909	0,28836	-7,25297	0,27294			0,00139	8,76E-05			--
	GT13.1	-0,3061	0,06807	0,34525	0,0639			-0,00136	0,000154			$Y_0<0$
	GT13.2	2,55193	0,81619	-2,51357	0,81352			0,000317	0,000116			--
	GT14.1	-0,15954	0,06397	0,21323	0,05828			-0,00174	0,000262			$Y_0<0$
	GT14.2	-0,41993	0,10223	0,46171	0,09936			-0,00096	0,000147			$Y_0<0$
	GT15.1	3,52952	0,06247	-3,53469	0,05643			0,00359	0,000164			--
	GT15.2	5,55073	5,34174	-2,81382	0,34777	-3,0048	4,97592	0,01199	0,00164	0,00064	0,0016	--
Seq. experiment	GT1.1	22,09379	26,71909	-8,83118	0,17712	-14,9616	26,51306					--
	GT1.2	10,72577	2,19499	-8,17922	0,16658	-4,18746	2,00956					--
	GT2.1	7,05377	0,42232	-5,98914	0,12902	-2,75598	0,30021	2,10E-02	8,38E-04	3,37E-04	6,83E-04	--
	GT2.2	12,70733	6,52566	-6,38726	0,1396	-7,5121	6,36896	2,28E-02	8,68E-04	1,09E-03	8,41E-04	--

Experiment	Sample	Y_0	Y_0	A1	A1	A2	A2	k1	k1	k2	k2	Comment
		Val.	Std E.	Val.	Std E.	Val.	Std E.	Val.	Std E.	Val.	Std E.	
Seq. experiment	GT3.1	20,45358	0,35256	-25,1552	0,23884	0,03946	0,07664	3,05E-02	1,45E-03	2,12E-03	6,55E-04	k2<0
	GT3.2	13,67474	0,09182	-17,9443	0,36026			2,00E-02	7,47E-04	5,80E-04	6,25E-04	--
	GT4.1	16,04474	0,5833	-6,13237	0,08555	-11,6119	0,51306	1,38E-02	3,51E-04	-6,66E-03	3,12E-03	--
	GT4.2	11,08504	0,15073	-3,62583	0,07869	-8,53368	0,09152	2,20E-02	6,91E-04			--
	GT5.1	1,55746	0,0719	-1,43702	0,06525			3,46E-02	1,09E-03	1,52E-03	1,23E-04	--
	GT5.2	0,44285	0,00701	-0,48528	0,08759			3,66E-02	1,81E-03	2,79E-03	1,13E-04	--
	GT6.1	11,09622	0,8713	-7,63643	0,1618	-5,28164	0,6966	2,20E-03	1,94E-04			--
	GT6.2	17,52477	0,18263	-7,94451	0,72363	-12,4418	0,68621	4,80E-02	9,00E-03			--
	GT7.1	2,135	0,02555	-1,00164	0,09292	-1,35954	0,08882	2,32E-02	8,90E-04	1,61E-03	4,72E-04	--
	GT7.2	14,93193	1,79953	-4,47007	0,24037	-11,4868	1,53797	2,43E-02	2,57E-03	5,25E-03	4,25E-04	--
	GT8.1	6,45592	0,17968	-4,4762	0,23329	-3,6001	0,1464	2,63E-02	3,06E-03	5,23E-03	5,60E-04	--
	GT8.2	7,73355	0,33914	-4,02791	0,24769	-4,5623	0,1447	1,70E-02	1,21E-03	1,23E-03	3,09E-04	--
Parallel experiment	25_GT_B	8,9036	2,90244	-1,79653	0,29721	-7,42751	2,56332	3,99E-02	4,52E-03	4,26E-03	7,00E-04	--
	25_GT_A	6,19829	0,56762	-1,45956	0,25088	-5,03459	0,32049	2,31E-02	2,12E-03	2,85E-03	5,62E-04	--

Table S4.3.3.2. Fitting parameters of the exponential decay models in respiration test using KRA samples

Experiment	Sample	Y_0	Y_0	A1	A1	A2	A2	k1	k1	k2	k2	Comment
		Val.	Std E.	Val.	Std E.	Val.	Std E.	Val.	Std E.	Val.	Std E.	
Seq. experiment	RT1.1	8,2837	0,06751	-8,5722	0,05958			6,46E-03	1,43E-04			--
	RT1.2	7,13145	0,04584	-7,66767	0,04029			6,22E-03	9,90E-05			--
	RT2.1	6,40608	0,04524	-7,08554	0,04306			7,43E-03	1,35E-04			--
	RT2.2	6,08414	0,10225	-6,52666	0,08473			5,58E-03	2,16E-04			--
	RT3.1											Not possible to fit

Experiment	Sample	Y_0	Y_0	A1	A1	A2	A2	k1	k1	k2	k2	Comment
		Val.	Std E.	Val.	Std E.	Val.	Std E.	Val.	Std E.	Val.	Std E.	
Seq. experiment	RT3.2	9,40513	0,11293	-9,84091	0,11693			7,70E-03	2,74E-04			--
	RT4.1											Not possible to fit
	RT4.2	29,97821	0,95088	-29,0946	0,93388			1,09E-03	4,50E-05			--
	RT5.1	15,89896	0,71402	-15,8177	0,70428			9,86E-04	5,46E-05			--
	RT5.2	8,77504	0,08971	-8,73243	0,08719			1,47E-03	2,03E-05			--
	RT6.1	10,24031	0,08171	-10,1202	0,07092			3,56E-03	5,49E-05			--
	RT6.2	14,78347	0,30957	-14,5377	0,26398			3,53E-03	1,49E-04			--
	RT7.1	16,01966	0,4136	-16,9722	0,36068			3,22E-03	1,43E-04			--
	RT7.2	20,27344	0,16909	-21,0812	0,14061			4,02E-03	6,79E-05			--
	RT8.1	11,60009	0,07561	-11,5875	0,0639			5,35E-03	8,34E-05			--
	RT8.2	10,39977	0,06765	-10,3225	0,05832			5,64E-03	8,60E-05			--
Parallel experiment	25_RT _B	44,21726	6,24194	-41,7536	6,13224			1,47E-03	2,78E-04			--
	25_RT _A	87,0292	29,9875	-1,6E-07	1,23523	-71,638	4,95E+6		9,00E-03			--

Table S4.3.3.3. Fitting parameters of the exponential decay models in gas production using BRA samples

Experiment	Sample	Y_0	Y_0	A1	A1	A2	A2	k1	k1	k2	k2	Comment
		Val.	Std E.	Val.	Std E.	Val.	Std E.	Val.	Std E.	Val.	Std E.	
Parallel experiment	101_GT_A	1,27062	0,36683	-1,24308	0,36435			0,000765	0,000268			--
	101_GT_B	0,61972	0,12719	-0,00614	0,03472	-0,6124	0,11835	12,04189	2,52E+21	0,00245	0,00087	--
	102_GT_A	5,46816	1,03723	-5,60823	1,01015			1,15E-03	2,83E-04			No fit for 21d
	102_GT_B	4,91473	0,19302	-4,81845	0,17951			0,00265	0,000183			--
	103_GT_A	1,1263	0,05404	-1,11626	0,04917			0,00319	0,000306			--

Experiment	Sample	Y_0	Y_0	A1	A1	A2	A2	k1	k1	k2	k2	Comment
		Val.	Std E.	Val.	Std E.	Val.	Std E.	Val.	Std E.	Val.	Std E.	
Parallel experiment	103_GT_B	1,17795	0,0563	-1,18284	0,05112			0,00332	0,000316			--
	104_GT_A	0,42283	0,08222	-0,43045	0,07995			0,00175	0,000489			--
	104_GT_B	0,31645	0,05099	-0,34137	0,04599			2,83E-03	7,50E-04			No fit for 21d
	106_GT_A	0,07644	0,00493	-0,06388	0,00443			0,0042	0,000868			--
	106_GT_B	0,08156	0,00398	-0,07059	0,00419			0,00543	0,000939			--
	107_GT_A	0,55732	0,02675	-0,56548	0,02368			0,00285	0,000276			--
	107_GT_B	0,49878	0,02545	-0,50575	0,02226			0,00331	0,000372			--
	108_GT_A	2,25834	0,05842	-2,29727	0,05162			0,00264	0,000132			--
	108_GT_B	1,9764	0,07298	-1,9892	0,06887			0,00171	9,88E-05			--
	109.5_GT_A	8,95521	0,25184	-8,8077	0,23206			0,00449	0,000332			--
	109.5_GT_B	25,45017	38,24475	-25,5209	38,22462			0,000151	0,000236			Y_0 too high
	139_GT_A	0,0964	0,06598	0,11506	0,04415			-0,00655	0,000957			k1<0
	139_GT_B	2,61592	0,42415	-2,56897	0,41573			0,00166	0,00036			--

Table S4.3.3.4. Fitting parameters of the exponential decay models in respiration test using BRA samples

Experiment	Sample	Y_0	Y_0	A1	A1	k1	k1	Comment
		Val.	Std E.	Val.	Std E.	Val.	Std E.	
Parallel experiment	101_RT_A	5,41823	0,21277	-5,46059	0,19824	0,00285	0,000189	--
	101_RT_B	4,48107	0,12511	-4,46537	0,11788	0,00255	0,000118	--
	102_RT_A	10,77998	0,18256	-10,6607	0,16511	0,00357	0,000124	--
	102_RT_B	11,23898	0,18169	-11,1782	0,16417	0,00379	0,000125	--
	103_RT_A	12,78885	0,27404	-12,6081	0,25061	0,00297	0,00012	--

Experiment	Sample	Y_0	Y_0	A1	A1	k1	k1	Comment
		Val.	Std E.	Val.	Std E.	Val.	Std E.	
Parallel experiment	103_RT_B	17,56745	0,49095	-17,4521	0,45676	0,00251	0,000121	--
	104_RT_A	11,74563	1,68947	-11,9048	1,66213	0,0013	0,000242	--
	104_RT_B	12,12747	0,49148	-11,8241	0,46798	0,00221	0,000147	--
	106_RT_A	5,88576	0,24954	-5,63299	0,23291	0,00202	0,000151	--
	106_RT_B	5,03144	0,21202	-4,8184	0,1982	0,00197	0,000145	--
	107_RT_A	6,46976	0,35077	-6,13103	0,32985	0,00204	0,000195	--
	107_RT_B	5,85624	0,34517	-5,49622	0,32056	0,00232	0,000254	--
	108_RT_A	7,96684	0,20129	-7,40044	0,18247	0,00385	0,00023	--
	108_RT_B	9,03567	0,1218	-8,73327	0,10972	0,00319	8,91E-05	--
	109.5_RT_A	14,52941	0,40468	-14,4221	0,38582	0,00153	6,41E-05	--
	109.5_RT_B	16,32893	0,28851	-15,8611	0,26512	0,00223	7,08E-05	--
	139_RT_A	10,45072	0,92947	-9,84117	0,85989	0,00395	0,000627	--
	139_RT_B	13,74724	1,40328	-13,3371	1,36515	0,00225	0,000339	--

Table S4.3.3.5. Fitting parameters of the exponential decay models in gas production using WIE samples

Experiment	Sample	Y_0	Y_0	A1	A1	k1	k1	Comment
		Val.	Std E.	Val.	Std E.	Val.	Std E.	
Parallel experiment	206_GT_A	-0,18131	0,10082	0,18389	0,09914	-0,00125	0,000512	Y_0 and k1 not possible to fit
	206_GT_B	1,97E+00	4,16E-01	-2,00E+00	4,08E-01	1,04E-03	2,79E-04	--
	207_GT_A	3,12187	0,15255	-3,24927	0,13855	0,00406	0,000413	--
	207_GT_B	3,58396	0,14351	-3,74919	0,13128	0,00433	0,000359	--
	208_GT_A	6,68659	0,77461	-6,87111	0,74479	0,00176	0,00029	--

Experiment	Sample	Y_0	Y_0	A1	A1	k1	k1	Comment
		Val.	Std E.	Val.	Std E.	Val.	Std E.	
Parallel experiment	208_GT_B	4,61808	0,30959	-4,76107	0,28837	0,0025	0,000272	--
	209_GT_A	9,1215	3,11629	-9,14148	3,09852	0,000506	0,000196	Y_0 too high
	209_GT_B	2,32637	0,10093	-2,39933	0,09145	0,00329	0,00027	--
	210_GT_A	2,17322	0,15001	-2,49164	0,1167	0,00237	0,000273	lag phase >73 days
	210_GT_B	3,45121	1,00228	-3,50618	0,99166	0,000929	0,000325	--
	216_GT_A	43,01895	277,0113	-42,9487	277,0014	7,34E-05	0,00048	Y_0 too high
	216_GT_B	-5,79189	3,57223	5,83422	3,56176	-0,00059	0,000327	Y_0 and k1 not possible to fit

Table S4.3.3.6. Fitting parameters of the exponential decay models in respiration test using WIE samples

Experiment	Sample	Y_0	Y_0	A1	A1	k1	k1	Comment
		Val.	Std E.	Val.	Std E.	Val.	Std E.	
Parallel experiment	206_RT_A	5,11527	0,1229	-5,20377	0,11178	290,51	13,87415	--
	206_RT_B	5,32463	0,18331	-5,39862	0,1686	339,9236	21,47079	--
	207_RT_A	11,53777	0,20523	-11,5579	0,18112	252,3321	9,64624	--
	207_RT_B	11,99397	0,13435	-12,3446	0,12037	200,6082	5,16048	--
	208_RT_A	18,2176	0,31034	-19,0963	0,28536	185,6001	8,02991	--
	208_RT_B	16,75469	0,29856	-17,6656	0,29705	165,0655	7,96835	--
	209_RT_A	15,42275	0,33162	-16,9479	0,34645	150,3492	8,38852	--
	209_RT_B	17,77563	0,43037	-19,8547	0,4977	133,7811	8,93825	--
	210_RT_A	8,21284	0,2016	-8,88492	0,19684	172,891	10,1834	--
	210_RT_B	10,29487	0,32187	-11,1717	0,30111	184,2658	13,13073	--
	216_RT_A	13,1275	0,79203	-12,288	0,7243	262,2077	29,60083	--
	216_RT_B	12,81246	0,62702	-12,0095	0,56241	227,7739	22,1934	--

S4.3.4. Extrapolation of carbon potential (Y_0)

In KRA, the Y_0 for the gas production test (GT_{Y0}) was discarded in four out of 36 data points, all of them belonging to the pre-test, and the remaining data was correlated with GT_{365} (Figure S4.3.3, top left). For the gas respiration, no Y_0 (RT_{Y0}) was discarded. Notably, the correlation between RT_{Y0} and RT_{365}, including the samples from the parallel experiment (KRA-25) resulted in a better correlation than using only samples from the sequential experiment. In BRA, one out of 18 GT_{Y0} was discarded and in WIE fourth out of 12 GT_{Y0} were discarded. No RT_{Y0} was discarded in the aerated pilots, and the carbon generation was correlated to GT_{365} and RT_{365} (Figure S4.3.3, top right and bottom). In general, all pilots showed high correlations ($R^2 > 0.6$, Pearson's coefficient r significant on a confidence level of 99.98%, two-sided test) between Y_0 and both gas production and respiration for 365 days. This indicates that the carbon potential can be extrapolated using gas generation results of one year and the accuracy increases when samples have reached the plateau.

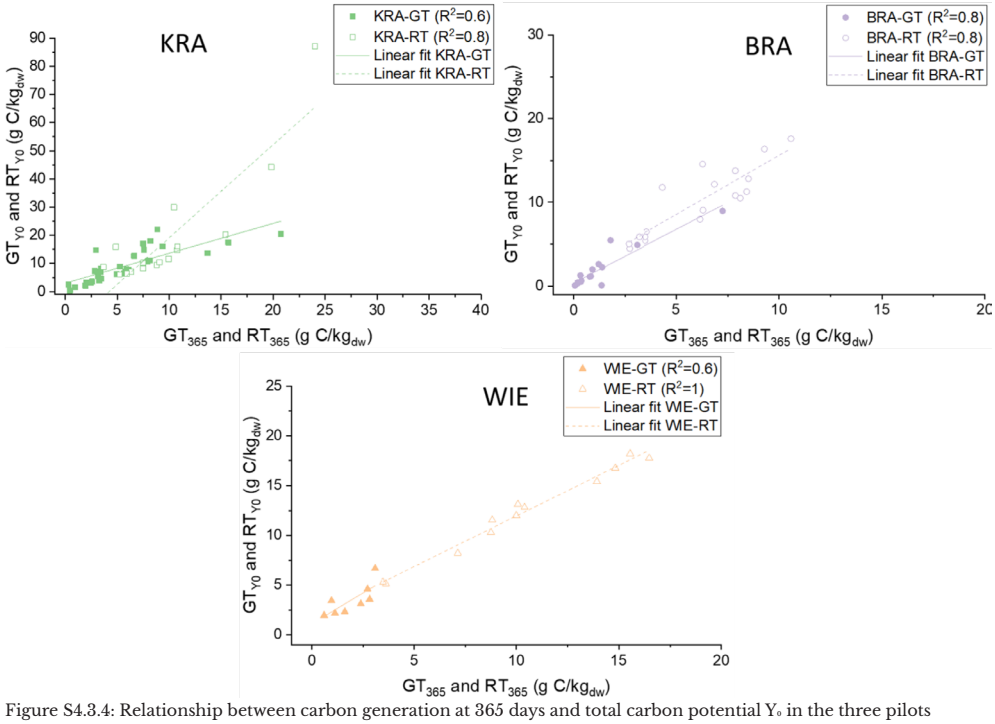

Figure S4.3.4: Relationship between carbon generation at 365 days and total carbon potential Y_0 in the three pilots

S4.3.5. Pre-test: Experiment 1 and 2

Methods

Experiment 1. Container test: This experiment aimed to evaluate the viability of using large containers for gas production tests, particularly to accommodate waste that would not fit through the 4.5 cm neck diameter of 1 L glass bottles. The experiment used 20 L

high-density polyethylene containers (C1 and C2) and 1 L glass bottles (BA and BB). The containers were filled with 1.5 kg and 4.5 kg of fresh, non-sieved waste from KRA, including bulky components. Similarly, two subsamples of approximately 250 g were placed without further pre-treatment in the glass bottles, which were sealed with butyl rubber stoppers. The experiment was conducted under anaerobic conditions, lasting at least 2.5 years in the containers and 3 years in the bottles.

Experiment 2. Storage conditions: The second experiment involved 14 non-sieved waste samples from KRA (GT9 to GT14) stored under cooling (4 °C) and frozen (-18 °C) conditions, as well as mixed samples (GT15) stored under cooling conditions before the gas production began. The experiment aimed to evaluate the effect of storage conditions on sample reactivity. The waste samples were stored for approximately two years (GT9-GT15: 2.3 years; GT15: 1.98 years) before initiating the anaerobic conditions. Two subsamples of approximately 250 g were placed without further pre-treatment in 1 L glass bottles (e.g., GT9.1 and GT9.2), which were sealed with butyl rubber stoppers. All weights were recorded.

Results

Results from 25 L containers (experiment 1) showed carbon generation that was approximately four times lower than the parallel experiments conducted in 1 L glass bottles over 1000 days, with averages of 3.4 kg C/t_{dw} and 14 kg C/t_{dw} respectively. Oxygen leakage during the first 4 months with oxygen concentrations up to 10 vol% in container 1 (C1) and up to 1% in container 2 (C2) lead to seal potential leaking paths and restart the anaerobic conditions. The initial aerobic conditions in C1 could explain the higher carbon production compared to C2. The initial presence of oxygen in the containers could have affected the anaerobic microorganisms, as well as the presence of inert waste such us pieces of metal or stones that were not present in the bottles due to the size limitation of the bottle entrance. The difficulties to keep an anaerobic environment at the beginning of the experiment lead to discard the 25L containers for the long-term experiment. However, they were monitored for more than 900 days and the parallels C1 and C2 showed a similar trend. Bottles A and B came from the same drilling as GT4 samples, and they showed a similar trend with a coefficient of variability of 10% for the experimental data at 600 days

The storage conditions (experiment 2) did not seem to affect carbon generation in samples and parallels stored under different cooling conditions. No significant difference ($p>0.5$) was found between cooled samples (Figure S4.3.5, blue and magenta lines) and frozen samples (Figure S4.3.5, light blue line) in the top and bottom layer. The middle layer showed a larger difference even between samples with the same cooling condition. This could be attributed to the highest heterogeneity of the waste in this layer. Also, previous studies have revealed a large variation in gas generation due to waste heterogeneity (Gebert et al., 2011; Hansen et al., 2004). The mixed sample under cooling conditions (GT15) showed a medium carbon generation compared to the rest of the samples on the same drilling well.

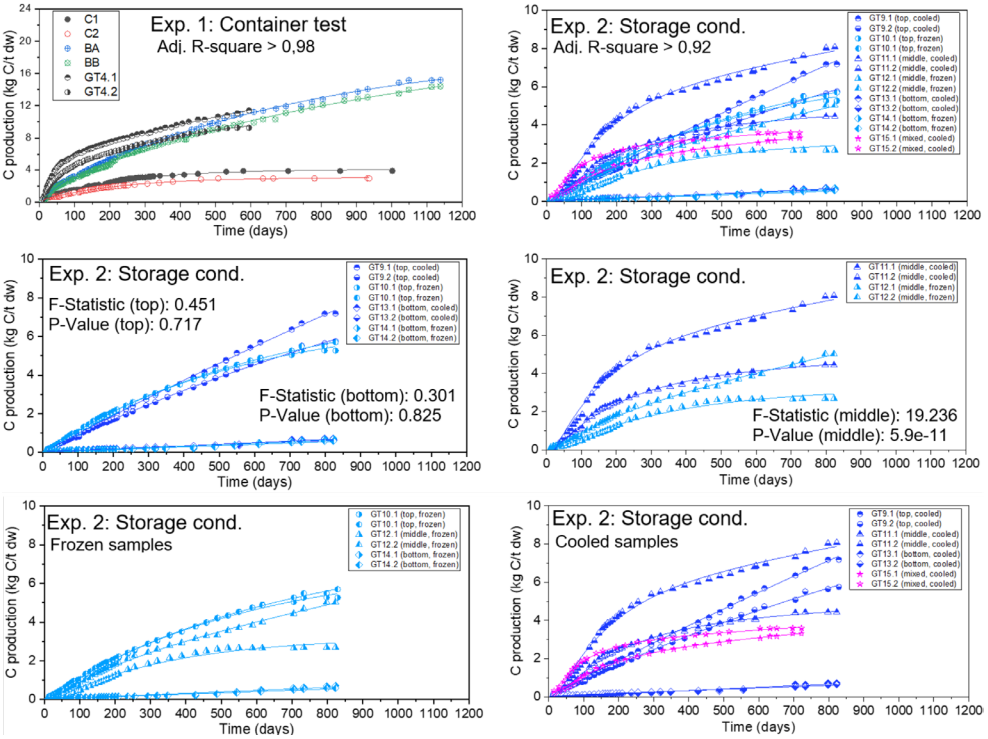

Figure S4.3.5: Course of carbon generation over time in laboratory experiment under anaerobic conditions in KRA testing different containers (top left) and temperature (top right, middle and bottom)

S4.3.6. Parallel anaerobic and aerobic incubation

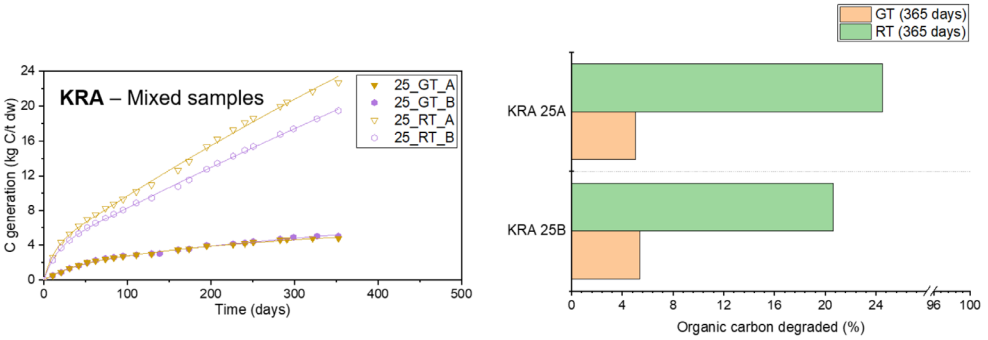

Figure S4.3.6.1: Course of carbon generation over time in laboratory experiment (left), and organic carbon degraded during 1 year (right) in mixed samples under anaerobic (GT) and aerobic (RT) conditions in KRA landfill pilot

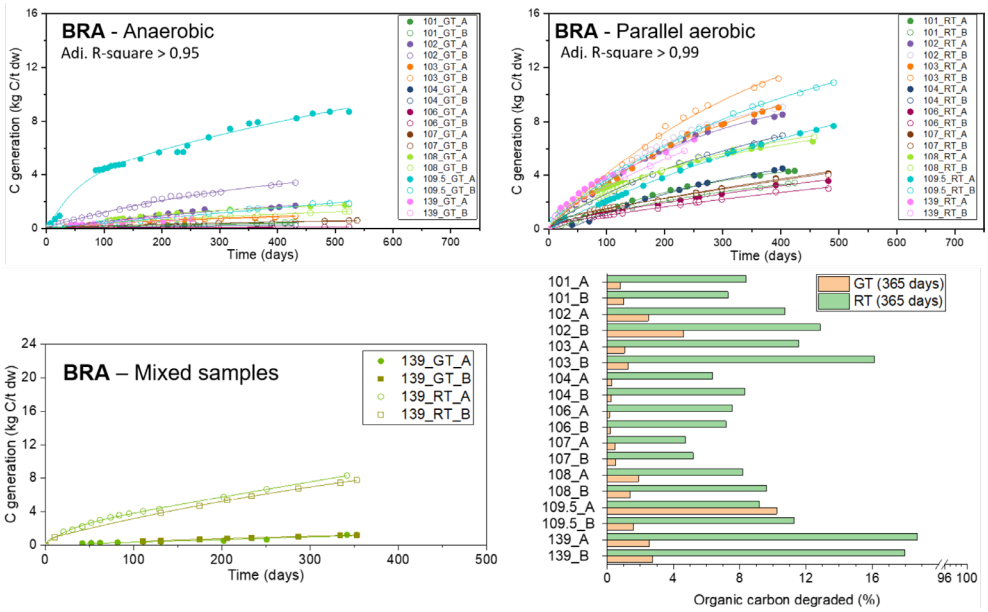

Figure S4.3.6.2: Course of carbon generation over time in laboratory experiment under anaerobic (GT) (top left), and aerobic (RT) (top right) conditions, and GT and RT in mixed samples (bottom left). Organic carbon degraded during 1 year during GT and RT (bottom right) in BRA landfill pilot

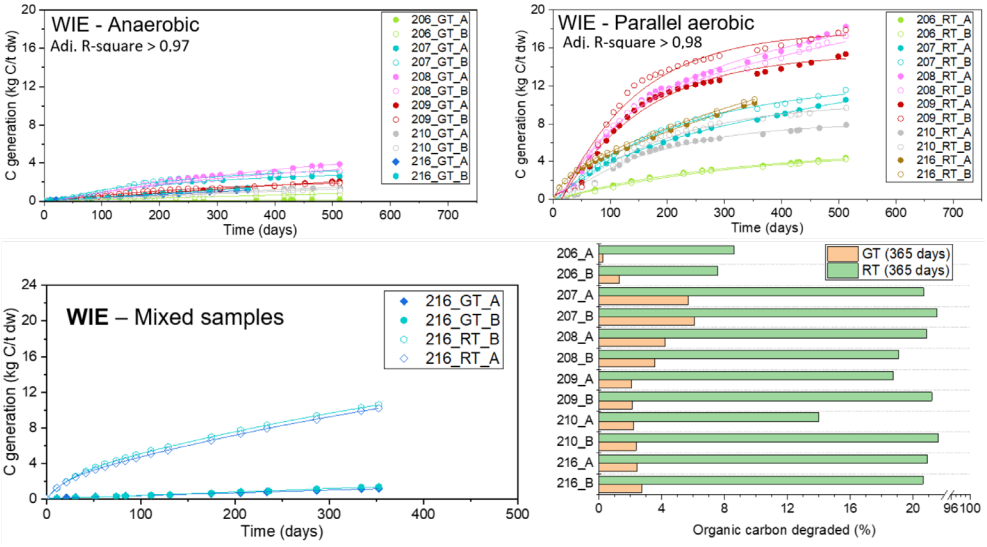

Figure S4.3.6.3: Course of carbon generation over time in laboratory experiment under anaerobic (GT) (top left), and aerobic (RT) (top right) conditions, and GT and RT in mixed samples (bottom left). Organic carbon degraded during 1 year during GT and RT (bottom right) in WIE landfill pilot

S4.3.7. Sequential anaerobic and aerobic incubations

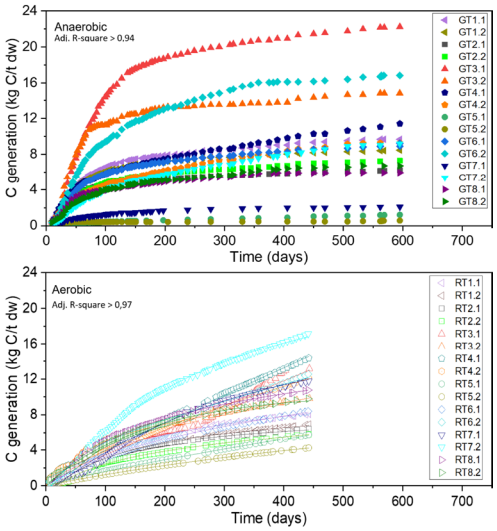

Figure S4.3.7: Course of carbon production (top) and respiration (bottom) over time in landfill pilot KRA.

Table S4.3.7. Mean and standard deviation of duration of experiment, gas production (GT), respiration (RT), and additional carbon released during the laboratory experiment per landfill pilot and layer group.

Landfill pilot	Layer group	Experimental data								
		Days GT	GT (kg C/t_{dw})		Days RT	RT (kg C/t_{dw})		Additional C released (%)		
		mean	mean	std	mean	mean	std	mean	median	std
KRA	top	595,0	8,3	5,3	441,8	9,0	3,6	227,1	109,4	250,6
	mid	595,0	10,3	7,2	442,2	10,7	4,3	176,3	91,2	195,3
	bot	595,0	6,4	0,5	441,1	10,3	0,7	162,8	162,8	24,6

S4.3.8. Kinetics of carbon generation

Table S4.3.8.1 Mean, median and standard deviation of duration of experiment, cumulative carbon, and organic carbon degraded during laboratory experiment per pilot and experiment.

Landfill pilot	Experiment	Condition	Laboratory experiment data								
			Duration of experiment (days)			Cumulative carbon (kg C/t_{dw})			Organic carbon degraded (%)		
			Mean	Median	Stdv	Mean	Median	Stdv	Mean	Median	Stdv
KRA	Pre-test	GT	679.6	616.0	158.5	4.4	3.9	3.8	2.62	2.19	2.63
	Parallel	GT	352.7	352.7	0.0	4.9	4.9	0.2	4.99	4.99	0.19
		RT	352.6	352.6	0.0	21.1	21.1	2.3	21.54	21.54	2.33
	Sequential	GT	595.0	595.0	0.0	8.8	8.7	5.7	4.58	3.39	2.62
		RT	441.9	442.0	0.7	9.8	9.8	3.6	6.31	5.44	3.28

Landfill pilot	Experiment	Condition	Laboratory experiment data								
			Duration of experiment (days)			Cumulative carbon (kg C/t_{dw})			Organic carbon degraded (%)		
			Mean	Median	Stdv	Mean	Median	Stdv	Mean	Median	Stdv
BRA	Parallel	GT	529.9	509.1	81.7	1.5	0.9	2.1	2.35	1.61	2.70
		RT	523.9	509.0	87.6	7.4	7.8	3.0	13.63	13.04	3.82
WIE	Parallel	GT	485.7	512.1	62.1	1.9	1.6	1.1	3.59	2.67	2.18
		RT	485.7	512.1	62.2	11.5	10.6	4.8	21.27	20.36	5.11

Table S4.3.8.2 Mean, median and standard deviation of carbon potentially degradable (Y_0) and degraded during the laboratory experiment per pilot and experiment.

Landfill pilot	Experiment	Condition	Carbon potential (Y_0)						Carbon degraded (laboratory) with respect to Y_0			
			Cumulative carbon (kg C/t_{dw})			Degradable organic carbon (%)			Cumulative carbon (%)		organic carbon (%)	
			Mean	Median	Stdv	Mean	Median	Stdv	Mean	Median	Mean	Median
KRA	Pre-test	GT	6.9	5.1	4.9	4.64	3.50	3.34	64.9	77.0	56.6	62.7
	Parallel	GT	7.55	7.55	1.9	7.71	7.71	1.95	64.8	64.8	64.8	64.8
		RT	65.6	65.6	30.3	67.03	67.03	30.92	32.1	32.1	32.1	32.1
	Sequential	GT	11.0	11.1	6.5	5.65	5.30	3.05	80.3	78.8	81.0	64.0
		RT	12.5	10.3	6.5	9.93	6.11	9.46	78.4	95.1	63.5	88.9
BRA	Parallel	GT	1.9	1.2	2.3	3.06	2.02	3.22	77.4	79.7	76.6	79.7
		RT	10.1	10.6	4.0	18.71	18.28	5.67	73.4	73.9	72.8	71.4
WIE	Parallel	GT	3.1	3.0	1.4	6.10	6.09	2.13	60.3	55.2	58.9	43.9
		RT	12.2	12.4	4.4	23.02	23.06	4.90	94.0	85.3	92.4	88.3

S4.3.9. Correlation with waste characteristics

Table S4.3.9.1. Sample size (n) for correlations between material characteristics and gas production (GT, pretest, parallel and sequential experiment) and respiration test (RT, parallel experiment) related to dry weight for 21 days and 365 days in **all landfill pilots**. WC = water content related to dry weight (%dw), EC = electroconductivity, TOC = total organic carbon (%dw), HI = Hydrogen index, OI = Oxygen index, R-ind = R-index, HP/TOC = hard plastics to TOC ratio, LOI = organic matter content, Y_0 = carbon potential. Bold = Pearson's coefficient r significant on a confidence level of 99.99%, two-sided test

	WC	EC	TOC	HI	OI	R-ind	HP/TOC	LOI	GT_{Y0}	GT_{365}	GT_{21}	RT_{Y0}	RT_{365}	RT_{21}
WC	39	12	39	39	39	40	28	29	66	66	62	32*	32*	32*
EC	--	12	12	12	12	12	12	3	24	24	23	24*	24*	24*
TOC	--	--	38	38	38	40	28	29	60	60	57	26*	26*	26*
HI	--	--	--	38	38	40	28	29	60	60	57	26*	26*	26*
OI	--	--	--	--	33	40	28	29	60	60	57	26*	26*	26*
R-ind	--	--	--	--	--	39	28	30	60	60	57	26*	26*	26*
HP/TOC	--	--	--	--	--	--	26	18	56	56	53	26*	26*	26*

A

	WC	EC	TOC	HI	OI	R-ind	H P / TOC	LOI	GT_{Y0}	GT_{365}	GT_{21}	RT_{Y0}	RT_{365}	RT_{21}
LOI	--	--	--	--	--	--	--	28	40	40	39	6*	6*	6*
GT_{Y0}	--	--	--	--	--	--	--	--	66	66	62	32*	32*	32*
GT_{365}	--	--	--	--	--	--	--	--	--	66	62	32*	32*	32*
GT_{21}	--	--	--	--	--	--	--	--	--	--	62	29*	29*	29*
RT_{Y0}	--	--	--	--	--	--	--	--	--	--	--	46	46	46
RT_{365}	--	--	--	--	--	--	--	--	--	--	--	--	46	46
RT_{21}	--	--	--	--	--	--	--	--	--	--	--	--	--	46

* Correlation does not include sequential experiment

Table S4.3.9.2. Pearson's coefficient rfor correlations between material characteristics and gas production (GT, pretest, parallel and sequential experiment) and respiration test (RT, parallel experiment) related to dry weight for 21 days and 365 days in **KRA**. WC = water content related to dry weight (%dw), EC = electroconductivity, TOC = total organic carbon (%dw), HI = Hydrogen index, OI = Oxygen index, R-ind = R-index, HP/TOC = hard plastics to TOC ratio, LOI = organic matter content, Y_0 = carbon potential. Bold = Pearson's coefficient r significant on a confidence level of 99.99%, two-sided test

	WC	EC	TOC	HI	OI	R-ind	H P / TOC	LOI	GT_{Y0}	GT_{365}	GT_{21}	RT_{Y0}	RT_{365}	RT_{21}
WC	1.00	--	0.11	0.08	-0.21	0.14	-0.33	0.26	0.19	0.08	0.07	--*	--*	--*
EC	--	--	--	--	--	--	--	--	--	--	--	--*	--*	--*
TOC	--	--	1.00	0.90	-0.58	0.62	0.12	0.86	0.45	0.45	0.39	--*	--*	--*
HI	--	--	--	1.00	-0.72	0.81	0.30	0.70	0.36	0.30	0.32	--*	--*	--*
OI	--	--	--	--	1.00	-0.84	-0.26	-0.42	-0.15	-0.09	0.02	--*	--*	--*
R-ind	--	--	--	--	--	1.00	0.28	0.39	0.07	-0.07	0.03	--*	--*	--*
H P / TOC	--	--	--	--	--	--	1.00	-0.10	0.00	-0.02	0.06	--*	--*	--*
LOI	--	--	--	--	--	--	--	1.00	0.38	0.47	0.33	--*	--*	--*
GT_{Y0}	--	--	--	--	--	--	--	--	1.00	0.82	0.71	--*	--*	--*
GT_{365}	--	--	--	--	--	--	--	--	--	1.00	0.84	--*	--*	--*
GT_{21}	--	--	--	--	--	--	--	--	--	--	1.00	--*	--*	--*
RT_{Y0}	--	--	--	--	--	--	--	--	--	--	--	1.00	0.88	0.90
RT_{365}	--	--	--	--	--	--	--	--	--	--	--	--	1.00	0.90
RT_{21}	--	--	--	--	--	--	--	--	--	--	--	--	--	1.00

* Correlation does not include sequential experiment

Table S4.3.9.3. Sample size (n) for correlations between material characteristics and gas production (GT, pretest, parallel and sequential experiment) and respiration test (RT, parallel experiment) related to dry weight for 21 days and 365 days in **KRA**. WC = water content related to dry weight (%dw), EC = electroconductivity, TOC = total organic carbon (%dw), HI = Hydrogen index, OI = Oxygen index, R-ind = R-index, HP/TOC = hard plastics to TOC ratio, LOI = organic matter content, Y_0 = carbon potential. Bold = Pearson's coefficient r significant on a confidence level of 99.99%, two-sided test

	WC	EC	TOC	HI	OI	R-ind	H P / TOC	LOI	GT_{Y0}	GT_{365}	GT_{21}	RT_{Y0}	RT_{365}	RT_{21}
WC	21	1	21	21	21	22	16	21	36	36	35	2*	2*	2*
EC	--	1	1	1	1	1	1	1	2	2	2	2*	2*	2*
TOC	--	--	20	20	20	22	16	21	36	36	35	2*	2*	2*

	WC	EC	TOC	HI	OI	R-ind	H P / TOC	LOI	GT_{Y0}	GT_{365}	GT_{21}	RT_{Y0}	RT_{365}	RT_{21}
HI	--	--	--	20	20	22	16	21	36	36	35	2*	2*	2*
OI	--	--	--	--	18	22	16	21	36	36	35	2*	2*	2*
R-ind	--	--	--	--	--	21	16	22	36	36	35	2*	2*	2*
H P / TOC	--	--	--	--	--	--	16	16	32	32	31	2*	2*	2*
LOI	--	--	--	--	--	--	--	21	36	36	35	2*	2*	2*
GT_{Y0}	--	--	--	--	--	--	--	--	36	36	35	2*	2*	2*
GT_{365}	--	--	--	--	--	--	--	--	--	36	35	2*	2*	2*
GT_{21}	--	--	--	--	--	--	--	--	--	--	35	2*	2*	2*
RT_{Y0}	--	--	--	--	--	--	--	--	--	--	--	16	16	16
RT_{365}	--	--	--	--	--	--	--	--	--	--	--	--	16	16
RT_{21}	--	--	--	--	--	--	--	--	--	--	--	--	--	16

* Correlation does not include sequential experiment

Table S4.3.9.4. Pearson's coefficient r for correlations between material characteristics and gas production (GT, pretest, parallel and sequential experiment) and respiration test (RT, parallel experiment) related to dry weight for 21 days and 365 days in **BRA**. WC = water content related to dry weight (%dw), EC = electroconductivity, TOC = total organic carbon (%dw), HI = Hydrogen index, OI = Oxygen index, R-ind = R-index, HP/TOC = hard plastics to TOC ratio, LOI = organic matter content, Y_0 = carbon potential. Bold = Pearson's coefficient r significant on a confidence level of 99.99%, two-sided test

	WC	EC	TOC	HI	OI	R-ind	H P / TOC	LOI	GT_{Y0}	GT_{365}	GT_{21}	RT_{Y0}	RT_{365}	RT_{21}
WC	1.00	-0.09	0.88	0.50	0.10	-0.76	-0.39	0.48	0.48	0.51	0.44	0.69	0.48	0.25
EC	--	1.00	0.10	-0.35	0.95	-0.62	0.88		0.32	0.79	0.84	0.45	0.52	0.73
TOC	--	--	1.00	0.41	0.15	-0.79	-0.10	0.32	0.64	0.62	0.56	0.70	0.71	0.37
HI	--	--	--	1.00	0.35	-0.31	0.06	0.44	-0.44	-0.48	-0.38	-0.38	-0.42	-0.47
OI	--	--	--	--	1.00	-0.53	0.97	-0.65	-0.07	0.18	0.36	0.20	0.26	0.55
R-ind	--	--	--	--	--	1.00	-0.28	0.00	-0.17	-0.35	-0.40	-0.91	-0.83	-0.71
H P / TOC	--	--	--	--	--	--	1.00		0.10	0.33	0.46	0.16	0.28	0.55
LOI	--	--	--	--	--	--	--	1.00	--	--	--	--	--	--
GT_{Y0}	--	--	--	--	--	--	--	--	1.00	0.92	0.91	0.40	0.33	0.12
GT_{365}	--	--	--	--	--	--	--	--	--	1.00	0.98	0.42	0.31	0.15
GT_{21}	--	--	--	--	--	--	--	--	--	--	1.00	0.36	0.23	0.08
RT_{Y0}	--	--	--	--	--	--	--	--	--	--	--	1.00	0.88	0.55
RT_{365}	--	--	--	--	--	--	--	--	--	--	--	--	1.00	0.81
RT_{21}	--	--	--	--	--	--	--	--	--	--	--	--	--	1.00

Table S4.3.9.5. Sample size (n) for correlations between material characteristics and gas production (GT, pretest, parallel and sequential experiment) and respiration test (RT, parallel experiment) related to dry weight for 21 days and 365 days in **BRA**. WC = water content related to dry weight (%dw), EC = electroconductivity, TOC = total organic carbon (%dw), HI = Hydrogen index, OI = Oxygen index, R-ind = R-index, HP/TOC = hard plastics to TOC ratio, LOI = organic matter content, Y_0 = carbon potential. Bold = Pearson's coefficient r significant on a confidence level of 99.99%, two-sided test

	WC	EC	TOC	HI	OI	R-ind	H P / TOC	LOI	GT_{Y0}	GT_{365}	GT_{21}	RT_{Y0}	RT_{365}	RT_{21}
WC	10	6	10	10	10	10	7	4	18	18	16	18	18	18
EC	--	6	6	6	6	6	6	1	12	12	11	12	12	12
TOC	--	--	10	10	10	10	7	4	14	14	12	14	14	14
HI	--	--	--	10	10	10	7	4	14	14	12	14	14	14
OI	--	--	--	--	9	10	7	4	14	14	12	14	14	14
R-ind	--	--	--	--	--	10	7	4	14	14	12	14	14	14
H P / TOC	--	--	--	--	--	--	6	1	14	14	12	14	14	14
LOI	--	--	--	--	--	--	--	3	2	2	2	2	2	2
GT_{Y0}	--	--	--	--	--	--	--	--	18	18	16	18	18	18
GT_{365}	--	--	--	--	--	--	--	--	--	18	16	18	18	18
GT_{21}	--	--	--	--	--	--	--	--	--	--	16	16	16	16
RT_{Y0}	--	--	--	--	--	--	--	--	--	--	--	18	18	18
RT_{365}	--	--	--	--	--	--	--	--	--	--	--	--	18	18
RT_{21}	--	--	--	--	--	--	--	--	--	--	--	--	--	18

Table S4.3.9.6. Pearson's coefficient r for correlations between material characteristics and gas production (GT, pretest, parallel and sequential experiment) and respiration test (RT, parallel experiment) related to dry weight for 21 days and 365 days in **WIE**. WC = water content related to dry weight (%dw), EC = electroconductivity, TOC = total organic carbon (%dw), HI = Hydrogen index, OI = Oxygen index, R-ind = R-index, HP/TOC = hard plastics to TOC ratio, LOI = organic matter content, Y_0 = carbon potential. Bold = Pearson's coefficient r significant on a confidence level of 99.99%, two-sided test

	WC	EC	TOC	HI	OI	R-ind	H P / TOC	LOI	GT_{Y0}	GT_{365}	GT_{21}	RT_{Y0}	RT_{365}	RT_{21}
WC	1.00	-0.19	0.84	0.73	-0.29	-0.54	-0.37	0.81	0.19	0.31	0.21	0.76	0.81	0.15
EC	--	1.00	-0.11	-0.68	0.92	0.46	0.38		-0.33	-0.45	0.15	-0.11	-0.17	0.66
TOC	--	--	1.00	0.80	0.00	-0.69	0.10	0.93	0.50	0.42	0.13	0.91	0.94	0.29
HI	--	--	--	1.00	-0.48	-0.74	-0.10	0.91	0.65	0.69	0.11	0.78	0.82	-0.10
OI	--	--	--	--	1.00	-0.02	0.48	-0.01	-0.02	-0.09	0.44	0.14	0.06	0.89
R-ind	--	--	--	--	--	1.00	-0.04	-0.85	-0.79	-0.91	-0.52	-0.89	-0.88	-0.31
H P / TOC	--	--	--	--	--	--	1.00		0.48	0.12	-0.13	0.15	0.09	0.53
LOI	--	--	--	--	--	--	--	1.00						
GT_{Y0}	--	--	--	--	--	--	--	--	1.00	0.82	0.21	0.68	0.64	0.36
GT_{365}	--	--	--	--	--	--	--	--	--	1.00	0.64	0.73	0.69	0.43
GT_{21}	--	--	--	--	--	--	--	--	--	--	1.00	0.48	0.41	0.71
RT_{Y0}	--	--	--	--	--	--	--	--	--	--	--	1.00	0.99	0.57
RT_{365}	--	--	--	--	--	--	--	--	--	--	--	--	1.00	0.48
RT_{21}	--	--	--	--	--	--	--	--	--	--	--	--	--	1.00

Table S4.3.9.7. Sample size (n) for correlations between material characteristics and gas production (GT, pretest, parallel and sequential experiment) and respiration test (RT, parallel experiment) related to dry weight for 21 days and 365 days in **WIE**. WC = water content related to dry weight (%dw), EC = electroconductivity, TOC = total organic carbon (%dw), HI = Hydrogen index, OI = Oxygen index, R-ind = R-index, HP/TOC = hard plastics to TOC ratio, LOI = organic matter content, Y_0 = carbon potential. Bold = Pearson's coefficient r significant on a confidence level of 99.99%, two-sided test

	WC	EC	TOC	HI	OI	R-ind	H P / TOC	LOI	GT_{Y0}	GT_{365}	GT_{21}	RT_{Y0}	RT_{365}	RT_{21}
WC	8	*5*	8	8	8	8	*5*	4	12	12	11	12	12	12
EC	--	*5*	*5*	*5*	*5*	*5*	*5*	1	10	10	10	10	10	10
TOC	--	--	8	8	8	8	*5*	4	10	10	10	10	10	10
HI	--	--	--	8	8	8	*5*	4	10	10	10	10	10	10
OI	--	--	--	--	7	8	*5*	4	10	10	10	10	10	10
R-ind	--	--	--	--	--	8	*5*	4	10	10	10	10	10	10
H P / TOC	--	--	--	--	--	--	*5*	1	10	10	10	10	10	10
LOI	--	--	--	--	--	--	--	4	2	2	2	2	2	2
GT_{Y0}	--	--	--	--	--	--	--	--	12	12	11	12	12	12
GT_{365}	--	--	--	--	--	--	--	--	--	12	11	12	12	12
GT_{21}	--	--	--	--	--	--	--	--	--	--	11	11	11	11
RT_{Y0}	--	--	--	--	--	--	--	--	--	--	--	12	12	12
RT_{365}	--	--	--	--	--	--	--	--	--	--	--	--	12	12
RT_{21}	--	--	--	--	--	--	--	--	--	--	--	--	--	12

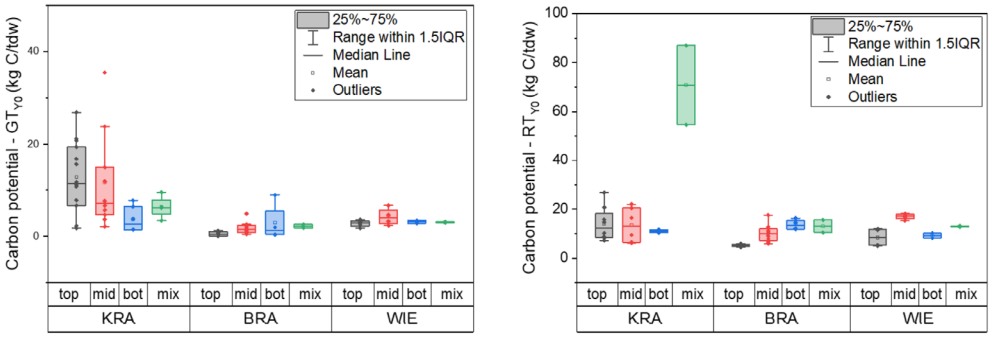

Figure S4.3.9.1: Carbon potential per group layer in KRA, BRA and WIE landfills. Anaerobic (GT_{Y0}, left), Aerobic (RT_{Y0}, right). For box plots: box = 25th-75th percentile, line = median, whiskers = 1.5 IQR, circle symbol = mean, rhombus symbol outside whiskers = outliers

A

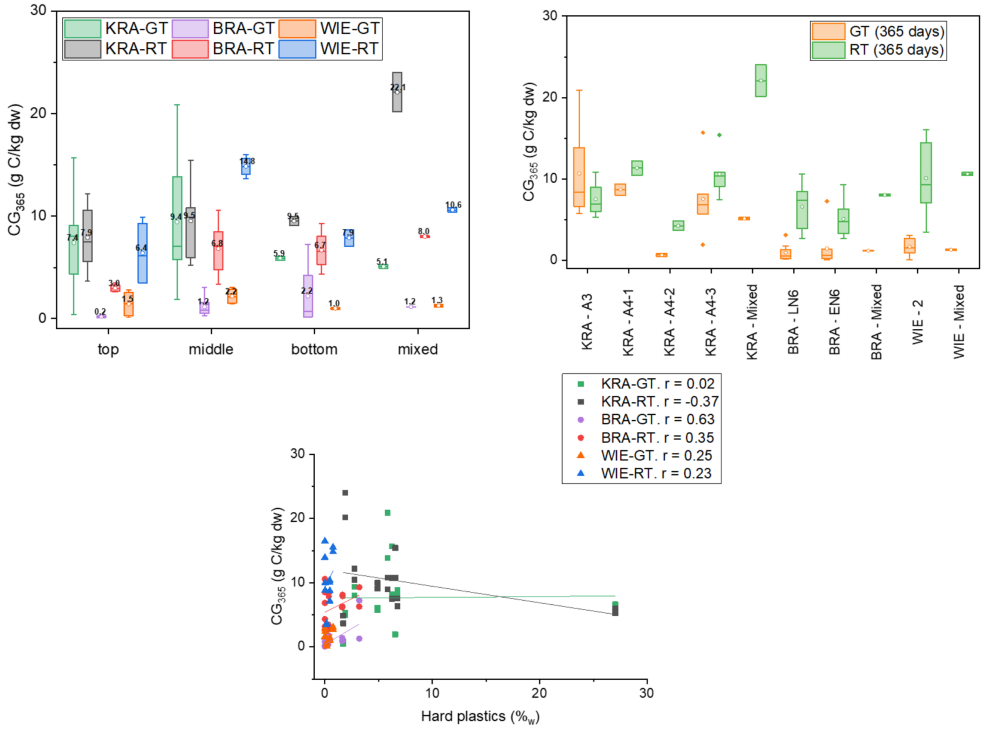

Figure S4.3.8.2: Carbon generation under anaerobic (GT) and aerobic (RT) conditions per depth and test (top left); carbon generation (GT, RT) per drill and test (top right), relationship between carbon generation (GT, RT) and hard plastic in percentage (bottom)

B

Supplementary Information Chapter 5

Carbon and nitrogen balancing to identify processes and assess progress of landfill in-situ stabilization

S5.1. Waste sampling to quantify mobile and adsorbed ammonium

The following subset of samples was selected to measure NH_4^+ adsorption characteristics (mobile, water-extractable and KCl-extractable NH_4^+):

- BRA: Samples 101 to 104 from well Ln6 located in compartment 11Z, and the mixed sample from compartment 11N, sample 139 (Figure S5.1.1, top).
- WIE: Samples 206, 207 and 209 from well 2, and the mixed sample 216 (Figure S5.1.1, middle)
- KRA: Samples 9, 11 and 13 from well A4-4 as well as their mixed sample, sample 15, and the mixed sample from other 9 wells, sample 25 (Figure S5.1.1, bottom).

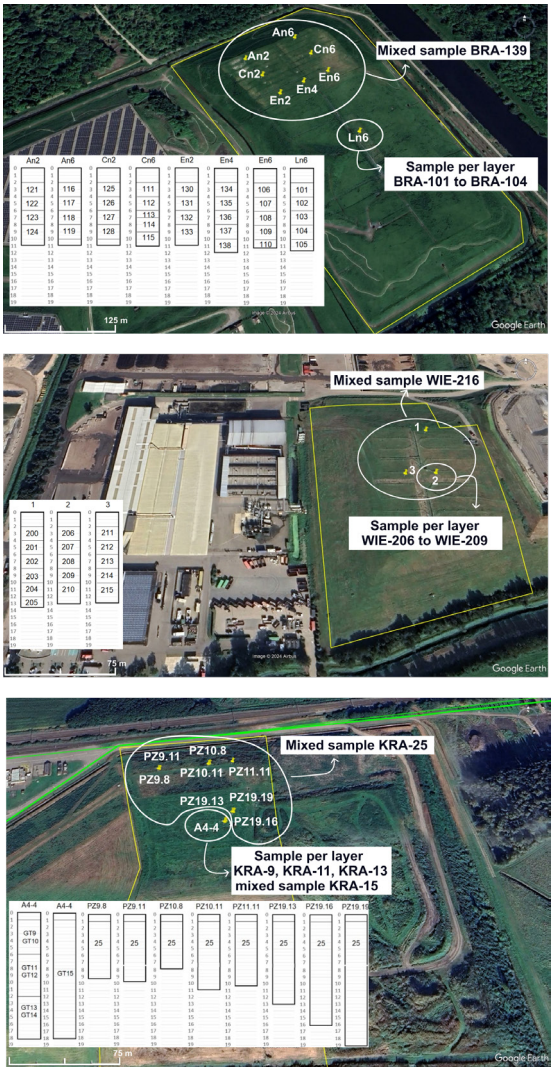

Figure S5.1.1: Aerial photographs (Google Earth) of waste sampling locations and schematic (bottom left in each subfigure) showing the waste samples used to quantify mobile and adsorbed ammonium. Top: BRA; middle: WIE; bottom: KRA.

S5.2. Correlations of free and adsorbed ammonium with waste properties

Correlations between NH_4^+-N fractions (pore water [NP], water-extractable [NW], and KCl-extractable [NK]) and selected waste properties were evaluated to identify factors influencing ammonium mobility and retention (Tables S5.2.1-S5.2.4).

Across the three pilots, ammonium fractions showed strong positive correlations with water content and total nitrogen, confirming that moisture availability and organic nitrogen pools strongly influence NH_4^+ solubility and sorption. Relationships with organic matter quality indices (R- and I-index) revealed that labile organic fractions enhance ammonification, while more refractory materials are associated with lower NH_4^+ availability.

In both aerated sites, water content correlated positively with NP, NW, and NK, indicating that moisture enhances ammonium mobilization. Strong correlations with TN and TOC demonstrate the coupling between organic carbon degradation and nitrogen release. NW and NK were particularly associated with labile carbon (RT_{Y_0}) and the I-index, reflecting the role of thermally labile compounds in nitrogen cycling. Negative correlations with TOC/TN ratios suggest that nitrogen enrichment accompanies stabilization. Ammonium fractions correlated positively with aerobic respiration metrics (RT) in BRA and WIE, suggesting that enhanced aeration promotes both organic carbon degradation and ammonium production, part of which becomes adsorbed to mineral or organic surfaces.

In contrast, KRA exhibited weak or negative correlations between NH_4^+ fractions and carbon or nitrogen parameters, consistent with the advanced flushing of soluble nitrogen under recirculation. Negative relationships with the I-index and gas production further support that most labile nitrogen has already been mobilised. Negative correlations with anaerobic gas potential (GT) in KRA suggest that water recirculation reduces adsorbed ammonium, likely due to flushing effects.

Together, these patterns illustrate the tight coupling between water content, organic matter lability, and microbial activity in regulating ammonium cycling in landfill waste. Aeration enhances nitrogen transformation and sorption capacity, whereas water recirculation promotes nitrogen export.

Table S5.2.1. Pearson's coefficient r for correlations between waste characteristics in BRA, WIE and KRA. WC = water content related to dry weight (%dw), EC = electroconductivity (mS/cm), TN = total nitrogen (%dw), TC = total carbon (%dw), TOC = total organic carbon (%dw), LOI = loss on ignition (%dw), TOC/TN = total organic carbon to total nitrogen ratio, HI = Hydrogen index, OI = Oxygen index, NP = nitrogen in the pore water (mg/kg_{dw}), NW = water-extractable nitrogen, NK = KCl-extractable nitrogen, GT_{365} = gas production in 365 days ($g\ C/kg_{dw}$), RT = respiration test, Y_0 = carbon potential. Bold = Pearson's coefficient r significant on a confidence level of 99.95%, two-sided test.

	BRA			WIE			KRA		
	NP (n=5)	NW (n=5)	NK (n=5)	NP (n=4)	NW (n=4)	NK (n=4)	NP (n=5)	NW (n=5)	NK (n=5)
WC	**0.95**	0.61	0.48	**0.98**	**0.93**	**0.99**	-0.63	**-0.83**	**-0.85**
pH	-0.26	**-0.77**	**-0.88**	-0.18	-0.32	-0.28	--	--	--
EC	-0.06	0.52	0.68	-0.38	0.05	-0.30	--	--	--
TN	**0.81**	0.67	0.71	**0.89**	**0.97**	**0.93**	0.40	-0.23	0.02

	BRA			WIE			KRA		
	NP (n=5)	NW (n=5)	NK (n=5)	NP (n=4)	NW (n=4)	NK (n=4)	NP (n=5)	NW (n=5)	NK (n=5)
TC	0.67	0.34	0.40	0.78	**0.95**	**0.82**	-0.41	-0.34	-0.46
TOC	0.58	0.22	0.31	**0.89**	**0.96**	**0.93**	-0.36	-0.36	-0.45
HI	-0.45	-0.43	-0.64	**0.95**	0.74	**0.91**	-0.09	0.03	-0.06
OI	-0.29	0.32	0.45	-0.33	0.16	-0.28	-0.11	-0.01	-0.03
R-ind	-0.65	**-0.90**	**-0.98**	-0.75	-0.80	-0.70	0.10	0.36	0.27
I-ind	0.63	**0.76**	**0.89**	0.64	0.61	0.57	-0.51	**-0.81**	**-0.80**
LOI	--	--	--	--	--	--	-0.20	-0.14	-0.24
TOC/TN	-0.61	**-0.96**	**-0.96**	-0.72	**-0.96**	-0.73	-0.38	-0.19	-0.34
GT_{Y_0}	-0.37	-0.29	0.04	0.33	0.55	0.27	**-0.87**	**-0.82**	**-0.90**
GT_{365}	-0.30	-0.24	0.10	0.36	0.46	0.28	-0.55	**-0.77**	**-0.80**
RT_{Y_0}	0.63	**0.82**	**0.91**	0.80	**0.98**	0.81	--	--	--
RT_{365}	0.25	0.51	**0.75**	**0.87**	**1.00**	**0.88**	--	--	--
NK	0.61	**0.93**	1.00	**0.99**	**0.89**	1.00	**0.79**	**0.95**	1.00
NP	1.00	**0.78**	0.61	1.00	**0.87**	**0.99**	1.00	0.58	**0.79**
NW	**0.78**	1.00	**0.93**	**0.87**	1.00	**0.89**	0.58	1.00	**0.95**

Table S5.2.2. Pearson's coefficient r for correlations between waste characteristics in **BRA**. WC = water content related to dry weight (%dw), EC = electroconductivity (mS/cm), TN = total nitrogen (%dw), TC = total carbon (%dw), TOC = total organic carbon (%dw), TOC/TN = total organic carbon to total nitrogen ratio, LOI = loss on ignition (%dw), HI = Hydrogen index, OI = Oxygen index, R-ind= R index, I-ind= I index, NP = nitrogen in the pore water (mg/kg_{dw}), NW = water-extractable nitrogen, NK = KCl-extractable nitrogen, GT_{365} = gas production in 365 days (g C/kg_{dw}), RT_{365} = gas respiration in 365 days (g C/kg_{dw}), Y_0 = carbon potential. Bold = Pearson's coefficient r significant on a confidence level of 99.95%, two-sided test.

BRA	WC (n=5)	pH (n=4)	EC (n=4)	TN (n=5)	TC (n=5)	TOC (n=5)	HI (n=5)	OI (n=5)	R-ind (n=5)	I-ind (n=5)	TOC/TN (n=5)	GT_{Y0} (n=5)	GT_{365} (n=5)	RT_{Y0} (n=5)	RT_{365} (n=5)	NK (n=5)	NP (n=5)	NW (n=5)
WC	1.00	-0.11	-0.22	0.88	0.83	0.77	-0.55	-0.51	-0.58	0.64	-0.45	-0.22	-0.12	0.61	0.31	0.48	0.95	0.61
pH	--	1.00	-0.95	-0.45	-0.28	-0.18	0.80	-0.80	0.81	-0.73	0.83	-0.71	-0.73	-0.65	-0.66	-0.88	-0.26	-0.77
EC	--	--	1.00	0.13	-0.05	-0.15	-0.56	0.95	-0.58	0.48	-0.62	0.88	0.82	0.40	0.50	0.68	-0.06	0.52
TN	--	--	--	1.00	0.90	0.86	-0.85	-0.25	-0.82	0.92	-0.61	0.16	0.27	0.86	0.71	0.71	0.81	0.67
TC	--	--	--	--	1.00	0.99	-0.86	-0.44	-0.53	0.72	-0.22	0.36	0.45	0.57	0.50	0.40	0.67	0.34
TOC	--	--	--	--	--	1.00	-0.84	-0.51	-0.46	0.67	-0.13	0.41	0.51	0.53	0.51	0.31	0.58	0.22
HI	--	--	--	--	--	--	1.00	-0.03	0.73	-0.88	0.42	-0.64	-0.71	-0.72	-0.77	-0.64	-0.45	-0.43
OI	--	--	--	--	--	--	--	1.00	-0.31	0.13	-0.43	0.21	0.13	0.12	0.20	0.45	-0.29	0.32
R-ind	--	--	--	--	--	--	--	--	1.00	-0.96	0.93	-0.10	-0.18	-0.96	-0.82	-0.98	-0.65	-0.90
I-ind	--	--	--	--	--	--	--	--	--	1.00	-0.78	0.29	0.39	0.96	0.89	0.89	0.63	0.76
TOC/TN	--	--	--	--	--	--	--	--	--	--	1.00	0.21	0.14	-0.87	-0.65	-0.96	-0.61	-0.96
GT_{Y0}	--	--	--	--	--	--	--	--	--	--	--	1.00	0.99	0.08	0.45	0.04	-0.37	-0.29
GT_{365}	--	--	--	--	--	--	--	--	--	--	--	--	1.00	0.20	0.56	0.10	-0.30	-0.24
RT_{Y0}	--	--	--	--	--	--	--	--	--	--	--	--	--	1.00	0.89	0.91	0.63	0.82
RT_{365}	--	--	--	--	--	--	--	--	--	--	--	--	--	--	1.00	0.75	0.25	0.51
NK	--	--	--	--	--	--	--	--	--	--	--	--	--	--	--	1.00	0.61	0.93
NP	--	--	--	--	--	--	--	--	--	--	--	--	--	--	--	--	1.00	0.78
NW	--	--	--	--	--	--	--	--	--	--	--	--	--	--	--	--	--	1.00

Table S5.2.3. Pearson's coefficient r for correlations between waste characteristics in **WIE**. WC = water content related to dry weight (%dw), EC = electroconductivity (mS/cm), TN = total nitrogen (%dw), TC = total carbon (%dw), TOC = total organic carbon (%dw), TOC/TN = total organic carbon to total nitrogen ratio, LOI = loss on ignition (%dw), HI = Hydrogen index, OI = Oxygen index, R-ind= R index, I-ind= I index, NP = nitrogen in the pore water (mg/kg_{dw}), NW = water-extractable nitrogen, NK = KCl-extractable nitrogen, GT_{365} = gas production in 365 days (g C/kg_{dw}), RT_{365} = gas respiration in 365 days (g C/kg_{dw}), Y_0 = carbon potential. Bold = Pearson's coefficient r significant on a confidence level of 99.95%, two-sided test.

WIE	WC (n=4)	pH (n=4)	EC (n=4)	TN (n=4)	TC (n=4)	TOC (n=4)	HI (n=4)	OI (n=4)	R-ind (n=4)	I-ind (n=4)	TOC/TN (n=4)	GT_{Y_0} (n=4)	GT_{365} (n=4)	RT_{Y_0} (n=4)	RT_{365} (n=4)	NK (n=4)	NP (n=4)	NW (n=4)
WC	1.00	-0.35	-0.18	0.97	0.89	0.97	0.86	-0.15	-0.70	0.54	-0.79	0.30	0.28	0.86	0.92	0.99	0.98	0.93
pH	--	1.00	-0.64	-0.50	-0.58	-0.52	0.13	-0.42	-0.31	0.55	0.19	0.49	0.66	-0.21	-0.24	-0.28	-0.18	-0.32
EC	--	--	1.00	0.07	0.28	0.07	-0.63	0.94	0.33	-0.52	-0.17	-0.08	-0.33	0.09	0.01	-0.30	-0.38	0.05
TN	--	--	--	1.00	0.97	1.00	0.72	0.10	-0.65	0.44	-0.86	0.31	0.23	0.91	0.94	0.93	0.89	0.97
TC	--	--	--	--	1.00	0.97	0.56	0.32	-0.59	0.35	-0.89	0.34	0.20	0.91	0.93	0.82	0.78	0.95
TOC	--	--	--	--	--	1.00	0.71	0.09	-0.62	0.42	-0.85	0.28	0.20	0.89	0.93	0.93	0.89	0.96
HI	--	--	--	--	--	--	1.00	-0.53	-0.81	0.79	-0.61	0.42	0.52	0.69	0.76	0.91	0.95	0.74
OI	--	--	--	--	--	--	--	1.00	0.08	-0.25	-0.35	0.24	-0.01	0.25	0.15	-0.28	-0.33	0.16
R-ind	--	--	--	--	--	--	--	--	1.00	-0.96	0.84	-0.87	-0.88	-0.86	-0.85	-0.70	-0.75	-0.80
I-ind	--	--	--	--	--	--	--	--	--	1.00	-0.67	0.86	0.94	0.68	0.67	0.57	0.64	0.61
TOC/TN	--	--	--	--	--	--	--	--	--	--	1.00	-0.73	-0.61	-0.99	-0.97	-0.73	-0.72	-0.96
GT_{Y_0}	--	--	--	--	--	--	--	--	--	--	--	1.00	0.97	0.68	0.61	0.27	0.33	0.55
GT_{365}	--	--	--	--	--	--	--	--	--	--	--	--	1.00	0.58	0.53	0.28	0.36	0.46
RT_{Y_0}	--	--	--	--	--	--	--	--	--	--	--	--	--	1.00	0.99	0.81	0.80	0.98
RT_{365}	--	--	--	--	--	--	--	--	--	--	--	--	--	--	1.00	0.88	0.87	1.00
NK	--	--	--	--	--	--	--	--	--	--	--	--	--	--	--	1.00	0.99	0.89
NP	--	--	--	--	--	--	--	--	--	--	--	--	--	--	--	--	1.00	0.87
NW	--	--	--	--	--	--	--	--	--	--	--	--	--	--	--	--	--	1.00

Table S5.2.4. Pearson's coefficient r for correlations between waste characteristics in **KRA**. WC = water content related to dry weight (%dw), EC = electroconductivity (mS/cm), TN = total nitrogen (%dw), TC = total carbon (%dw), TOC = total organic carbon (%dw), TOC/TN = total organic carbon to total nitrogen ratio, LOI = loss on ignition (%dw), HI = Hydrogen index, OI = Oxygen index, R-ind= R index, I-ind= I index, NP = nitrogen in the pore water (mg/kg_{dw}), NW = water-extractable nitrogen, NK = KCl-extractable nitrogen, GT_{365} = gas production in 365 days (g C/kg_{dw}), RT_{365} = gas respiration in 365 days (g C/kg_{dw}), Y_0 = carbon potential. Bold = Pearson's coefficient r significant on a confidence level of 99.95%, two-sided test.

KRA	WC (n=5)	TN (n=5)	TC (n=5)	TOC (n=5)	HI (n=5)	OI (n=5)	R-ind (n=5)	I-ind (n=5)	LOI (n=5)	TOC/TN (n=5)	GT_{Y_0} (n=5)	GT_{365} (n=5)	NK (n=5)	NP (n=5)	NW (n=5)
WC	1.00	0.22	0.66	0.72	0.47	-0.50	0.20	0.41	0.49	0.46	0.76	0.44	-0.85	-0.63	-0.83
TN	--	1.00	-0.36	-0.20	-0.14	-0.38	-0.11	-0.16	-0.37	-0.58	0.08	-0.32	0.02	0.40	-0.23
TC	--	--	1.00	0.98	0.87	-0.56	0.64	0.16	0.97	0.96	0.20	0.34	-0.46	-0.41	-0.34
TOC	--	--	--	1.00	0.91	-0.68	0.69	0.08	0.95	0.91	0.20	0.24	-0.45	-0.36	-0.36
HI	--	--	--	--	1.00	-0.85	0.93	-0.34	0.92	0.81	-0.12	-0.17	-0.06	-0.09	0.03
OI	--	--	--	--	--	1.00	-0.85	0.52	-0.60	-0.39	0.08	0.45	-0.03	-0.11	-0.01
R-ind	--	--	--	--	--	--	1.00	-0.66	0.74	0.60	-0.34	-0.51	0.27	0.10	0.36
I-ind	--	--	--	--	--	--	--	1.00	0.00	0.16	0.62	0.98	-0.80	-0.51	-0.81
LOI	--	--	--	--	--	--	--	--	1.00	0.96	-0.05	0.19	-0.24	-0.20	-0.14
TOC/TN	--	--	--	--	--	--	--	--	--	1.00	0.06	0.35	-0.34	-0.38	-0.19
GT_{Y_0}	--	--	--	--	--	--	--	--	--	--	1.00	0.57	-0.90	-0.87	-0.82
GT_{365}	--	--	--	--	--	--	--	--	--	--	--	1.00	-0.80	-0.55	-0.77
NK	--	--	--	--	--	--	--	--	--	--	--	--	1.00	0.79	0.95
NP	--	--	--	--	--	--	--	--	--	--	--	--	--	1.00	0.58
NW	--	--	--	--	--	--	--	--	--	--	--	--	--	--	1.00

S5.3. Carbon and nitrogen in the leachate

Table S5.3.1. Dissolved inorganic carbon (DIC), dissolved organic carbon (DOC_L), Kjeldahl nitrogen (Nkj), DOC_L and Kjeldahl nitrogen normalized to chloride (DOC_L/Cl and Nkj/Cl), nitrate nitrogen plus nitrite nitrogen (NO_3-N+NO_2-N) per landfill pilot (BRA, WIE, KRA) and compartment. Yearly mean and standard deviation in brackets.

Landfill pilot	Measurement period	DIC [mg/l]	DOC_L [mg/l]	DOC_L/Cl	Nkj [mg/l]	Nkj /Cl	NO_3-N+NO_2-N [mg/l]
BRA-11N	2017	727.5 (151.2)	135.2 (47.4)	0.1 (0.0)	326.1 (57.3)	0.4 (0.0)	0.1
BRA-11N	2018	730.0 (113.4)	182.0 (72.0)	0.2 (0.1)	355.6 (48.2)	0.4 (0.1)	0.3 (0.2)
BRA-11N	2019	745.2 (110.5)	160.6 (39.7)	0.3 (0.3)	349.1 (85.4)	0.4 (0.1)	1.4
BRA-11N	2020	821.6 (315.4)	175.4 (41.1)	0.2	407.4 (99.6)	0.5 (0.1)	1.3 (1.4)
BRA-11N	2021	741.4 (83.6)	174.6 (27.9)	0.2 (0.0)	406.2 (61.7)	0.6 (0.0)	0.2
BRA-11N	2022	791.2 (116.7)	192.4 (37.8)	0.2 (0.1)	460.8 (101.8)	0.6 (0.1)	0.2 (0.1)
BRA-11N	2023	722.5 (97.7)	182.0 (29.6)	0.3	453.9 (100.6)	0.8 (0.1)	0.4 (0.1)
BRA-11N	2024	708.5 (223.0)	218.0 (11.0)	0.4 (0.0)	873.3 (1742.9)	0.7 (0.1)	0.3 (0.1)
BRA-11Z	2017	561.0 (89.2)	88.7 (43.0)	0.1 (0.0)	132.3 (61.5)	0.1 (0.1)	0.3
BRA-11Z	2018	531.0 (103.1)	99.1 (28.8)	0.1 (0.0)	124.6 (17.1)	0.1 (0.0)	0.1
BRA-11Z	2019	555.1 (73.5)	101.2 (25.7)	0.1 (0.0)	126.3 (51.6)	0.1 (0.0)	0.0
BRA-11Z	2020	508.7 (105.9)	80.7 (19.0)	0.1 (0.0)	109.0 (29.6)	0.1 (0.0)	0.3
BRA-11Z	2021	545.1 (59.4)	95.0 (51.1)	0.1 (0.1)	117.2 (20.7)	0.2 (0.0)	1.1
BRA-11Z	2022	553.4 (84.6)	79.4 (17.0)	0.1 (0.0)	117.2 (29.4)	0.1 (0.0)	0.3 (0.1)
BRA-11Z	2023	478.2 (94.8)	66.6 (15.2)	0.1 (0.0)	95.4 (27.6)	0.2 (0.0)	0.4 (0.1)
BRA-11Z	2024	372.5 (116.5)	52.3 (9.9)	0.1 (0.0)	71.7 (11.5)	0.2 (0.0)	0.3 (0.1)
BRA-12	2017	872.7 (245.4)	215.5 (115.8)	0.2 (0.1)	473.5 (219.5)	0.4 (0.1)	0.2
BRA-12	2018	665.6 (237.2)	174.5 (82.4)	0.2 (0.1)	376.3 (148.9)	0.3 (0.1)	0.3 (0.3)
BRA-12	2019	572.8 (178.0)	138.4 (51.9)	0.1 (0.0)	284.0 (125.2)	0.2 (0.1)	2.5 (2.4)
BRA-12	2020	596.2 (202.0)	141.3 (65.7)	0.1	287.8 (150.1)	0.3 (0.1)	4.5 (5.5)
BRA-12	2021	588.2 (113.6)	122.0 (33.3)	0.1	242.9 (80.7)	0.2 (0.0)	0.6 (0.3)
BRA-12	2022	626.0 (146.6)	158.4 (131.9)	0.2 (0.1)	266.4 (93.3)	0.3 (0.1)	0.5 (0.4)
BRA-12	2023	519.4 (147.1)	89.8 (30.7)	0.2 (0.0)	156.6 (74.1)	0.3 (0.1)	0.8 (0.9)
BRA-12	2024	459.6 (218.0)	118.8 (39.5)	0.2 (0.1)	155.3 (65.6)	0.3 (0.1)	0.3 (0.2)
WIE	2017	836.6 (123.5)	213.7 (62.6)	0.4 (0.1)	537.7 (116.6)	1.0 (0.1)	1.3 (2.1)
WIE	2018	911.2 (164.7)	275.4 (99.1)	0.4 (0.1)	645.0 (154.9)	1.0 (0.3)	0.2 (0.1)
WIE	2019	828.5 (75.6)	235.4 (33.1)	0.4 (0.0)	540.9 (78.3)	0.9 (0.1)	0.3
WIE	2020	892.9 (72.5)	280.9 (27.4)	0.4 (0.1)	655.0 (66.0)	1.0 (0.1)	0.3
WIE	2021	933.5 (50.2)	317.7 (19.0)	0.5 (0.1)	689.6 (48.6)	1.0 (0.1)	0.5 (0.1)
WIE	2022	1042.4 (201.7)	357.7 (76.5)	0.5 (0.1)	845.6 (176.5)	1.2 (0.2)	0.3 (0.1)
WIE	2023	952.1 (213.4)	339.2 (79.4)	0.5 (0.1)	792.6 (182.1)	1.3 (0.3)	0.4 (0.2)
WIE	2024	905.4 (58.5)	306.4 (37.8)	0.6 (0.1)	590.7 (85.6)	1.2 (0.3)	0.3 (0.1)
KRA	2018	1761.8 (164.2)	874.2 (109.4)	0.7 (0.1)	1561.7 (179.2)	1.3 (0.1)	0.2 (0.0)
KRA	2019	1677.6 (127.3)	879.6 (179.5)	0.8 (0.1)	1471.2 (170.6)	1.3 (0.1)	0.8 (1.1)

Landfill pilot	Measurement period	DIC [mg/l]	DOC_L [mg/l]	DOC_L/Cl	Nkj [mg/l]	Nkj /Cl	NO_3-N + NO_2-N [mg/l]
KRA	2020	1588.7 (78.3)	904.1 (395.6)	0.9 (0.3)	1439.3 (102.2)	1.4 (0.1)	2.3 (6.8)
KRA	2021	1500.8 (118.3)	678.6 (128.3)	0.7 (0.1)	1318.7 (90.3)	1.3 (0.0)	1.1 (2.3)
KRA	2022	1428.6 (92.3)	672.7 (121.5)	0.7 (0.1)	1295.7 (116.0)	1.3 (0.1)	0.5 (0.5)
KRA	2023	1178.9 (199.1)	479.4 (57.3)	0.6 (0.1)	1142.9 (181.2)	1.4 (0.2)	0.3 (0.0)

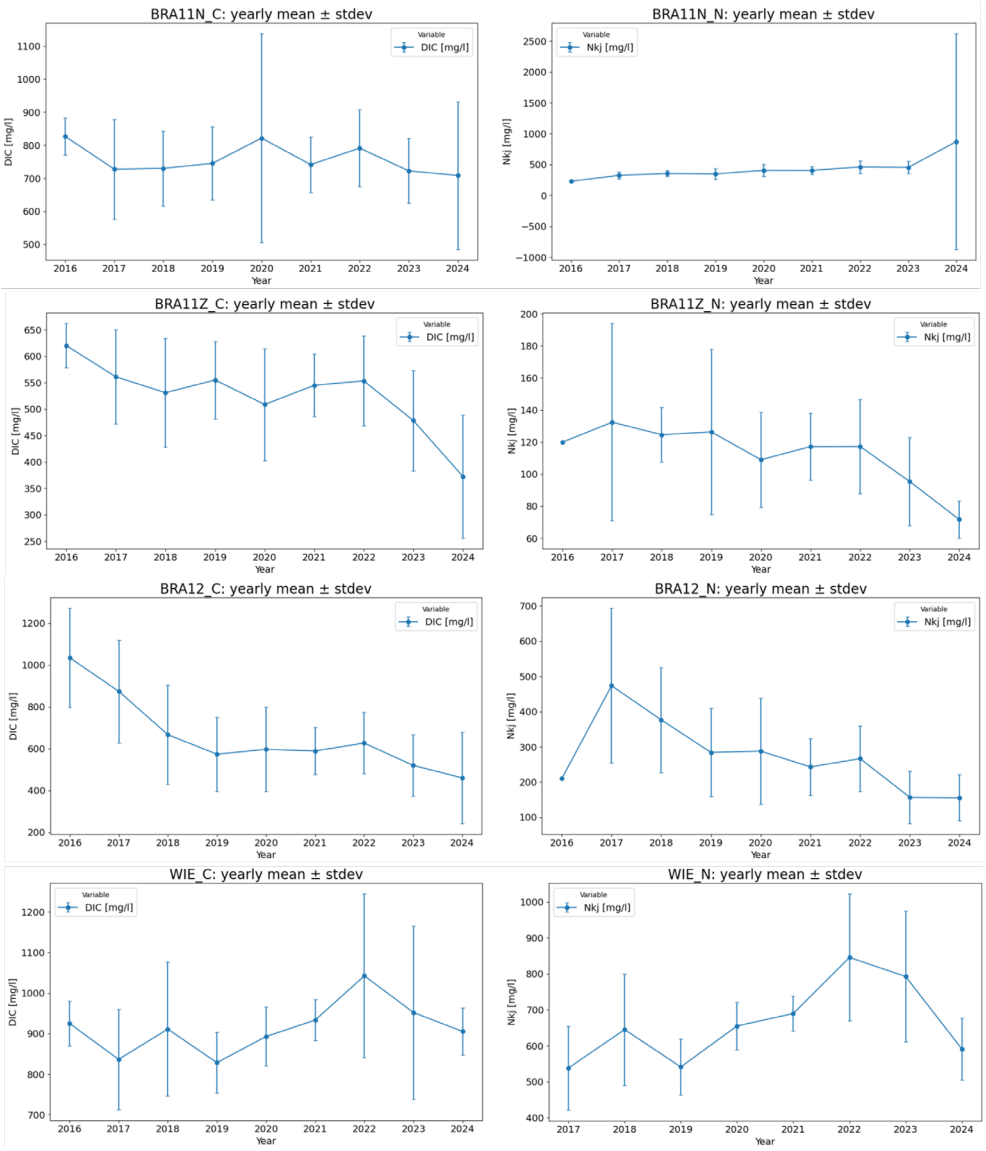

Figure S5.3.1. Yearly mean and standard deviation of Dissolved inorganic carbon (DIC), and Kjeldahl nitrogen (Nkj) in BRA and WIE landfill pilots and compartments.

B

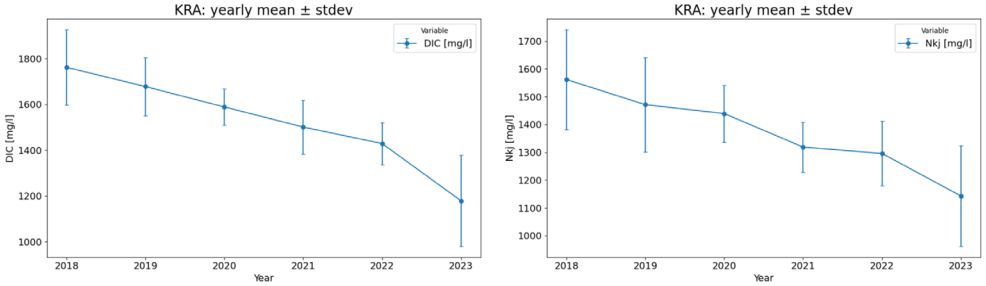

Figure S5.3.2. Yearly mean and standard deviation of Dissolved inorganic carbon (DIC), and Kjeldahl nitrogen (Nkj) in KRA landfill pilot.

S5.4. Carbon and nitrogen in the landfill gas

Table S5.4.1. Gas pressure, flow (not normalized) and composition (CH_4, CO_2, and O_2) in landfill pilots: BRA (2017-09-08 to 2024-09-08), WIE (2017-08-15 to 2024-04-16) and KRA (2012-03-01 to 2023-12-31). Yearly mean and standard deviation in brackets

Landfill pilot	Measurement period	Measurements				
		Pressure (hPa)	Flow (m^3/h)	CH_4 (vol. %)	CO_2 (vol. %)	O_2 (vol. %)
BRA	2017	-25.1 (3.2)	679.8 (166.0)	4.1 (3.7)	13.3 (1.9)	4.7 (1.5)
	2018	-25.1 (6.8)	287.6 (84.7)	8.6 (2.6)	17.0 (3.3)	3.1 (2.9)
	2019	-30.0 (8.5)	269.8 (61.8)	10.8 (2.5)	18.1 (2.5)	4.4 (5.1)
	2020	-40.4 (10.7)	294.3 (129.5)	8.8 (3.8)	15.7 (5.3)	5.1 (4.3)
	2021	-24.9 (16.5)	294.2 (177.4)	8.3 (4.0)	15.4 (5.9)	5.0 (5.6)
	2022	-33.7 (14.1)	284.4 (138.5)	7.4 (3.0)	14.6 (4.1)	6.0 (4.1)
	2023	-33.2 (11.3)	444.8 (133.4)	4.4 (1.6)	13.5 (2.5)	6.7 (2.2)
	2024	-32.1 (9.2)	504.1 (78.7)	3.2 (1.1)	8.5 (3.0)	11.0 (3.4)
WIE	2017	-17.0 (5.6)	594.9 (204.7)	3.9 (3.0)	17.3 (2.9)	3.3 (2.6)
	2018	-23.3 (6.5)	432.2 (133.7)	6.7 (4.0)	19.7 (4.7)	2.3 (4.3)
	2019	-24.6 (8.0)	379.7 (128.9)	10.7 (3.7)	21.1 (2.7)	1.1 (2.2)
	2020	-38.2 (7.3)	481.6 (150.0)	6.9 (2.4)	18.0 (3.2)	2.3 (2.5)
	2021	-39.1 (8.4)	419.6 (130.7)	9.1 (2.3)	19.3 (2.2)	2.2 (1.6)
	2022	-33.7 (13.8)	555.5 (171.5)	6.3 (3.0)	15.8 (5.6)	5.0 (4.6)
	2023	-35.1 (10.6)	498.4 (137.9)	7.3 (1.7)	15.1 (3.1)	6.9 (2.7)
	2024	-38.7 (4.4)	417.2 (114.1)	8.1 (1.8)	13.5 (2.2)	8.4 (2.2)
KRA	2018	-	55.3 (29.9)**	36.6 (2.9)	24.8 (0.8)	1.9 (0.6)
	2019	-4.0 (3.4)*	78.7 (45.0)**	41.0 (2.5)	26.7 (4.8)	1.9 (1.0)
	2020	-6.4 (3.9)*	65.9 (78.6)**	41.1 (4.1)	24.4 (1.7)	1.4 (1.2)
	2021	-7.2 (3.4)*	54.8 (23.1)**	43.5 (3.4)	27.3 (1.3)	0.6 (0.5)
	2022	-5.6 (3.8)*	42.4 (22.8)**	42.7 (4.4)	25.8 (1.3)	0.4 (0.5)
	2023	-7.6 (5.4)*	36.1 (17.7)**	42.8 (0.7)	26.8 (4.6)	0.5 (0.5)

*Measured in the bulk gas of Kragge
** Measured in the bulk gas in Kragge 2

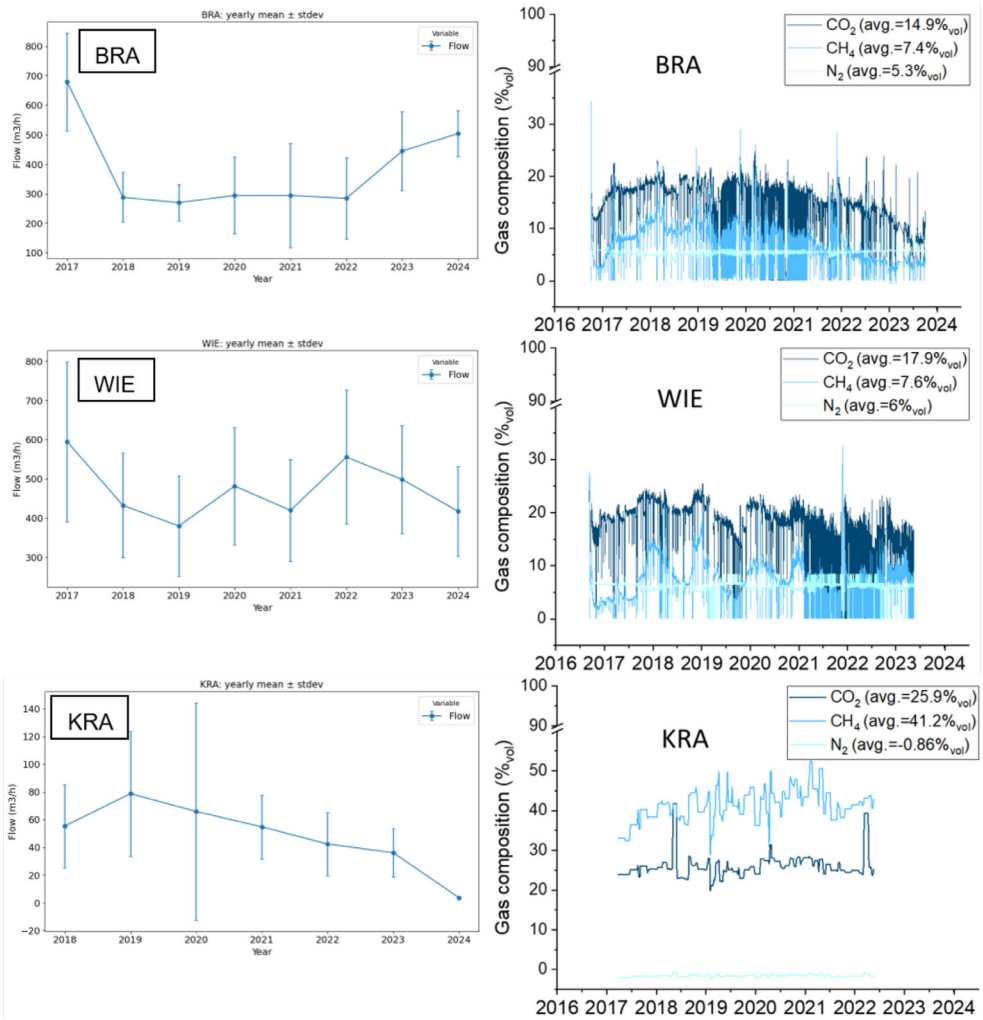

Figure S5.4.1. Yearly mean and standard deviation of gas flow and gas composition in BRA, WIE and KRA. Gas flow in KRA corresponds to the bulk gas in Kragge 2 landfill.

B

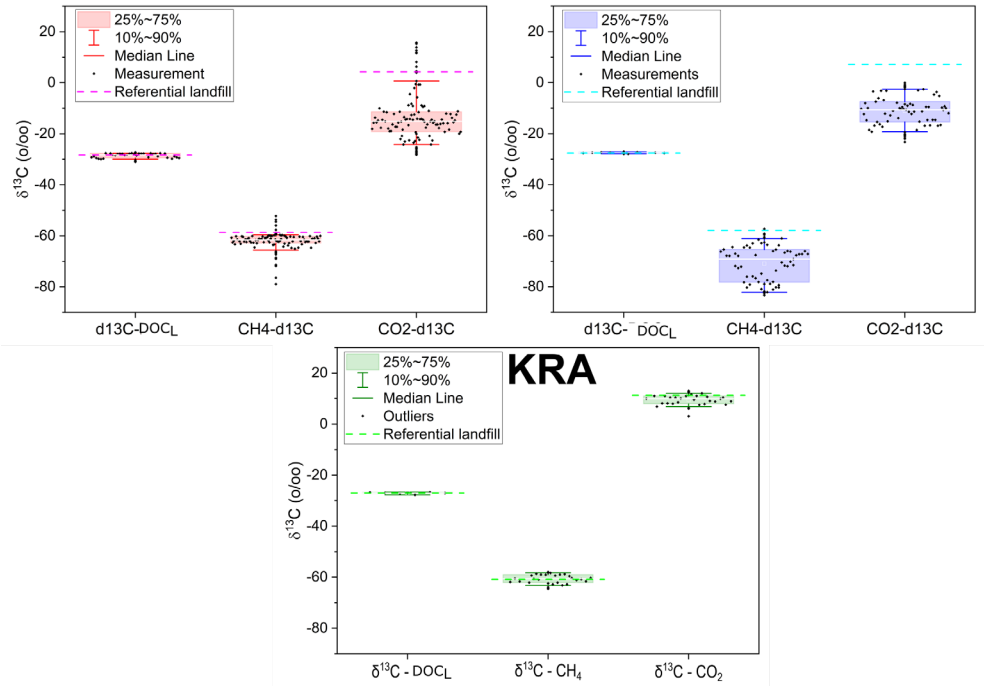

Figure S5.4.2. Stable carbon isotope ratios (d13C) for dissolved organic carbon (DOC_L) in the leachate, and methane (CH_4) and carbon dioxide (CO_2) in the landfill gas. Referential landfill values correspond to compartments outside the stabilization area.

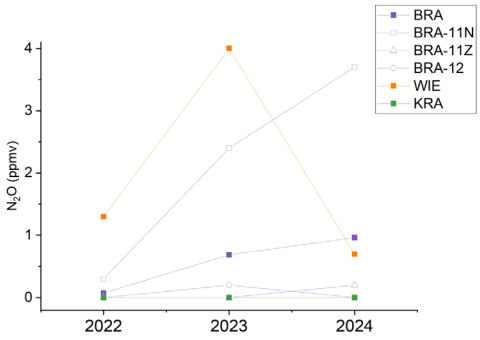

Figure S5.4.3. N_2O concentration in BRA, WIE and KRA

Acknowledgements

This journey would not have been possible without my promotors, Prof. Julia Gebert and Prof. Timo Heimovaara. I would like to express my profound gratitude for giving me the opportunity to work on this PhD, which was part of the CURE project supported by the Dutch National Science Foundation (NWO) under project no. OCENW.GROOT.2019.092. The research was also supported by the Dutch Sustainable Landfill Foundation through the iDS project.

Prof. Julia Gebert, I am deeply grateful to have had you as my daily supervisor and promotor. I always wanted to have a female boss and a role model in my career, and I could not have wished for a better one. Since I arrived in the Netherlands, you were always one step ahead with things I would need, not only for work but also in my personal life. I will always remember your warm welcome to the Netherlands and all the moments we shared outside work. You are not only an excellent researcher but also a friend and a person I admire greatly.

Prof. Timo Heimovaara, thank you for your guidance, curiosity, and for encouraging me to use Python for data processing; it truly made my work more efficient. I was not very enthusiastic about coding at first, but I was lucky to have Dr. Andre van Turnhout in our team and his “Fun with Python” sessions, which helped me understand why it was essential to learn it. Thank you, Andre, for your patience and support during this learning process.

I would also like to thank Dr. Susan Yi. Having another environmental engineer in the team, with both laboratory and field experience, was invaluable. Thank you for all the fieldwork we shared and for your support in the lab whenever needed. To the last two postdocs who joined the project, Dr. Leonardo and Dr. Nasim, it was reassuring to know that you were always willing to help.

Liang, Cristhian, Frank and Nick, having other PhD candidates in our project was wonderful, not only because we shared the same academic journey but also because of all the moments we spent together outside work. I think those times were essential for our well-being. Liang, thank you for always being willing to help, not only with coding and fieldwork but even once in the lab when no one else was around. You were always a reliable colleague and friend. Cristhian, having another Latino in the group was fun; thank you for all the laughs we shared and for your spontaneity. Liang and Cristhian, thank you also for all the meals we shared; Lychee Restaurant is still my favourite. Thank you both as well for agreeing to be my paranymphs and for making the time for my defence, especially Liang for travelling from another country to be there. I truly appreciate it. Frank and Nick, I will never forget our trip to Vienna to pick up the reactors. It was really fun. Nick, your driving endurance is

amazing, haha. Thank you also for always being there to discuss the sometimes mysterious behaviour of the waste, and for your help whenever I had to go to WUR. Frank, thank you for hosting me; I bought The Game after playing it for the first time at your house. Nick, special thanks also for your help in the lab with the waste milling and characterisation. I appreciate it a lot, as it is not an easy job.

Our collaborative project would not have been possible without the companies, researchers and professors involved, both within and outside TU Delft. Thank you for your valuable feedback and time. Special thanks to Dr. Heijo Scharff and Dr. Hans Oonk for the scientific discussions, and to Hans Lammen, Carmen Cruz and Twan Kanen for the operational insights. I am also grateful to the technical teams within those companies, Marco, Frank, Cees-Jan, Mariette and others, who made sampling faster and more enjoyable.

At TU Delft, many thanks to technicians Roland, Jolanda, and especially Cristina, for all the hours we spent together in the lab. I would also like to thank those who were not directly involved in the project but still offered their help, such as Mark, who came up with creative ideas to speed up and improve bottle flushing, or Karel, who rescued my samples from the centrifuge late one evening when almost everyone was already at home. At WUR, thanks to Gerlinde for your help in the lab with the DOC fractionation measurements.

Finally, within the research group I would like to thank the student assistants and the bachelor's and master's students who collaborated on the project: Justus, Lucia, Julia R., Luca, Raj, Tejas, Robbert, Zhenlu, Ties, Simon, Merel, Ruben, Paul, and many others. Your input was important in helping us understand a little more about the complexity of landfills. Special thanks to Julia R., who supported me during the most intense period of laboratory work, and to Robbert for giving me the opportunity to supervise you and for the valuable work you carried out in your thesis.

In my department, Geoscience, I would like to thank my office mates Susan, Wen, Valentina and Tristan, from the time when there were no flex desks and postdocs and PhDs shared the same office. Thank you for all the meals we shared, the drinks at PSOR, and for being there almost every day. Our office was never empty. Susan and Valentina, it was sad to say goodbye when your postdocs finished, but I have many good memories from that time. Wen and Tristan, our PhD journey is also about to finish. It was really nice to share the office with you from the beginning of our PhD. Even when we started our postdocs, we did not want to move to the postdocs office, and luckily we managed to stay in the same office.

I would also like to thank the CEG suport team, especially Marlijn, for always being ready to help despite the busyness of your work. I will always remember the dragon boat event and you as the captain of the boat, leading us with the drum. It was really fun. I would also like to thank Malihe, Willemijn, Jasper, Entela, George, Parvin and Sepi for being part of the PhD committee and for all the events we organised together. I thank Kevin for giving me the opportunity to represent my section in the PhD committee, and Ian, Wei and Vidushi for

continuing that work in the PhD committee and the department council. Thank you also to Mathab, Chris, Sian, Yuen, Mario, Bhini, Andrea, Nazeir, Sara, Elham, Mohamet and many others for all the social activities we shared. Special thanks to Laura, my dear friend who was always there during the good days but especially during the difficult ones. This journey would not have been the same without you. Thank you for all the time we shared together, especially outside work. Your friendship is something valuable that I will carry with me long after the PhD.

There were also activities that greatly supported my well-being during this journey. I would like to thank Lea, Elli, Amelie and Franco for letting me be part of the FoodSharing Delft committee, and Garazi, Nora, Chae and Katherine for being part of it as well. Our shared passion for reducing food waste and living more sustainably brought us together. Thank you for your time and your patience during the busy days of the PhD. Thank you also for the dinners we organised, where I met wonderful people like Frank, who, besides sustainability, also enjoys Latin culture. Those were fun times. I would also like to thank Lotfi for the initiative of creating and, after many years, still managing the volleyball club. Thank you for all the matches and tournaments; I had a lot of fun and met amazing people.

My deep thanks go to my dear friends Sofi and Elena. Together with Laura, we were always ready to party, and of course Macumba is still our favourite Latin party. Special thanks to Sofi, who is also my flatmate and makes our home feel more special and familiar. I would also like to thank Ana and Fede, for all the moments we shared and for helping with the illustration and formatting of this dissertation, and to Miki, who unfortunately is no longer with us but in spirit is also defending this thesis with me.

None of this would have been possible without the unwavering support of my parents. “Education is the key to success,” they always said. Their effort and sacrifices made it possible for me to take every opportunity to learn and discover my passion for research. Rocio, Rigoberto, Francisco, Carlos, Rocio, Maricruz and Julio, my dear family, thank you for all your support, the videocalls and your visits to the Netherlands when I could not go to Peru. They meant a lot to me. I would also like to thank my family in the Netherlands, Paola, Bernd, Sofi and Saskia. Thank you for your warm welcome, your support, and for my first bike, which is very important in this country. I would also like to thank John, my boyfriend, who made life easier and more enjoyable. Thank you for always being there, for your infinite patience, and for taking care of my well-being, especially during the final phase of the PhD. Thank you also to your family, who is now part of my family as well. Thank you for all the messages of encouragement and for celebrating my small victories.

I am grateful for the chance to have met such wonderful people and for the family that has supported me through every stage of this journey, which culminates today.

Paola Nathali Meza Ramos
November, 2025. Delft, The Netherlands.

Curriculum Vitae

Paola Nathali Meza Ramos

02/05/1991	Born in Huancayo, Peru
2003-2007	Secondary Education Zarate School, Huancayo, PE.
2009-2013	B. Sc. in Environmental Engineering National University Agraria La Molina, Lima, PE.
2013-2018	Environmental consulting For private and public insitutions, PE.
2018-2019	Master in Waste Management and Treatment Autonomous University of Madrid, Madrid, ES.
2019-2020	Master in Waste and Wastewater Management for Resource Recovery Autonomous University of Madrid, Madrid, ES.
2019-2020	Environmental consulting For private insitutions, ES.
2020-2025	Ph. D. in Landfill Response to in-situ Stabilisation Delft University of Technology, Delft, NL.
2025-2026	Postdoc in Waste Assesment after Stabilization Delft University of Technology, Delft, NL.

List of publications

Peer reviewed

• Meza, N., Lammen, H., Kanen, T., Heimovaara, T., & Gebert, J. (2026). Generated, recovered and modelled carbon in three landfill pilots under in-situ stabilization. *(in preparation).*

• Yi, S., Meza, N., & Gebert, J. (2025). Application of the nitrogen-to-argon ratio to understand nitrogen transformation pathways in landfills under in-situ stabilization. Waste Management, 194, 13–23. https://doi.org/10.1016/j.wasman.2024.12.042

• Meza, N., Lammen, H., Cruz, C., Heimovaara, T., & Gebert, J. (2022). Spatial variability of gas composition and flow in a landfill under in-situ aeration. Detritus, 19, 104–113. https://doi.org/10.31025/2611-4135/2022.15191

• Gebert, J., de Jong, T., Meza, N., Rees-White, T., Beaven, R. P., & Lammen, H. (2022). Spatial variability of leachate tables, leachate composition and hydraulic conductivity in a landfill stabilized by in-situ aeration. Detritus, 19, 114–120. https://doi.org/10.31025/2611-4135/2022.15189

Conference Proceedings

• Meza, N., Lammen, H., Heimovaara, T., & Gebert, J. (2024). Comparing modelled, recovered and generated carbon in a landfill under in-situ aeration. EurAsia Waste Management Symposium 2024.

• Meza, N., Heimovaara, T., Kanen, T., & Gebert, J. (2023). Comparing modelled, recovered and produced gas in a MSW landfill under leachate recirculation. Sardinia 2023, 19th International Symposium on Waste Management and Sustainable Landfilling.

• Gebert, J., Meza, N., Osorio, C. C., & Lammen, H. (2023). Assessing the efficiency of landfill aeration with a carbon mass balance approach. Sardinia 2023, 19th International Symposium on Waste Management and Sustainable Landfilling.

(Winner of the John Pacey Award for Best Contribution in Landfill Gas Management).

• Meza, N., Lammen, H., Cruz, C., Heimovaara, T., & Gebert, J. (2021). Spatial variability of gas composition and flow in a landfill under in-situ aeration. Sardinia 2021, 18th International Symposium on Waste Management and Sustainable Landfilling.

Other publications

• Wang, L.*, Meza, N.*, & Andrade, C.* (2023, July). The journey of waste: Understanding landfills through the CURE project. DRUPPEL Magazine, 42, 12–14. https://dispuutwaterandenvironment.com/druppel/druppel-jul-2023-volume-42/

*Denotes equal contribution.